IDENTIFICATION OF SHIP HYDRODYNAMIC COEFFICIENTS FROM SIMPLE TRIAL MANEUVERS DURING REGULAR SHIP OPERATIONS

by

GENGSHEN LIU

B.S., Harbin Shipbuilding Engineering Institute
(1967)

Submitted to the Department of
Ocean Engineering
in Partial Fulfillment of the
Requirements of the Degrees of

OCEAN ENGINEER

and

MASTER OF SCIENCE IN NAVAL ARCHITECTURE AND MARINE ENGINEERING

at the

MASSASCHUSETTS INSTITUTE OF TECHNOLOGY

June 1984

Signature of Author Gengshen Liu
Department of Ocean Engineering,
22 May 1984

Certified by
Thesis Supervisor

Accepted by
Chairman, Ocean Engineering
Departmental Committee

ABSTRACT

The hydrodynamic coefficients(for maneuvering simulation) of tanker Esso Osaka were "measured" by applying Extended Kalman Filter(EKF) with the measurements of surge, sway, yaw velocities(u, v, and r) and yaw angle ψ. Efforts are made in this thesis to complete the same task with new system models which require a lesser number of variables to be measured.

Three different models for system identification are tried: (1) using measurements of u, v, and ψ; (2) using measurements of u and ψ; and (3) using measurement of ψ. And discussions on the state model are made from the point of view of both physics and system engineering. And for each model, the analyses on identifibility are made to predict the possibility of success. All models are tested by applying EKF techniques. Except for the model with single measurement ψ, the results are very encouraging. The identification result by using measurements of u, v, ψ is not inferior to that acquired by the four measurement model, which coincides equipped with the conclusion by the mathematical analysis on these two model approaches. This success means that all the modern ships equipped with the dual axis Doppler sonar and gyrocampasses become ships of opportunity on which simple maneuvers are needed to be carried out during normal operation at sea in order to get enough measurement data for identifying the hydrodynamic coefficients.

The result of identification of the hydrodynamic coefficients by the two measurements of u and ψ is also satisfactory for determining the simulation model of the ship and even though it is not as good as that acquired through three measurements. This success result from two measurements is very significant, since it indicates that most ships can be used as ships of opportunity for these simple trials.

It is confirmed again that the application of system identificaiton theory to the maneuvering problems of ships has a bright future. The EKF technique is really very powerful in this area.

ACKNOWLEDGEMENTS

The inspiring advices of Professor M. A. Abkowitz has provided the encouragement which made possible this effort. His profound knonwledge and guidance with skill and patience was most valuable during the whole work. The author takes pleasure to express his heartfelt gratitute.

The author wish to thank professor Michael. Triantafyllou and Dr. Dana R. Yoerger for helpful discussions.

The author also wish to express the appreciation to Mr. Bobby Burke and Mr. Arthur Anger for the optimistic attitude and valuable suggestion during consulation with them on computer work.

CONTENTS

	Page
ABSTRACT	2
ACKNOWLEDGEMENTS	3
Chapter 1 INTRODUCTION	6
Chapter 2 SYSTEM MODEL OF SHIPS	11
2.1 State Variables and Assumptions for the State Model	12
2.1.1 Coordinates Selected and Variables Describing Ship's Motion	13
2.1.2 Assumptions	14
2.2 Overview of Governing Equations	16
2.3 State Model	24
2.4 Measurement Model	28
2.4.1 Different Measurement Models	28
2.4.2 The Relation Between State Model and Measurement Model	30
Chapter 3 IDENTIFICATION TECHNIQUES	32
3.1 Premises	32
3.2 Identifibility	33
3.2.1 Identifibility of a Time-invariant Linear System	33
3.2.2 Primary Analysis on the Identifibility of Our Systems	35
3.2.3 An Alternative Analysis on the Identifibility of the Three Measurement Model	38
3.3 Identification Technique Applied	40

Page

Chapter 4 RESULTS OF THE IDENTIFICATION BY DIFFERENT SYSTEM MODELS 42

4.1 Results of the Three and Two Measurement Models 42

4.2 Result of the One Measurement Model 44

4.3 One Attempt of Using r Derived from ψ 44

Chapter 5 CONCLUSIONS AND SUGGESTIONS 150

5.1 Conclusions 150

5.2 Suggestions 151

REFERENCES 153

Chapter 1 INTRODUCTION

Along with the development of science and technology, especially the wide application of computers, the technique of simulation has been more and more used. This is also the case in the study of the maneuverability of marine vehicles. An accurate mathematical model of a ship is of great importance, since it describes the dynamical characteristics properly and realistically.

With a good mathematical model, one can judge the maneuvering capacity, hence the operability of the ship, to see if it can maneuver adequately in the environment in which it operates. In other words, to see if it can perform its missions safely and effectively, especially in the restricted waters, such as in the harbor, shallow water and so on. After appearance of the giant ships such like VLCC(Very Large Crude Carriers) and LNG(Liquified Natural Gas) tanker, the problem of safety has become more important. Because accidents like collisions or groundings of these types of vessels may cause extensive damage to life, property and environment.

The correct mathematical models of ships may become the basis on which modern electronic devices and computer systems on board, (such as auto pilot, satellite navigator, automatically controlled power plant system,...) can be properly designed, and standard procedure of operation of the ships can be properly developed.

In addition, good mathematical models of the ship can be used

beneficially by the owners to train pilots on realistic simulators.

Furthermore, the mathematical models of ships are also helpful for the design practice. The surface ship is a good example, since the manerverability study of a surface ship is mainly concerned with the dynamic stability, the ships' response to the control surface and the turnning capacity in various environments. In the design stage, several alternative designs could be simulated and compared, then the optimal design can be reached. For the ships already in service, the possibility of improvement in design can be explored. J.S. Kim's work[15] is an example of this.

The mathematical models of ships are determined by both their structures and the values of the parameters in them. Structures of the models are developed through the application of Newton's laws of dynamics to the ships and the environments in which they operate. Professor Martin A. Abkowitz has given a good demonstration in his works.[1] Of course, in practice, simplification and revision during the derivation are always needed, and the experiences in hydrodynamics are often involved.

After the structure of the mathematical model has been determined, the most important thing is to find the values of the parameters in the model correctly, or in other words, to estimate them either theoretically or experimentally. The traditional method was through model testing, although the method of using ships of full scale to do experiment might also be an option.

However, the full scale ship test is difficult to be carried out and is also very expensive, while the disvantages of scale effect from model tests may make model tests not ideal nor satisfactory. Therefore, efforts were put in searching for new techniques which can be effectively used in the practice.

When the ship and the environment are together taken as a system, the technique of "system identification" can be used to measure the parameters in the mathematical model, by carrying out very simple sea trials of the ships. Among different methods of system identification, under the guidance of professor Matin A. Abkowitz, the Extended Kalman Filter(EKF) was first chosen for the ship maneuvering dynamics in M.I.T, and it has worked very successfully.[2--9].

Among all the work done in this area, the most stimulating one is the work done by Hwang and Kwok[8,9] on the 280,000-dwt tanker Esso Osaka in deep water and shallow water respectively which really provided a very convincible demonstration. The effective simulation model was identified and the motion predictions by the model for all the trial maneuvers compare very favorably with the measured motions of the Esso Osaka. Hence the EKF has been confirmed as a powerful tool in measuring the parameters of the model.

However, when Esso Osaka carried out the specially designed sea trials, four kinds of measurements were required which were u,v,r and ψ respectively, therefore four different kinds of sensors were required correspondingly. It is well known that not

all the ships are equipped with the apparatus which measures sway velocity v and the yaw rate r, especially the latter. To mount these special apparatus will not only be expensive but also time-consuming. For this reason, the example of Esso Osaka would have no extensive practical significance, because, to use this kind of technique, there are very few ships of opportunity existing in the realistic world. A ship of opportunity is on that can conduct simple trials during a normally scheduled voyage with only the normal instrumentation on board. If we can use only three measurements of u, v and ψ at the sea trials to get satisfactory results of identification, there would be more ships of opportunity, since, some new built advanced ships are equipped with dual-axis Doppler sonar systems. If we can use only two measurements of u and ψ, then most of the ships could become the ships of opportunity. Since every ship has its gyrocampass and most of the ships have some kind of the speed log to measure the surge velocity u. Then, because the identification of the parameters in the mathematical model----in our case they are hydrodynamic coefficients----can be carried out by means of simple sea trials, the effective mathematical model of most ships can be established economically. So the application of EKF to the ship maneuvering problem will be of great significance. Furthermore, if only the measurement of ψ is needed in order to get satisfactory identification, Then every ship becomes a ship of opportunity, since every ship has a gyrocampass. Then the technique of EKF can applied to all the ships for setting up

their mathematical models.

The good prospects resulting from this analysis is very encouraging.

With all the data of the sea trials of Esso Osaka at hand, all the three cases mentioned above have been tried by using 3, 2 and 1 measurement data in successive case. Since the identification procedures for a same ship in deep water and shallow water are parallel, only the case of deep water was studied here.

In Chapter2 the mathematical models of the ship systems with 3, 2 and 1 measurements correspondingly are discussed from the point of view of system engineering. During the discussion, assumptions are also mentioned.

In Chapter3, brief analyses of the identifibility of the ship systems are made. This initial prediction about the success for different systems was given as the starting point of our work. And the philosophy of identification for the three different cases are illustrated briefly.

Chapter4 gives the results of all the three cases and comments are made for each one.

The conclusions were summarized in chapter5, and recommendations for the future work and the practical application of EKF to the ship maneuver problems are made.

Chapter 2 SYSTEM MODEL OF SHIPS

It is very clear that when we use the technique of system identificaion to deal with the maneuverability of ships, we will not only consider the ship, but take the ship together with the environment in which it operates as a system. The model describing the very system is in fact a group of equations. For identification problems, by and large, the system model consists of two parts:

1. The state model described by the equations:

$$\dot{\underline{x}}(t) = \underline{f}[\underline{x}(t), \underline{\xi}(t), \underline{w}(t), \underline{p}(t), t] \quad \text{.....(2.1)}$$

where $\underline{x}(t)$: system state vector.

$\underline{\xi}(t)$: input signal.

$\underline{w}(t)$: input disturbance.

$\underline{p}(t)$: unknown parameters of the system.

2. The observation model or measurement model described by the equations:

$$\underline{z}(t) = \underline{h}[\underline{x}(t), \underline{\xi}(t), \underline{w}(t), \underline{p}(t), \underline{v}(t), t] \quad \text{.....(2.2)}$$

where besides the symbols defined above,

$\underline{v}(t)$: observation noise.

$\underline{z}(t)$: output signal or observed vector.

In general, the order of the differential equation $\underline{f}$ may or may not be known, and there is always the unknown parameter vector $\underline{p}(t)$. Therefore both of them are to be identified. Fortunately, for our case, the order of the differential equation $\underline{f}$ is known as we will show later. All we need to identify are the parameters -- hydrodynamic coefficients in the equations. To complete this task we first should start from setting up the system models.

2.1 State Variables and Assumptions for the State Model

The state model of a ship system is a group of differential equations which governing the maneuvering motion of the ship. To represent a complicated physical system by only a group mathematical equations, requires comprehensively analytical work, and the first thing is to make assumptions and define the variables with physical meanings which will be used in the equations. Proper assumptions together with carefully chosen variables will make the physical problems greatly simplified while at the same time all the main characteristics of the problem are described authentically.

2.1.1 Coordinates Selected and Variables Describing Ship's Motion

Strictly speaking, for all kinds of ships including surface ships, underwater marine vehicles, even the special marine vehicles like hovercrafts, their motions are 6 degrees of

freedom. To describe motions of a ship, a coordinate system is needed, either it is fixed to the ground or it is fixed to the ship. Since the forces and moments involved in the dynamics of the ship system are essentially hydrodynamic, so to make the calculation of these hydrodynamic loading easier, we prefer to fix the coordinates onto the ship.

The coordinate system chosen in this work is a Cartisian Coordinate. Considering the symmetrical property of the geometry of the ship, the system is located on the ship as shown in Fig. 2.1

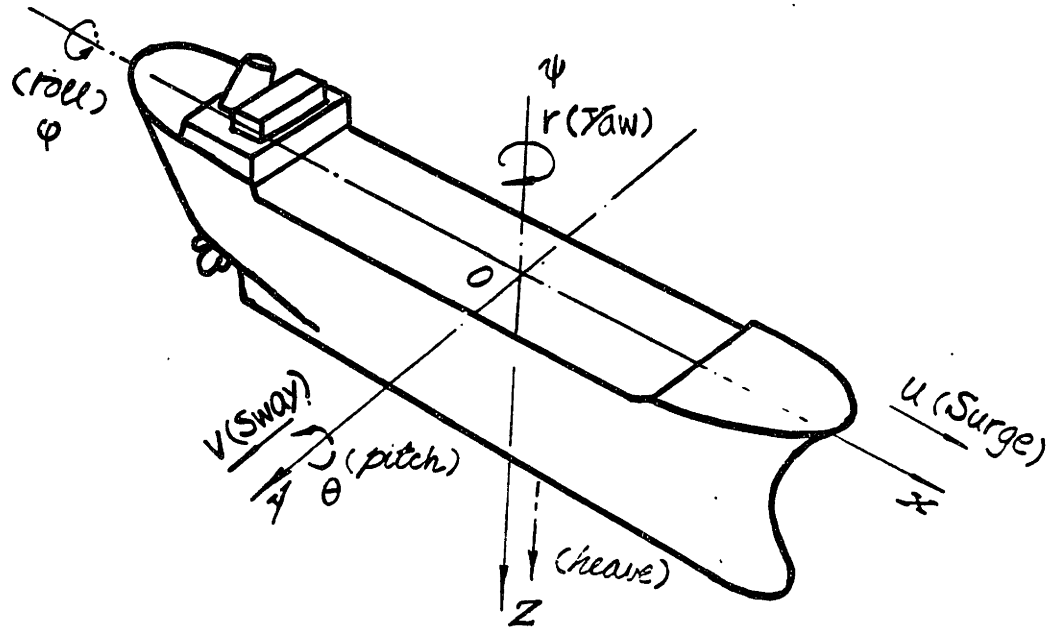

fig.2.1 Coordinate system for the ship

The origin is at the midship of x-axis which is the intersection of the longitudinal centre plane of the ship and the

calm water surface. The positive directions of x-axis, y-axis and z-axis point toward bow, starboard and keel respectively. Therefore this is an orthogonal right hand system.

In this coordinate system, the motion of the ship is, in fact, described by the negatively relative motion of the environment. There are six basic motions which can be classified. Three of them are translational motions which are surge motion along x-axis described by u, sway motion along y-axis described by v and heave motion along z-axis described by w. The left three of them are rotations which are roll motion around x-axis described by p, pitch motion around y-axis described by q and yaw motion around z-axis described by r. Therefore, in general, the mathematical equations derived from the Newton's law are formed with these six state variables.

2.1.2 Assumptions

The motions of ships are very complicated. The real motions of ships are of 6 degrees of freedom and there may be cross-couplings between them, for example, the cross-coupling between roll and sway, surge and heave, yaw and roll etc. However, the complexity of the motions depends in a large scale on the type of ship -- size, shape, displacement,...; the tightness of the maneuvering -- velocity, acceleration,.... Therefore, for different ships, with correct analysis, the insignificant factors can be ignored and the problem of maneuvering motions can thus be simplified. As an example, the

motions of our object -- the big tanker Esso Osaka were very much simplified after the following analyses.

1) Tanker Esso Osaka is very large in size(o.a.: 343.00m; w: 53m, T: 22.05m), and the service speed of it is low(15 knots), so the motion of it could not be of high Froude number.

2) For the large merchant ships like Esso Osaka, the maneuvering problems are mainly concerned with offshore maneuvering, docking and harbor operation, so the very tight maneuvers at high speed are most unlikely.

Under the conditons mentioned above, the following assumptions will be reasonable.

1) Heaving, pitching and rolling motions are of no significance to basic maneuvering of the Esso Osaka, hence can be ignored. The maneuvering motion of it can thus be taken as the motion in the horizontal plane, so it has only 3 degrees of freedom. The corresponding variables for describing it, or the state variables, are u, v and r.

2) Like all ships, Esso Osaka has port-starboard symmetry, so no cross-couplings with the vertical motions.

3) The accelerations described by $\dot{u}$, $\dot{v}$ and $\dot{r}$ are only linearly related to the hydrodynamic forces and moments.

4) The environment is in the steady mode during a particular maneuver, which means that the changes in the environment such as the currents, the water depth and so on, are assumed

producing little or no extroneous exicitations and therefore negligible.

The convention of these variables are shown in fig.2.2, where ψ is the yaw angle and $\dot{\psi} = r$ is the yaw rate.

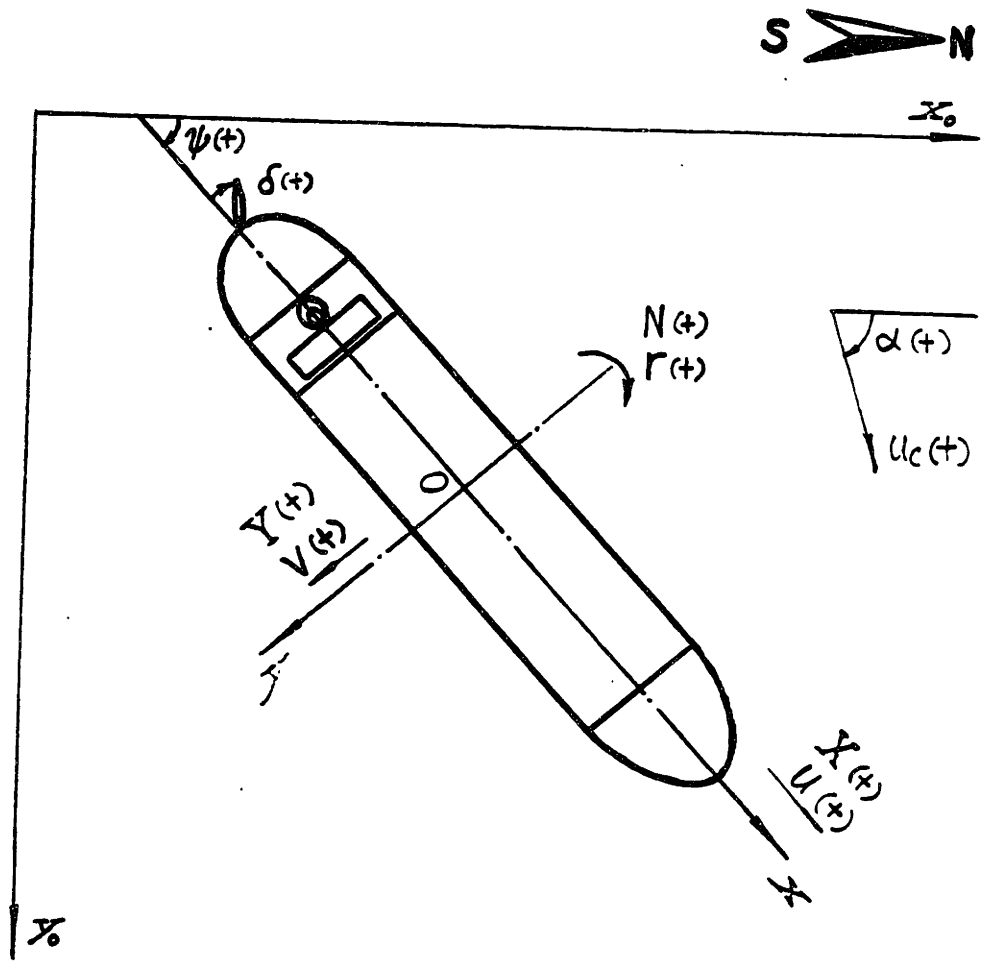

fig.2.2 Coordinate system and sign convention

2.2 Overview of Governing Equations

The governing equations of the ship system result from the application of Newton's second law. The whole procedure of

derivation is exactly the same as what is shown in professor Abkowitz's work[1]. We start from the three basic equations:

$$m[\dot{u}_r - rv_r - x_G r^2] = X(\dot{u}_r, \dot{v}_r, \dot{r}, u_r, v_r, r, \delta, \ldots)$$

$$m[\dot{v}_r + ru_r + x_G \dot{r}] = Y(\dot{u}_r, \dot{v}_r, \dot{r}, u_r, v_r, r, \delta, \ldots)$$

$$I_z \dot{r} + mx_G[\dot{v}_r + ru_r] = N(\dot{u}_r, \dot{v}_r, \dot{r}, u_r, v_r, r, \delta, \ldots) \quad \ldots\ldots(2.3)$$

where X, Y are the external forces acting in the x and y direction respectively, N is the external moment about the z-axis.

Considering the current with magnitude u and direction of 2.

$$u_r = u - u_c \cos(\psi - \alpha)$$

$$v_r = v + u_c \sin(\psi - \alpha)$$

$$\dot{u}_r = \dot{u} + u_c r \sin(\psi - \alpha)$$

$$\dot{v}_r = \dot{v} + u_c r \cos(\psi - \alpha) \quad \ldots\ldots\ldots\ldots\ldots(2.4)$$

Of course, u_c is taken as constant, because we already made the assumption in 2.1.2.

The result of the derivation are the simultaneous differential equations of u_r, v_r, r, with the hydrodynamic coefficients as the parameters. They are:

$$\dot{u}_r = \frac{f_1}{m - X_{\dot{u}_r}}$$

$$\dot{v}_r = \frac{(I_z - N_{\dot{r}})f_2 - (mx_G - Y_{\dot{r}})f_3}{f_4}$$

$$\dot{r} = \frac{(m - Y_{\dot{v}_r})f_3 - (mx_G - N_{\dot{v}_r})f_2}{f_4} \qquad \ldots\ldots\ldots\ldots (2.5)$$

where

$$f_1 = X_{u_r}\Delta u_r + X_{u_r u_r}(\Delta u_r)^2 + X_{u_r u_r u_r}(\Delta u_r)^3 + X_{v_r v_r} v_r^2 + X_{\delta\delta}\delta^2 + (X_{rr} + mx_G)r^2$$

$$+ (X_{v_r r} + m)v_r r + X_{v_r \delta} v_r \delta + X_{r\delta} r\delta + X_{\delta\delta u_r}\delta\delta\Delta u_r + X_{rru_r} r^2\Delta u_r + X_{v_r v_r u_r} v_r^2\Delta u_r$$

$$+ X_{v_r r u_r} v_r r\Delta u_r + X_{v_r \delta u_r} v_r \delta\Delta u_r + X_{r\delta u_r} r\delta\Delta u_r$$

$$f_2 = Y_0 + Y_{v_r} v_r + (Y_r - mu_r)r + Y_\delta \delta + Y_{v_r u_r} v_r \Delta u_r + Y_{ru_r} r\Delta u_r + Y_{\delta u_r}\delta\Delta u_r$$

$$+ Y_{v_r v_r v_r} v_r^3 + Y_{rrr} r^3 + Y_{\delta\delta\delta}\delta^3 + Y_{v_r rr} v_r r^2 + Y_{v_r \delta\delta} v_r \delta\delta + Y_{v_r u_r u_r} v_r (\Delta u_r)^2 + Y_{rv_r v_r} r v_r^2$$

$$+ Y_{r\delta\delta} r\delta^2 + Y_{ru_r u_r} r(\Delta u_r)^2 + Y_{\delta v_r v_r}\delta v_r^2 + Y_{\delta rr}\delta r^2 + Y_{\delta u_r u_r}\delta(\Delta u_r)^2 + Y_{v_r r\delta} v_r r\delta$$

$$f_3 = N_0 + N_{v_r} v_r + (N_r - mx_G u_r)r + N_\delta \delta + N_{v_r u_r} v_r \Delta u_r + N_{ru_r} r\Delta u_r + N_{\delta u_r}\delta\Delta u_r$$

$$+ N_{v_r v_r v_r} v_r^3 + N_{rrr} r^3 + N_{\delta\delta\delta}\delta^3 + N_{v_r rr} v_r r^2 + N_{v_r \delta\delta} v_r \delta\delta + N_{v_r u_r u_r} v_r (\Delta u_r)^2 + N_{rv_r v_r} r v_r^2$$

$$+ N_{r\delta\delta} r\delta^2 + N_{ru_r u_r} r(\Delta u_r)^2 + N_{\delta v_r v_r}\delta v_r^2 + N_{\delta rr}\delta r^2 + N_{\delta u_r u_r}\delta(\Delta u_r)^2 + N_{v_r r\delta} v_r r\delta$$

$$f_4 = (m - Y_{\dot{v}_r})(I_z - N_{\dot{r}}) - (mx_G - N_{\dot{v}_r})(mx_G - Y_{\dot{r}})$$

But these equations are not suitable for use both in simulation and system identification for the following reasons:

1) The hydrodynamic coefficients are not constants , but are the functions of the speed of ships, or in more detail, are the functions of the relative speed at the points where the hydrodynamic forces act. While the nondimentionalized coefficients are constant at the low speed range. And furthermore, the nondimentionalization of the hydrodynamic coefficients also sets up the bridge between the simulation model and the full sized ship. Therefore the equations are prefered to be changed into the form with nondimentionalized hydrodynamic coefficients.

2) As we noticed the equations (2.1) are the same for all the ships with motions only in the horizontal plane. However, there are too many coefficients which degrade the practical application. At the same time the significance of the coefficients may be quite different for different ships and some of them may be mutually dependent when the concrete ship is studied in more detail. Therefore, there is the possibility that we can reconstruct the equations through analyses based on the experiences in hydrodynamics. In this way, the equations may be simplified and be made more realistic.

For our case, the main modifications will be carried out as follows:

1) A new variable c had been introduced which is the mean velocity over the rudder. The purpose of introducing it is to make the nondimentionalization of the force and moment induced by rudder deflection more appropriate.

$$c = \sqrt{\frac{A_p}{A_R}[(1-w)u_r+ku_{A\infty}]^2 + \frac{A_R-A_p}{A_R}(1-w)^2u_r^2} \qquad (2.6)$$

where A_R is the span area of the rudder.

A_p is the area of part of the rudder covered by the propeller culumn as shown in fig.2.3

w : wake fraction.

k is a factor which is a function of distance x and $k = \frac{u_A}{u_{A\infty}}$

$$u_{A_\infty} = -(1-w)u + \sqrt{(1-w)^2u^2 + \frac{8}{\pi}K_t(nd)^2}$$

K_t : thrust coefficient of the propeller.

n : rotating rate of the propeller.

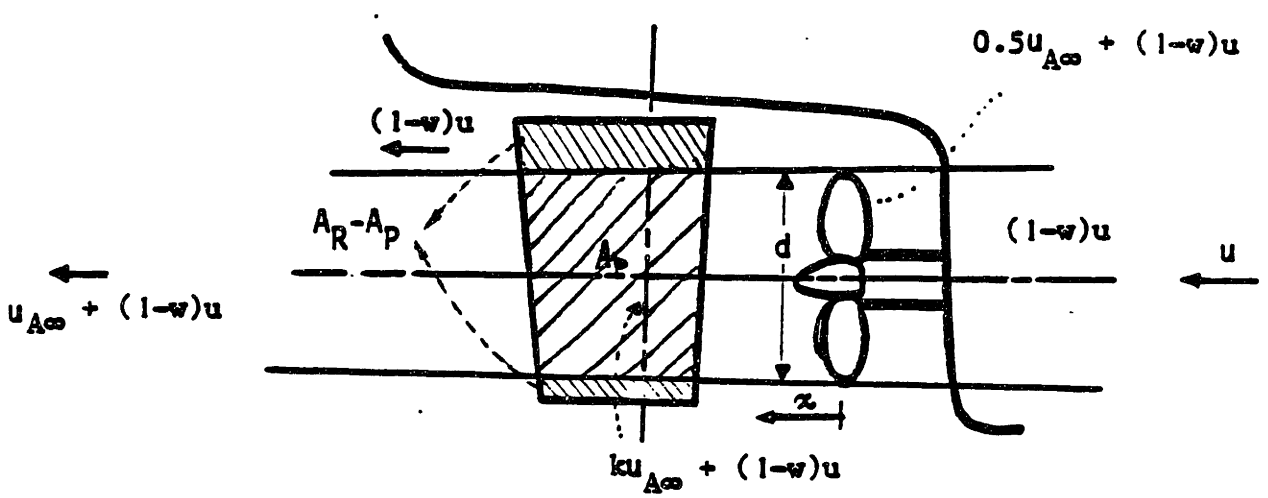

fig.2.3 Geometrical relationship between the propeller and the rudder

The more interesting thing is that this physically meaningful modification covers the effects represented by $X_{u_r\delta\delta}$, $X_{v_r\delta u_r}$, $X_{r\delta u_r}$, $Y_{\delta u_r}$, $Y_{\delta u_r u_r}$, $N_{\delta u_r}$ and $N_{\delta u_r u_r}$. Thus all these terms have to be removed and as the result, the model becomes simpler.

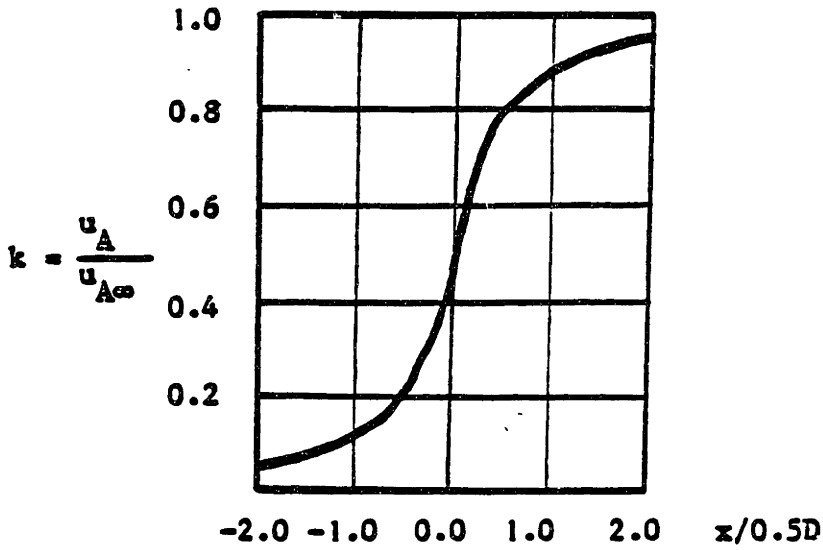

fig.2.4 Function k = k(x)

2) Esso Osaka is propelled by a single propeller, hence at zero serge speed, the sway force Y and yaw moment N are not zero, there are the bias factors Y_o and N_o. To account for this phenomenon, u_r is not suitable for the use of the nondimentionalization of Y_o and N_o, and based on the hydrodynamic analysis, $0.5u_{A_\infty}$ is used instead. And

3) The coefficients of X force are reset through replacing X'_u, X'_{uu}, X'_{uuu} with η_1, η_2, η_3 and C_R to make the equations more suitable for simulation and identification.

η_1, η_2 and η_3 are artificial coefficients resulted from the mathematically logical anaylsis. These three new coefficients satisfy the following relationship:

$$(1-t)T \longrightarrow \eta_1 u^2 + \eta_2 nu + \eta_3 n^2 \qquad \text{.....(2.7)}$$

where t is the thrust deduction factor.

T is the thrust.

η_1, η_2, η_3 have no physical meaning, and the relation expressed here is purely based on the numerical skill.

C_R is resistance coefficient which is related to R, the resistance of the ship in the straight course acting on the ship hull, propeller and other appendages. And the relation between them is

$$(1-t)T-R = (1-t)K_t\rho n^2 d^4 - \frac{\rho}{2} C_R S u^2 \qquad \text{.....(2.8)}$$

where S is the wetted surface of the ship and appendages.

4) A new variable e is created to replace δ.

$$e \approx \delta - \frac{v}{c} + \frac{rL}{2c} \qquad \text{.....(2.9)}$$

e is called the inflow angle to the rudder. With the introduction of e, three new formed force and moment derivatives X_{ee}, Y_{eee} and N_{eee} are used to replace the

higher order force and moment derivatives involving in the following way:

$$X_{\delta\delta}\delta^2+X_{v_r\delta}v_r\delta+X_{r\delta}r\delta+X_{\delta\delta u_r}\delta\delta\Delta u_r+X_{v_r\delta u_r}v_r\delta\Delta u_r+X_{r\delta u_r}r\delta\Delta u_r$$

$$\longrightarrow X_{ee}ee$$

$$Y_{\delta\delta\delta}\delta^3+Y_{\delta u_r}\delta\Delta u_r+Y_{\delta v_r v_r}\delta v_r{}^2+Y_{\delta rr}\delta r^2+Y_{\delta u_r u_r}\delta(\Delta u_r)^2+Y_{r\delta\delta}r\delta^2$$

$$Y_{v_r\delta\delta}v_r\delta^2+Y_{v_r r\delta}v_r r\delta$$

$$\longrightarrow Y_{eee}eee$$

$$N_{\delta\delta\delta}\delta^3+N_{\delta u_r}\delta\Delta u_r+N_{\delta u_r u_r}\delta(\Delta u_r)^2+N_{v_r r\delta}v_r r\delta+N_{v_r\delta\delta}v_r\delta\delta$$

$$+N_{r\delta\delta}r\delta^2+N_{\delta v_r v_r}\delta v_r{}^2+N_{\delta rr}\delta r^2$$

$$\longrightarrow N_{eee}eee$$

The benefit in simplifying the model is very obvious.

5) With the relation $v_r \approx kr$, based on the analysis on the properties of the nonlinear hydrodynamic coefficients involving v_r and r, all the v_r, r cross-correlated third order sway force derivatives acceptably merge into a new item Y_{vrr}.[2]

i.e.

$$\begin{aligned} & Y_{v_r rr}v_r r^2+Y_{rv_r v_r}rv_r{}^2+Y_{v_r v_r v_r}v_r{}^3+Y_{rrr}r^3 \\ \approx\ & (Y_{v_r rr}+kY_{rv_r v_r}+k^2Y_{v_r v_r v_r}+Y_{rrr}/k)v_r r^2 \\ \approx\ & \bar{Y}_{v_r rr}v_r r^2 \end{aligned} \qquad \ldots\ldots\ldots\ldots\ldots\ldots\ldots\ldots(2.10)$$

6) Hydrodynamic analysis showes that the higher order partial derivatives of forces and moment to u_r together with v_r and/or r are the items accounting for the effect of propeller overloading and they can be replaced by the items containing only the first order derivatives of the forces and moment to δ. The detail is as follows:

$$Y_{v_r u_r} v_r \Delta u_r + Y_{r u_r} r \Delta u_r + Y_{r u_r u_r} r (\Delta u_r)^2 + Y_{v_r u_r u_r} v_r (\Delta u_r)^2$$

$$\longrightarrow \frac{Y'_\delta}{2} (c - c_0) \frac{\rho}{2} L^3 r - Y'_\delta (c - c_0) \frac{\rho}{2} L^2 v_r$$

$$N_{v_r u_r} v_r \Delta u_r + N_{r u_r} r \Delta u_r + N_{r u_r u_r} r (\Delta u_r)^2 + N_{v_r u_r u_r} v_r (\Delta u_r)^2$$

$$\longrightarrow \frac{1}{2} N'_\delta (c - c_0) \frac{\rho}{2} L^4 r - N'_\delta (c - c_0) \frac{\rho}{2} L^3 v_r$$

where c_0 is the value of the mean velocity over the rudder corresponding to the equilibrium propeller loading at forward speed u .

X_{rru_r}, $X_{v_r v_r u_r}$ are negligible and omitted.

7) To reflect the speed loss effect, new item Xvrvr2r2 is added and there is:

$$X_{vvrr} v_r^2 r^2 = X'_{v_r^2 r^2} [\frac{\rho}{2} L^4 U^{-2}] v_r^2 r^2 \qquad \text{.....(2.11)}$$

2.3 State Model

Under the assumptions we made and after the modifications mentioned above the final form of the state model of Esso Osaka is shown as follows.

$$\dot{u} = \dot{u}_r - u_c \cdot r \cdot \sin(\psi-\alpha)$$

$$\dot{v} = \dot{v}_r - u_c \cdot r \cdot \cos(\psi-\alpha)$$

$$\dot{u}_r = \frac{f_1}{m-X_{\dot{u}_r}}$$

$$\dot{v}_r = \frac{1}{f_4}[(I_z-N_{\dot{r}})f_2-(mx_G-Y_{\dot{r}})f_3]$$

$$\dot{r} = \frac{1}{f_4}[(m-Y_{\dot{v}_r})\ f_3-(mx_G-N_{\dot{v}_r})f_2] \qquad \text{.....(2.12)}$$

where

$$f_1 = \eta_1'[\tfrac{\rho}{2}L^2]\ u^2{}_r+\eta_2'[\tfrac{\rho}{2}L^3]nu_r+\eta_3'[\tfrac{\rho}{2}L^4]n^2-C_R'[\tfrac{\rho}{2}Su_r{}^2]+X'_{v_r^2}[\tfrac{\rho}{2}L^2]v_r^2$$
$$+\ X'_{e^2}[\tfrac{\rho}{2}L^2c^2]e^2+(X'_{r^2}+m'x_G')[\tfrac{\rho}{2}L^4]r^2+(X_{v_rr}+m')[\tfrac{\rho}{2}L^3]v_rr$$
$$+\ X'_{v_r^2r^2}[\tfrac{\rho}{2}L^4U_r^{-2}]v_r{}^2r^2$$

$$f_2 = Y_0'[\tfrac{\rho}{2}L^2\ (\tfrac{u_{A\infty}}{2})^2]+\{Y'_{v_r}[\tfrac{\rho}{2}L^2U_r]v_r-Y'_\delta(c-c_0)\tfrac{\rho}{2}L^2v_r\}$$
$$+\{(Y'_r-m'u_r')\ [\tfrac{\rho}{2}L^3U_r]r+\tfrac{Y'_\delta}{2}\ (c-c_0)\ \tfrac{\rho}{2}L^3\ r\}+Y'_\delta[\tfrac{\rho}{2}L^2c^2]\delta$$
$$+Y'_{v_r^3}[\tfrac{\rho}{2}L^2U_r^{-1}]v_r^3+Y'_{v_r^2r}[\tfrac{\rho}{2}L^3U_r^{-1}]v_r^2\ r+Y'_{r^2v_r}[\tfrac{\rho}{2}L^4U_r^{-1}]r^2v_r$$
$$+Y'_{r^3}[\tfrac{\rho}{2}L^5U_r^{-1}]r^3+Y'_{e^3}[\tfrac{\rho}{2}L^2\ c^2]e^3$$

$$f_3 = N_0'[\tfrac{\rho}{2}L^3\ (\tfrac{u_{A\infty}}{2})^2]+\{N'_{v_r}[\tfrac{\rho}{2}L^3U_r]v_r-N'_\delta(c-c_0)\ \tfrac{\rho}{2}L^3v_r\}$$
$$+\{N'_r-m'x_G'u_r')[\tfrac{\rho}{2}L^4U_r]r+\tfrac{1}{2}N'_\delta(c-c_0)\tfrac{\rho}{2}L^4\ r\}+N'_\delta[\tfrac{\rho}{2}L^3c^2]\delta$$
$$+N'_{v_r^3}[\tfrac{\rho}{2}L^3U_r^{-1}]v^3{}_r+N'_{v_r^2r}[\tfrac{\rho}{2}L^4U_r^{-1}]\ v_r{}^2r+N'_{r^2v_r}[\tfrac{\rho}{2}L^5U_r^{-1}]r^2v_r$$
$$+N'_{r^3}[\tfrac{\rho}{2}L^6U_r^{-1}]r^3+N'_{e^3}[\tfrac{\rho}{2}L^3\ c^2]e^3$$

$$f_4 = (m'-Y'_{\dot{v}_r})[\tfrac{\rho}{2}L^3]\ (I_z'-N'_{\dot{r}})[\tfrac{\rho}{2}L^5]-(m'x_G'-N'_{\dot{v}_r})[\tfrac{\rho}{2}L^4](m'x_G'-Y'_{\dot{r}})[\tfrac{\rho}{2}L^4]$$

$$u_r = u-u_c\ \cos(\psi-\alpha)$$

$$v_r = v+u_c\ \sin(\psi-\alpha)$$

$$c = \sqrt{\frac{A_p}{A_R}[(1-w)u_r + ku_{A\infty}]^2 + \frac{A_R - A_p}{A_R}(1-w)^2 u_r^2}$$

$$U_r = \sqrt{u_r^2 + v_r^2}$$

u_c: the current velocity which is taken as constant.

α: the direction angle of the current.

In the appearance of the model, 4 variables are involved, i.e. u, v, r and ψ except for the case of

$$u_c = 0$$

in which ψ disappears. For this reason, the system is easily taken as a system with four state variables. This can be seen in the work done on Esso Osaka before, when the model of the system was expressed in the space form,

$$\dot{\psi} = r \qquad \text{.....(2.13)}$$

is added then there is

$$\dot{\underline{x}} = \underline{A}\underline{x} + \underline{w}$$

$\underline{x} = \begin{pmatrix} u_r \\ v_r \\ r \\ \psi \end{pmatrix}$ is the state vector.

.....(2.14)

But we must keep in mind that it is not true if we examine it seriously. First, physically, since the motion of the ship is of only three degrees of freedom, there should only be three independent variables to describe the state of this dynamic system. Second, even start from the point of view of the system

engineering, since r and ψ are not independent to each other, so 4 is in fact a pseudo number, and

$$\dot{\psi} = r$$

is not a state equation. As it will be shown later on, the understanding of this number is helpful in the study of the identifibility of our system.

2.4 Measurement Model

2.4.1 Different Measurement Models

Measurement model is another important part of the system model of a given system. With the same state model the different measurement model can consist the different system models which behave quite different in the view of point of system identification.

Hwang and Kwok in their work used a four measurement model as follows:

$$\underline{z} = \underline{H}\underline{x} \quad \text{.....(4.1)}$$

where $\underline{z} = \begin{bmatrix} u_r \\ v_r \\ r \\ \psi \end{bmatrix}$ is the vector of the same order of $\underline{x}$, so the matrix $\underline{H}$ is a unit matrix:

$$\underline{H} = \begin{bmatrix} 1 & 0 & 0 & 0 \\ 0 & 1 & 0 & 0 \\ 0 & 0 & 1 & 0 \\ 0 & 0 & 0 & 1 \end{bmatrix}$$

Thus, they set up a fourth order system model with full state measurements. With this model Hwang and Kwok very successfully identified the linear and nonlinear hydrodynamic coefficients for Esso Osaka by means of using EKF for the cases of deep water and shallow water respectively. The results are very encouraging in deed, since that was the first time of successfully "measuring" the hydrodynamic coefficients of a real ship by the technique of EKF. However, it is not so attractive for the practical use,

since the requirement of four measurements can only be met by very few ships. Vessels are not commonly equipped with the equipment of measuring sway velocity and only the very special ships have heading rate gyros.

To explore the possibility of using less measurements to do the same identificaion, we need to change the measurement model, and therefore may change the state model as well. Nevertheless, in order to compare with the four measurement model directly, we keep the state model unchanged. In our plan, three different cases are to be studied according to the practical situations of the ships, so we shall set up three different measurement models combining the same state model to compose three different system models and then examine them one by one.

For three measurements, u_r, v_r and ψ are the output variables to be measured, the measurement model is in the form:

$$\underline{z} = \underline{H}\underline{x}$$

$$\underline{z} = \begin{bmatrix} u_r \\ v_r \\ \psi \end{bmatrix}$$

$$\underline{H} = \begin{bmatrix} 1 & 0 & 0 & 0 \\ 0 & 1 & 0 & 0 \\ 0 & 0 & 0 & 1 \end{bmatrix} \qquad \text{.....(2.16)}$$

For the case of two measurements, v_r is omitted from considerations, even though for some modern ships the onboard dual-axis Doppler sonar system is available. Because all ships are

equipped with gyrocampasses but not Doppler sonar systems. In this case the measurement model becomes:

$$\underline{z} = \underline{H}\underline{x}$$

$$\underline{z} = \begin{bmatrix} u_r \\ \psi \end{bmatrix}$$

$$\underline{H} = \begin{bmatrix} 1 & 0 & 0 & 0 \\ 0 & 0 & 0 & 1 \end{bmatrix} \qquad \text{.....(2.17)}$$

While for one measurement, we keep the yaw angle as the variable to be measured. One can argue that almost every ship is equipped with the equipment for measuring surge velocity, why don't you choose u_r to form the single measurement model? The reason is that though almost any ship has the equipment for measuring both u_r and ψ, the ship with accurate speed log or sonar will have the gyrocampasses with high accuracy while the opposite may not be true. And also we know that the more information we have the better we can make the system identification, so when we have the data of two variables we will not throw off the data with higher accuracy. With this idea, the single measurement model will be:

$$z = \underline{H}\underline{x}$$

$$z = \psi$$

$$\underline{H} = [\ 0\ 0\ 0\ 1\ ] \qquad \text{.....(2.18)}$$

2.4.2 The Relation Between State Model and Measurement Model.

A system model consists of state model and measurement model. These two submodels are not independent, on the contrary, there is the mutual influence between them. From the automatic control theory it is well known that different state models may differ in the requirement of the kind of the variables to be measured, and also may differ in the requirements of the accuracy of the measurements, or in other words, differ in the allowance of the noise of the measurements. On the other hand, different measurement model may cause changes in the state model. Take our case as an example, if we are not going to use the dual-axis Doppler sonar system, but only measure the velocities of the ship relative to the water, then the equations involving u and v will not be included in the state model, and then ψ will immediately disappear, the model hence only have three state variables.

Therefore, strictly speaking, when we change the measurement model, we should examine the state model carefully to see if there is any necessity of modification. And at the same time we should reexamine the design of the sea trials for the measurement of the variables to see if some revision is needed. Nevertheless, for our situation, because our work is of exploring and we are not going to conduct a series of new sea trials but to make use of the data already obtained from the four measurement sea trials, so we are not going to change the state model as used by Hwang[8]. But we should keep in mind that this is not the best choice.

Chapter 3 IDENTIFICATION TECHNIQUES

3.1 Premises

It is obvious that the system corresponding to our ship and the environment in which it operates is a nonlinear system. It is well known that the Kalman filtering technique belongs to the category of linear system. Although the EKF technique developed directly from it can be used for the nonlinear systems, it is not applicable to all the nonlinear systems. From the point of view of system engineering, analyses on the system model of Esso Osaka have been made and the results confirm the possibility of successful application of EKF to it. In this thesis the analyses will not be repeated while the useful conclusions are listed as follows:

1) To compare with the 4 second measuring time interval, the time constant of Esso Osaka is much larger, therefore the system model describing the dynamics of Esso Osaka can be taken as time invariant.

2) The process noise $\underline{w}$ is modelled as zero mean, white and Gaussian distributed. The reason is that the process modelled here is basically of low order and involves slow speed dynamics.

3) The measurement noise $\underline{n}$ is also assumed to be zero mean, white and Gaussian distributed. Because, the noise sources are independent and during the sea trials the time constants of all the sensor dynamics are shorter than 1 second, while the time interval used in filtering is 4 seconds which is quite safe for

our assumption.

All these treatments were proven acceptable by the identification work done on Esso Osaka before.

3.2 Identifibility

The problem of identifibility for the nonlinear system is quite complicated, but at the same time it is very important. Everyone likes to know the possibility of success before he starts to work. Although our work is an exploratory work and we shall try each of our models anyway, we still like to know the hope of success for each case. And it is also hoped to get some experiences on predicting the identifibility of a ship system like ours.

Hwang in his work demonstrated how to analyze the identifibility of the parameters by engineering analysis. Based on the analysis, suggestions were made of dividing the hydrodynamic coefficients into different groups, designing different sea trials for different groups and using some special technique like parallel processing to improve the results of identification and so on. No doubt, all these analyses are valid for our work, because the system of the ship doesn't change, nor the objectives of identification.

3.2.1 Identifibility of a Time-invariant Linear System

In this thesis, we try to start from a different angle to consider this problem. We consider a linear system:

$$\dot{\underline{x}} = \underline{A}\underline{x} + \underline{w} \quad \text{.....(3.1)}$$

$$\underline{z} = \underline{C}\underline{x} + \underline{v} \quad \text{.....(3.2)}$$

where $\underline{w}$ and $\underline{v}$ are white-noise with correlation matrices:

$$E[\underline{w}\underline{w}^T] = \underline{Q}$$

$$E[\underline{v}\underline{v}^T] = \underline{R}$$

The Kalman filter is described by:

$$\dot{\hat{\underline{x}}} = \hat{\underline{x}} + \underline{K}(\underline{z} - \underline{H}\hat{\underline{x}}) \quad \text{.....(3.3)}$$

where $\underline{K} = \underline{P}\underline{C}^T\underline{R}^{-1}$

and $\dot{\underline{P}} = \underline{A}\underline{P} + \underline{P}\underline{A}^T + \underline{Q} - \underline{P}\underline{C}^T\underline{R}^{-1}\underline{C}\underline{P}$ .....(3.4)

The vector $\hat{\underline{x}}$ is the estimation of $\underline{x}$, and the matrix $\underline{P}$ is the covariance matrix of the errors $\underline{e}$ in the estimates. And

$$\underline{e} = \hat{\underline{x}} - \underline{x} \quad \text{.....(3.5)}$$

Then we approach our problem by considering two sub problems. The first one is whether our system is identifiable by applying the Kalman filtering, in other words, if the solution of the $\underline{P}$ matrix of equation (3.6) approach a stable steady state at which

$$\dot{\underline{P}} = 0 \quad \text{.....(3.6)}$$

The second problem is that because our system can not be exactly described by our model, $\underline{P}$ matrix in the filter calculation is not the actual covariance matrix, but a calculated one.

So we like to know whether when $\underline{P}$ approaches a stable steady state the actual covariance matrix $\tilde{\underline{P}}$ also approaches a satisfactory stable steady state. If not, we shall say that there exists divergence of the Kalman filter. Then the result of the identification in this case is still unacceptable. There are two kinds of divergence of the Kalman filter, according to Fitzgerald. In his paper[1971], both of them were discussed theoretically in details and illustrated by examples. The methods of predicting the possibility of divergence are also provided.

After making the structure of the problem of identifibility clear, the following procedure is designed for our work:

i) Taking the systems of Esso Osaka as a linear time invariant system to make a primary prediction of whether they are identifiable, that is, to try the first problem by using linear system theories. Details are in the next section.

ii) Although we can follow the methods in Fitzgerald's paper to check the divergence of the filter, the work involving too many calculations of matrices makes us prefer the other choice. That is to check the accuracy of the identification by directly simulating the maneuver of Esso Osaka with the identified hydrodynamic coefficients.

3.2.2 Primary Analysis on the Identifibility of Our Systems

For linear time invariant system with the system model:

$$\dot{\underline{x}} = \underline{A}\underline{x} + \underline{B}\underline{\xi} + \underline{w} \quad \text{.....(3.7)}$$

$$\underline{z} = \underline{C}\underline{x} + \underline{v} \quad \text{.....(3.8)}$$

the sufficient condition for it to be identifiable is that the system is stable and observable. While for a stable linear time-invariant system the observability can be surveyed by the following rules:

$$\underline{\Delta} \triangleq [\underline{C}^T | \underline{A}^T\underline{C}^T | (\underline{A}^T)^2\underline{C}^T | \cdots\cdots | (\underline{A}^T)^{n-1}\underline{C}^T] \quad \text{.....(3.9)}$$

Assume $\underline{A}$ is n x n matrix,

$\underline{C}$ is m x n matrix, if $\underline{\Delta}$ of rank n, than the system is observable.

Our systems are stable systems since the stability of the systems is only related to the characteristics of matrix $\underline{A}$, and it does not change for all the cases. And from the analyses in Chapter2, our systems can be approximated as linear, time invariant. Follow the formula:

$$\dot{\underline{x}}(t) = \underline{f}[\underline{x}(t), \underline{\xi}(t), \underline{w}(t), \underline{p}(t), t]$$

$$\longrightarrow \quad \dot{\underline{x}} = \underline{A}\underline{x} + \underline{B}\underline{\xi} + \underline{w}$$

$$\underline{A} = \left[\frac{\partial f}{\partial u} \quad \frac{\partial f}{\partial v} \quad \frac{\partial f}{\partial r} \quad \frac{\partial f}{\partial \psi}\right] \quad \text{.....(3.10)}$$

we can start to make tedious but straightfoward algebraic calculation. Since we consider the system as time invariant, to make the problem simple, we choose t = 0 in calculating the partial derivatives. The final result of matrix $\underline{A}$ is:

$$A = \begin{bmatrix} 9.100048\text{x}10^{-4} & 9.21502459\text{x}10^{-1} & 2.61012284\text{x}10^{-1} & 0 \\ 0 & 3.393093071 & 2.78326392\text{x}10 & 0 \\ 0 & 7.56308300\text{x}10^{-3} & -9.78519310\text{x}10^{-2} & 0 \\ 0 & 0 & 1 & 0 \end{bmatrix}$$

$$\text{.....(3.11)}$$

This is a 4 x 4 matrix. The ranks of the checking matrices corresponding to the three system models are:

n = 4 for the model of measuring u, v and ψ.

n = 4 for the model of measuring u and ψ.

n = 3 for the model of only measuring only ψ.

From this result we can draw the conclusion that our models with three and two measurements are identifiable, while the identifibility of the system with only measuring ψ is in doubt. Because the principle of observability only checks the condition of sufficiency, the result of n = 3 does not mean that the system is surely unidentifiable, though from engineering experiences it is most likely unidentifiable. Anyway, it worth a try even for the single measurement model.

But we must bear in mind that for an utterly new system, if we want to make the analyses on observability as mentioned before, we have to consider the effect of the a priori information on the results. Because some of the parameters of the systems are to be estimated, so before the identification, their values are far from accurate. As to our case, the prediction of observability is based on the successful work of identifying the parameters by the model with full(four) state variables being measured. Therefore it is convinient and no this kind of problem.

3.2.3 An Alternative Analysis on the Identifibility of the Three Measurement Model

The state model for Esso Osaka, as mentioned in Chapter2, is of pseudo-4th order, because the yaw velocity r and the yaw angle ψ are not independent, r is the time derivative of ψ. To achieve good results of identification, the accuracies of the measurements of r and ψ should match each other, otherwise it will increase the process noise of the system. Because the unmatching measurements of r and ψ will infuluence the equation

$$\dot{\psi} = r$$

directly. Generally speaking, it is not difficult to get very accurate measurements for modern ships as the data for Esso Osaka already showed. The measurement data of r for Esso Osaka acquired by the special heading rate gyro are also very accurate, and thus with these data, the hydrodynamic coefficients of the mathematical model of Esso Osaka were very successfully identified. Since in the state equations, yaw velocity r is more directly involved, it seems more important to compare it with yaw angle ψ. However, we know, with the accurate measurement of ψ, we can derive the yaw velocity r from it by mathematics with enough accuracy. So from this sense, the three measurements of u, v and ψ is not inferior to the four measurements of u, v, r and ψ for the latter can be derived from the former.

Thus based on the success of using four measurements, before we start to try the system model with three measurements, we can

predict the identifibility by another way which is very simple. For our case, the data of u, v and ψ which we shall use in the three measurement model are the same of those obtained from the sea trials designed for the four measurements. Then we use the data of ψ to derive the data of r*, and compare r with r*. If they are properly consistent to each other, there should be no doubt about the identifibility for the new system.

Fig.3.1 shows the two curves of r and r*. just as we expected, they are very consistent to each other. Therefore, the successful result of the identification by using the three measurement model is not unexpected.

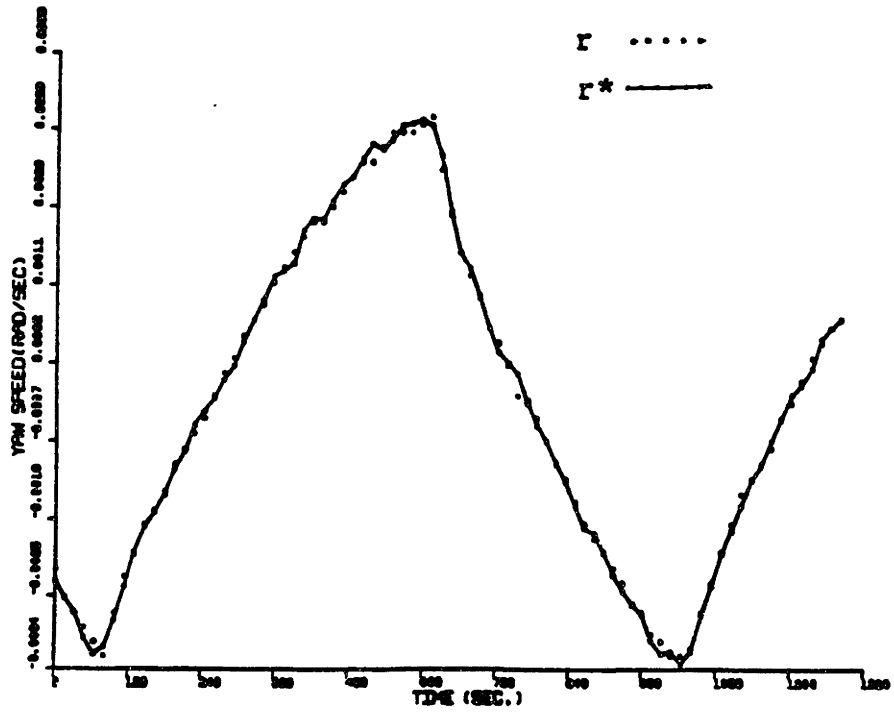

fig.3.1 Curves of r and r*

3.3 Identification Technique Applied

In our work, the method used for identification is called State-Augmented Extended Kalman Filtering. The change in the measurement model changes the structure of the system model; hence the completed program has to be changed. However, the principle and the procedure of the estimation of the hydrodynamic coefficients have not been changed. The theory of EKF will not be discussed in this thesis. Reference could be made to Gelb's work[3]. Here we only want to discuss some technical problems related to the application of EKF very briefly.

1) From Hwang and Kwok's work[8,9], the parallel processing method and the method of exaggerated over- and under- estimated initial guess have been proved the very useful remedy for the simultaneous drift phenomenon. In our work we use the same technique. The brief idea is that for each measured variable, we shift the phase of the data file to get a new data file, then we use these two files as the input at the same time. Since the simultaneous drift is caused by the cancellation effect between the contribution of hydrodynamic coefficients such as Yv and Yr; and Nv and Nr. While for two different maneuvers the contribution of the same coefficient is of different pattern, so if the measurement data of two different maneuvers are processed at the same time, the phenomenon of simultaneous drift may be improved.

2) To help further, we use the the technique of exaggerated over- and under- estimated initial guesses as well, that is, over

estimate one of Yv and Yr to a large extent and under estimate the other as initial guesses, and the same thing is applied to Nv and Nr. In this way we hope we can prevent the improper simultaneous drifting phenomenon to appear early and give enough time for the estimation curves of the hydrodynomic coefficients to keep a steady level.

These two techniques are illustrated in great detail in Hwang's work[8].

3) when we choose the identified values from the curves of the coefficients, the analyses based on engineering experiences are always made. We shall see which part of the curve more likely approaches the true value of the coefficients from the point of view of the maneuveribility.

4) For the final check of the validity of the identified values, we simulate the maneuver by using the state model of Esso Osaka with the identified hydrodynamic coefficients as the parameters. Then we compare the simulation curves with the measured maneuvering of the ship to determine if the results of the identification are satisfactory or not.

Chapter 4 RESULTS OF THE IDENTIFICATION BY DIFFERENT SYSTEM MODELS

The measurement data of the 10°-10° zigzag maneuver of Esso Osaka during the sea trials are used for the identification of the linear hydrodynamic coefficients. The measurement data of 35° circle maneuver are used for the identification of the nonlinear hydrodynamic coefficients. The linear hydrodynamic coefficients are first to be identified and the accuracy of the identification is checked by the simulation of the 10°-10° zigzag maneuver. The qualified values of linear hydrodynamic coefficients are put into the state model and fixed, then the modified models are used to identify the nonlinear hydrodynamic coefficients. The identified results are also checked by the simulation of 35° turning maneuvering.

4.1 Results of the Three and Two Measurement Models

The results of the identification by the three measurement and two measurement model are very successful. Not only are the procedure of the identification for these two models very smooth, but the values of the estimation of the hydrodynamic coefficients are also satisfactory. The simulation of the dynamics of Esso Osaka in both 10°-10° zigzag maneuvering and 35° turning maneuvering by using the values identified from each model was made. The results of the simulation are satisfactory, because they are highly consistent to the measurements.

The comparison between the simulations by using the values of hydrodynamic coefficients obtained from ship model test, four

measurement model and three measurement model. The result of comparison is not surprising:

(1) It is confirmed again that the method of making identification with EKF is greatly superior to the method of ship model test. However, model test results can be used to predict maneuverability before the ship is built.

(2) In system identification by applying EKF, the three measurement model is not inferior to the four measurement model at all. The reason is that as we mentioned in Chapter2 and chapter 3, these two models are of the same order and the measurement of the yaw angle is highly accurate. When the measurement of yaw velocity r is accurate enough, there is no essential difference between them. And we can further imagine that in case the measurement of r is not accurate enough, the inconsistency between r and $\dot{\psi}$ will increase the process noise of the system model and thus may make the identificaition result by the four measurement model inferior to that of the three measurement model.

The simulation of the dynamics of Esso Osaks by using values of the hydrodynamic coefficients from the two measurement model is not as good as that from the three measurement model. But compared with the simulation of using the values of hydrodynamic coefficients from model test, it is still quite satisfactory. Considering the significance of avoiding the measurement of sway velocity v, this result is very encouraging.

4.2 Result of the One Measurement Model

Although the one measurement model gave the result of identification of the linear hydrodynamic coefficients, we had to stop at this stage. Because the values from the residual test during the identification are not valid, and the 10°-10° zigzag maneuvering simulation by using these identified values of the hydrodynamic coefficients is unsatisfactory. It is not difficult to understand it physically.

4.3 One Attempt of Using r Derived from ψ

From the one measurement model, an attempt by using the r derived from ψ was tried. The motivation is that since the state model of the system of the ship involves directly r not ψ, and we are very confident about getting very accurate value of r from ψ, because of the highly accurate values of ψ. We hoped that if the appearance of ψ in the state model caused large process noise, by pretreating ψ into r, it might be mended. However the result turned out negative.

All these results are presented by tables and figures in this chapter.

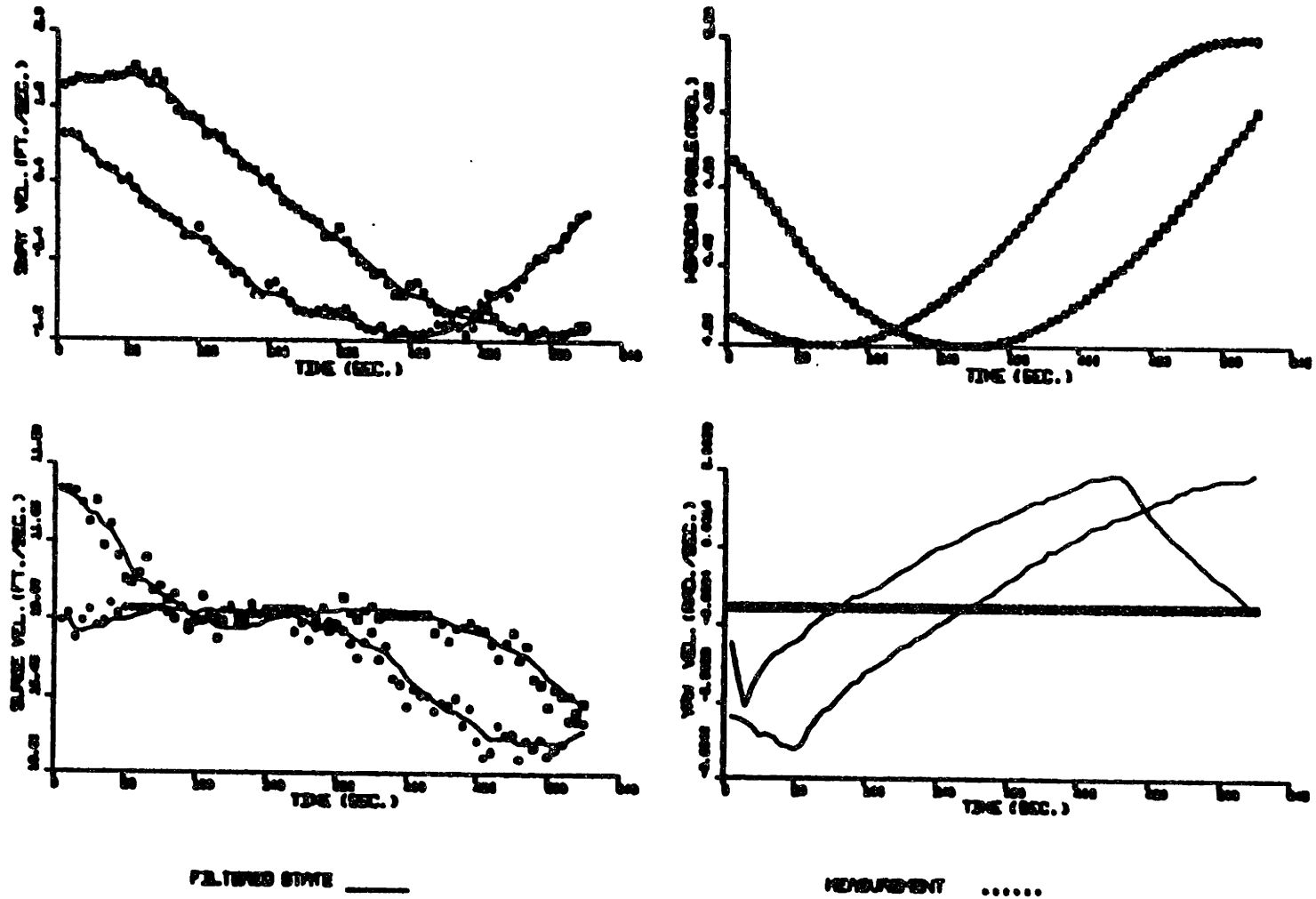

fig.4.1.1(a) Results of Identification of Linear Coefficients with Three Measurements

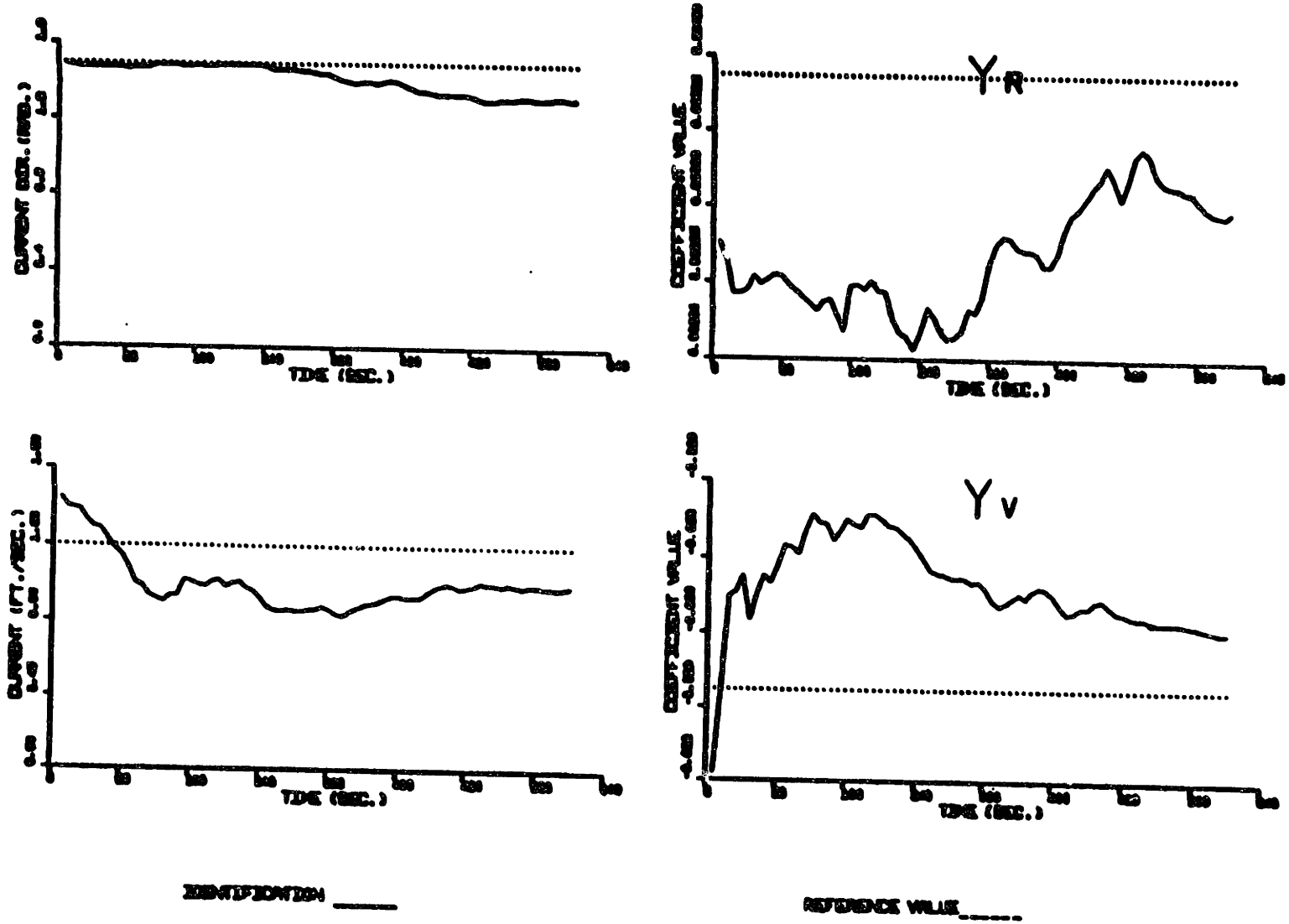

fig.4.1.1(b) Results of Identification of Linear Coefficients with Three Measurements

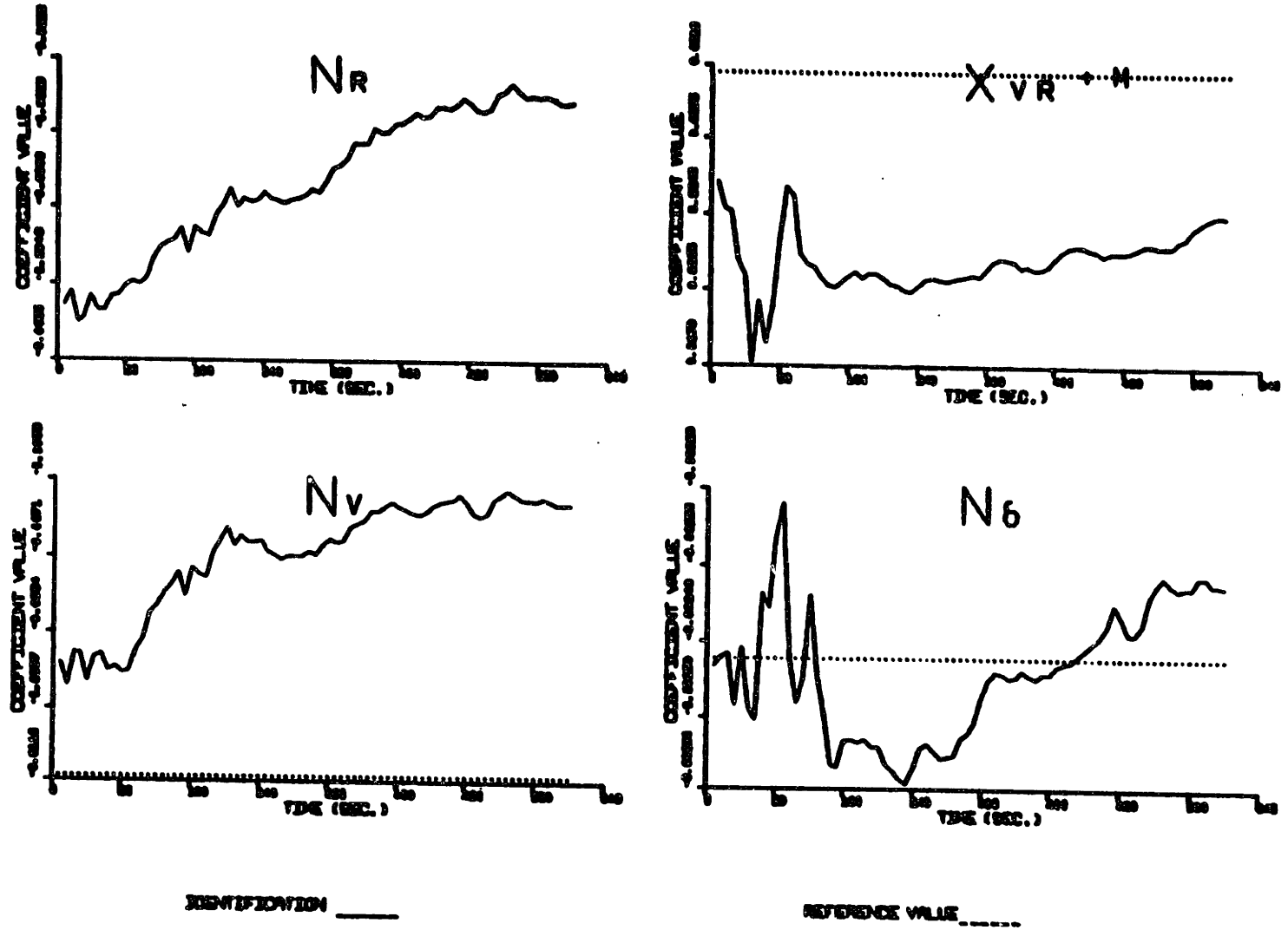

fig.4.1.1(c) Results of Identification of Linear Coefficients with Three Measurements

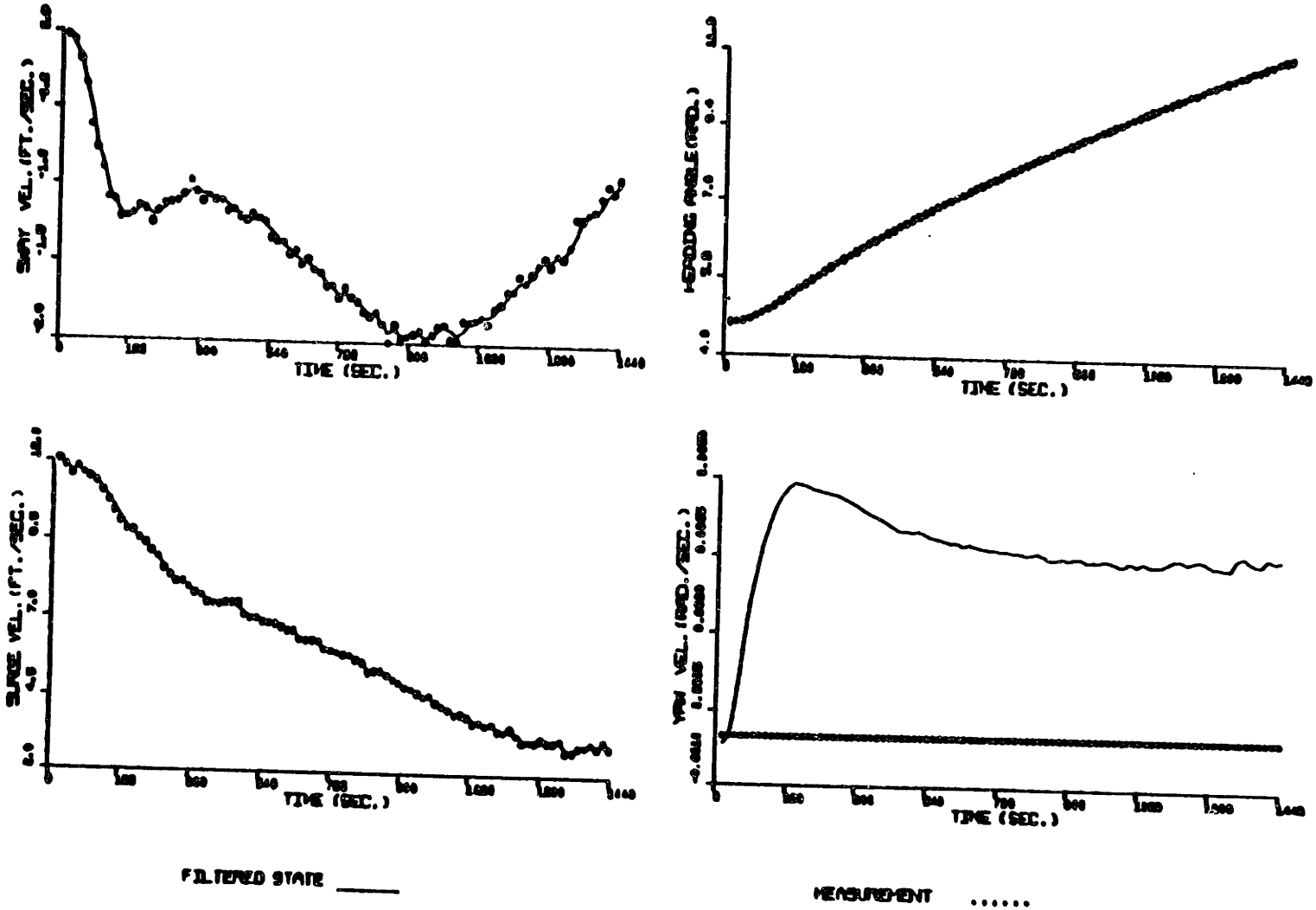

fig.4.1.2(a) Results of Identification of Nonlinear Coefficients with Three Measurements

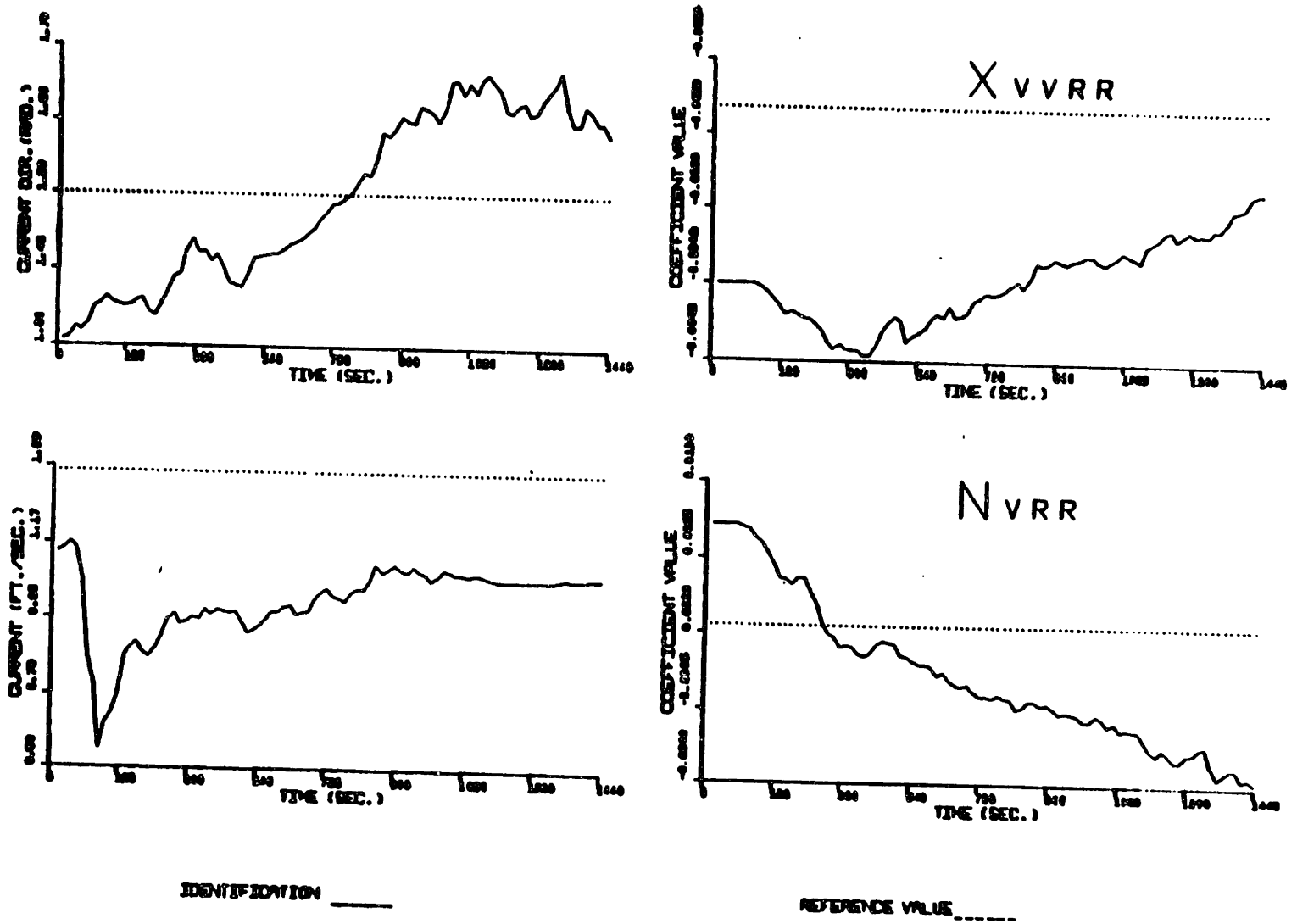

fig.4.1.2(b) Results of Identification of Nonlinear Coefficients with Three Measurements

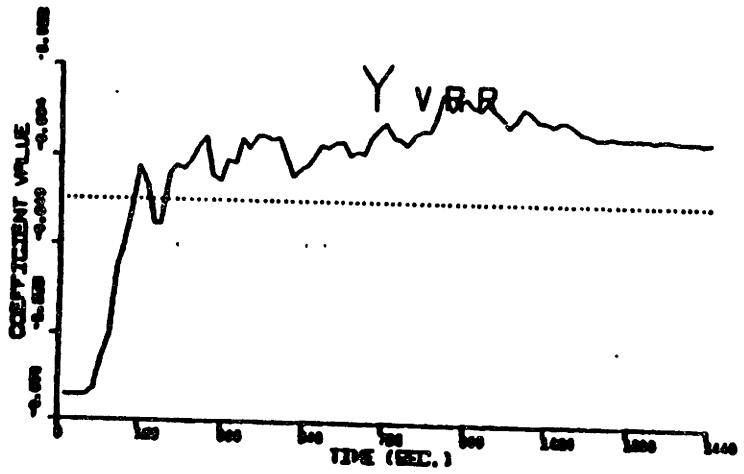

fig.4.1.2(c) Results of Identification of Nonlinear Coefficients with Three Measurements

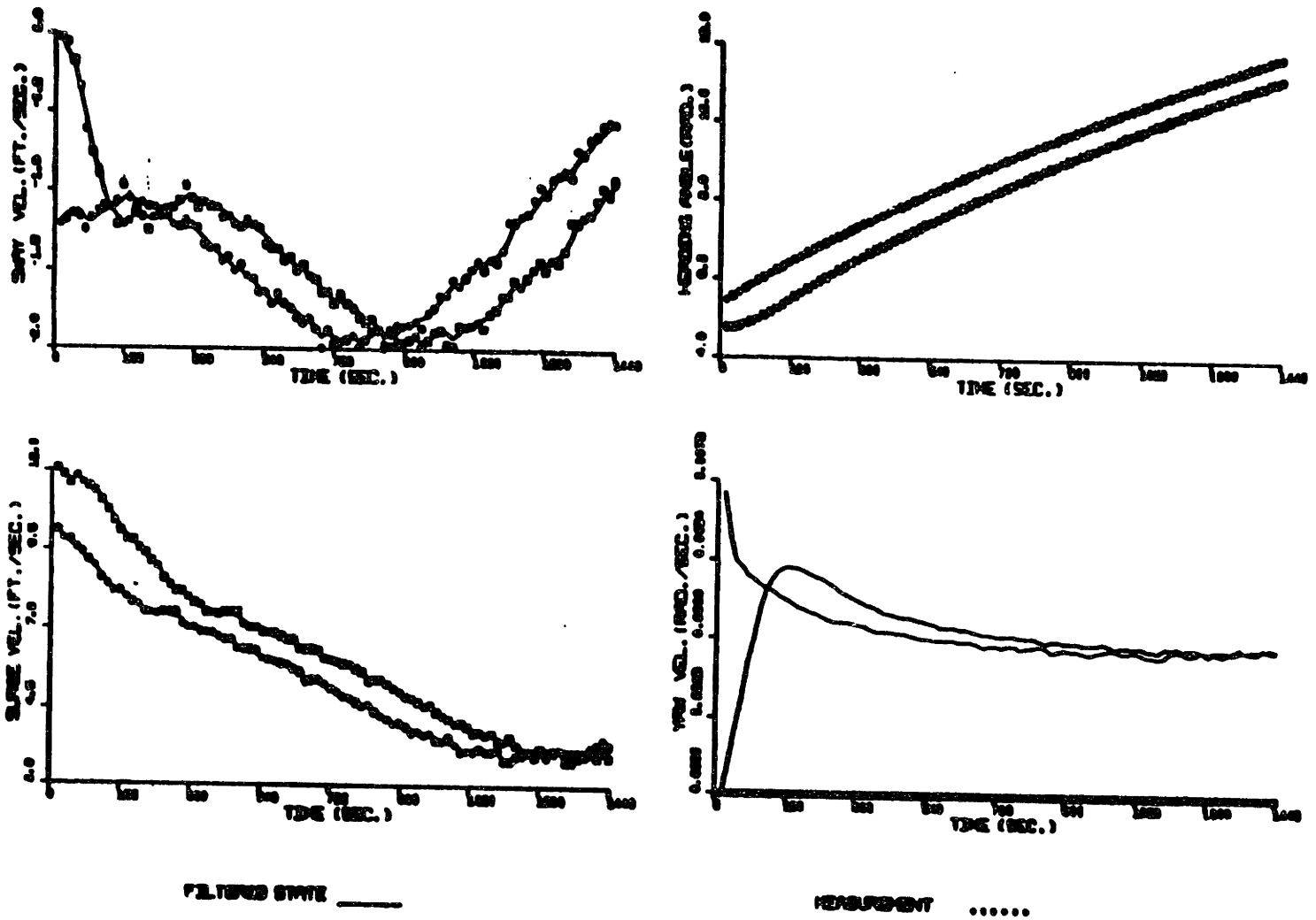

fig.4.1.2(d) Results of Identification of Nonlinear Coefficients with Three Measurements

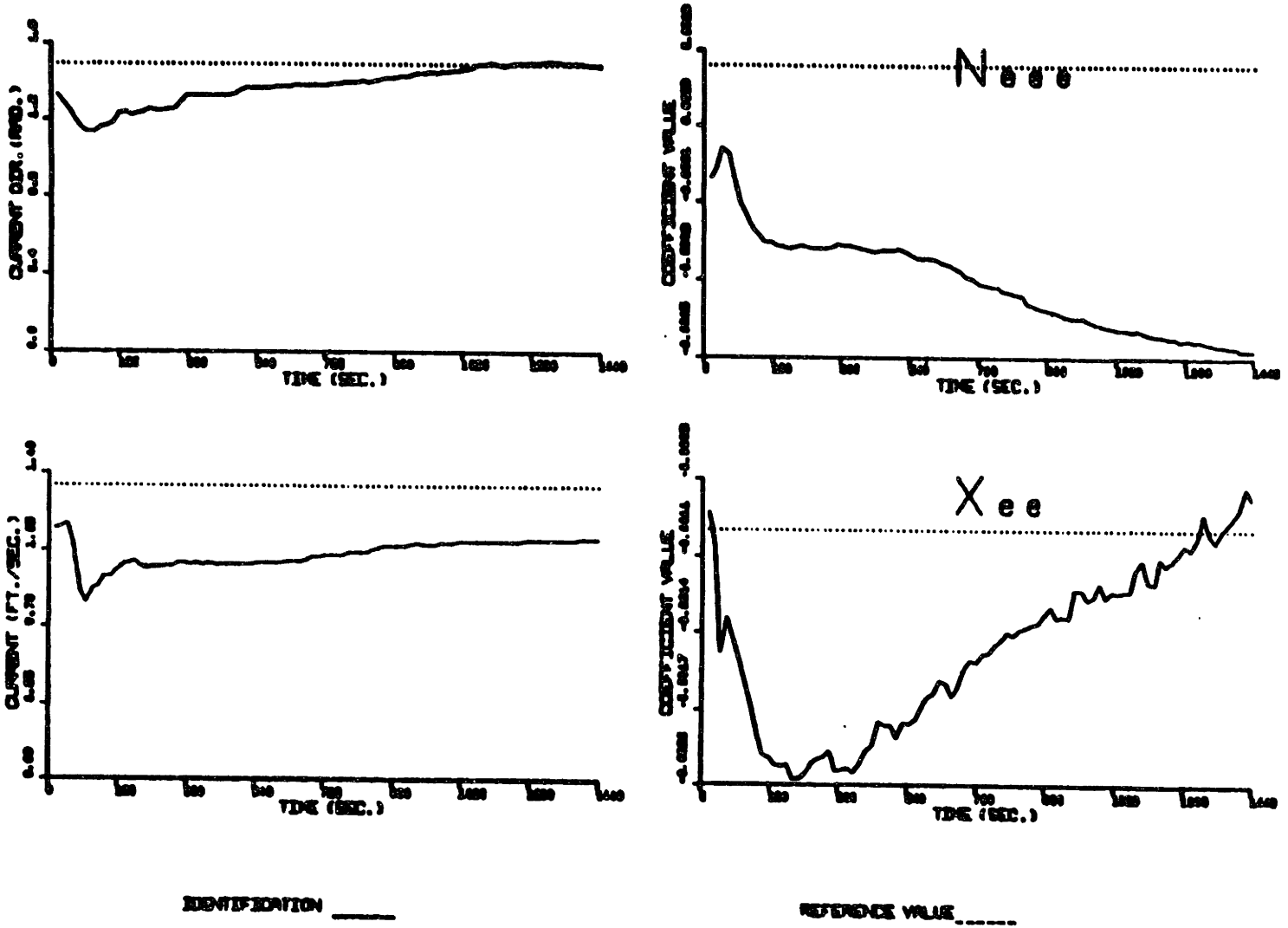

fig.4.1.2(e) Results of Identification of Nonlinear Coefficients with Three Measurements

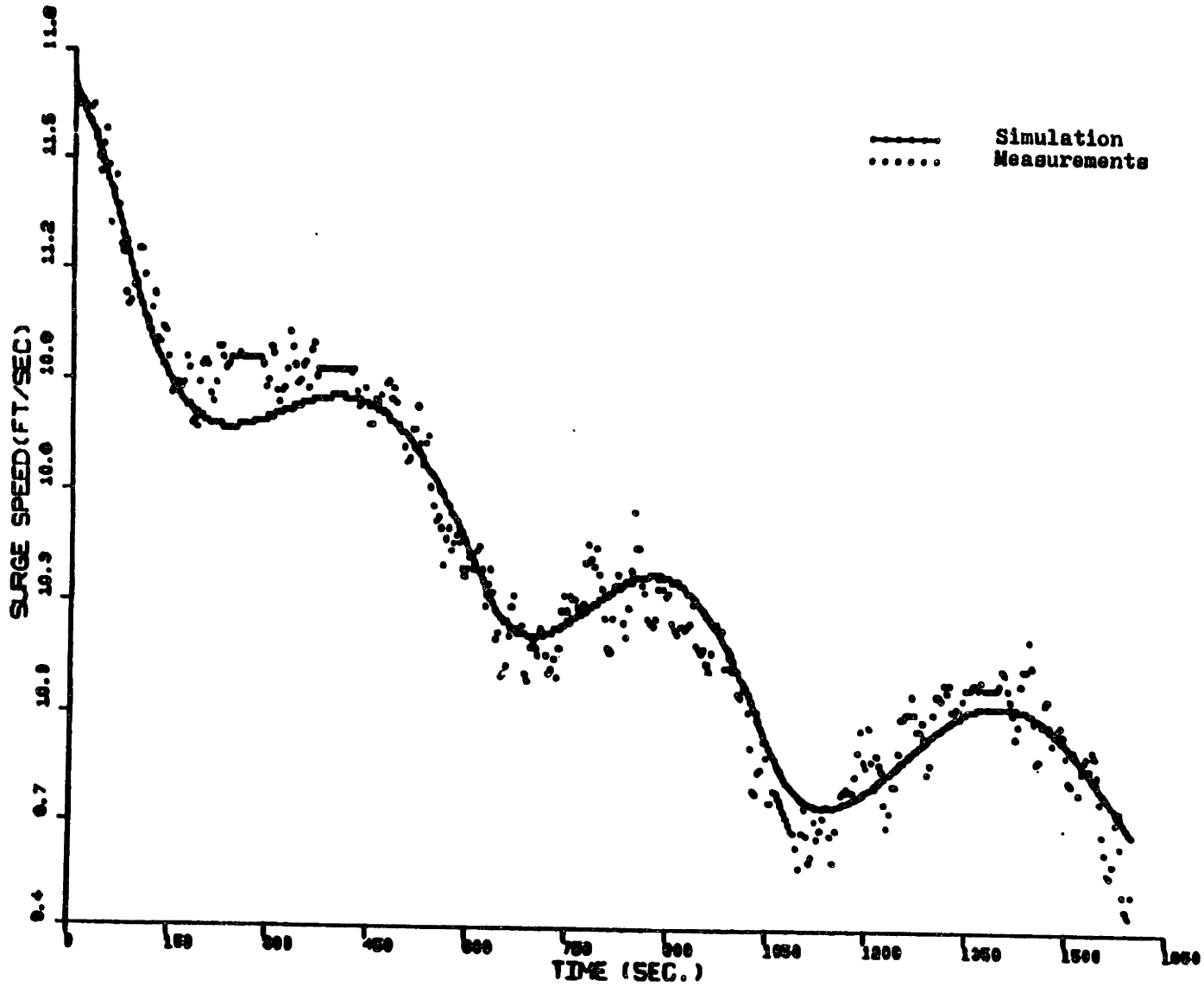

fig.4.1.3(a) Comparison between the Measurements and the Simulation of 10^{o}-10^{o} Maneuver by Using the Coefficients Identified with Three Measurements----Surge Speed u.

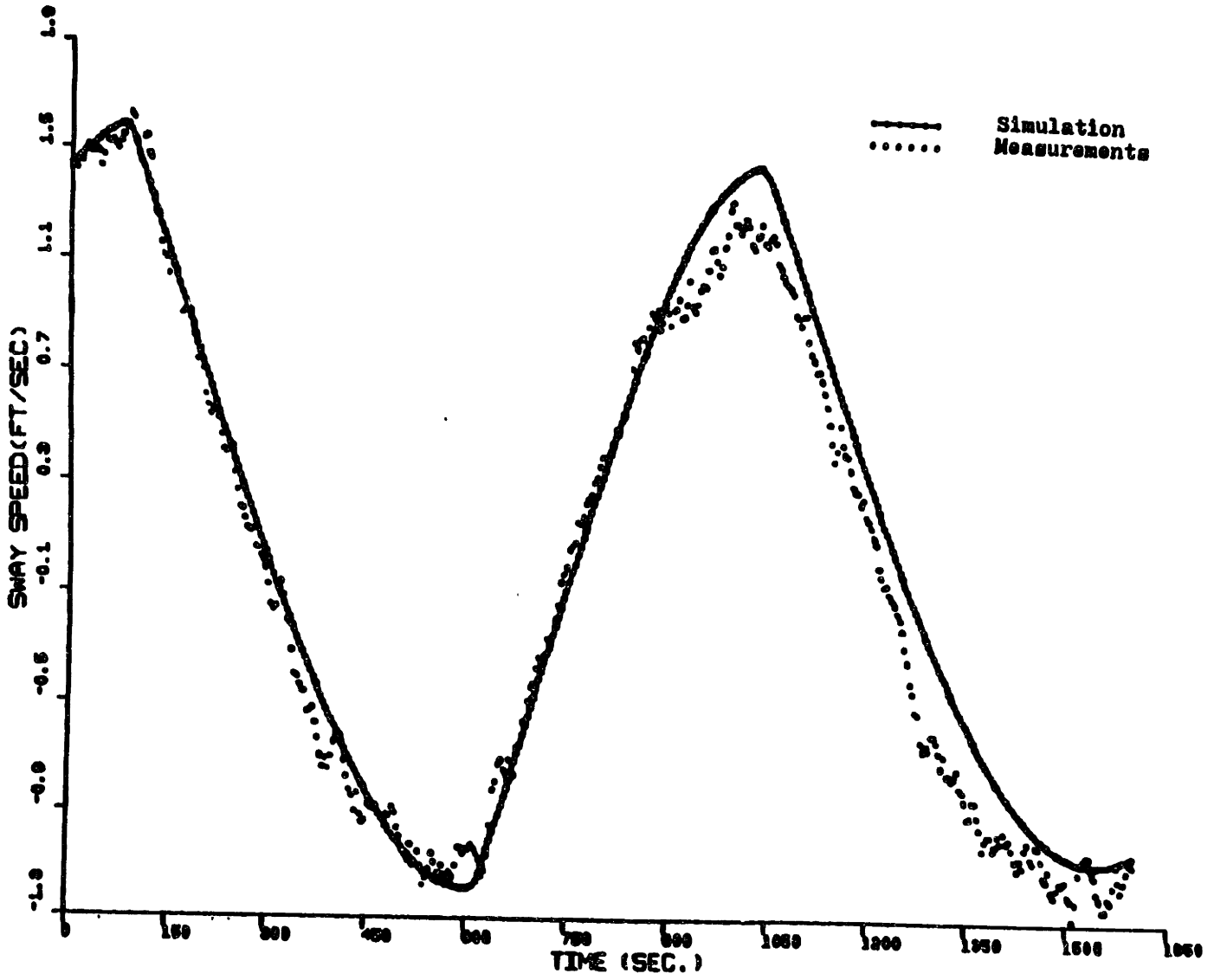

fig.4.1.3(b) Comparison between the Measurements and the Simulation of 10^{o}-10^{o} Maneuver by Using the Coefficients Identified with Three Measurements----Sway Speed v.

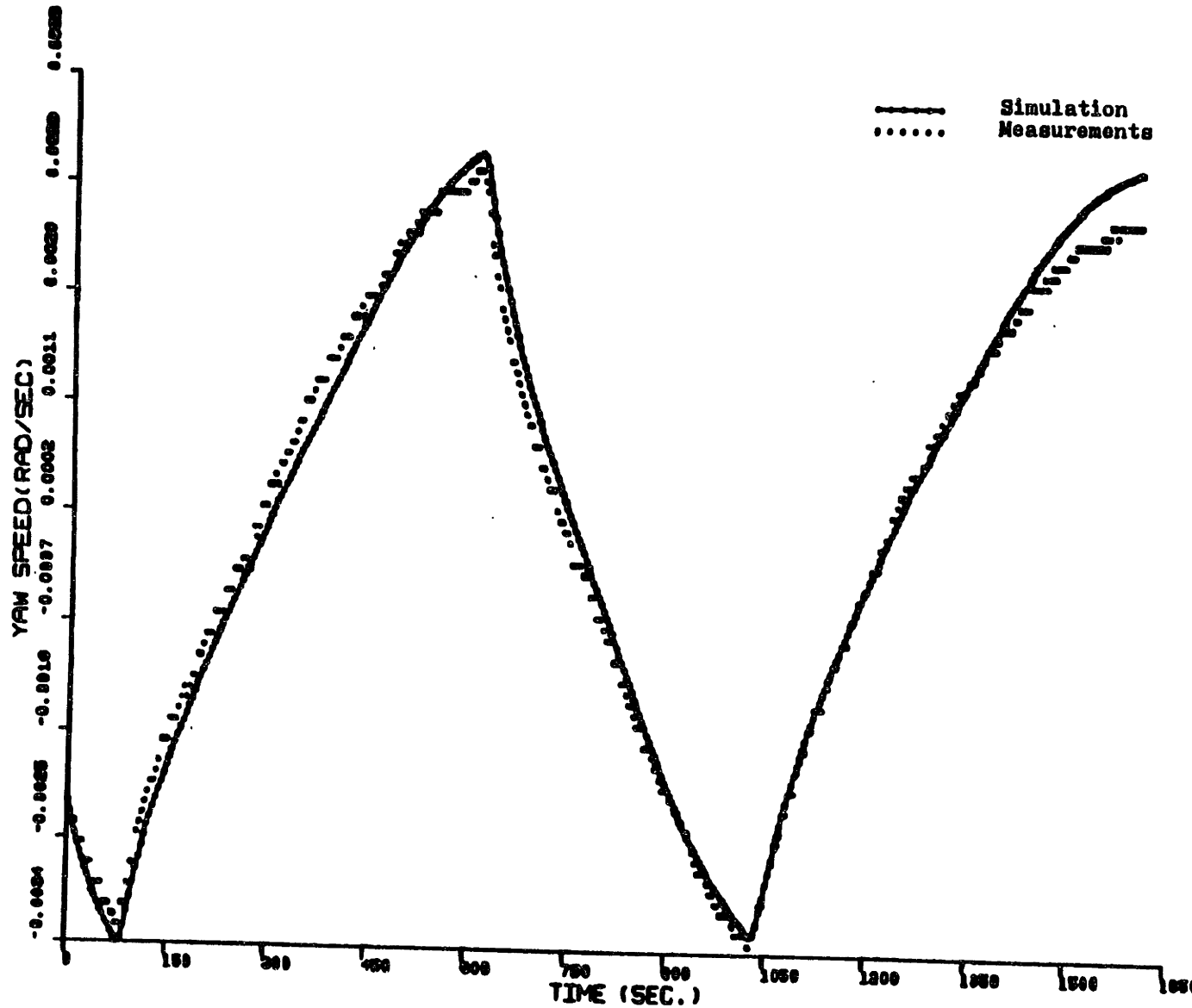

fig.4.1.3(c) Comparison between the Measurements and the Simulation of 10^{o}-10^{o} Maneuver by Using the Coefficients Identified with Three Measurements----Yaw Speed r.

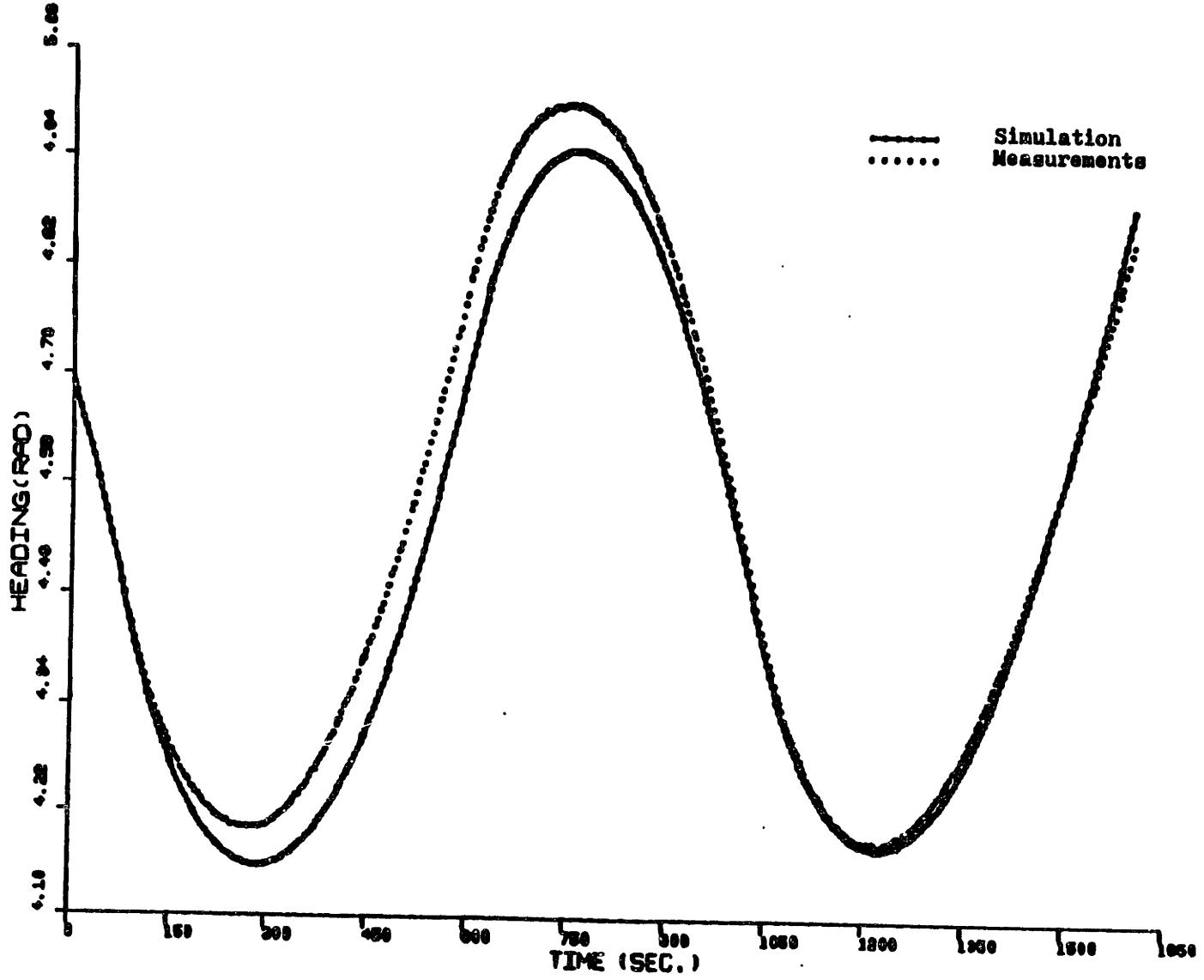

fig.4.1.3(d) Comparison between the Measurements and the Simulation of 10^{o}-10^{o} Maneuver by Using the Coefficients Identified with Three Measurements----Yaw Angle ψ.

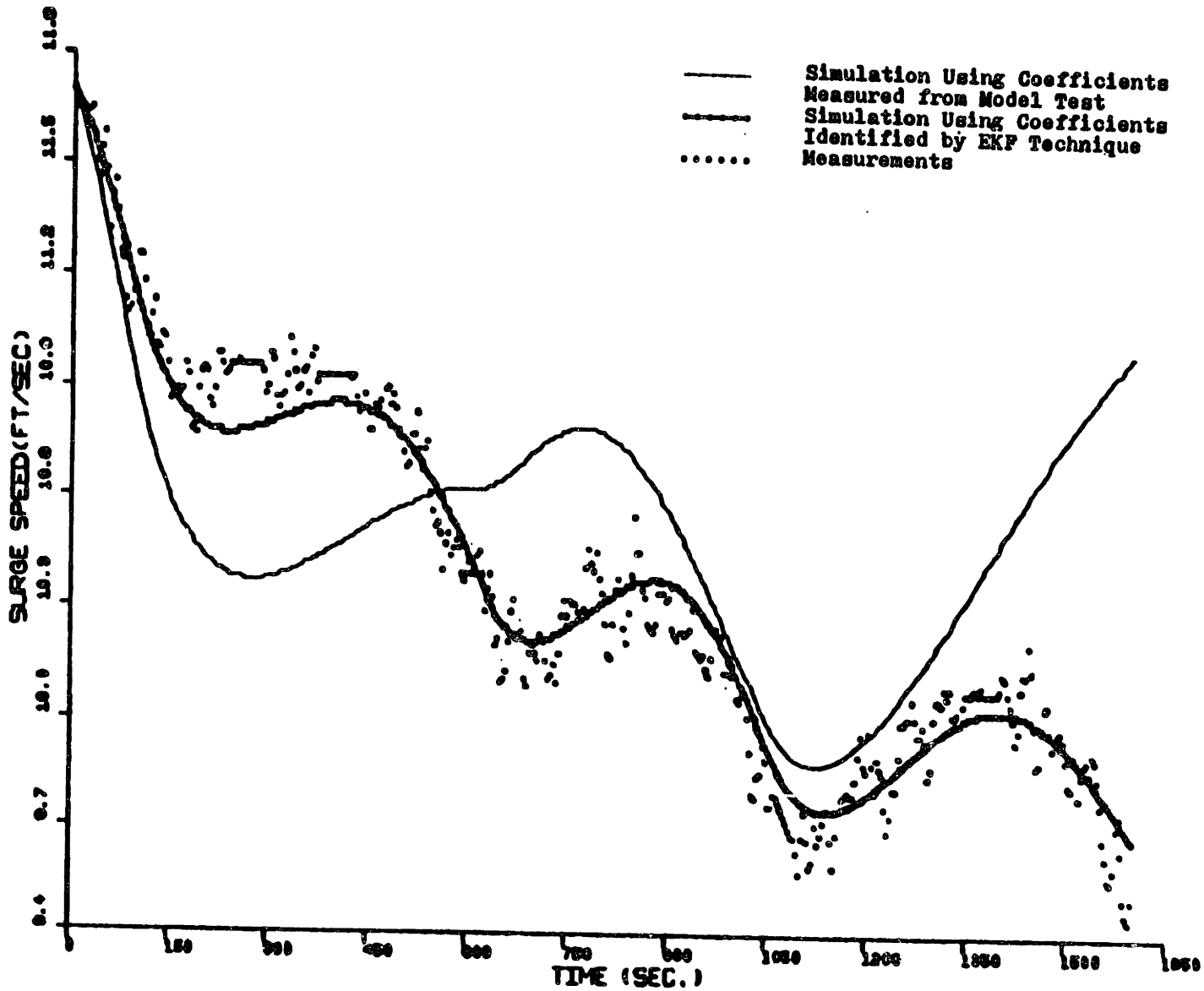

fig.4.1.4(a) Comparison between the Simulations of 10^{o}-10^{o} Maneuver by Using the Coefficients "Measured" from Model Test and Identified with Three Measurements----Surge Speed u.

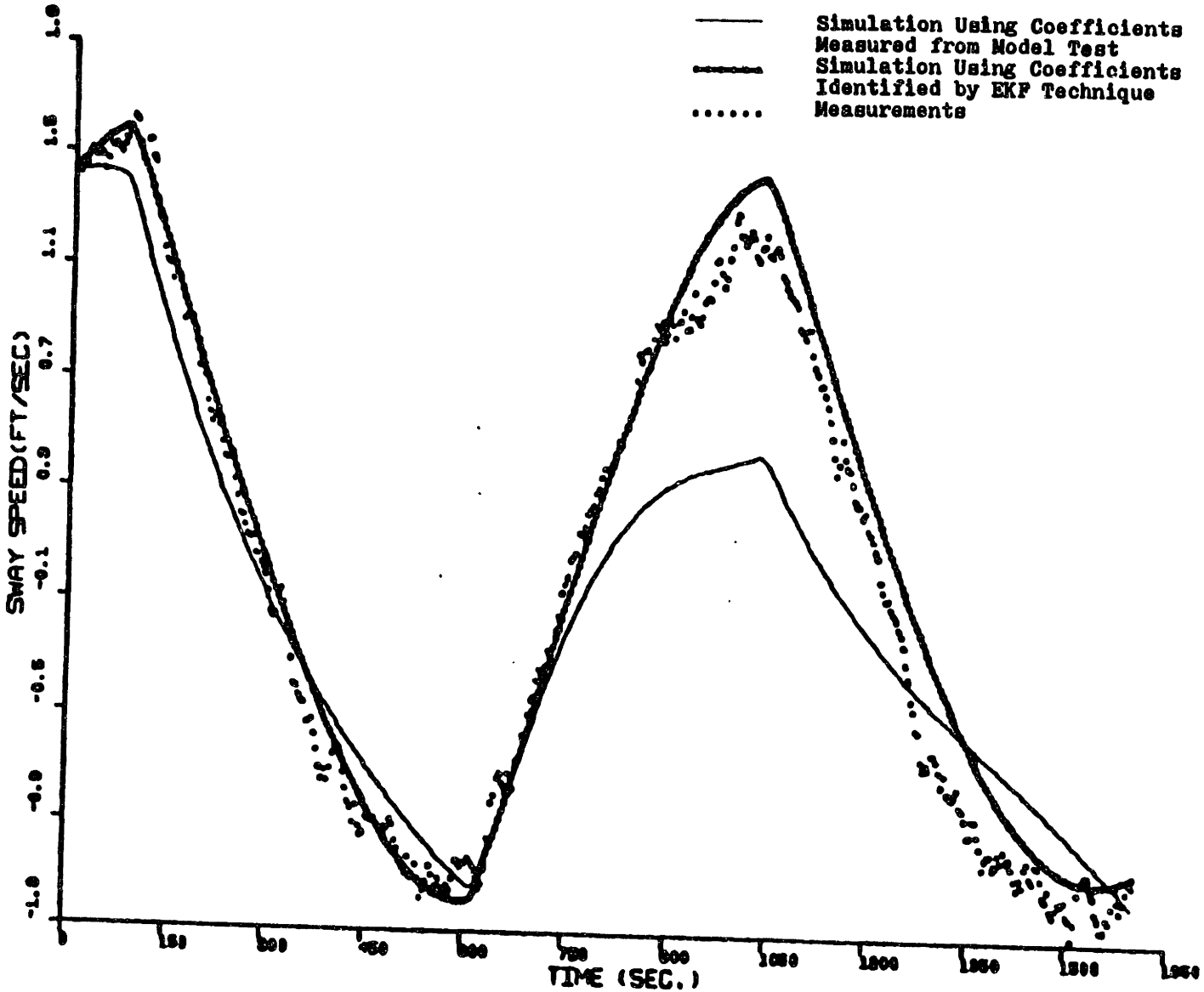

fig.4.1.4(b) Comparison between the Simulation of 10°-10° Maneuver by Using the Coefficients "Measured" from Model Test and Identified with Three Measurements----Sway Speed v.

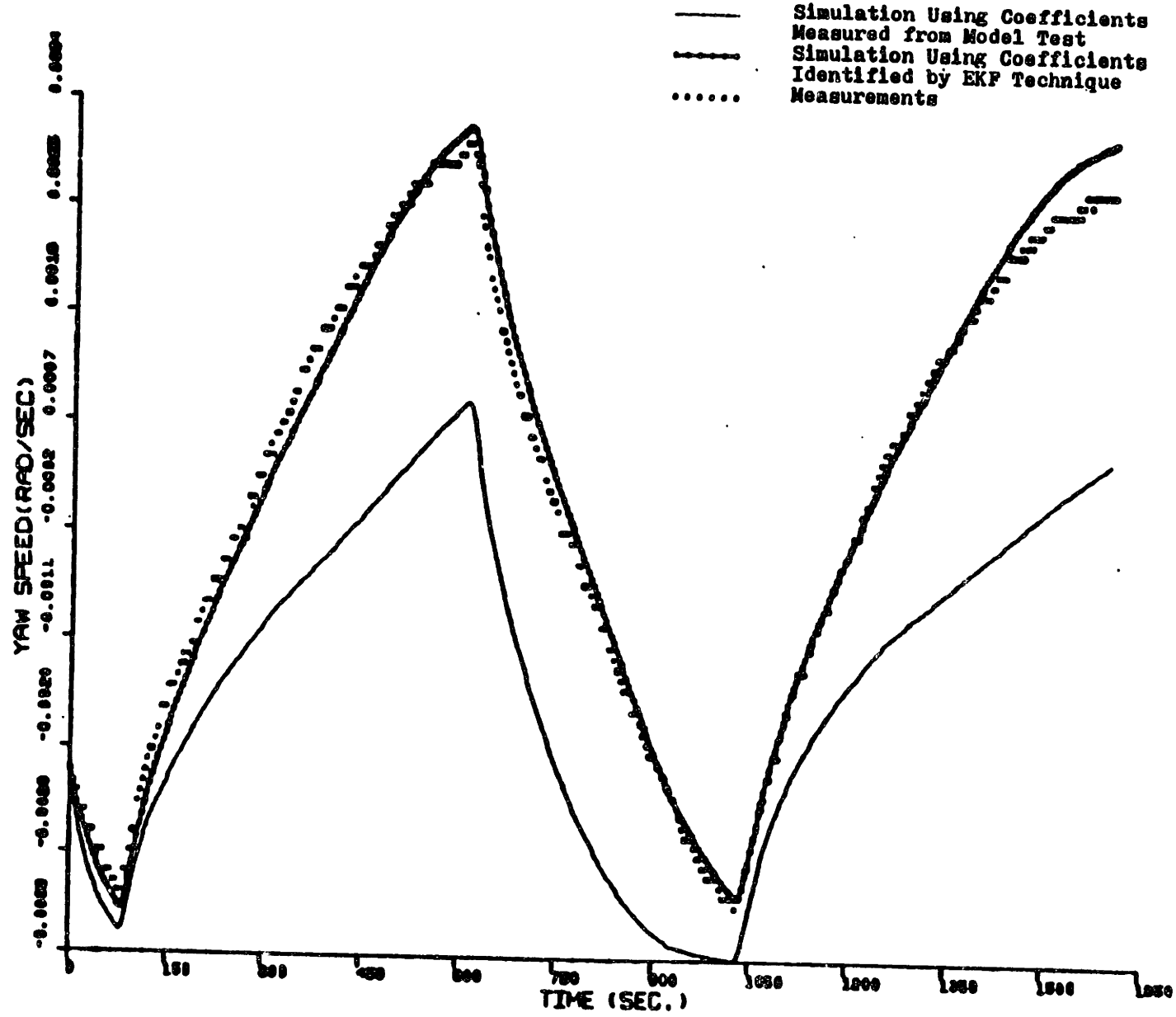

fig.4.1.4(c) Comparison between the Simulations of 10^{o}-10^{o} Maneuver by Using the Coefficients "Measured" from Model Test and Identified with Three Measurements----Yaw Speed r.

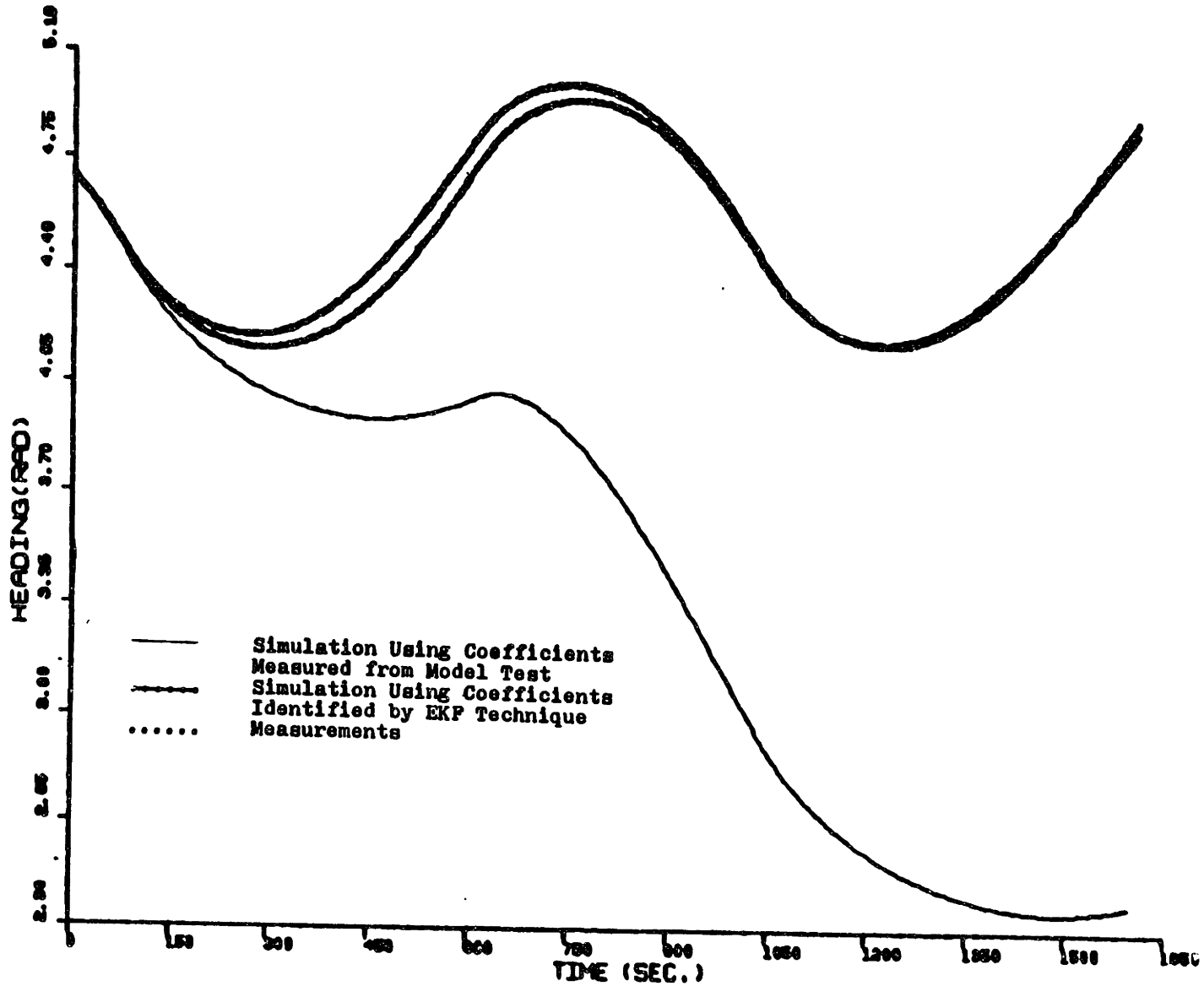

fig.4.1.4(d) Comparison between the Simulations of 10^{o}-10^{o} Maneuver by Using the Coefficients "Measured" from Model Test and Identified with Three Measurements----Yaw Angle ψ.

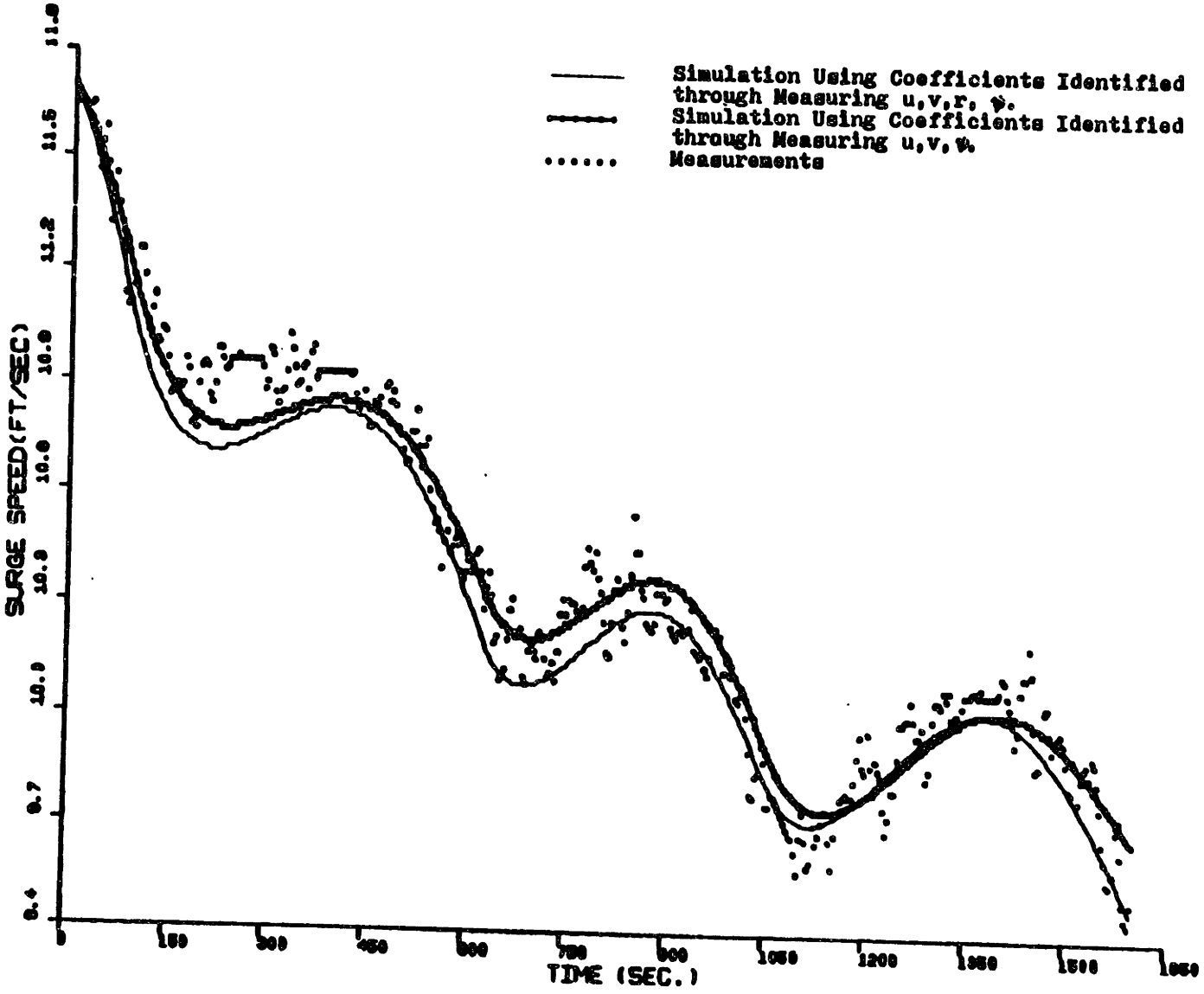

fig.4.1.5(a) Comparison between the Simulation of 10^{o}-10^{o} Maneuver by Using the Coefficients Identified with Four and Three Measurements Respectively ----Surge Speed u.

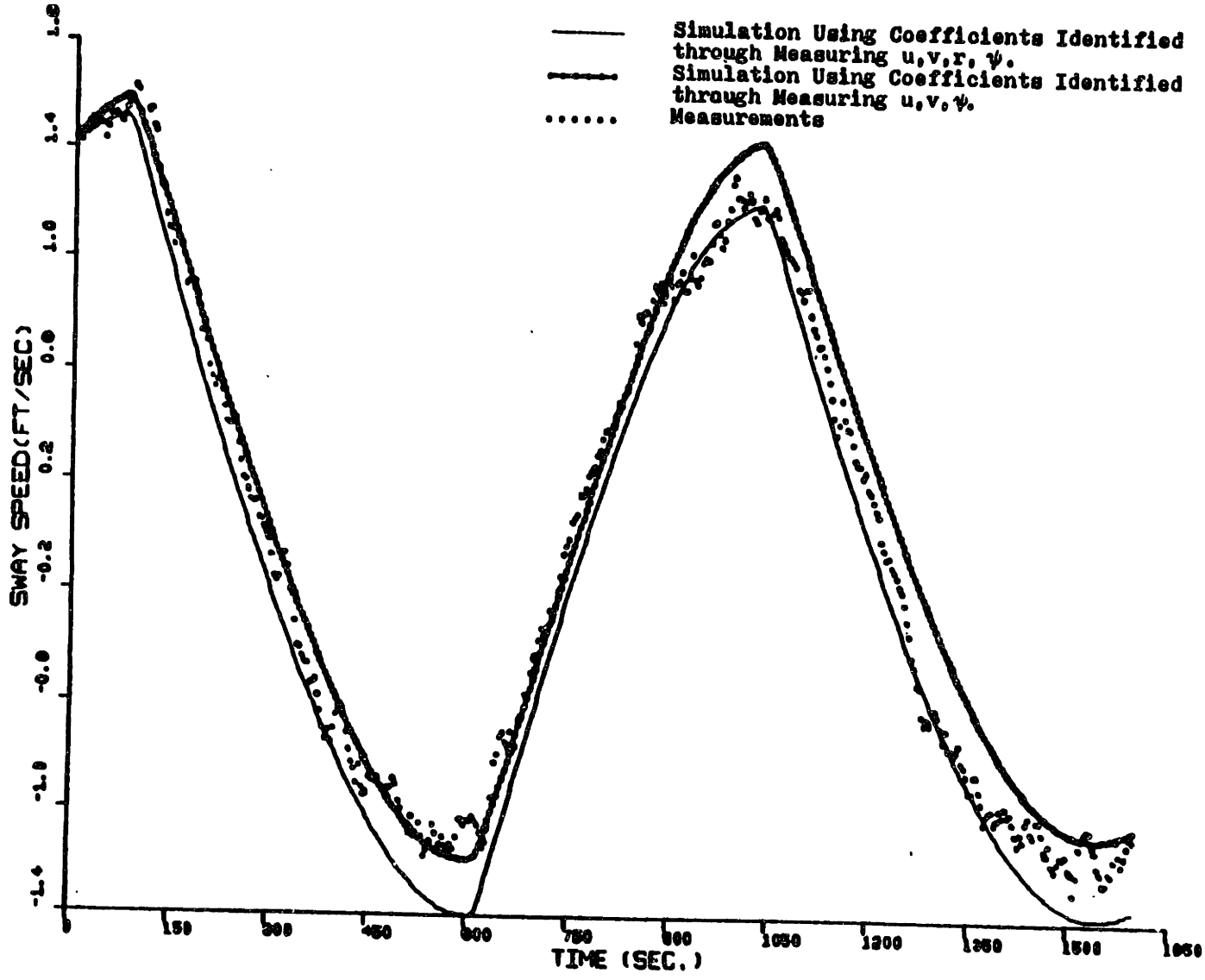

fig.4.1.5(b) Comparison between the Simulations of 10^{o}-10^{o} Maneuver by Using the Coefficients Identified with Four and Three Measurements Respectively ----Sway Speed v.

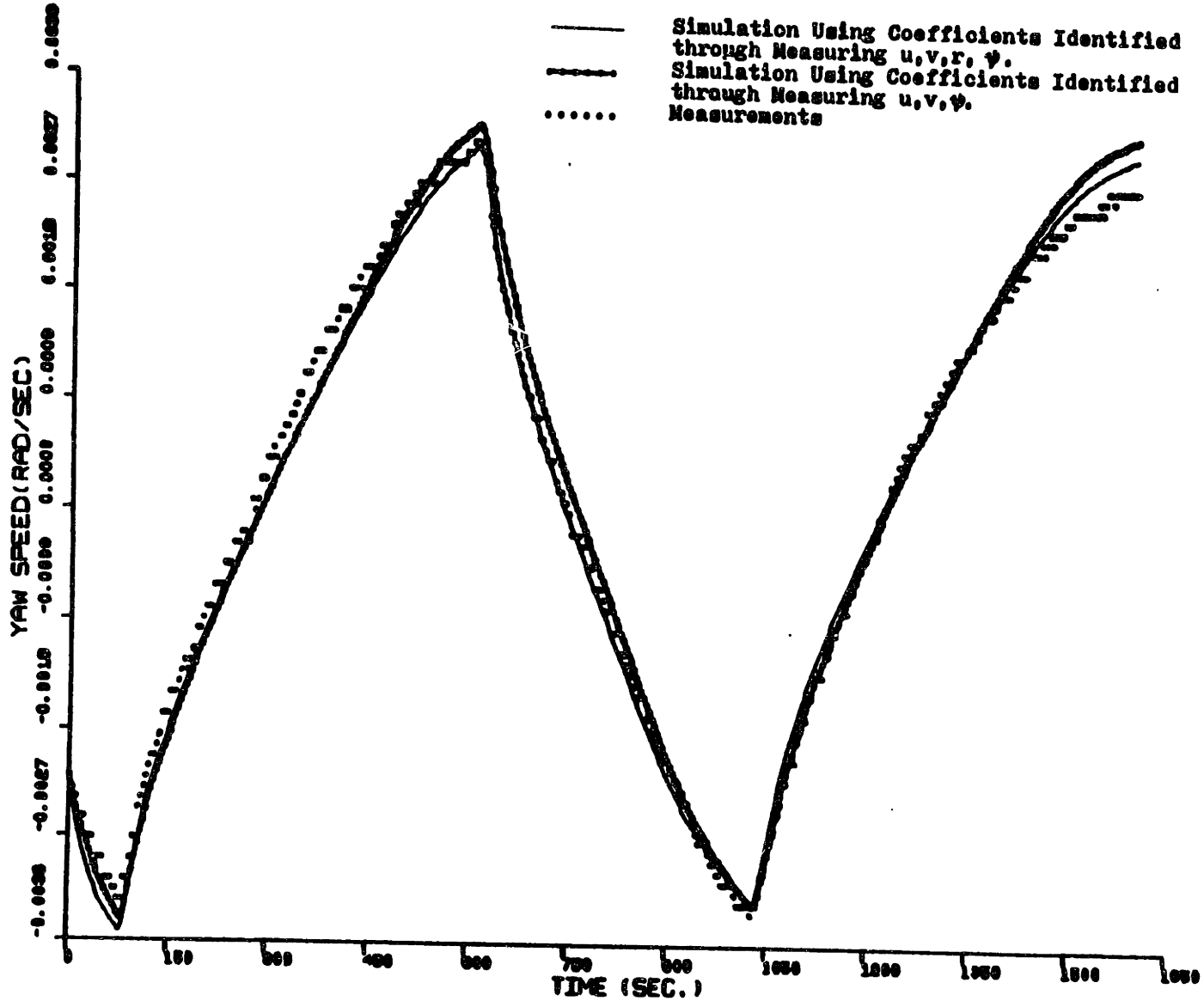

fig.4.1.5(c) Comparison between the Simulations of 10^{o}-10^{o} Maneuver by Using the Coefficients Identified with Four and Three Measurements Respectively ----Yaw Speed r.

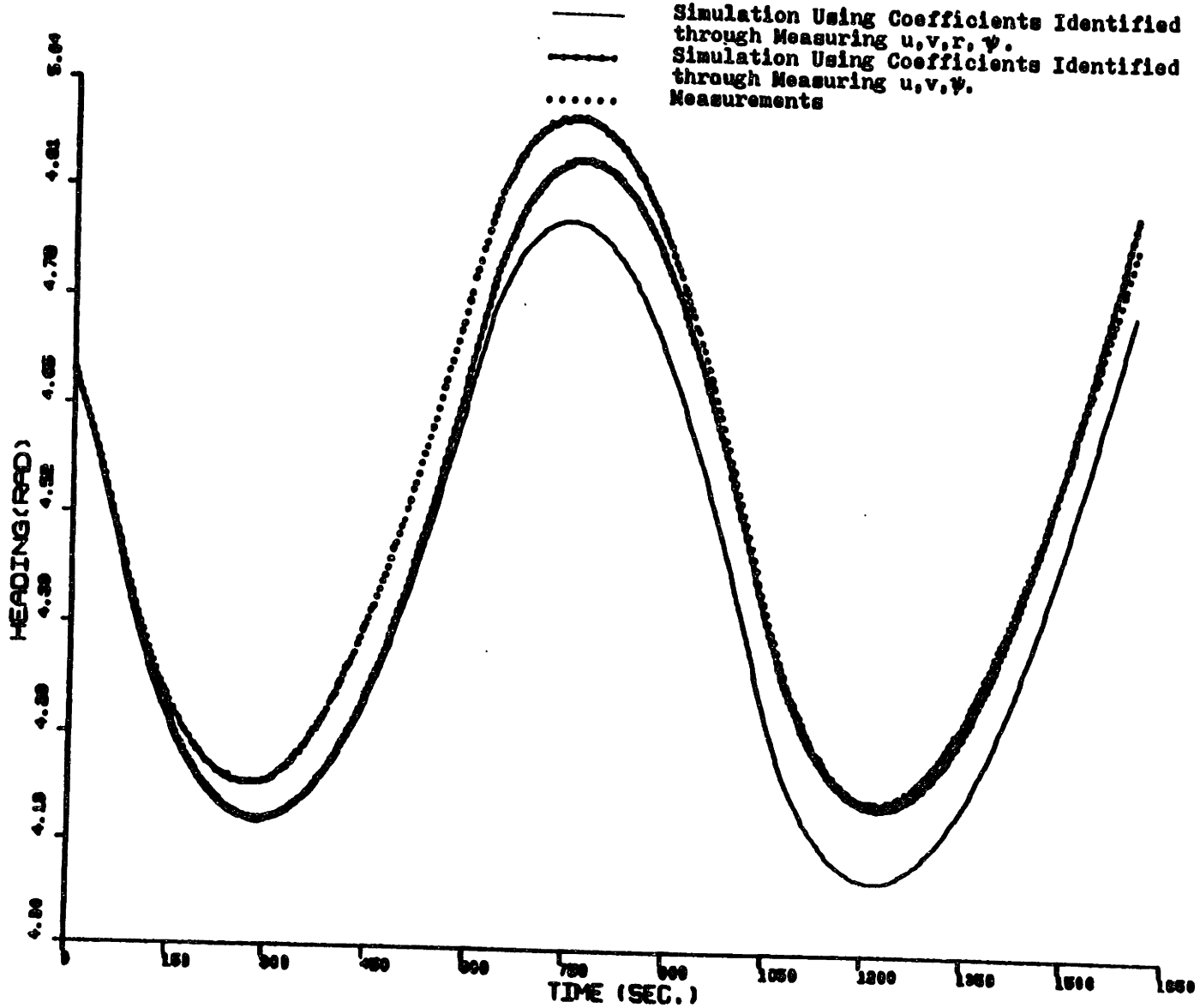

fig.4.1.5(d) Comparison between the Simulations of 10°-10° Maneuver by Using the Coefficients Identified with Four and Three Measurements Respectively ----Yaw Angle ψ.

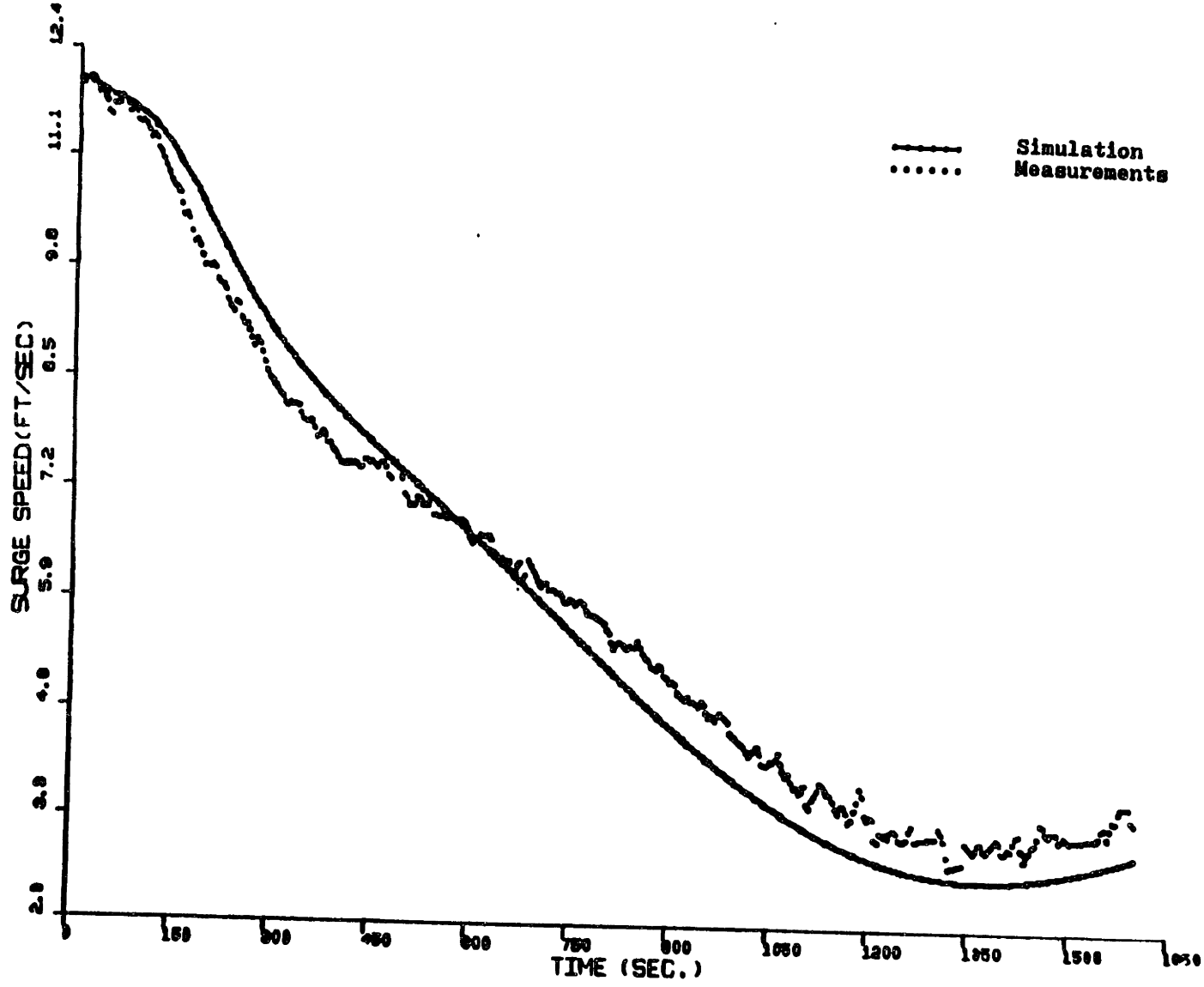

fig.4.1.6(a) Comparison between the Measurements and the Simulation of the Maneuver of 35°Turning by Using the Coefficients Identified with Three Measurements----Surge Speed u.

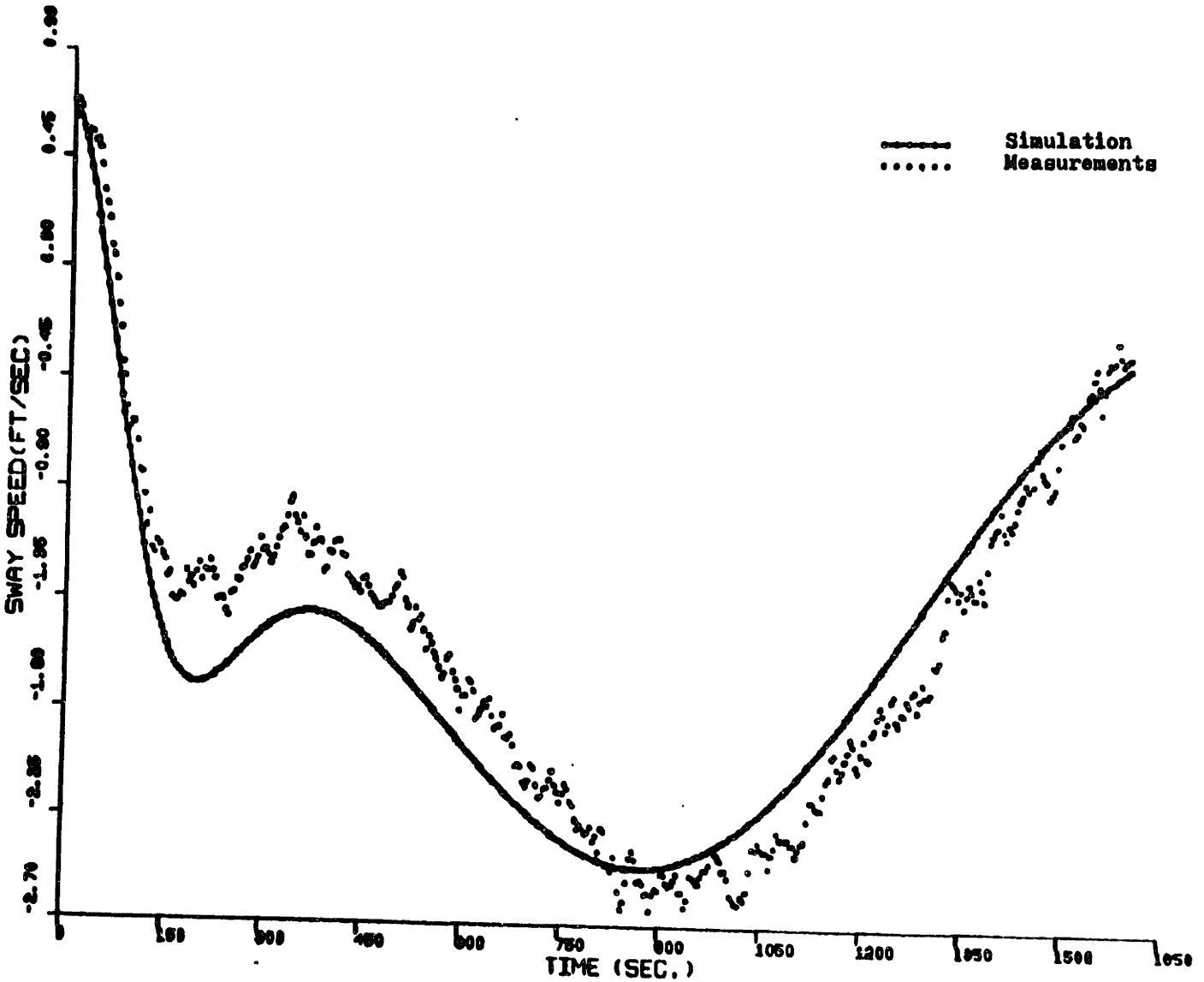

fig.4.1.6(b) Comparison between the Measurements and the Simulation of the Maneuver of 35^{o} Turning by Using the Coefficients Identified with Three Measurements----Sway v.

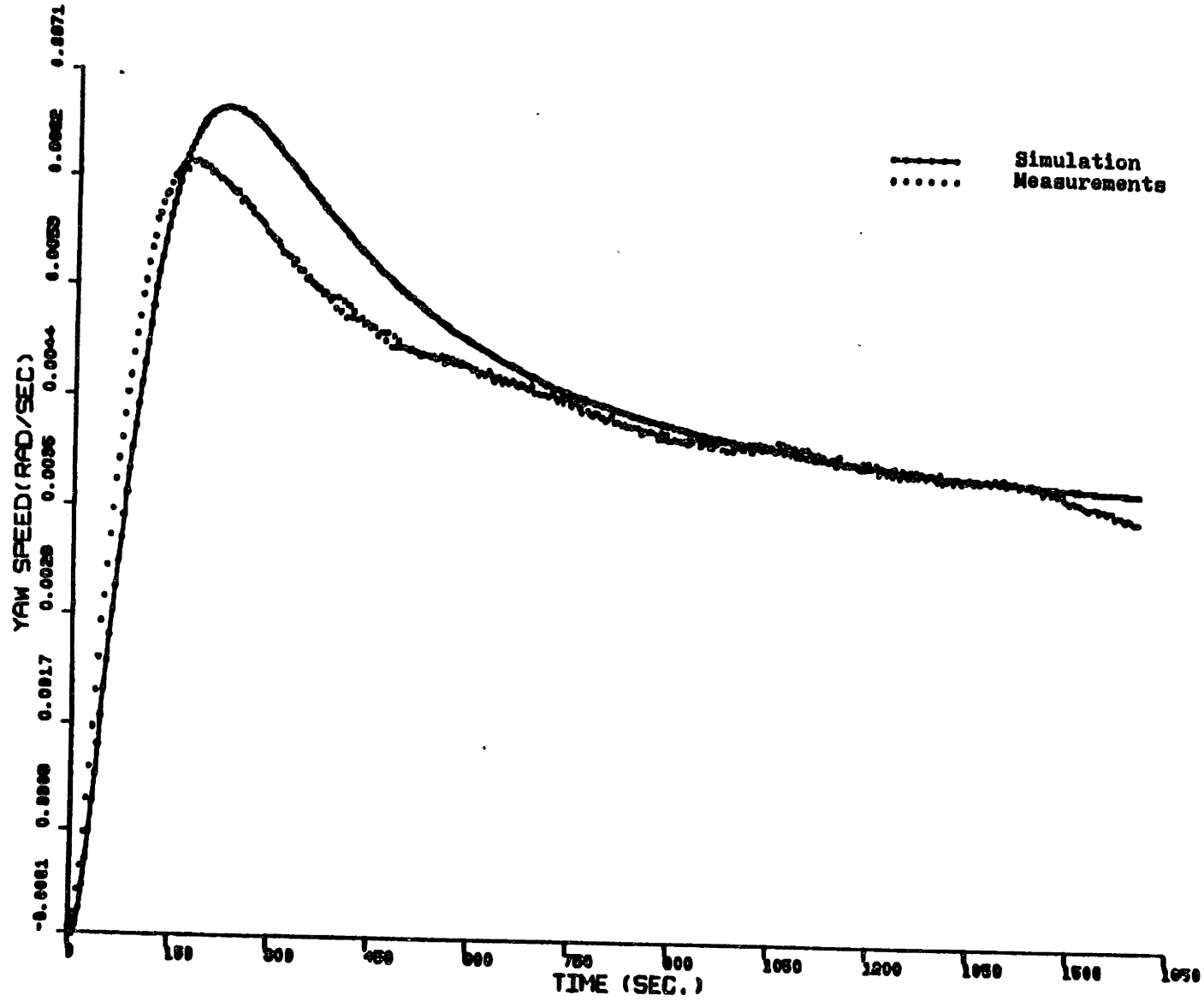

fig.4.1.6(c) Comparison between the Measurements and the Simulation of the Maneuver of 35^{o} Turning by Using the Coefficients Identified with Three Measurements----Yaw Speed r.

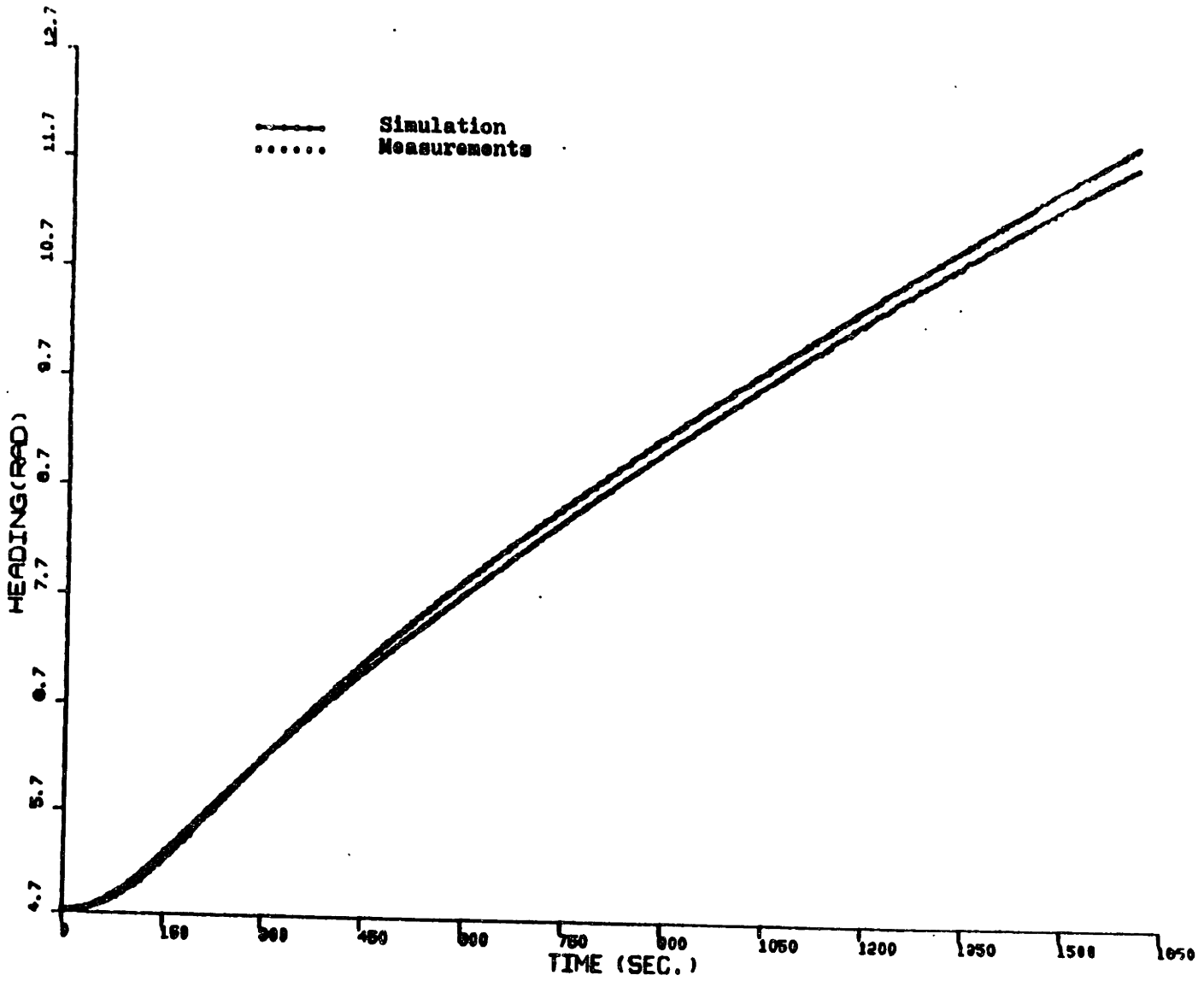

fig.4.1.6(d) Comparison between the Measurements and the Simulation of the Maneuver of 35^{0} Turning by Using the Coefficients Identified with Three Measurements----Yaw Angle ψ.

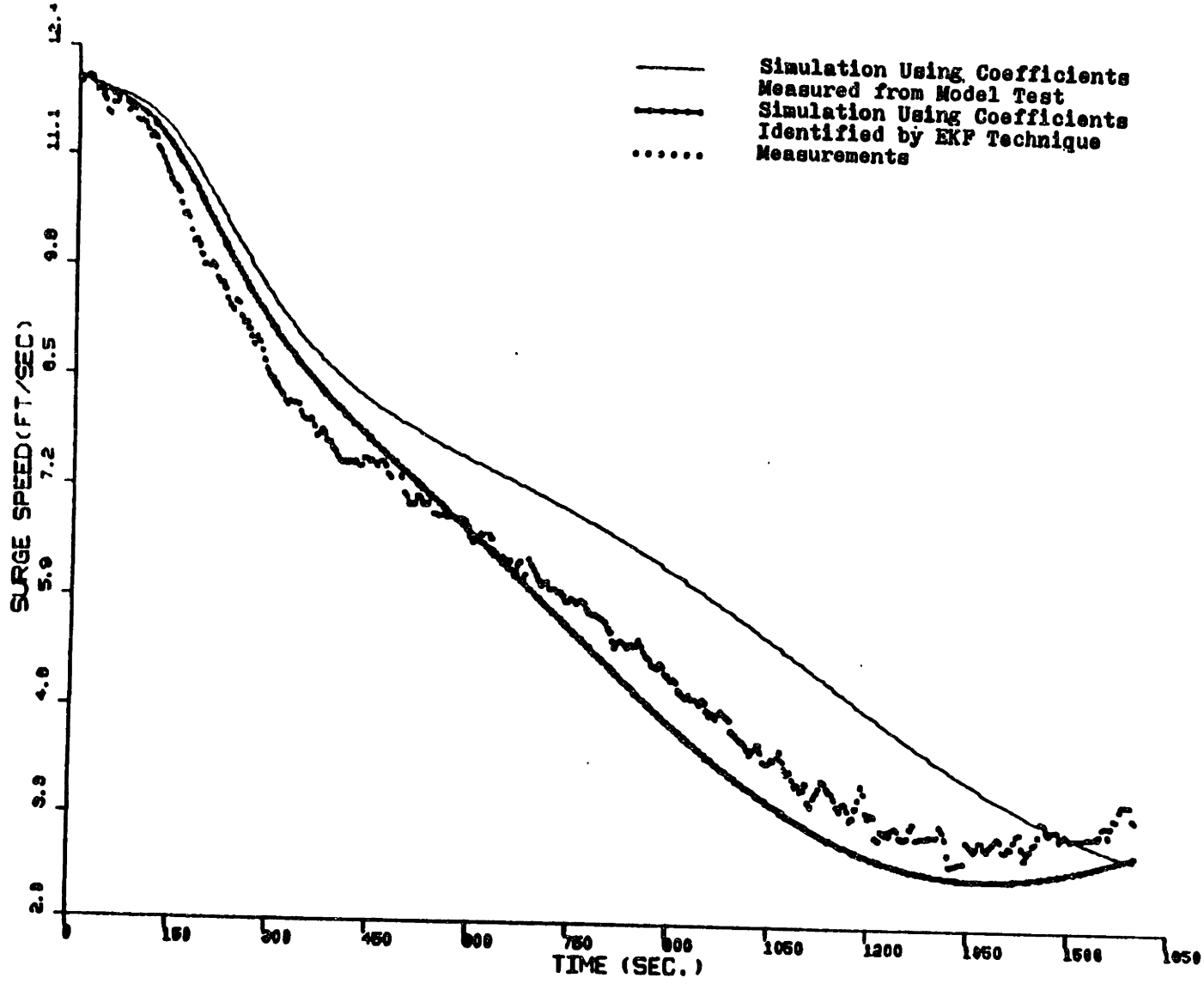

fig.4.1.7(a) Comparison between the Simulation of the Maneuver of 35^{o} Turning by Using the Coefficients "Measured" from Model Test and Identified with Three Measurements----Surge Speed u.

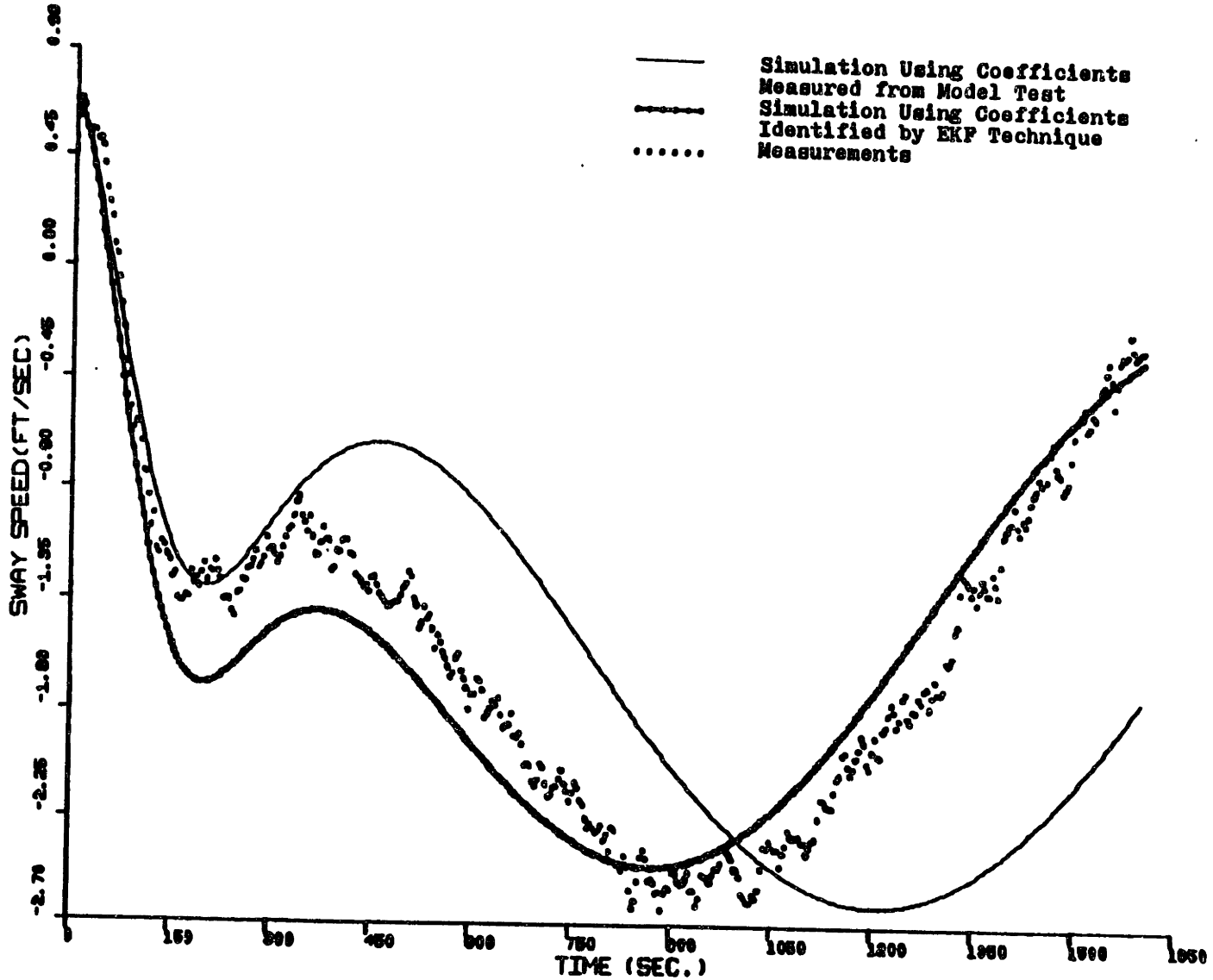

fig.4.1.7(b) Comparison between the Simulations of the Maneuver of 35^{o} Turning by Using the Coefficients "Measured" from Model Test and Identified with Three Measurements----Sway Speed v.

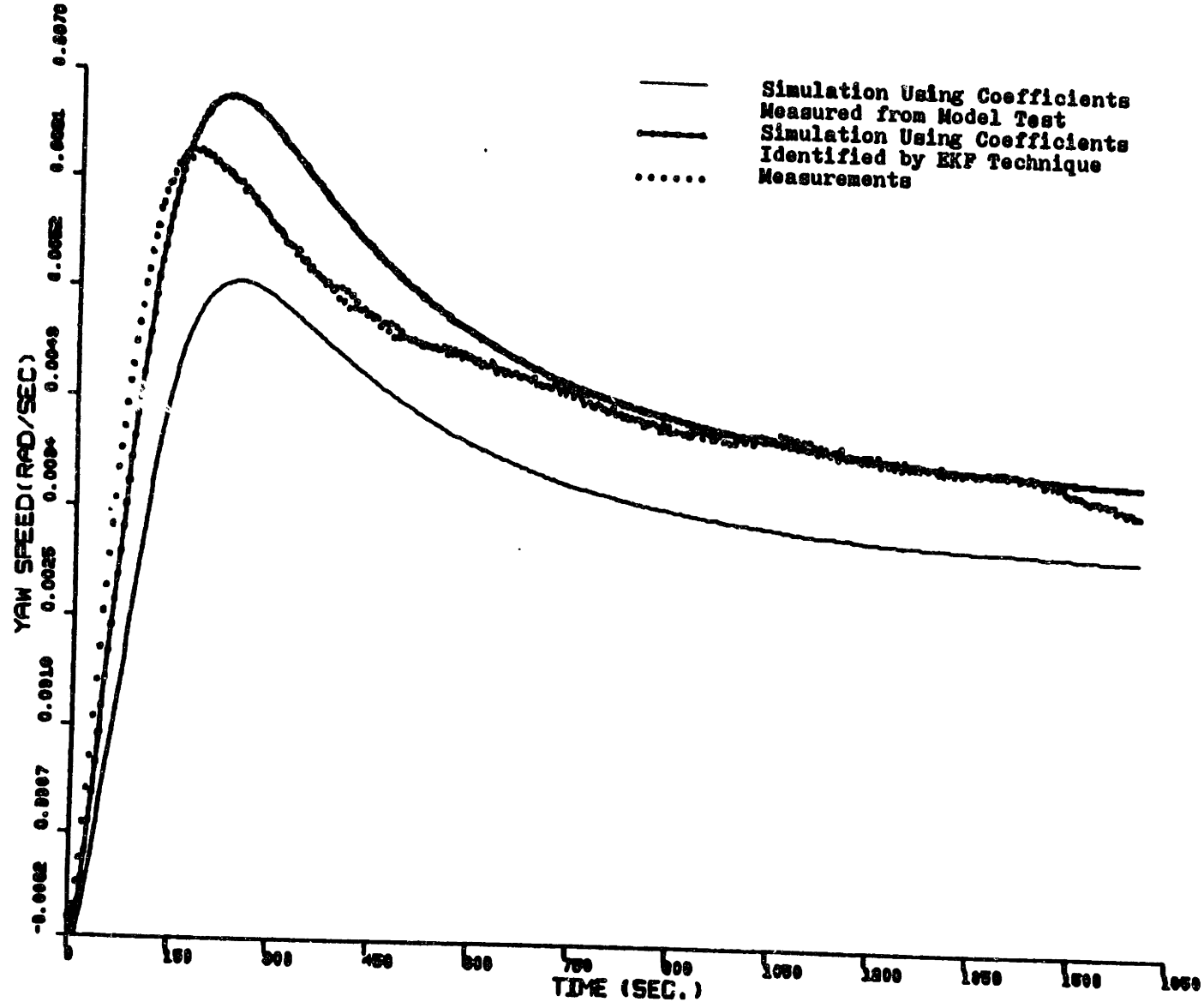

fig.4.1.7(c) Comparison between the Simulations of the Maneuver of 35° Turning by Using the Coefficients "Measured" from Model Test and Identified with Three Measurements----Yaw Speed r.

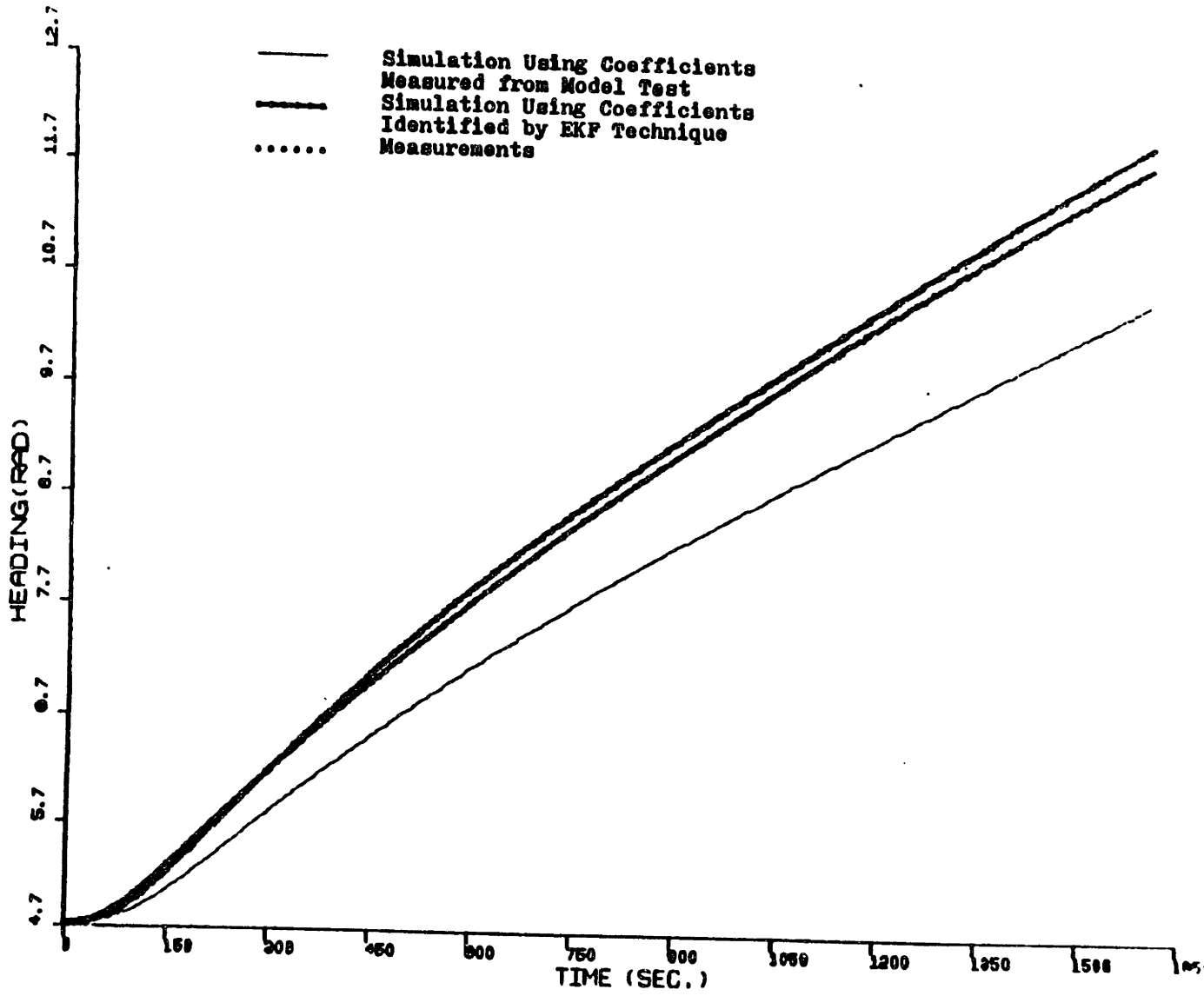

fig.4.1.7(d) Comparison between the Simulations of the Maneuver of 35^{o} Turning by Using the Coefficients "Measured" from Model Test and Identified with Three Measurements----Yaw Angle ψ.

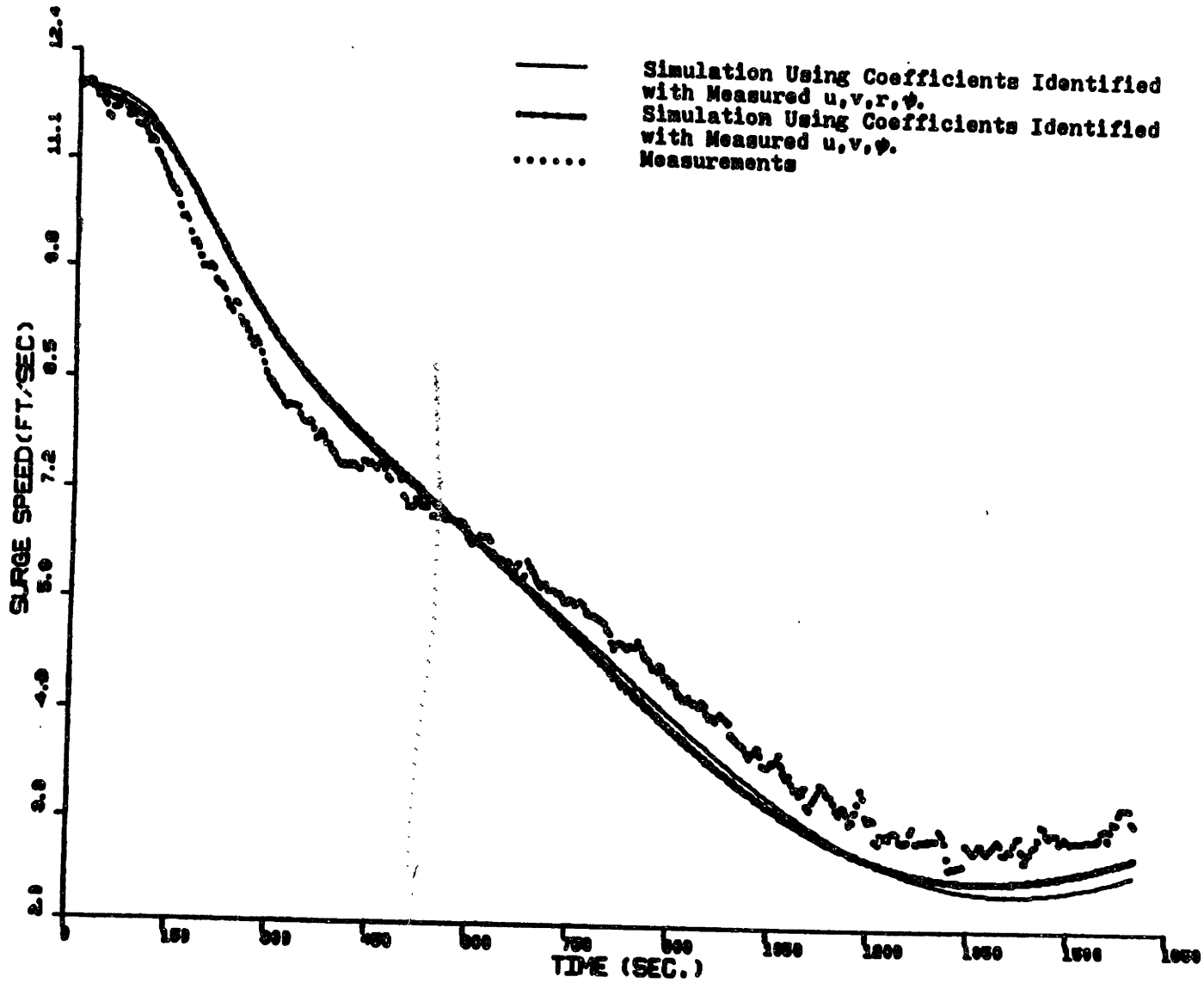

4.1.8(a) Comparison between the Simulations of the Maneuver by Using the Coefficients Identified with Four and Three Measurements Respectively ----Surge Speed u.

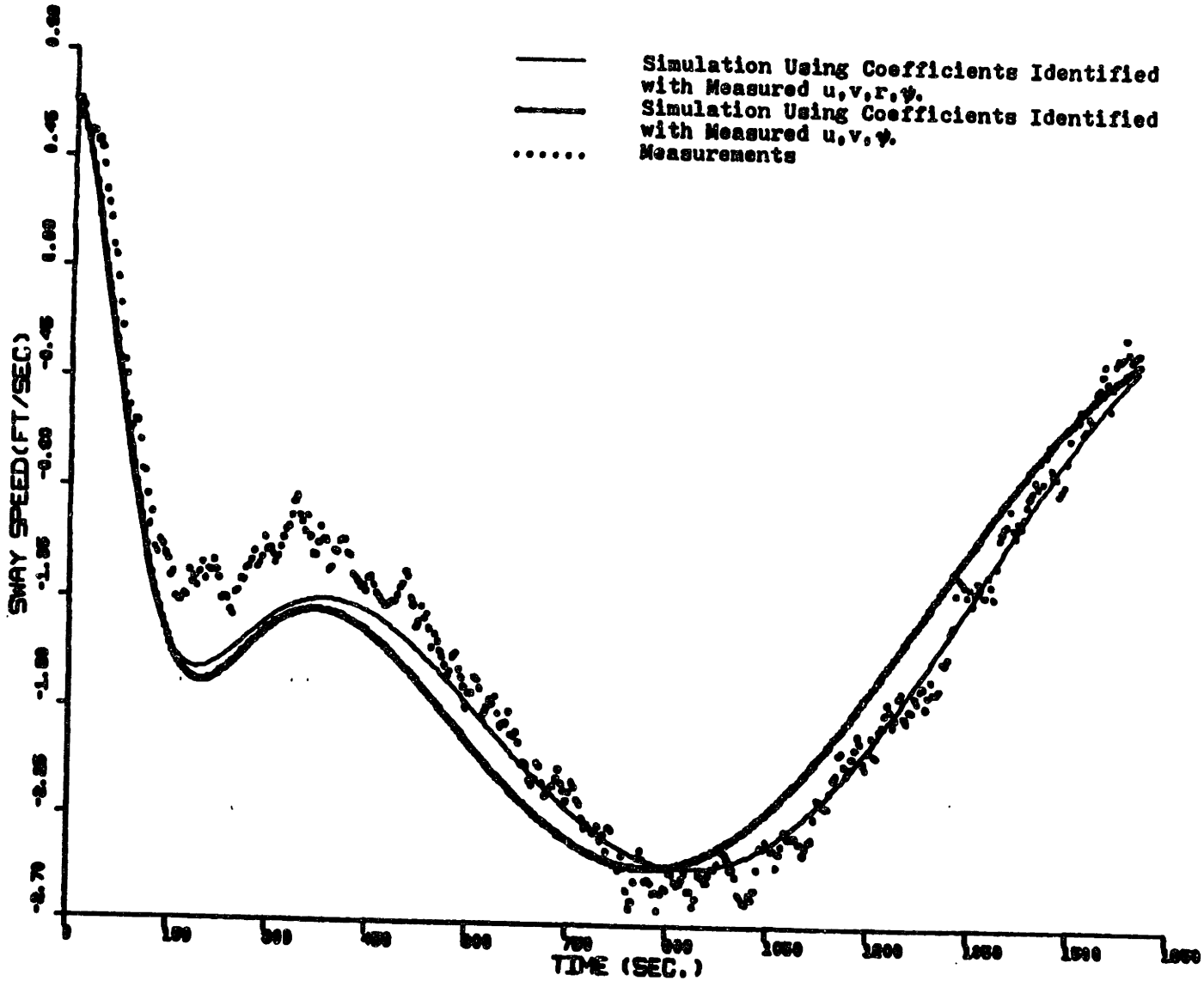

fig.4.1.8(b) Comparison between the Simulations of the Maneuver by Using the Coefficients Identified with Four and Three Measurements Respectively ----Sway Speed v.

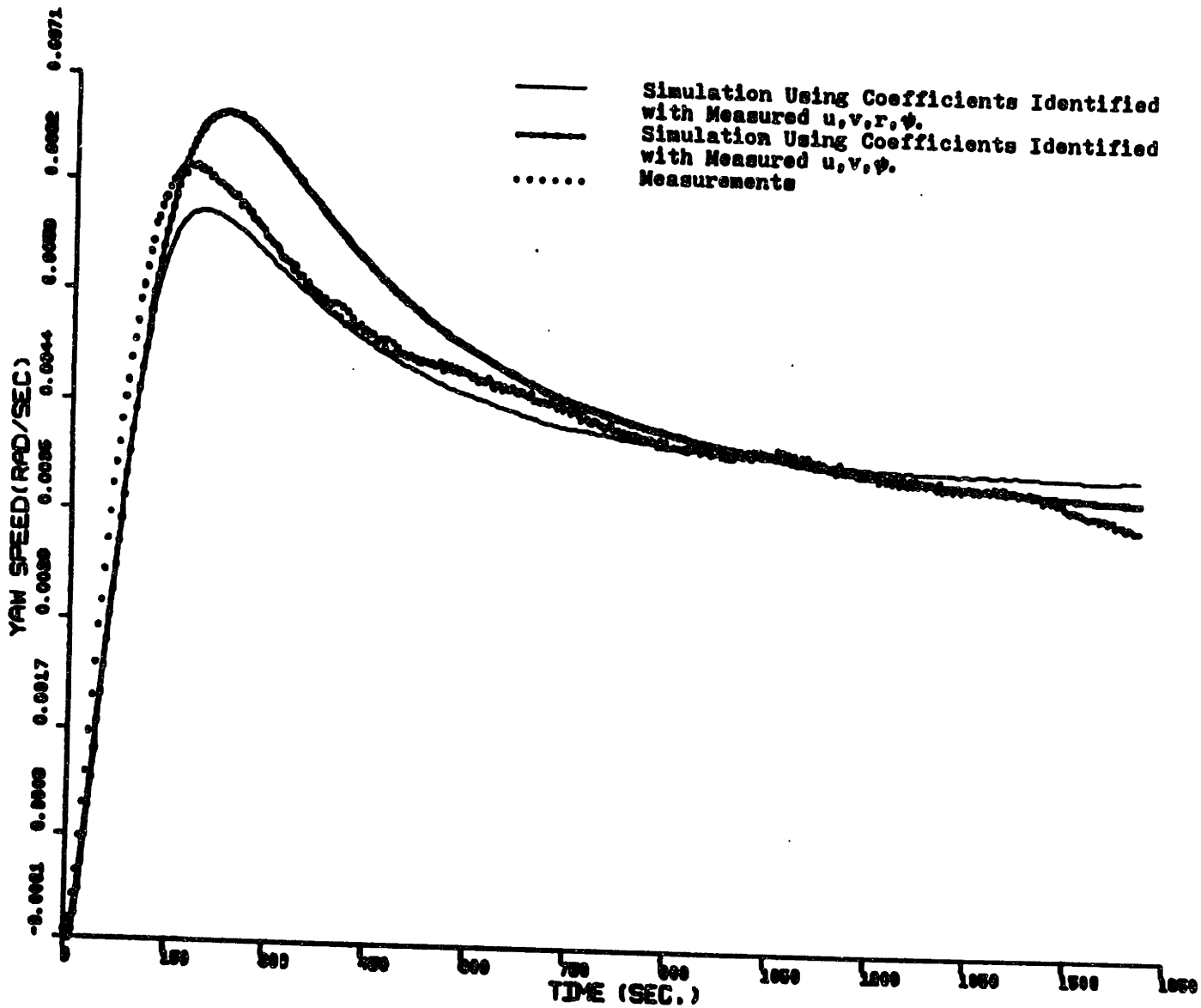

fig.4.1.8(c) Comparison between the Simulations of the Maneuver by Using the Coefficients Identified with Four and Three Measurements Respectively ----Yaw Speed r.

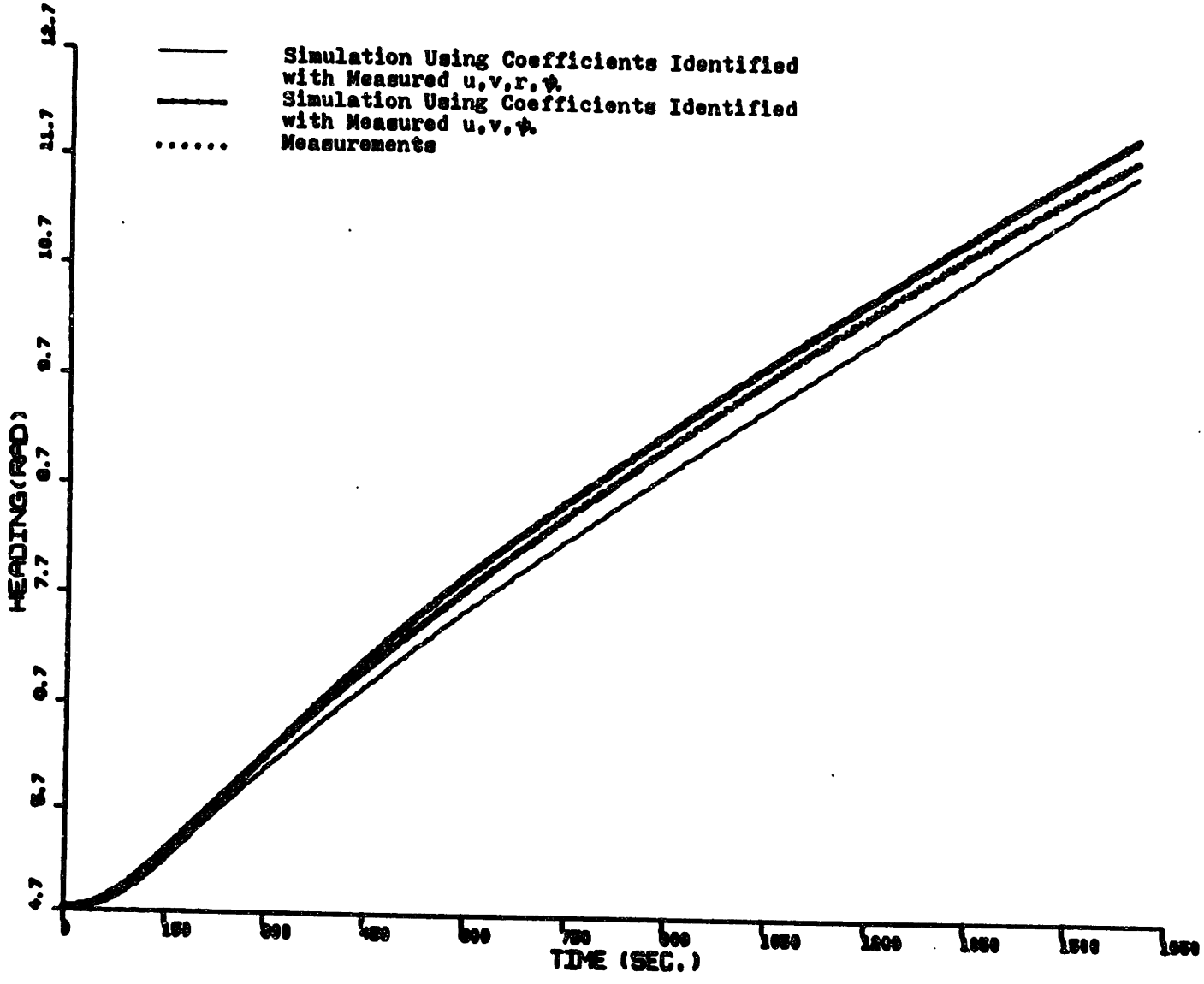

fig.4.1.8(d) Comparison between the Simulation of the Maneuver by Using the Coefficients Identified with Four and Three Measurements Respectively ----Yaw Angle ψ.

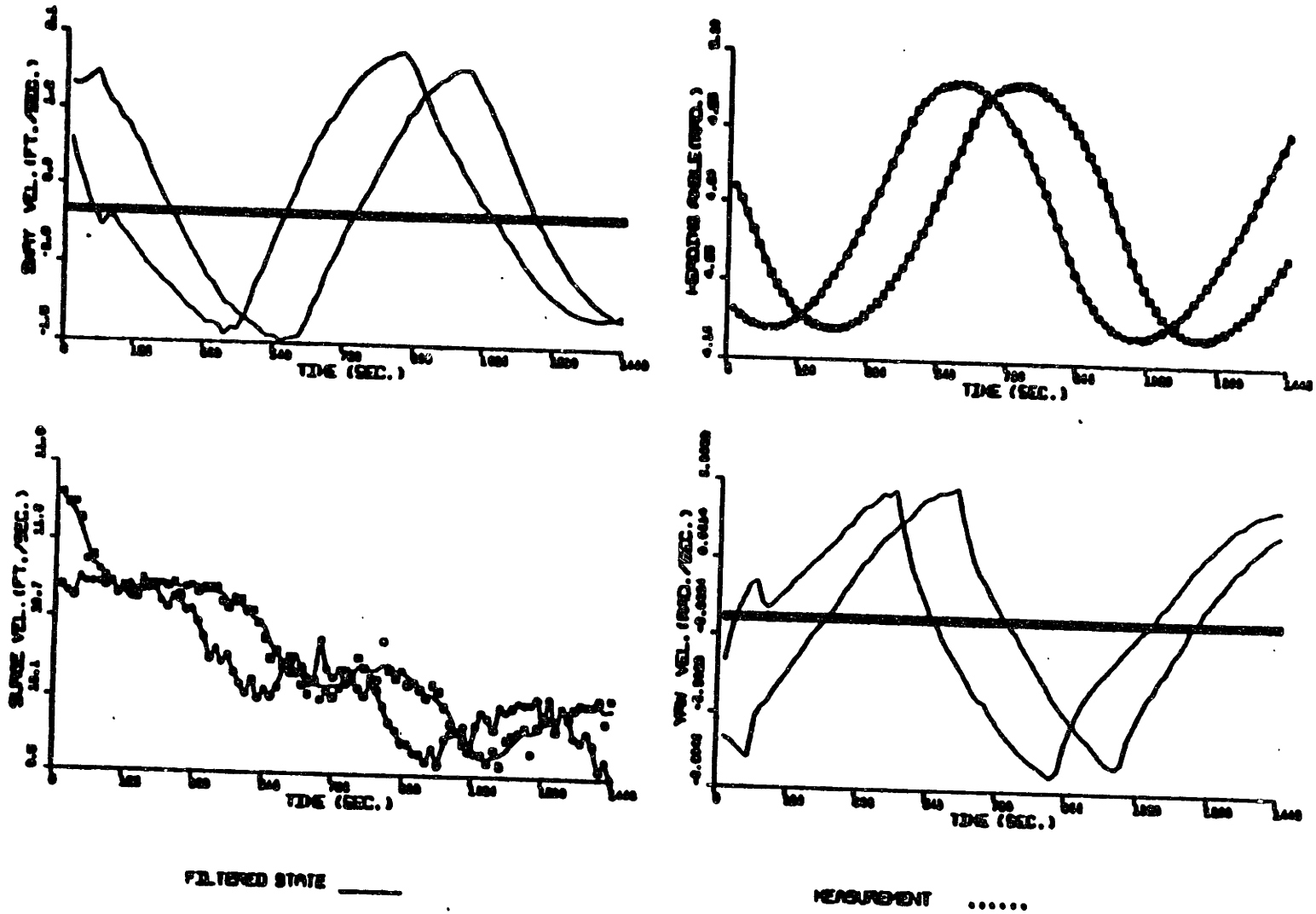

fig.4.2.1(a) Results of Identification of Linear Coefficients with Two Measurements

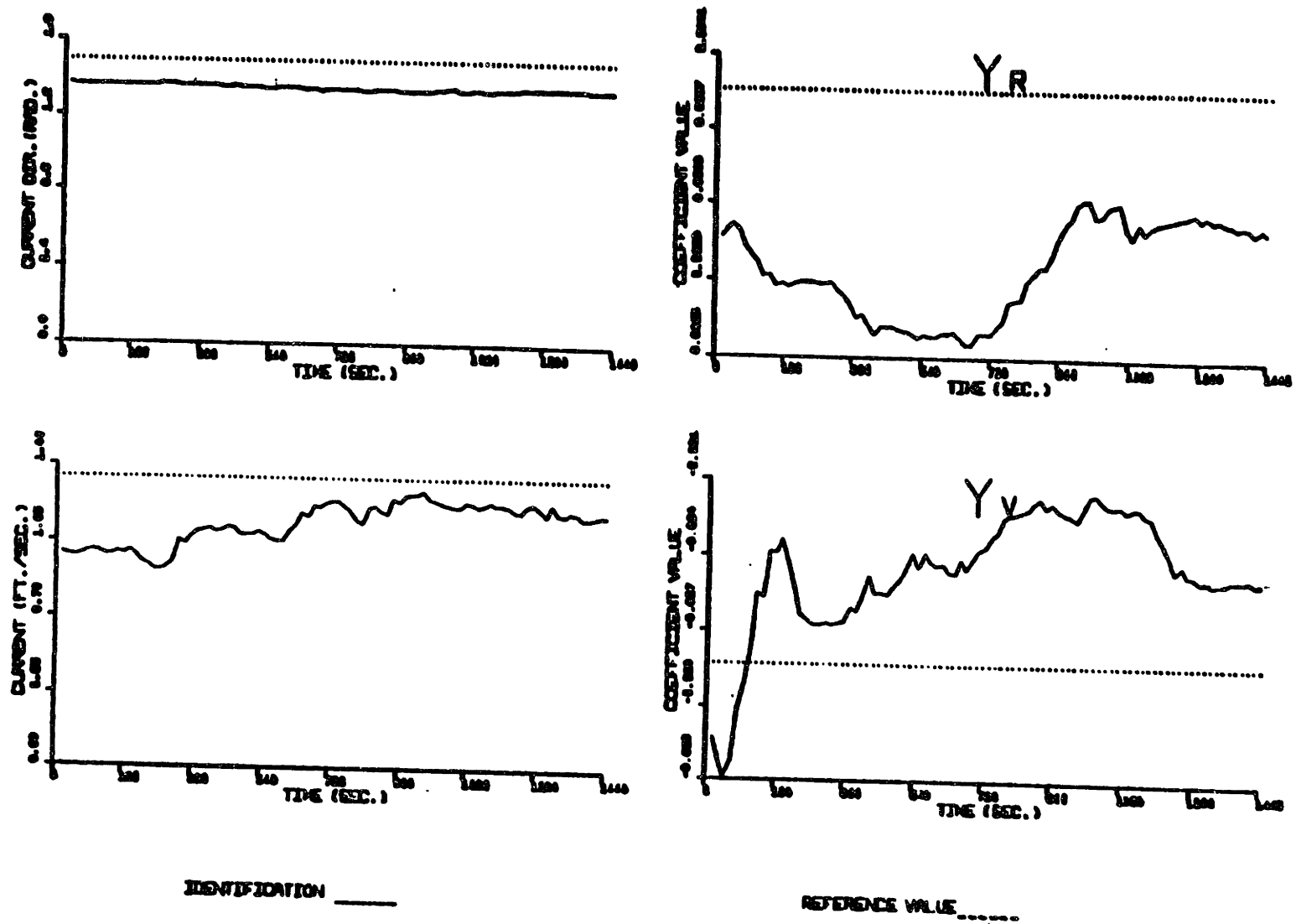

fig.4.2.1(b) Results of Identification of Linear Coefficients with Two Measurements

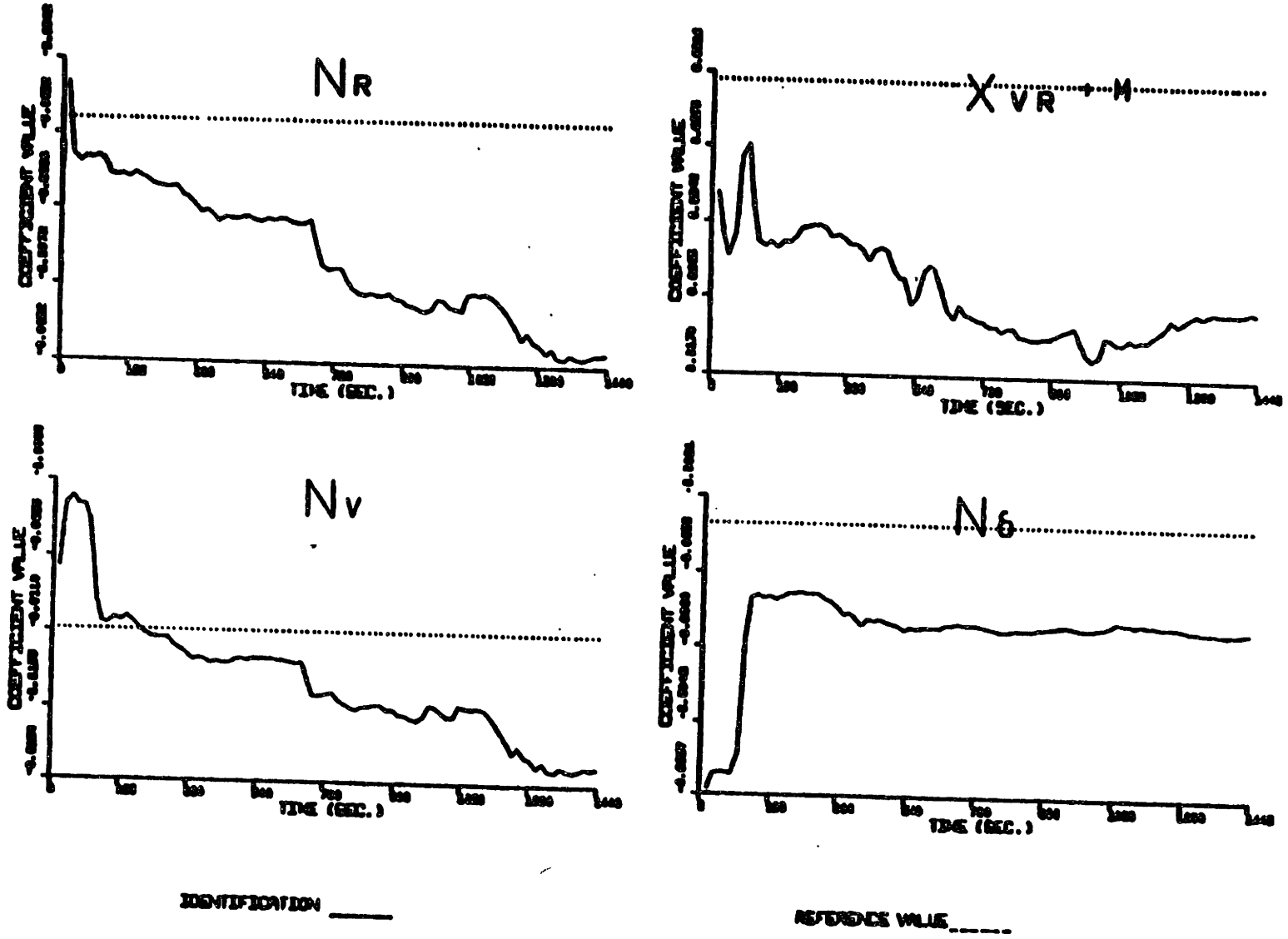

fig.4.2.1(c) Results of Identification of Linear Coefficients with Two Measurements

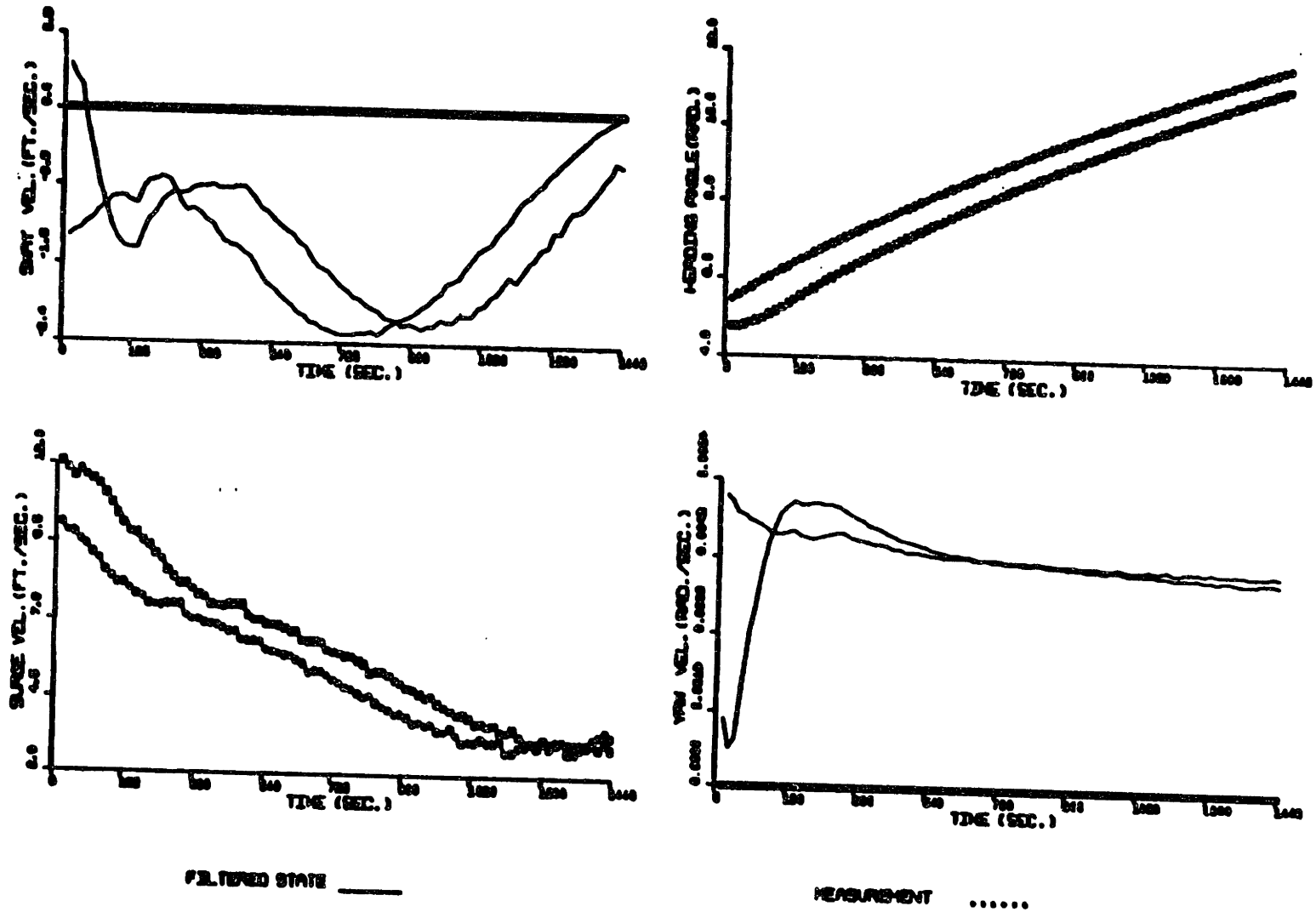

fig. 4.2.2(a) Results of Identification of Nonlinear Coefficients with Two Measurements

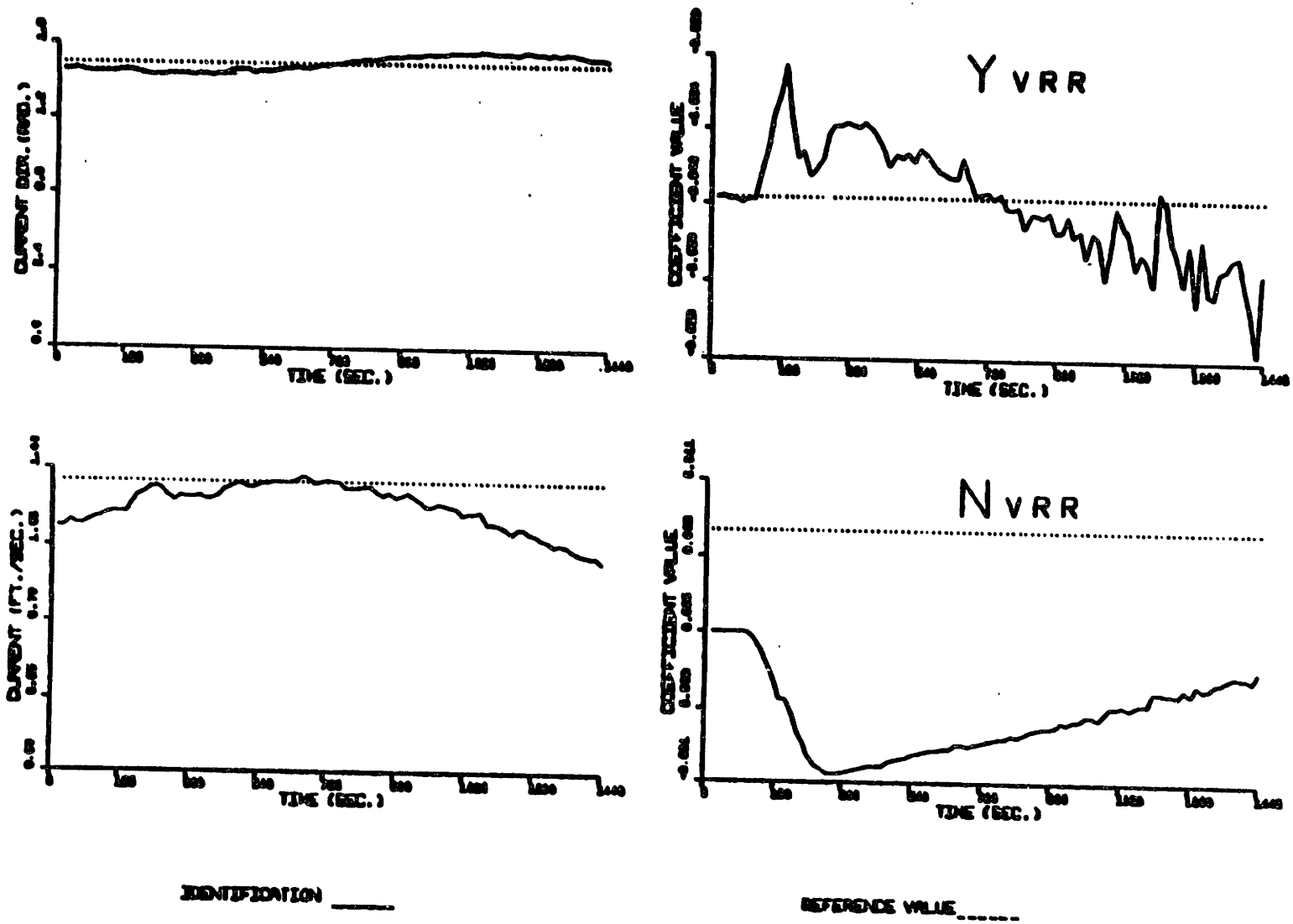

fig.4.2.2(b) Results of Identification of Nonlinear Coefficients with Two Measurements

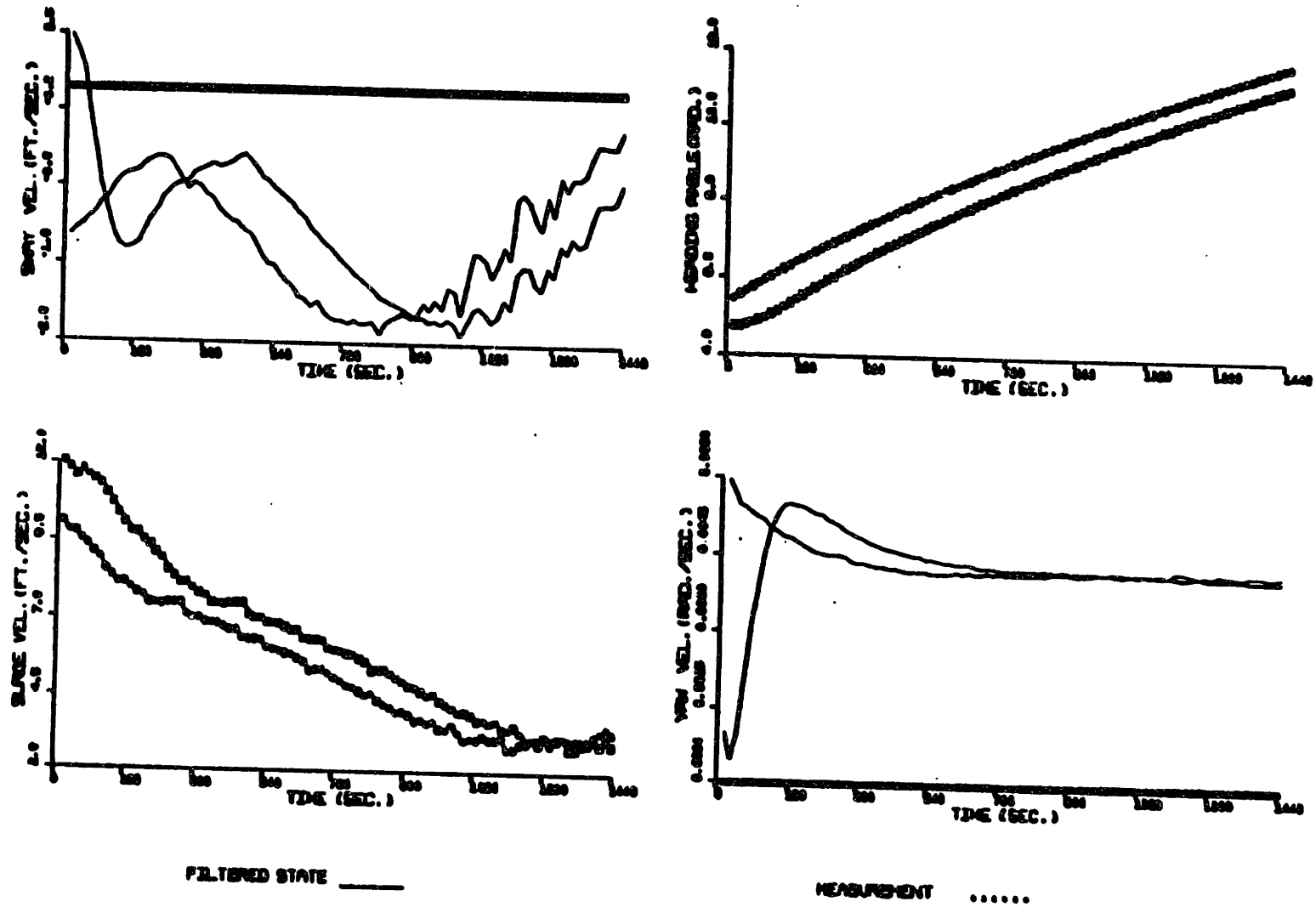

fig.4.2.2(c) Results of Identification of Nonlinear Coefficients with Two Measurements

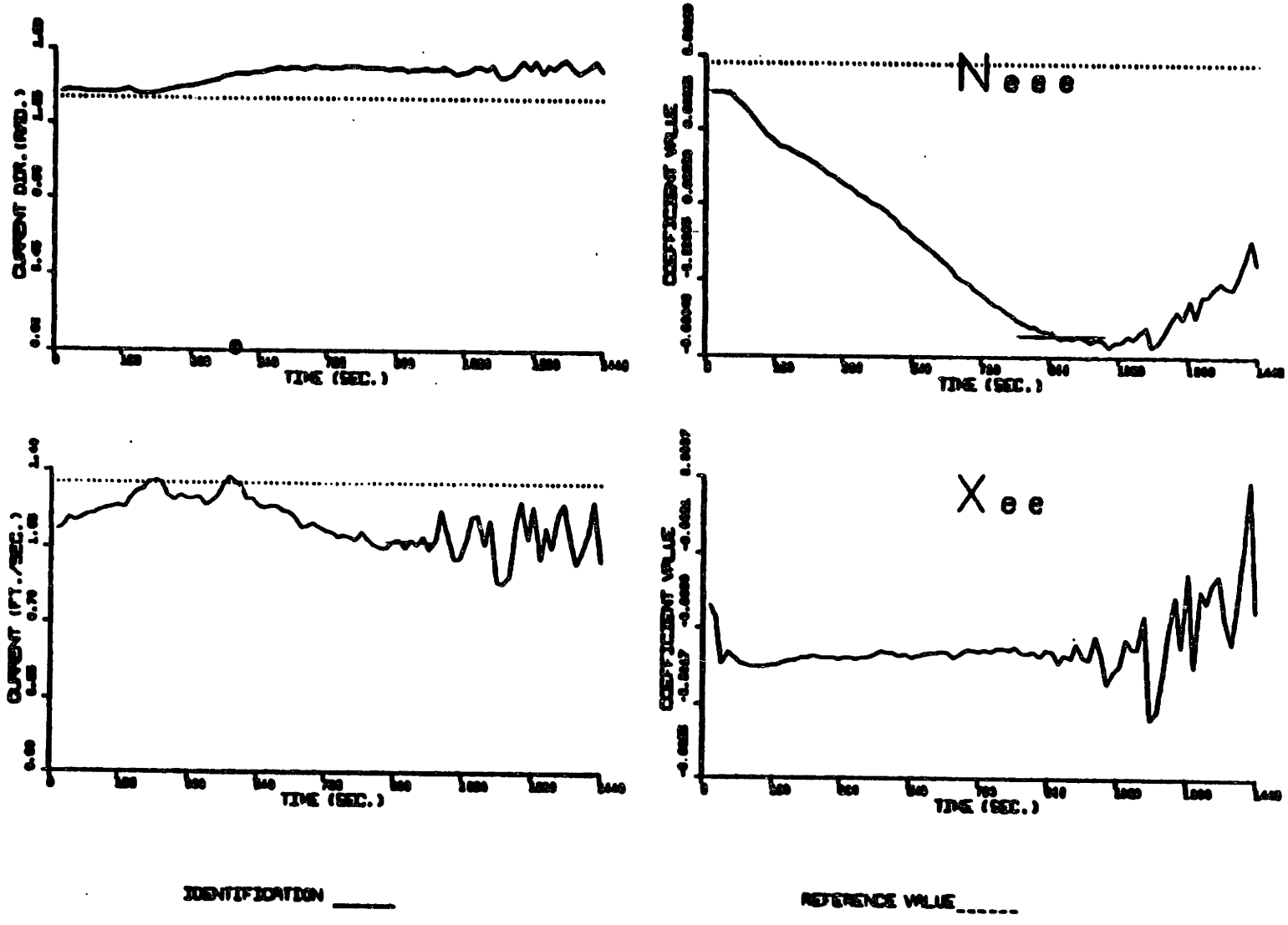

fig.4.2.2(d) Results of Identification of Nonlinear Coefficients with Two Measurements

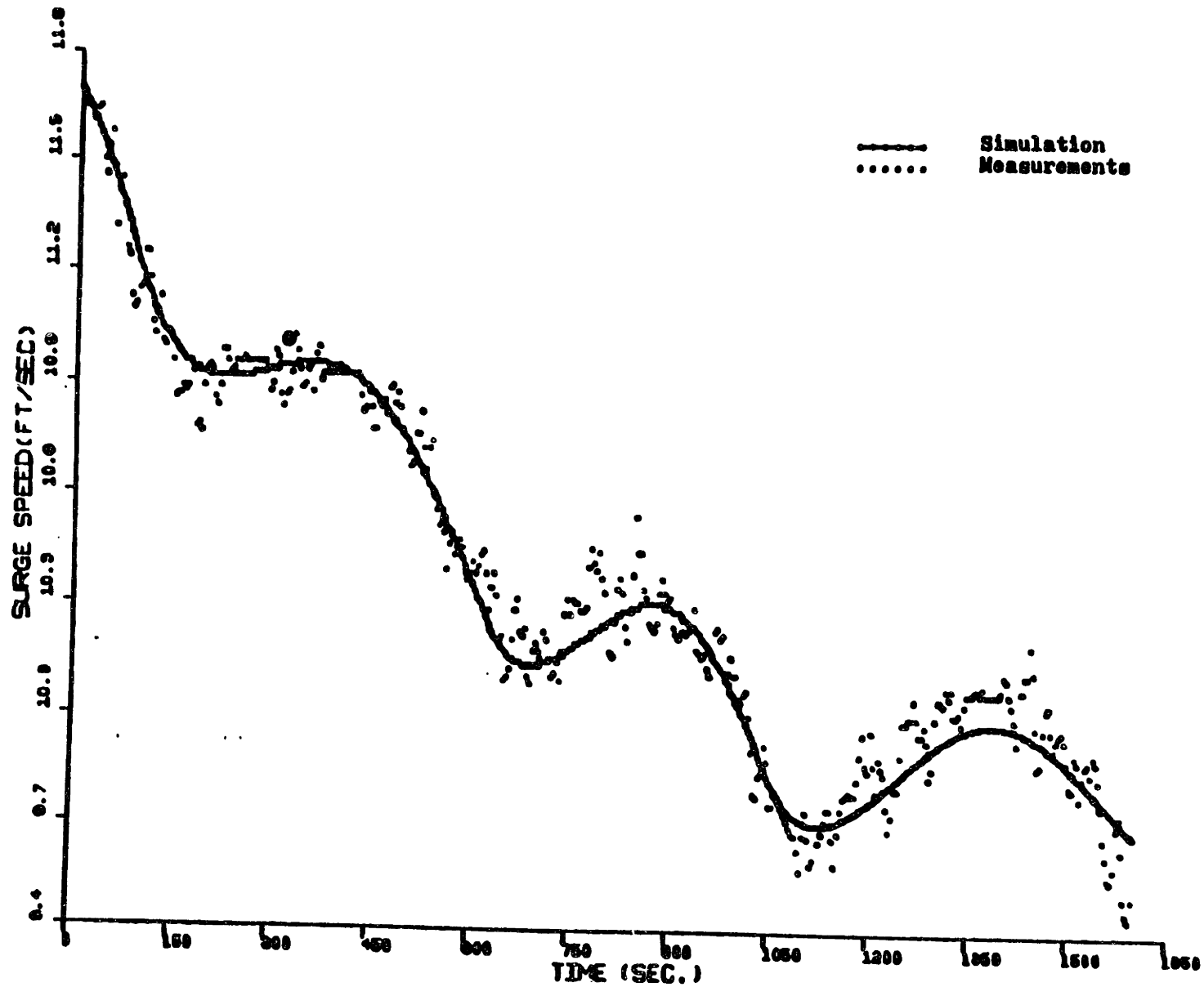

fig.4.2.3(a) Comparison between the Measurements and the Simulation of 10^{o}-10^{o} Maneuver by Using the Coefficients Identified with Two Measurements----Surge Speed u.

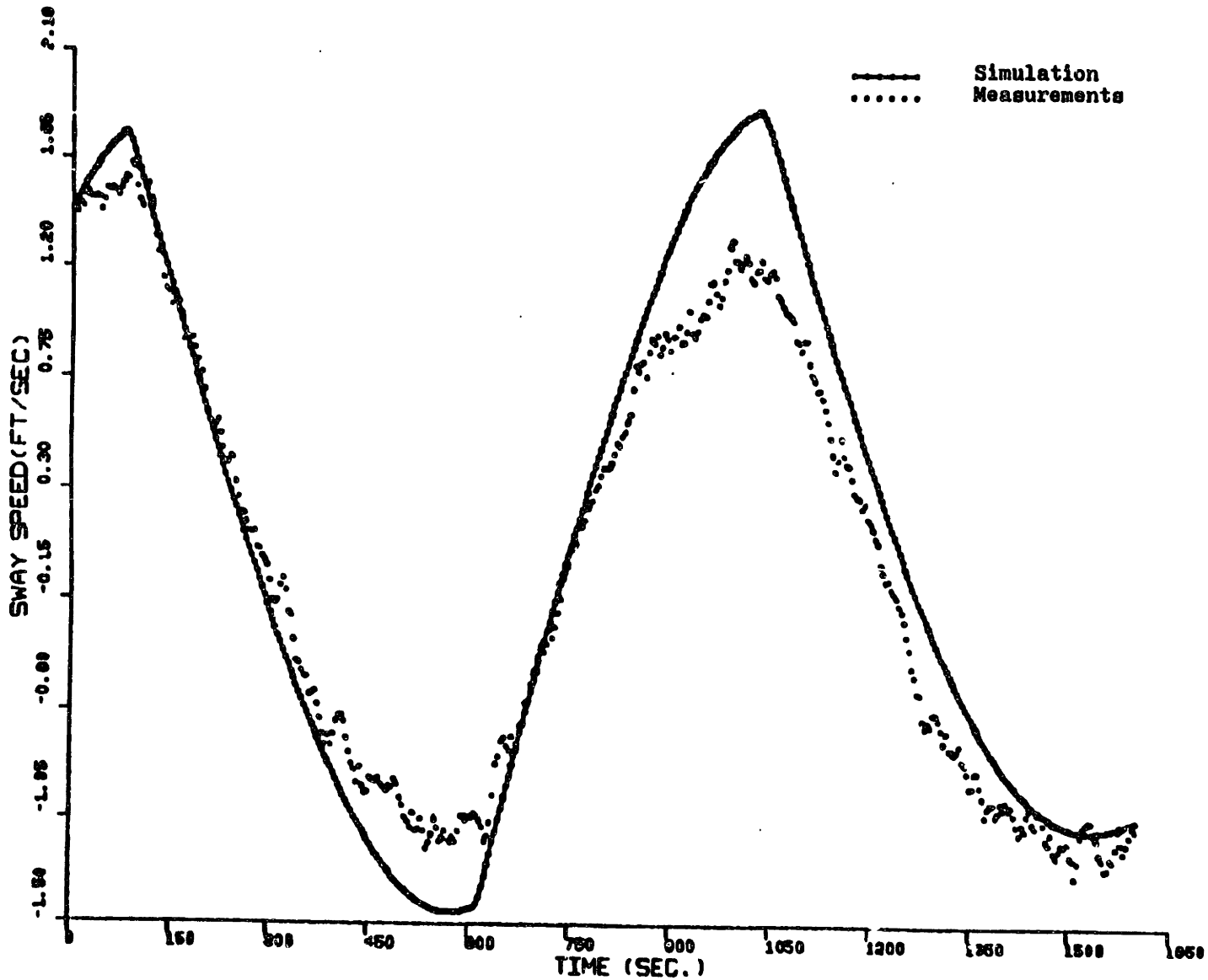

fig.4.2.3(b) Comparison between the Measurements and the Simulation of 10^{o}-10^{o} Maneuver by Using the Coefficients Identified with Two Measurements----Sway Speed v.

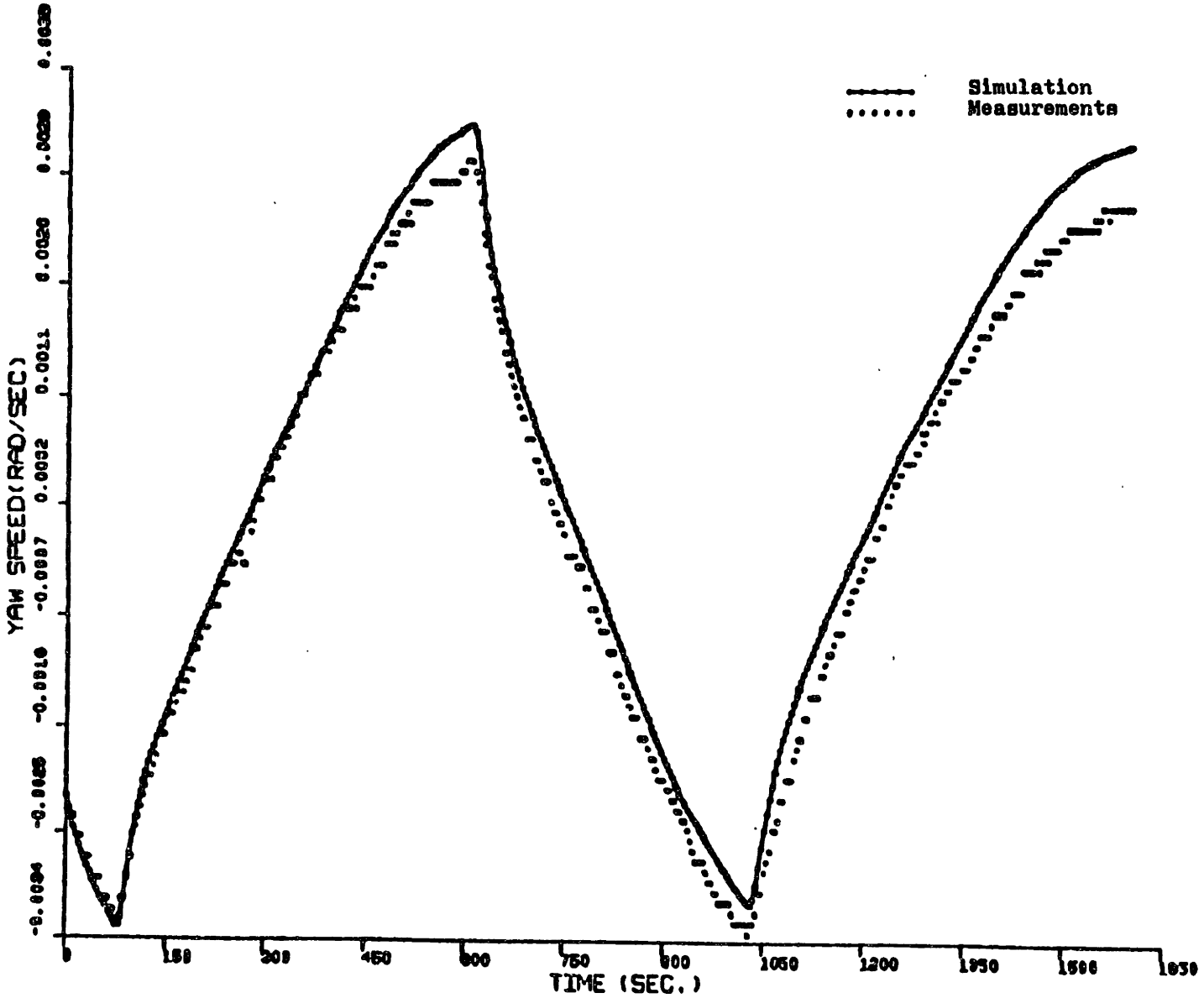

fig.4.2.3(c) Comparison between the Measurements and the Simulation of 10^{o}-10^{o} Maneuver by Using the Coefficients Identified with Two Measurements----Yaw Speed r.

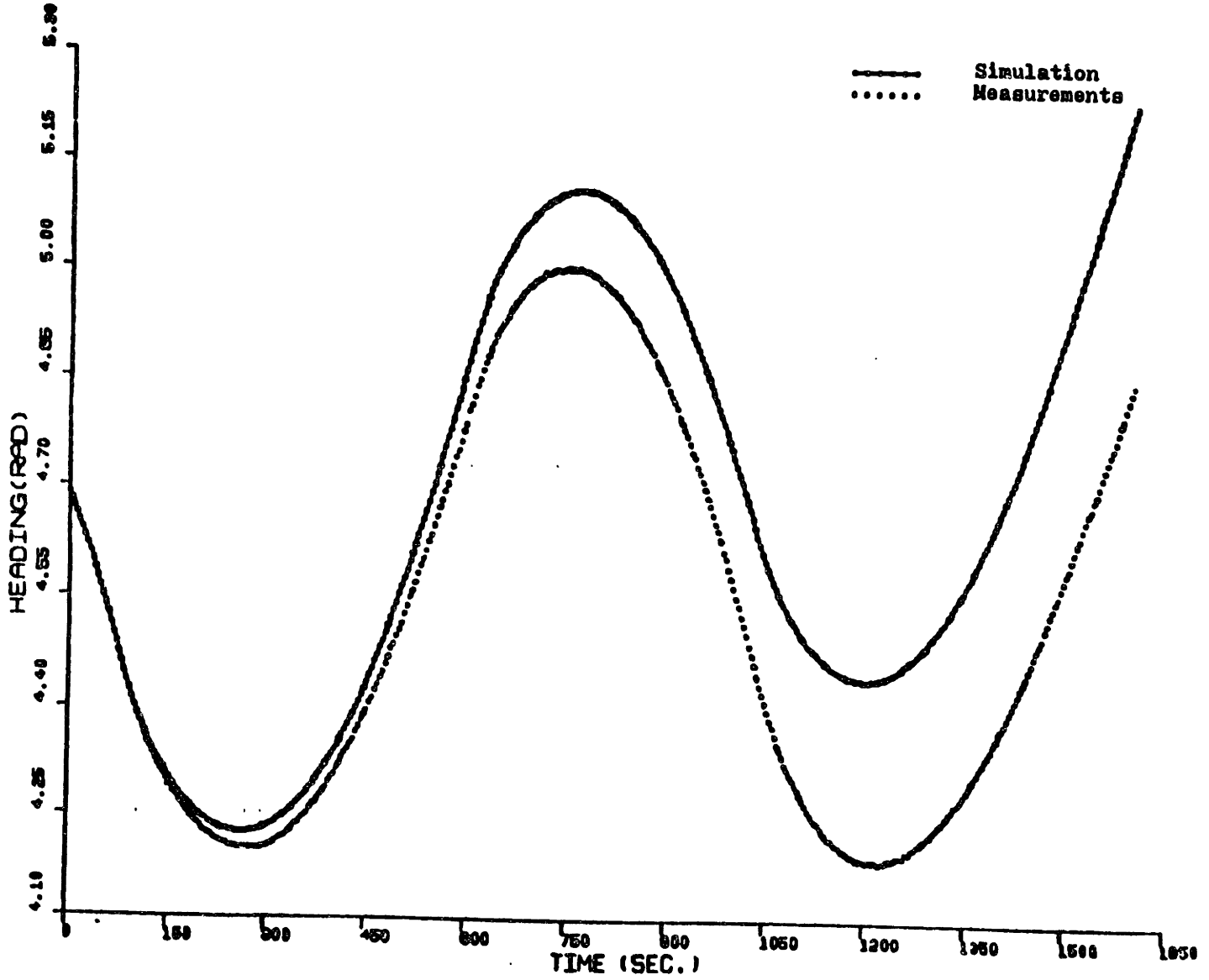

fig.4.2.3(d) Comparison between the Measurements and the Simulation of 10^{o}-10^{o} Maneuver by Using the Coefficients Identified with Two Measurements----Yaw Angle ψ.

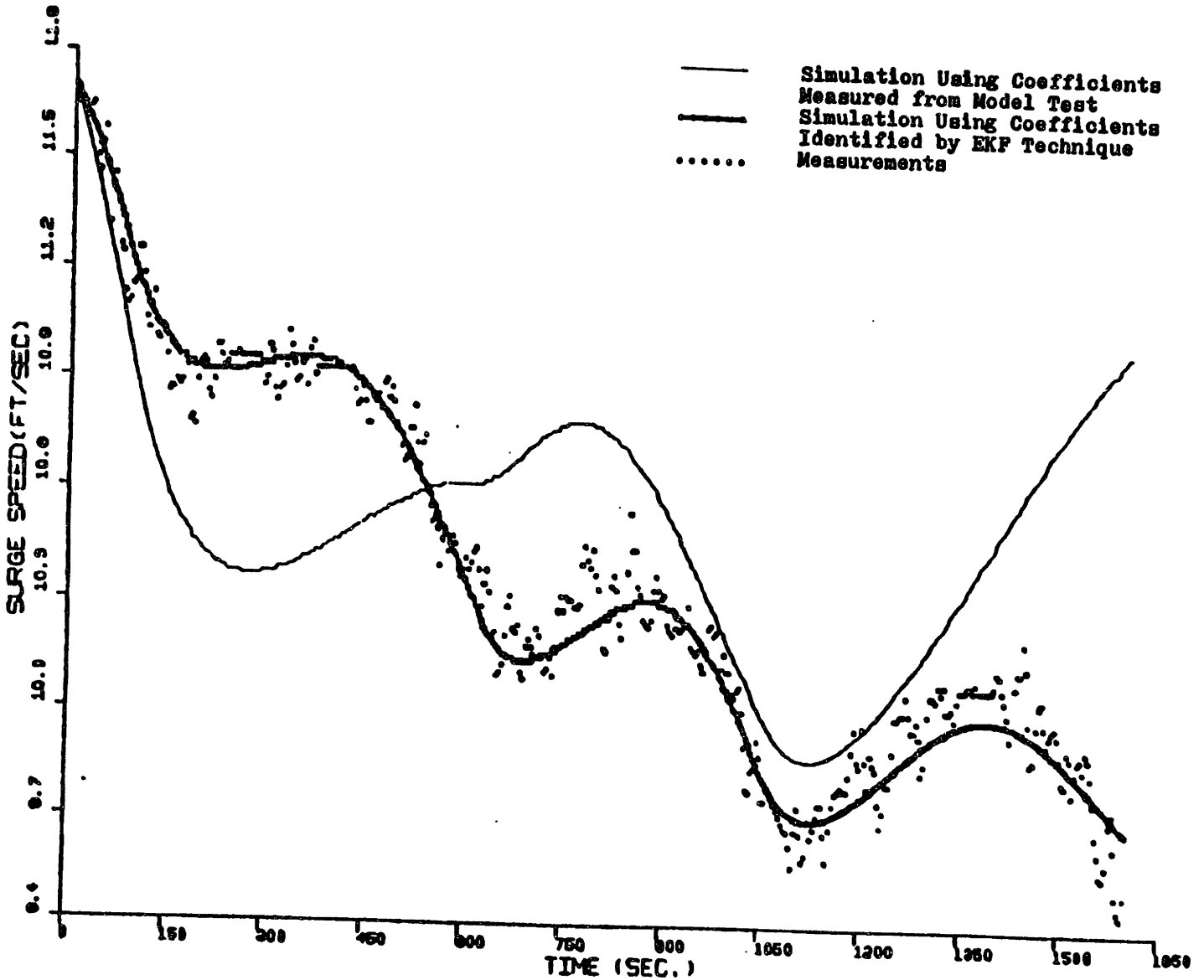

fig.4.2.4(a) Comparison between the Simulation of 10^{o}-10^{o} Maneuver by Using the Coefficients "Measured" from Model Test and Identified with Two Measurements----Surge Speed u.

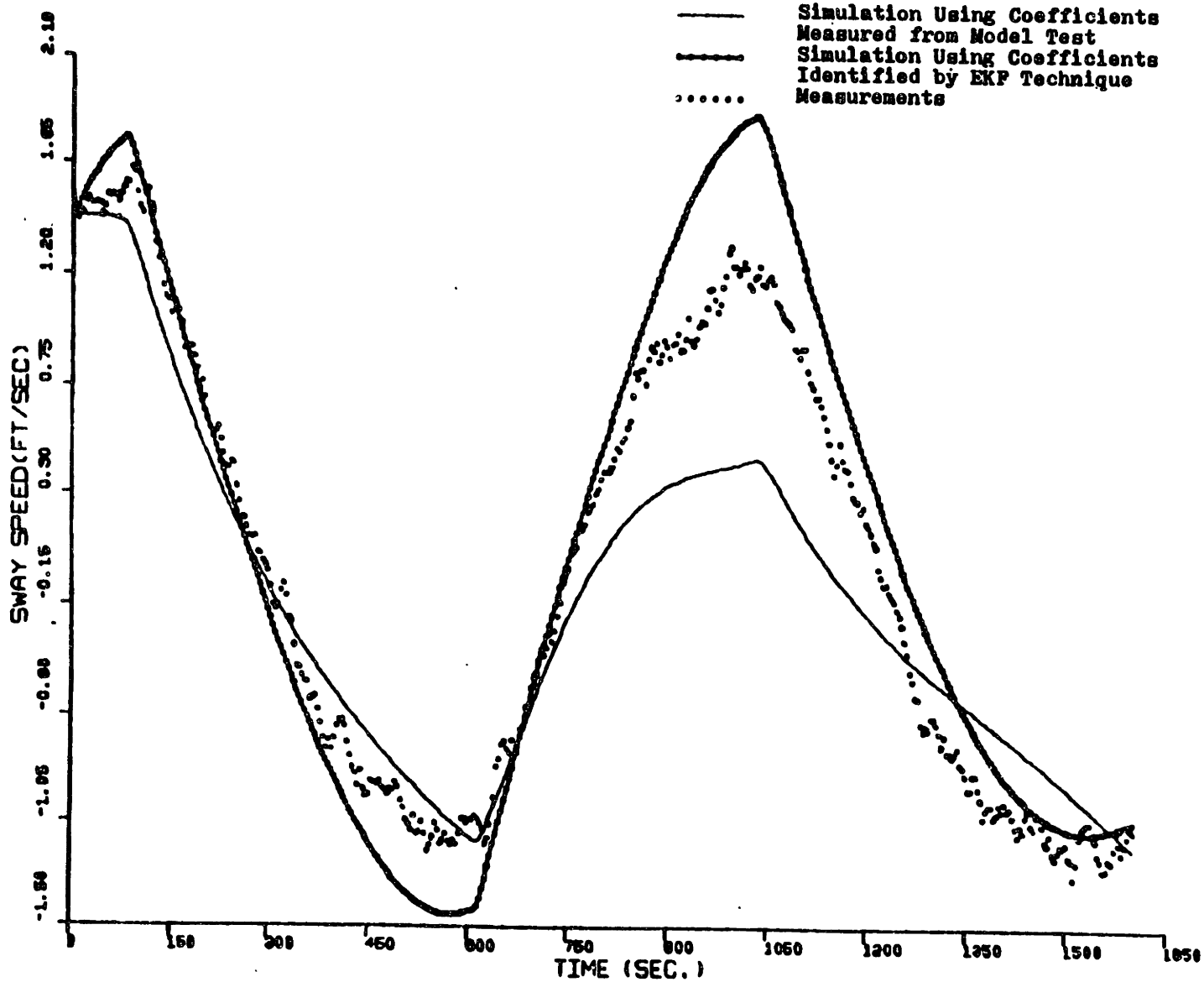

fig.4.2.4(b) Comparison between the Simulation of 10^{o}-10^{o} Maneuver by Using the Coefficients "Measured" from Model Test and Identified with Two Measurements----Sway Speed v.

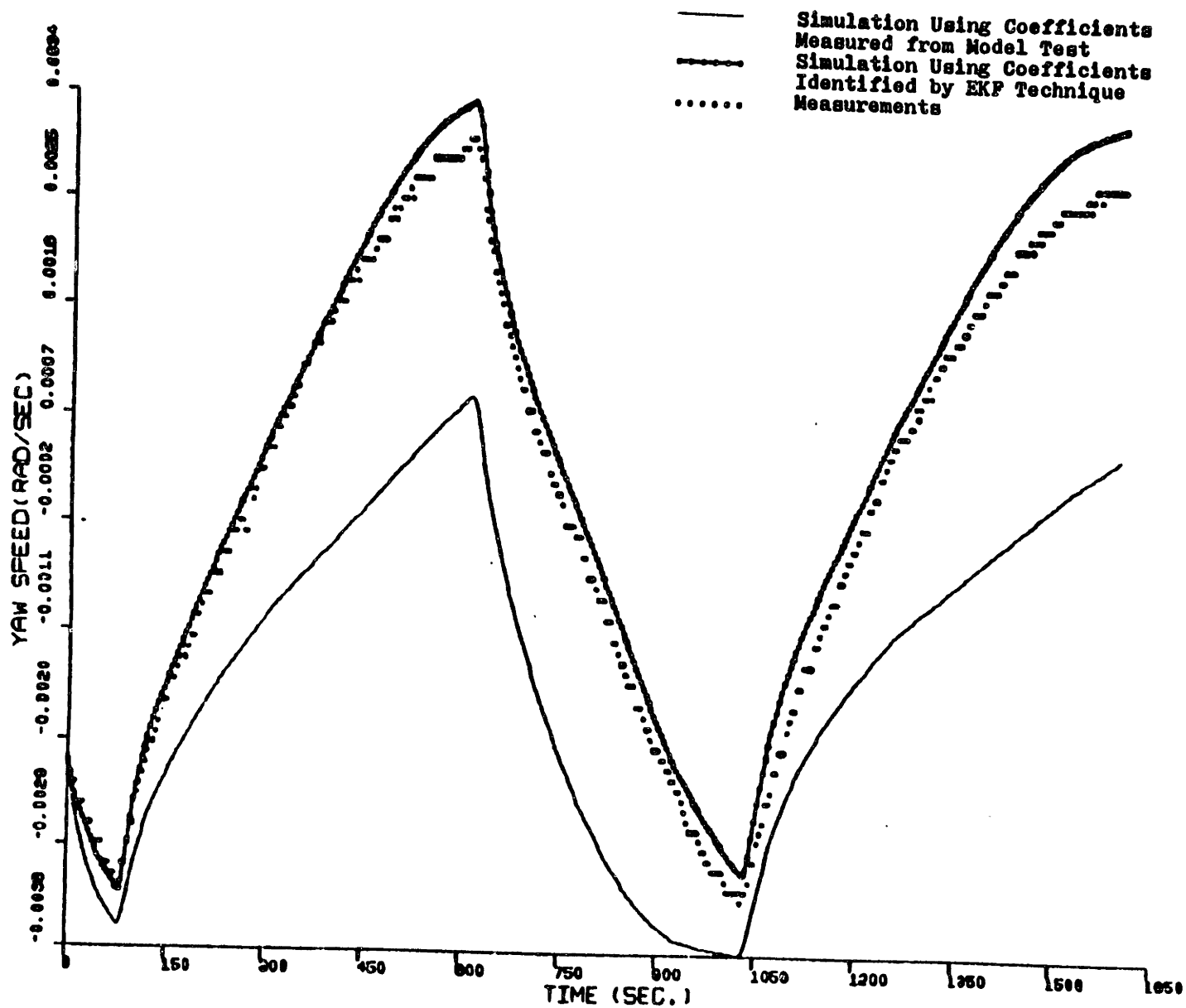

fig.4.2.4(c) Comparison between the Simulation of 10^{o}-10^{o} Maneuver by Using the Coefficients "Measured" from Model Test and Identified with Two Measurements----Yaw Speed r.

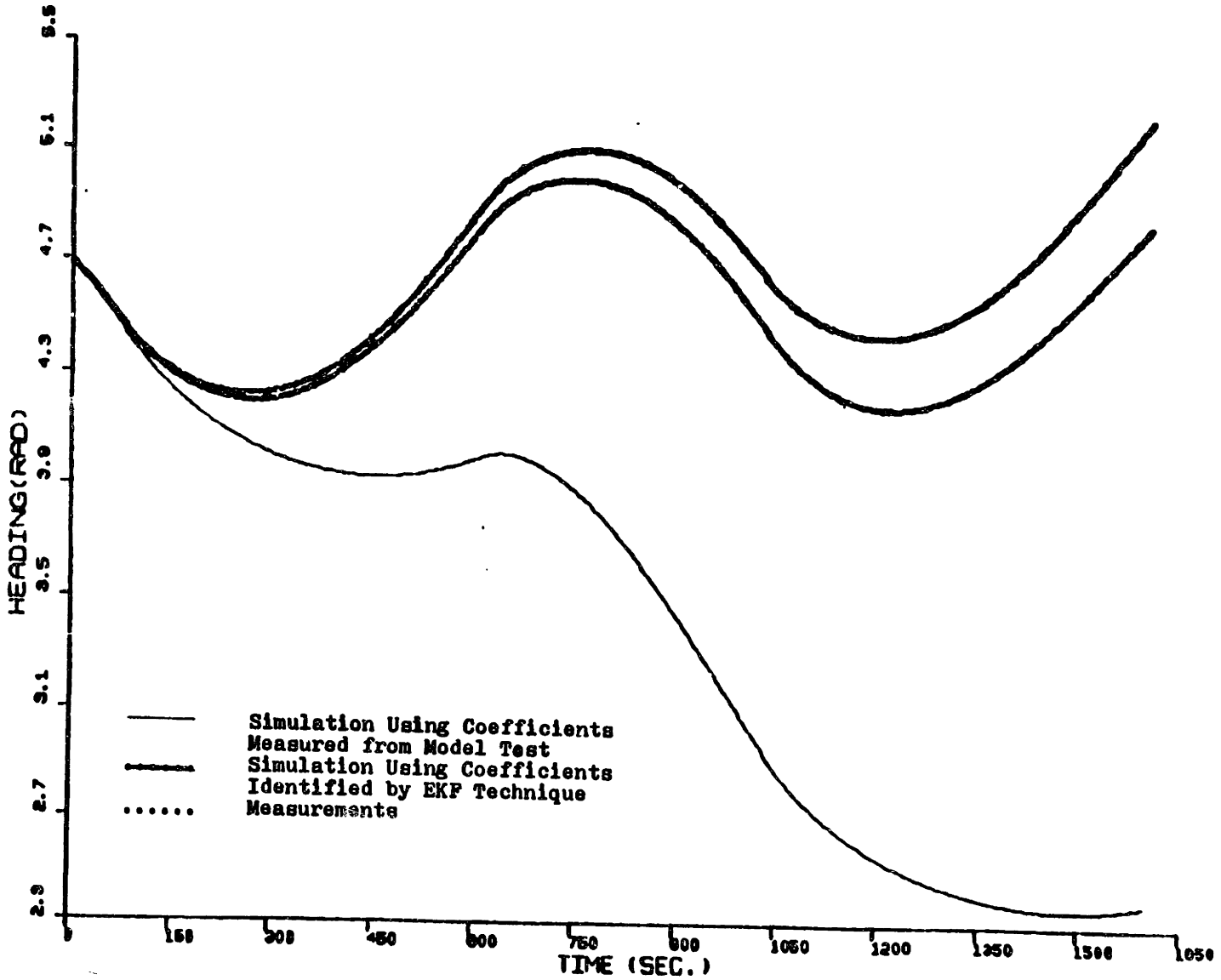

fig.4.2.4(d) Comparison between the Simulation of 10^{o}-10^{o} Maneuver by Using the Coefficients "Measured" from Model Test and Identified with Two Measurements----Yaw Angle ψ.

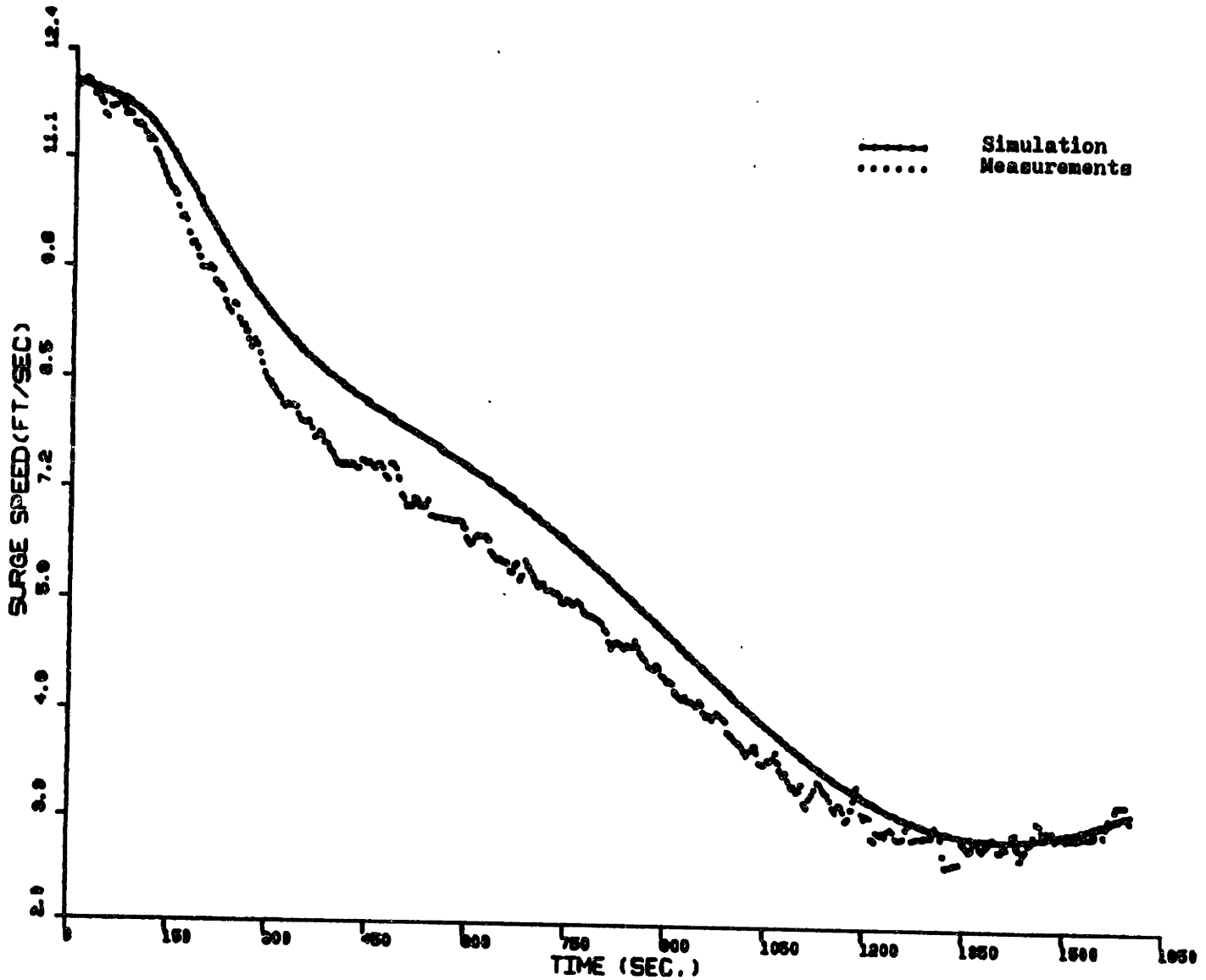

fig.4.2.5(a) Comparison between the Measurements and the Simulation of the Maneuver of 35^{o} Turning by Using the Coefficients Identified with Two Measurements----Surge Speed u.

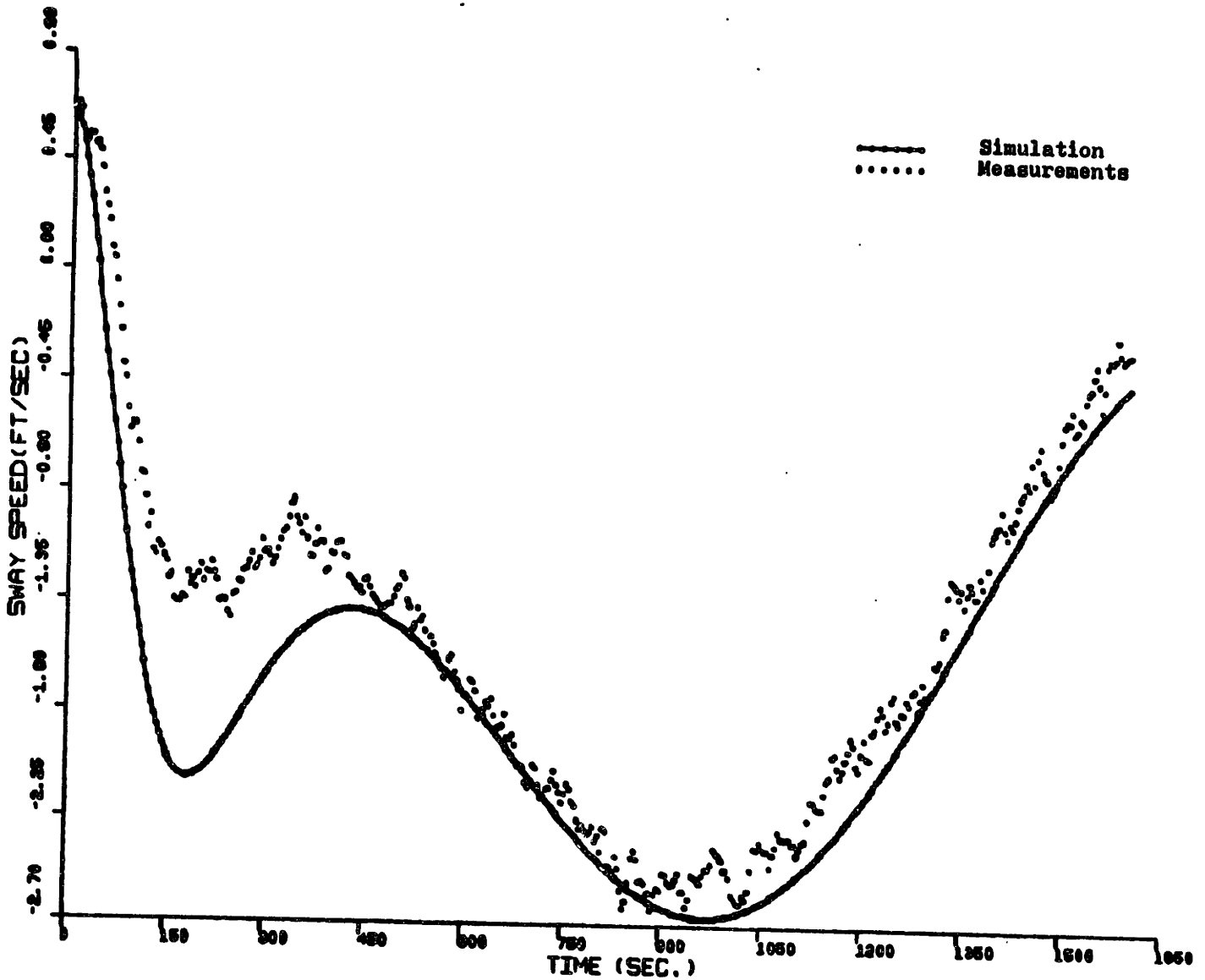

fig.4.2.5(b) Comparison between the Measurements and the Simulation of the Maneuver of 35^{o} Turning by Using the Coefficients Identified with Two Measurements----Sway Speed v.

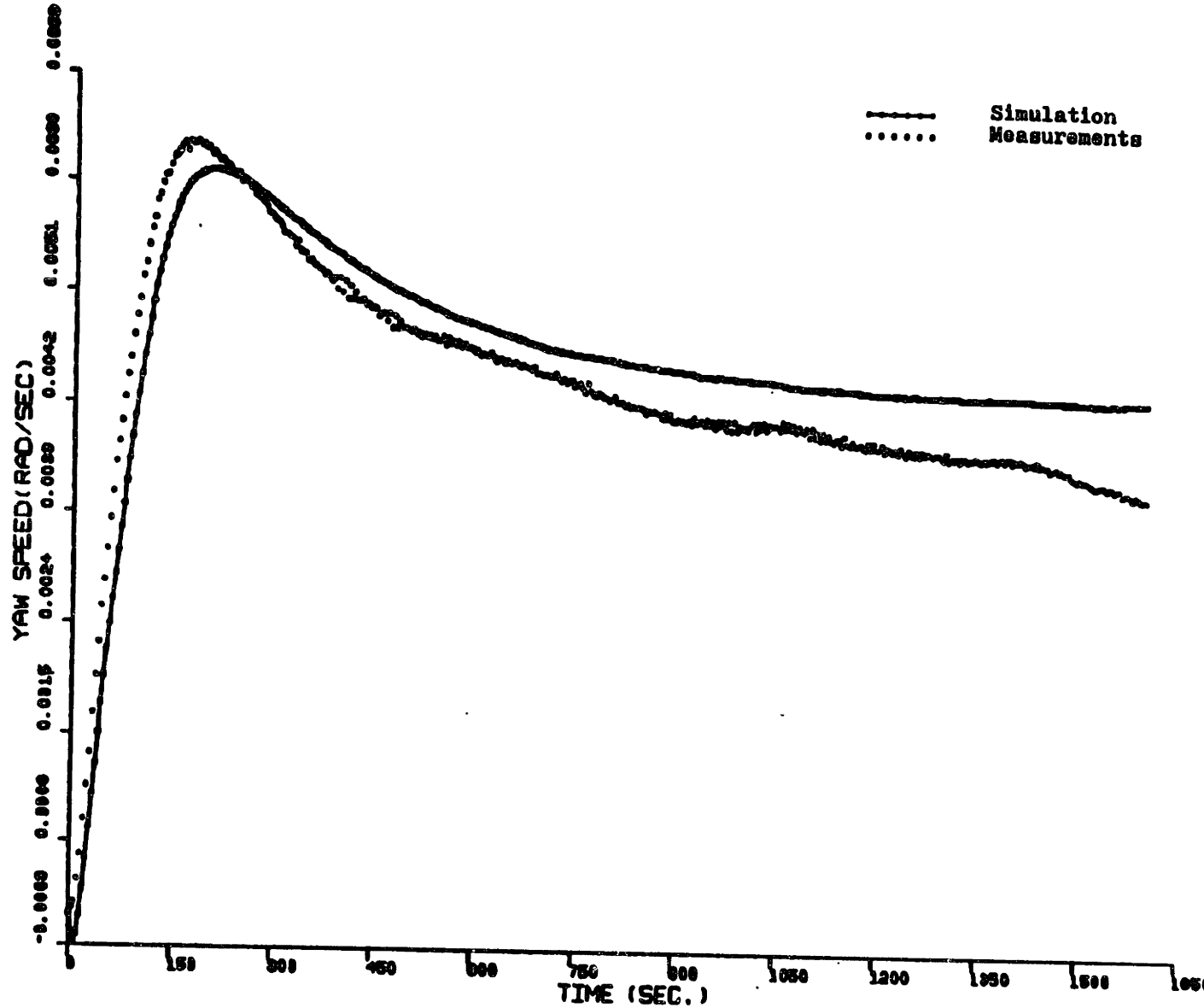

fig.4.2.5(c) Comparison between the Measurements and the Simulation of the Maneuver of 35° Turning by Using the Coefficients Identified with Two Measurements----Yaw Speed r.

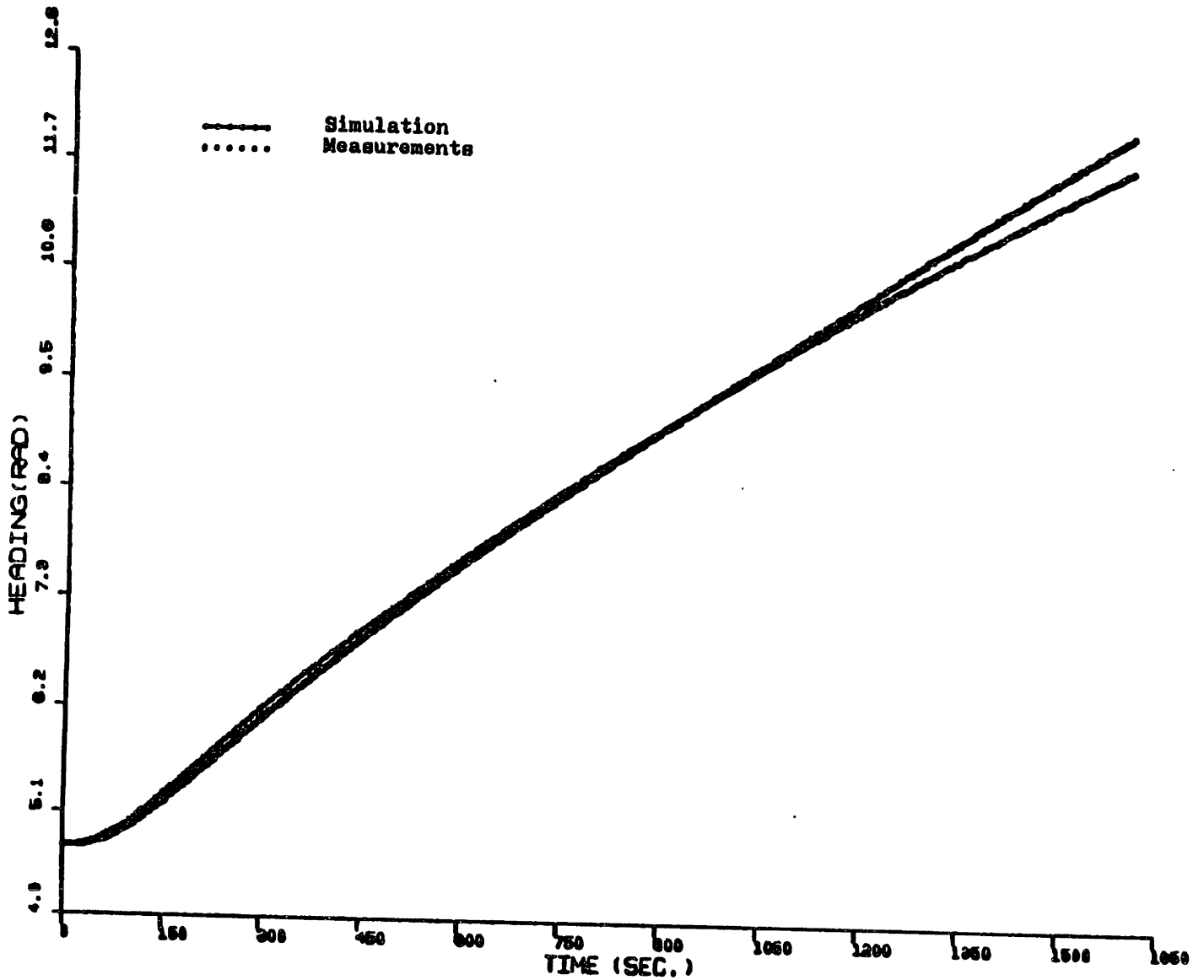

fig.4.2.5(d) Comparison between the Measurements and the Simulation of the Maneuver of 35° Turning by Using the Coefficients Identified with Two Measurements----Yaw Angle ψ.

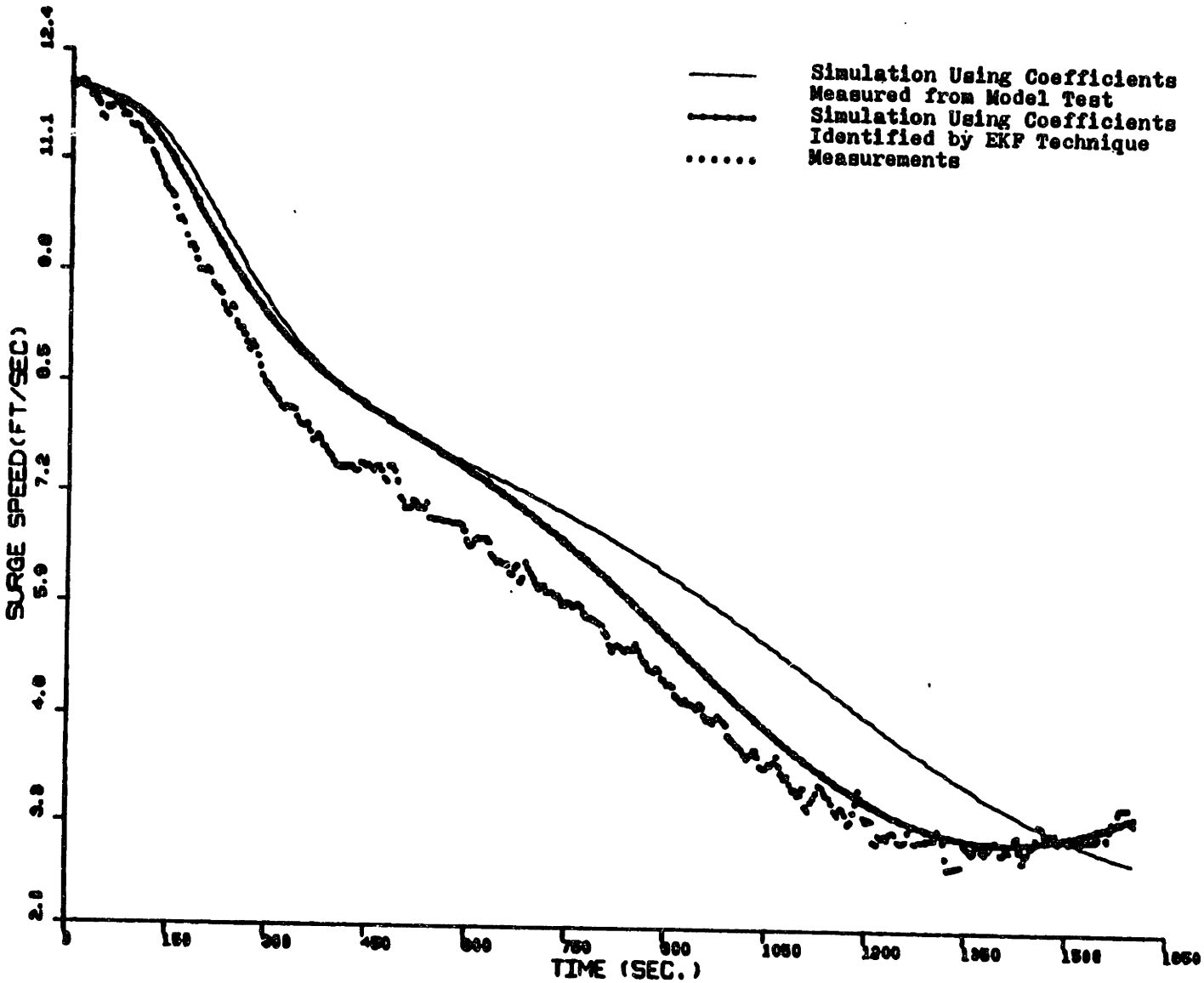

fig.4.2.6(a) Comparison between the Simulations of the Maneuver of 35^{o} Turning by Using the Coefficients "Measured" from Model Test and Identified with Two Measurements----Surge Speed u.

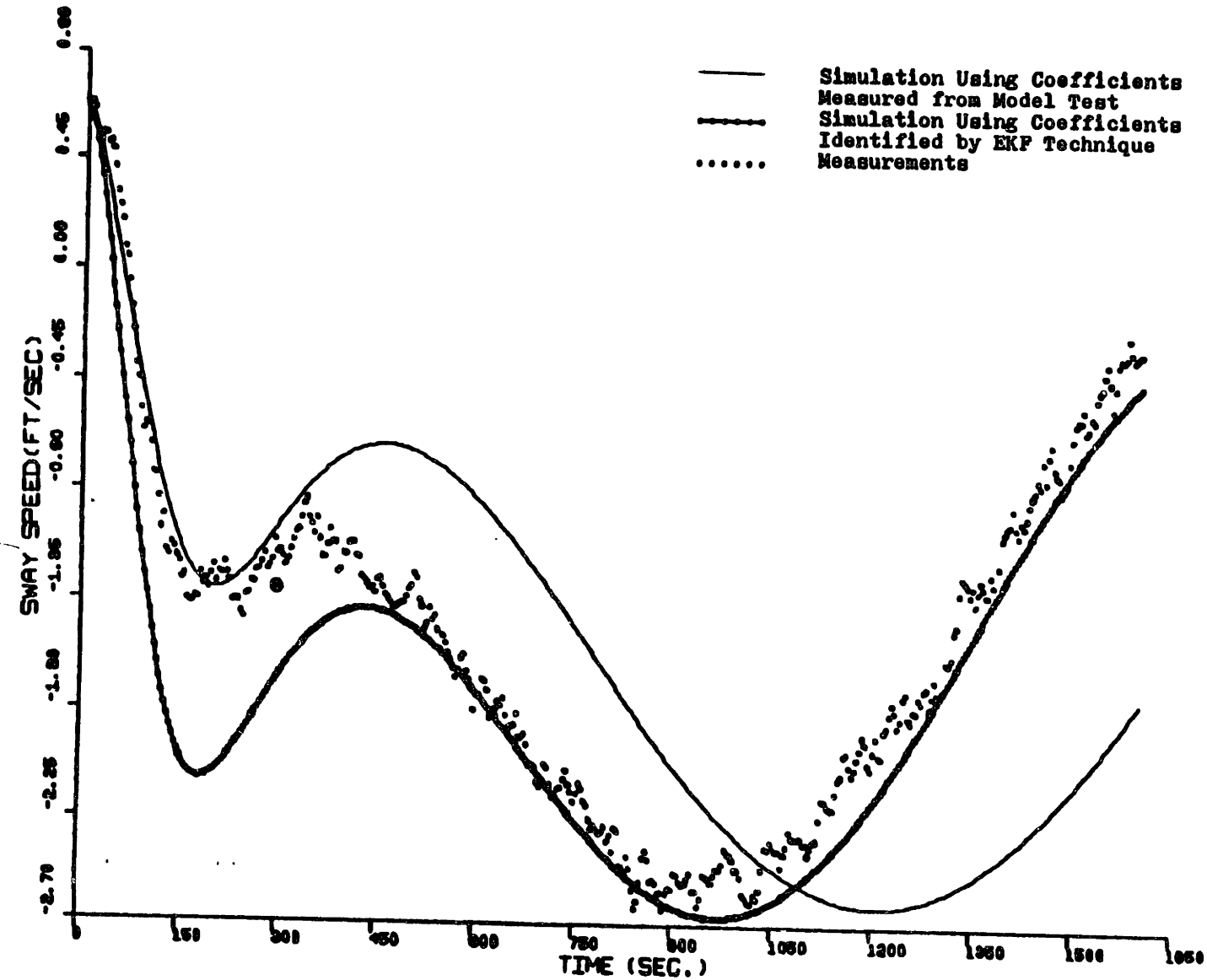

fig.4.2.6(b) Comparison between the Simulations of the Maneuver of 35° Turning by Using the Coefficients "Measured" from Model Test and Identified with Two Measurements----Sway Speed v.

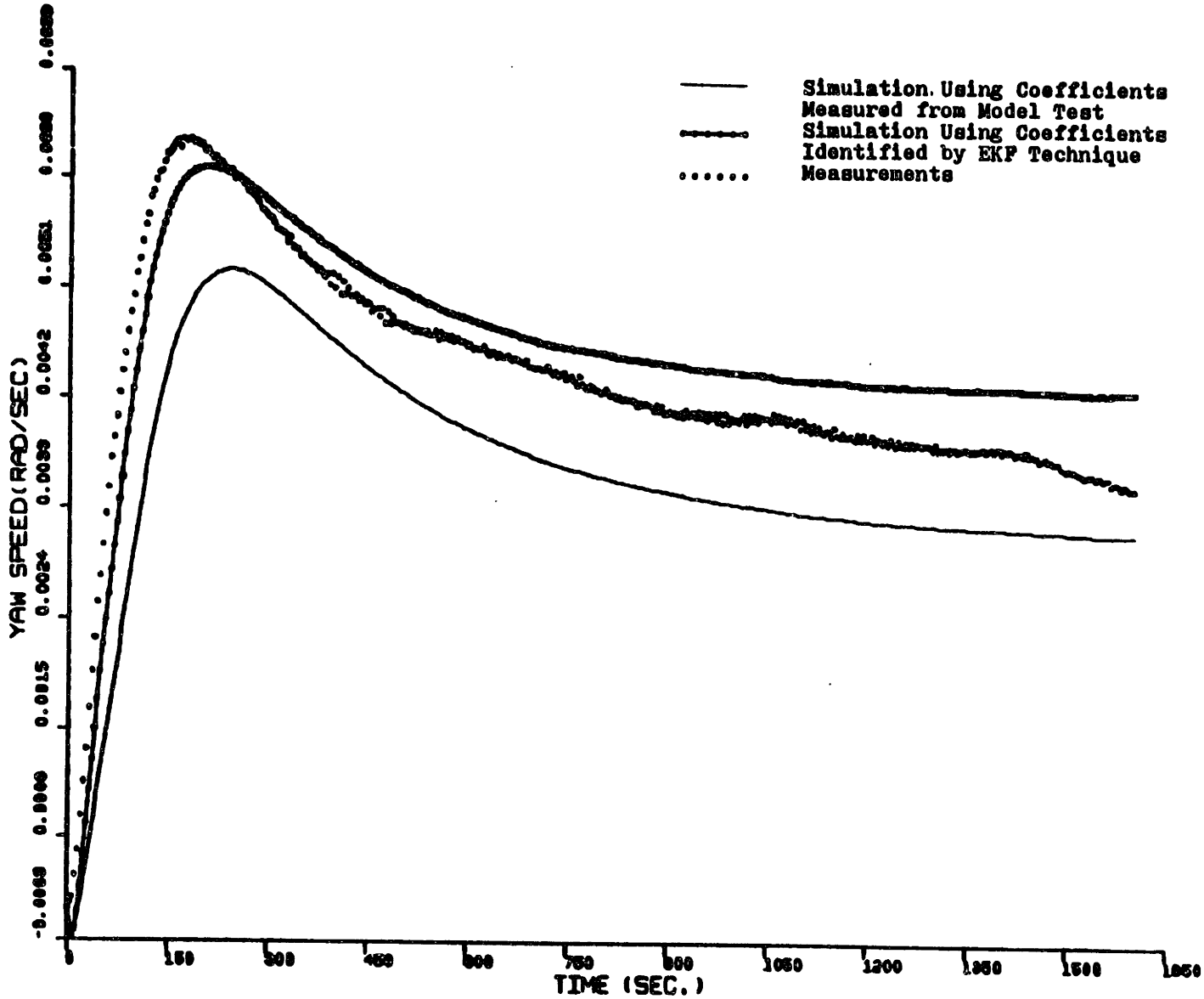

fig.4.2.6(c) Comparison between the Simulations of the Maneuver of 35^{o} Turning by Using the Coefficients "Measured" from Model Test and Identified with Two Measurements----Yaw Speed r.

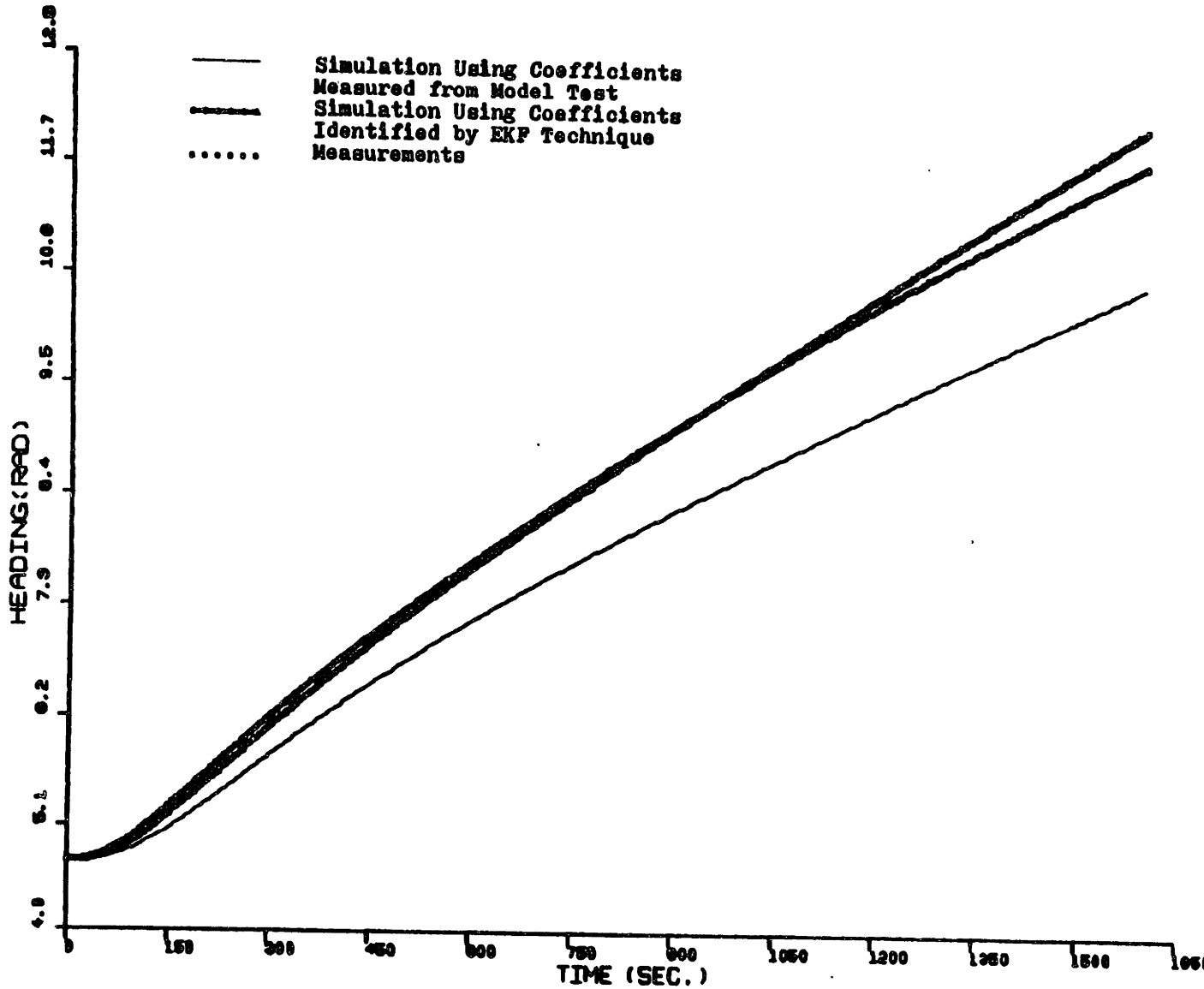

fig.4.2.6(d) Comparison between the Simulations of the Maneuver of 35^{o} Turning by Using the Coefficients "Measured" from Model Test and Identified with Two Measurements----Yaw Angle ψ.

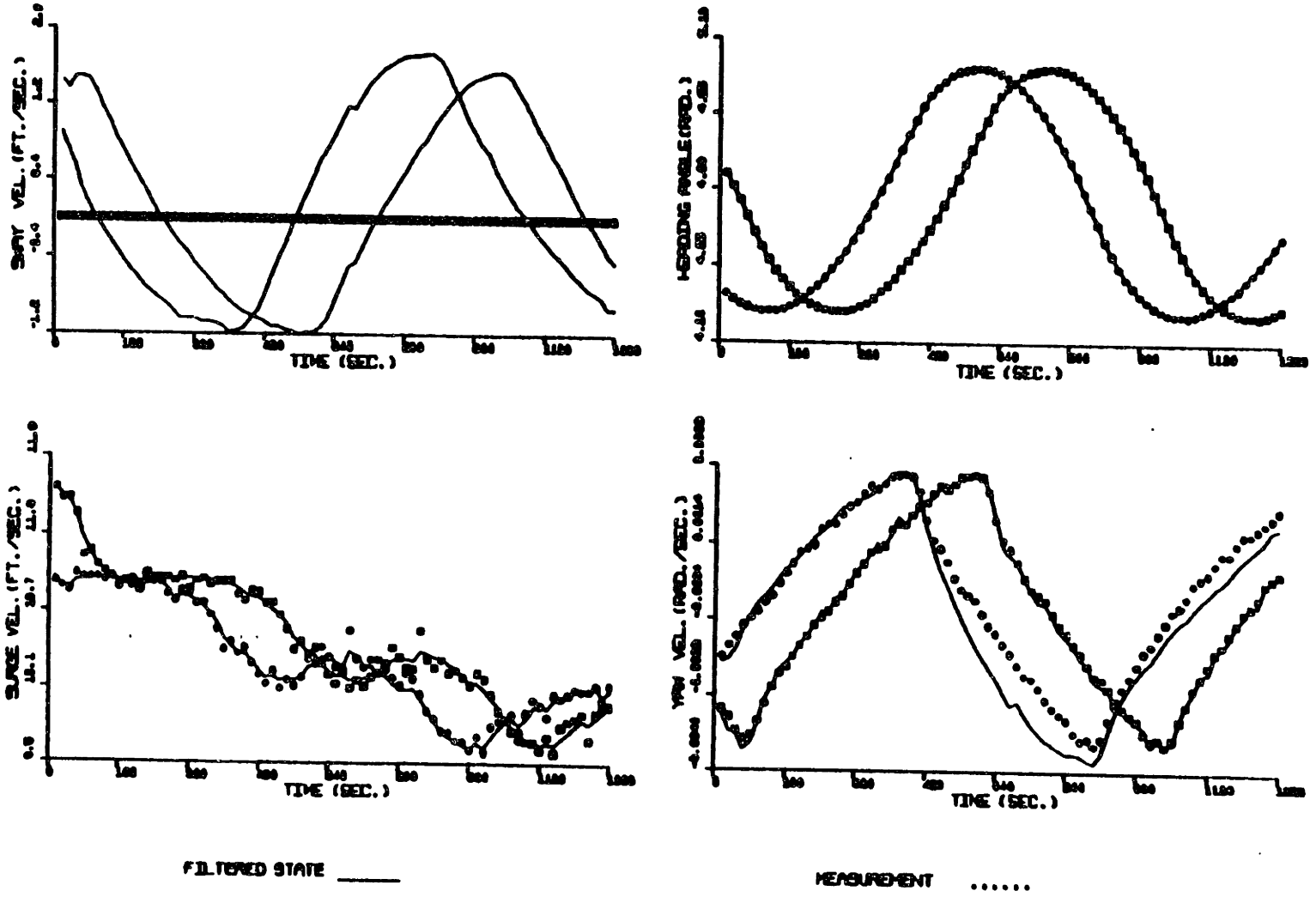

fig.4.3.1(a) Results of Identification of Linear Coefficients with Measured u, ψ and Derived $\dot{\psi}$.

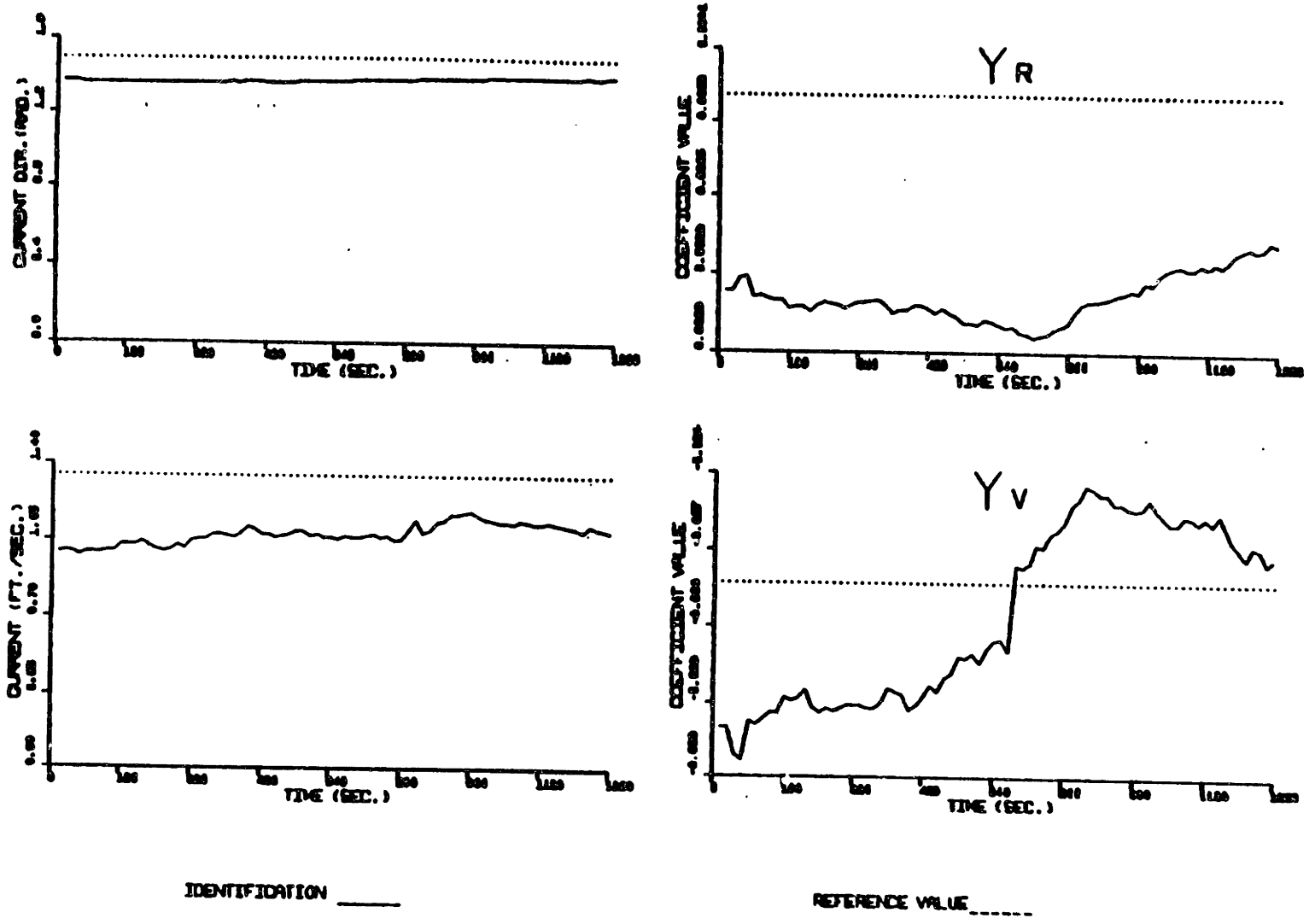

fig.4.3.1(b) Results of Identification of Linear Coefficients with Measured u, ψ and Derived $\dot{\psi}$.

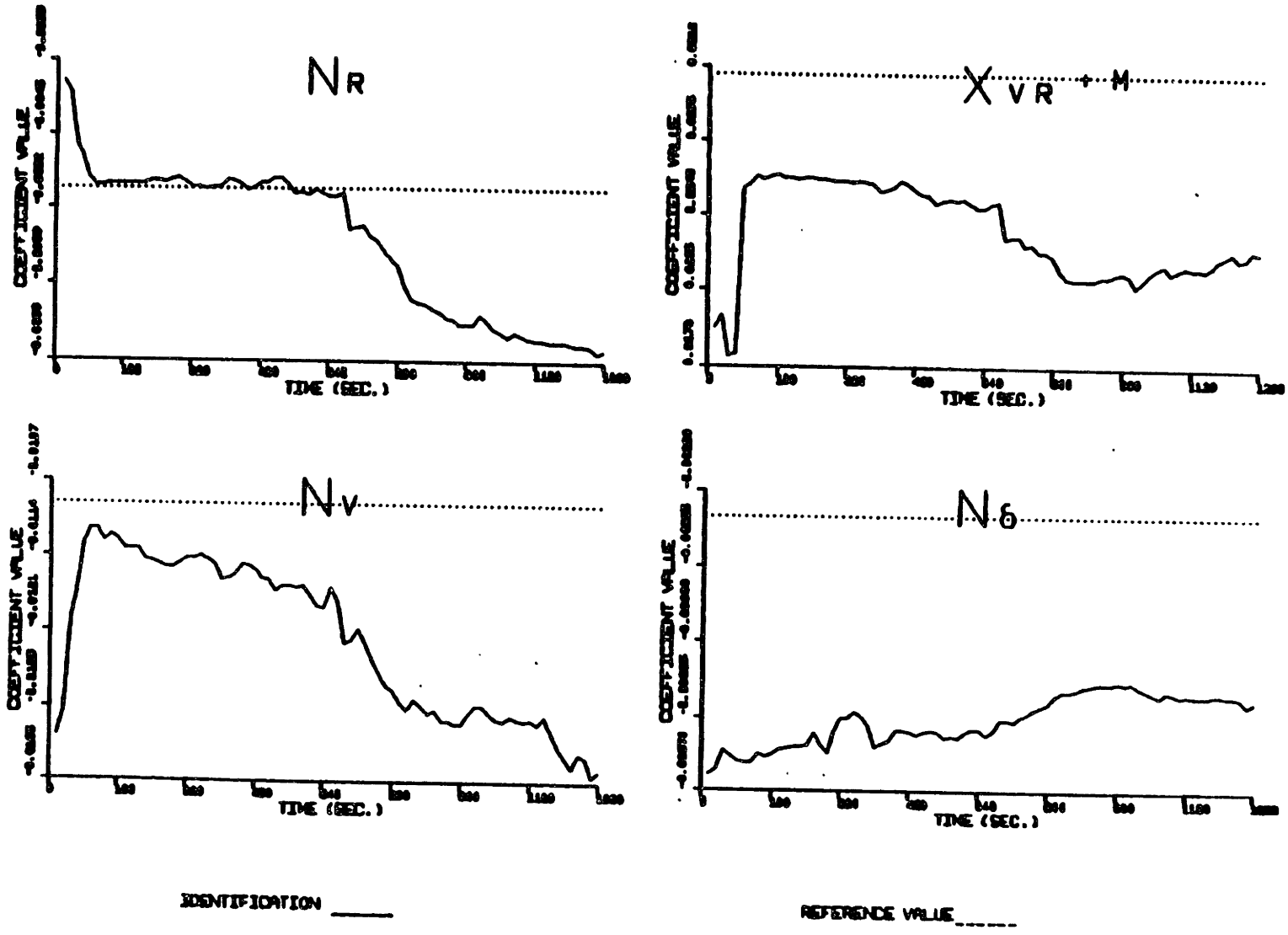

fig.4.3.1(c) Results of Identification of Linear Coefficients with Measured u, ψ and Derived $\dot{\psi}$.

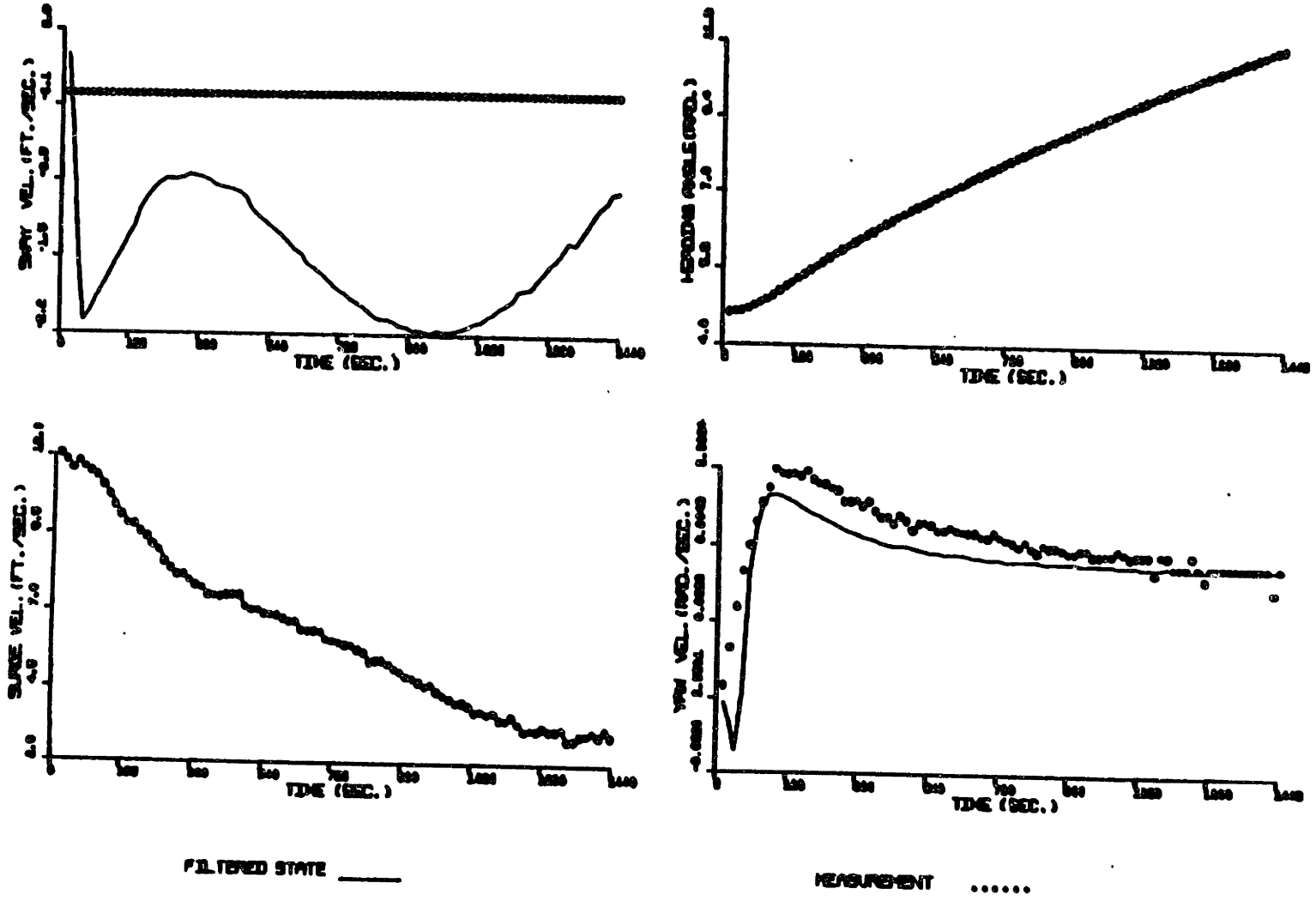

fig.4.3.2(a) Results of Identification of Nonlinear Coefficients with Measured u, ψ and Derived $\dot{\psi}$.

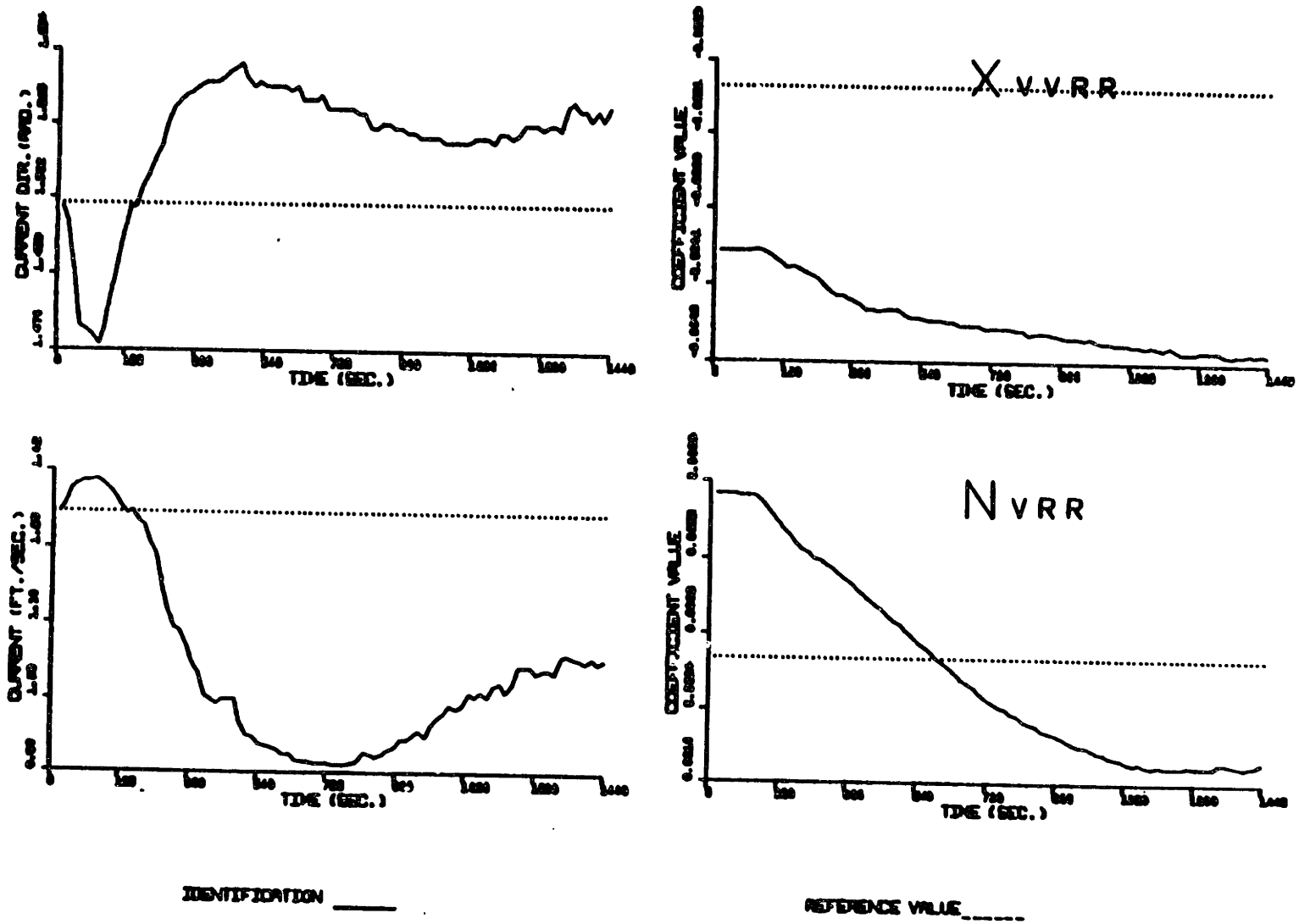

fig.4.3.2(b) Results of Identification of Nonlinear Coefficients with Measured u, ψ and Derived $\dot{\psi}$.

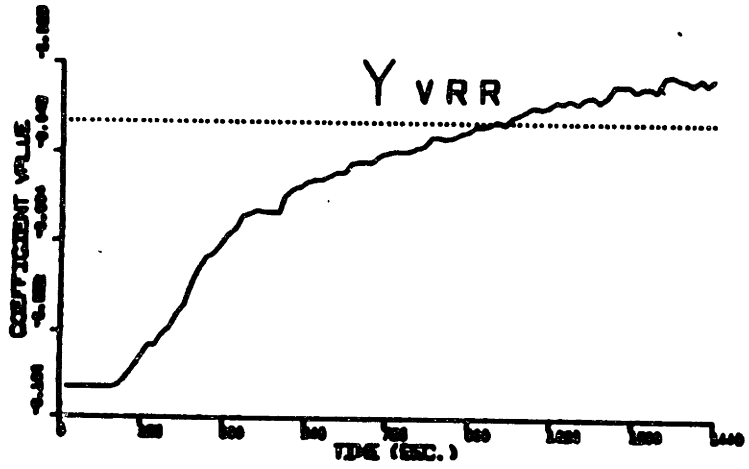

IDENTIFICATION _____ REFERENCE VALUE_____

fig.4.3.2(c) Results of Identification of Nonlinear Coefficients with Measured u, ψ and Derived $\dot{\psi}$.

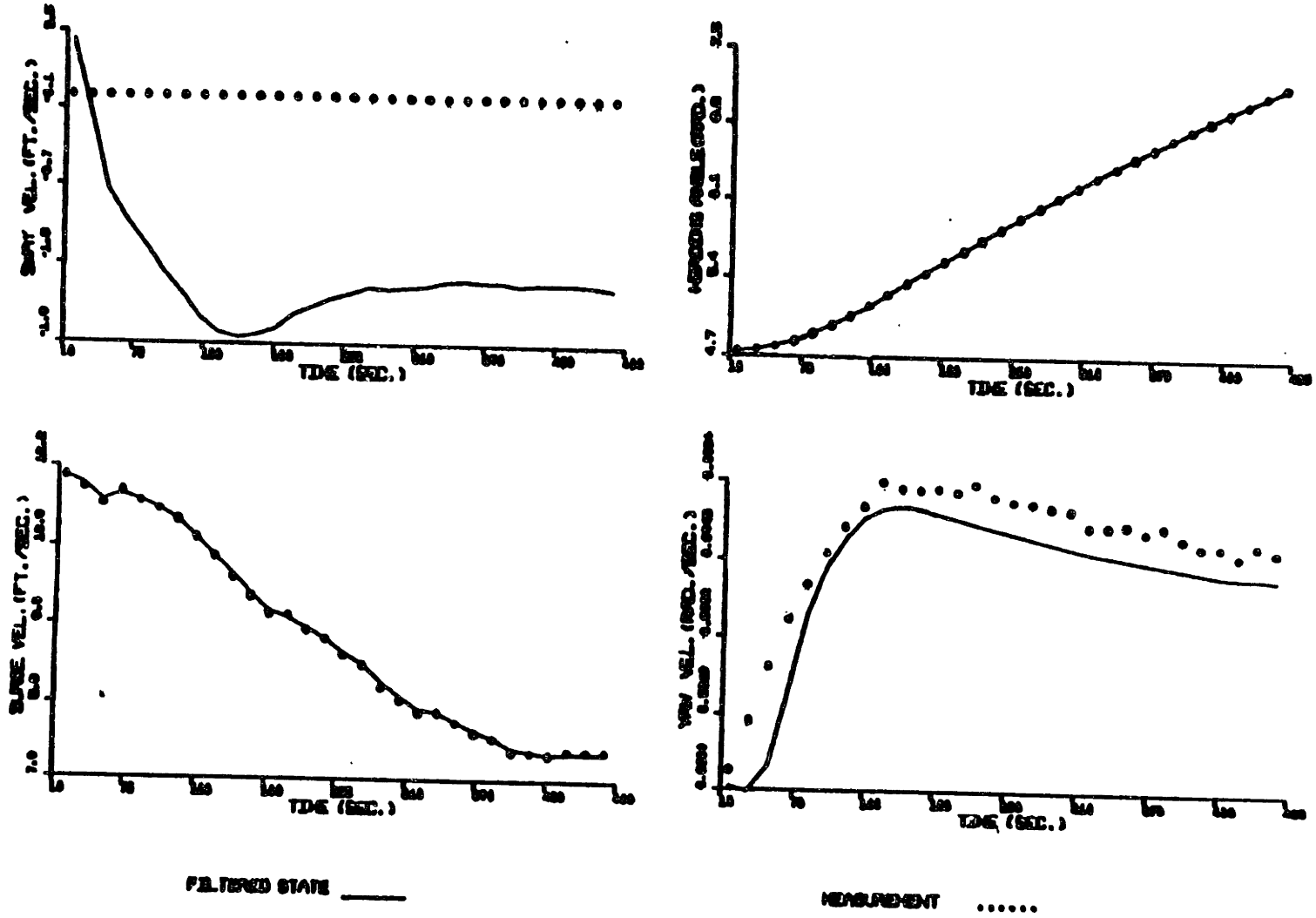

fig.4.3.2(d) Results of Identification of Nonlinear Coefficients with Measured u, ψ and Derived $\dot{\psi}$.

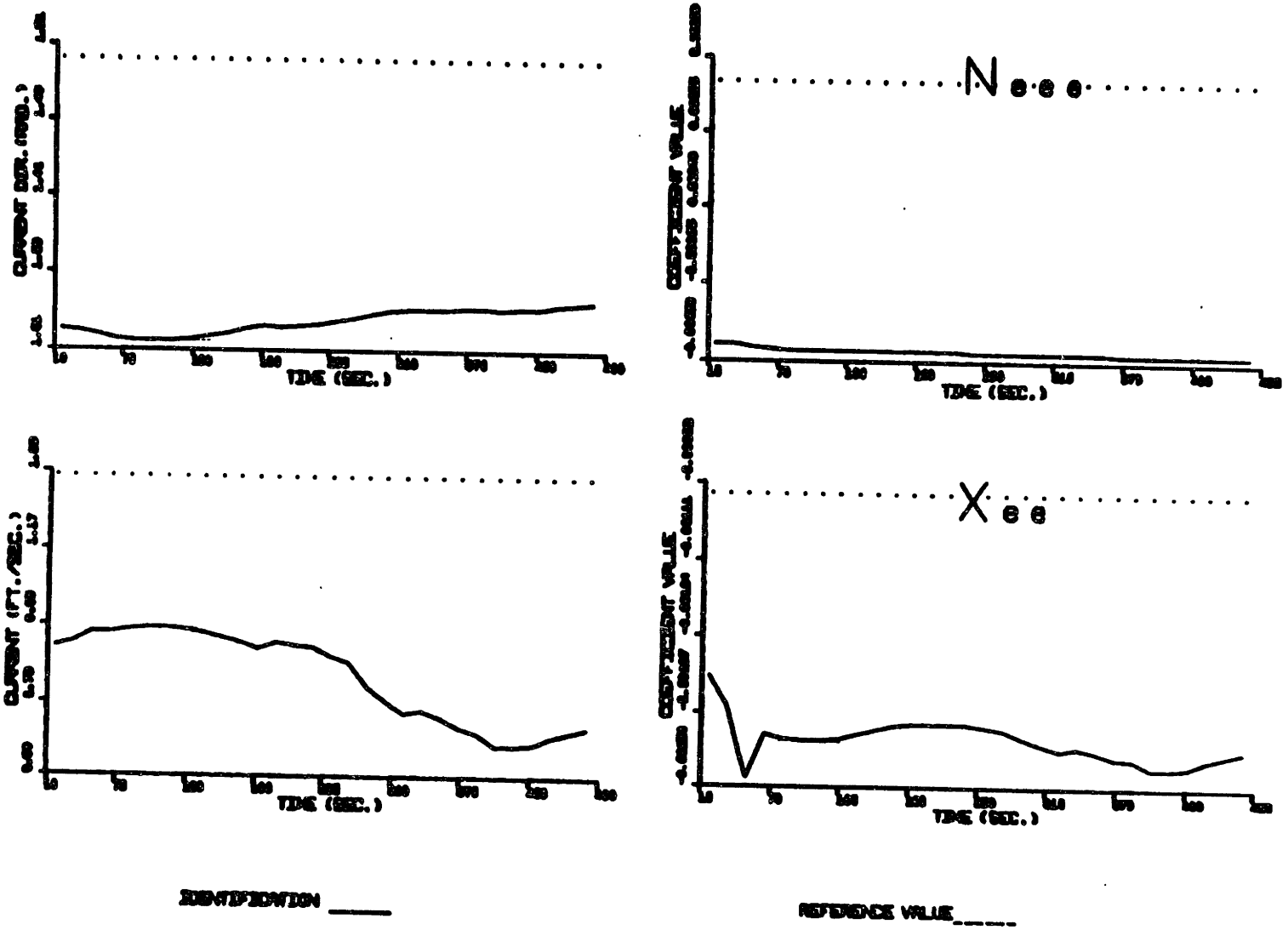

fig.4.3.2(e) Results of Identification of Nonlinear Coefficients with Measured u, ψ and Derived $\dot{\psi}$.

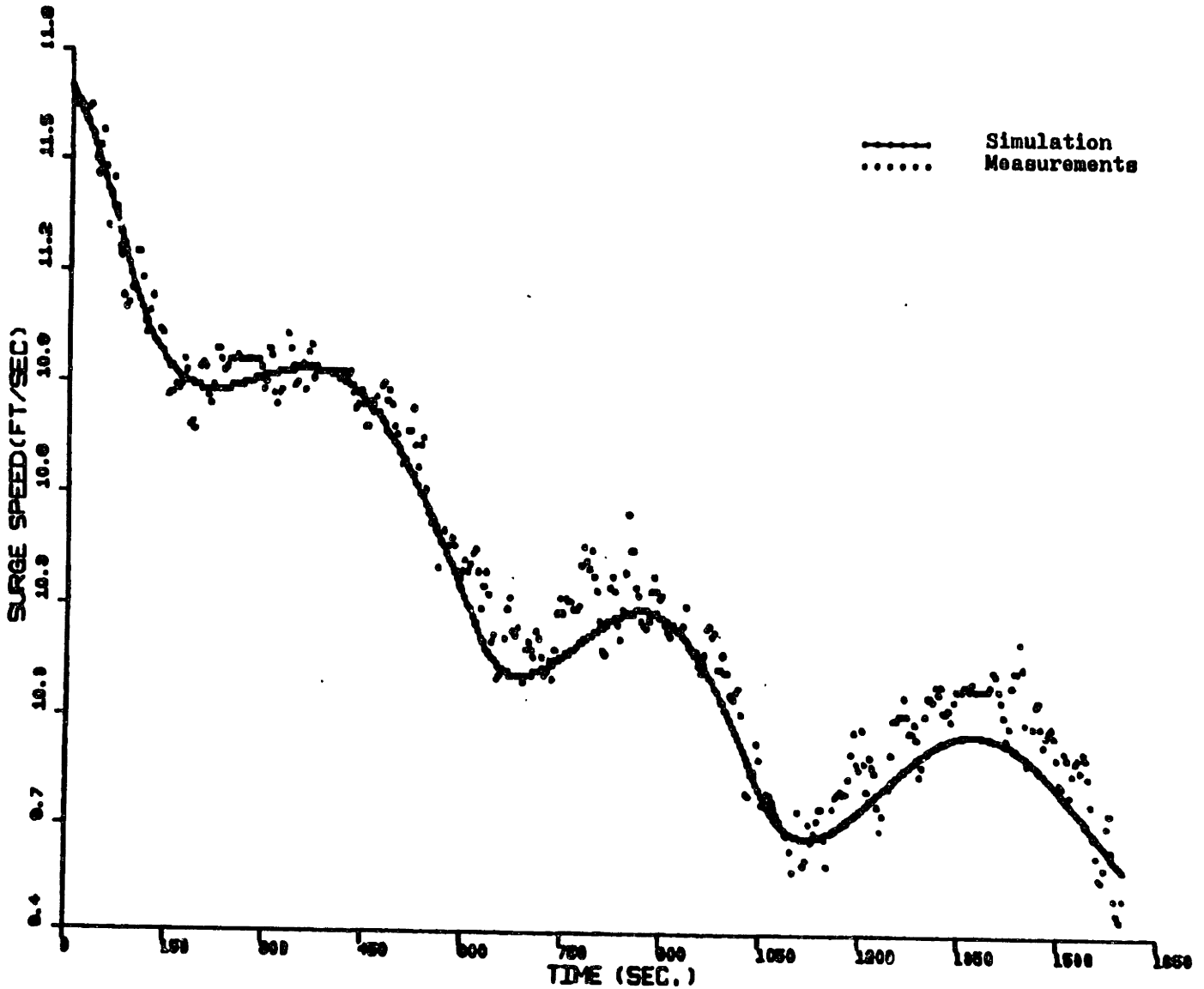

fig.4.3.3(a) Comparison between the Measurements and the Simulation of 10^{o}-10^{o} Maneuver by Using the Coefficients Identified with Measured u, ψ and Derived $\dot{\psi}$----Surge Speed u.

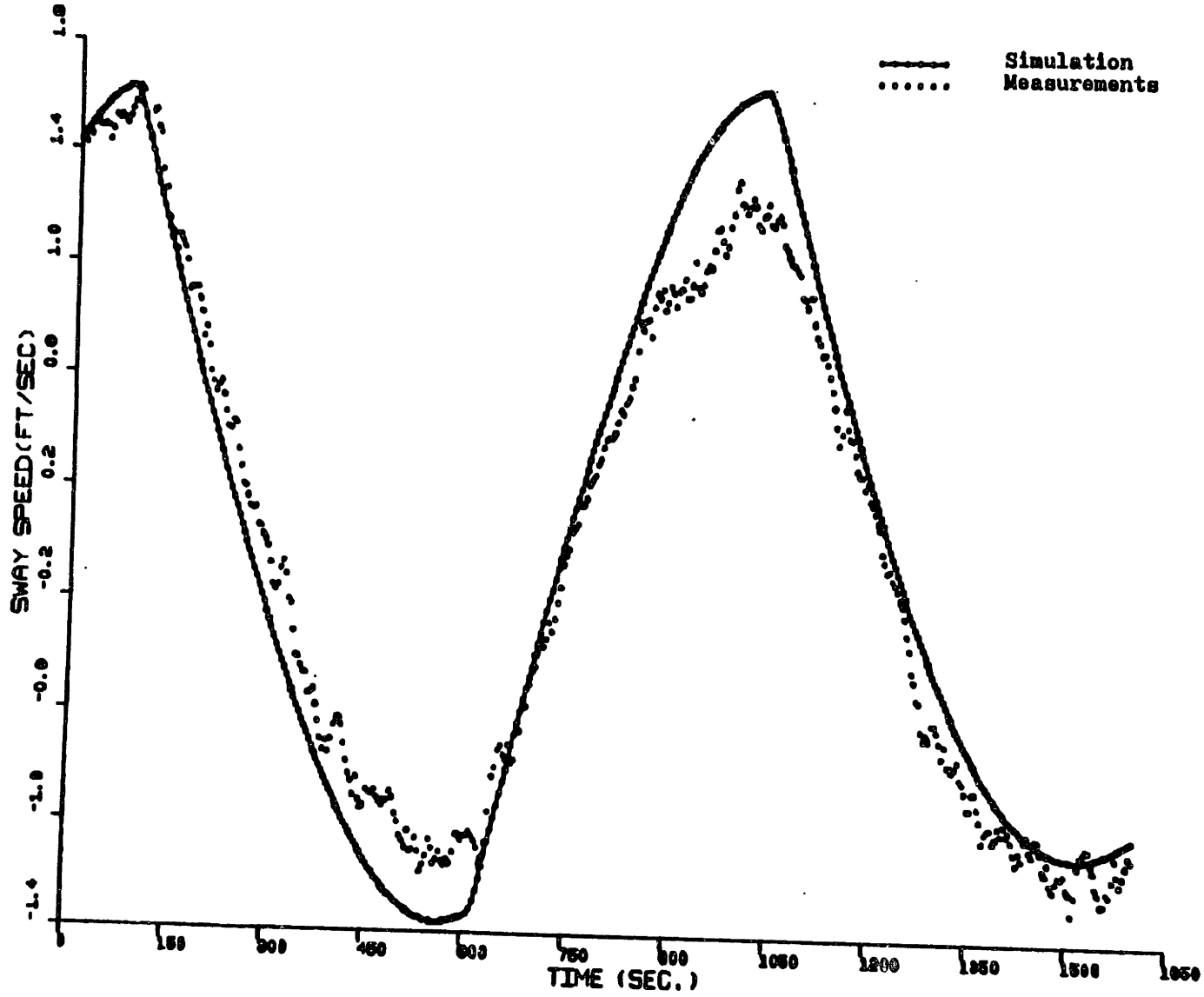

fig.4.3.3(b) Comparison between the Measurements and the Simulation of 10^{o}-10^{o} Maneuver by Using the Coefficients Identified with Measured u, ψ and Derived $\dot{\psi}$ ----Sway Speed v.

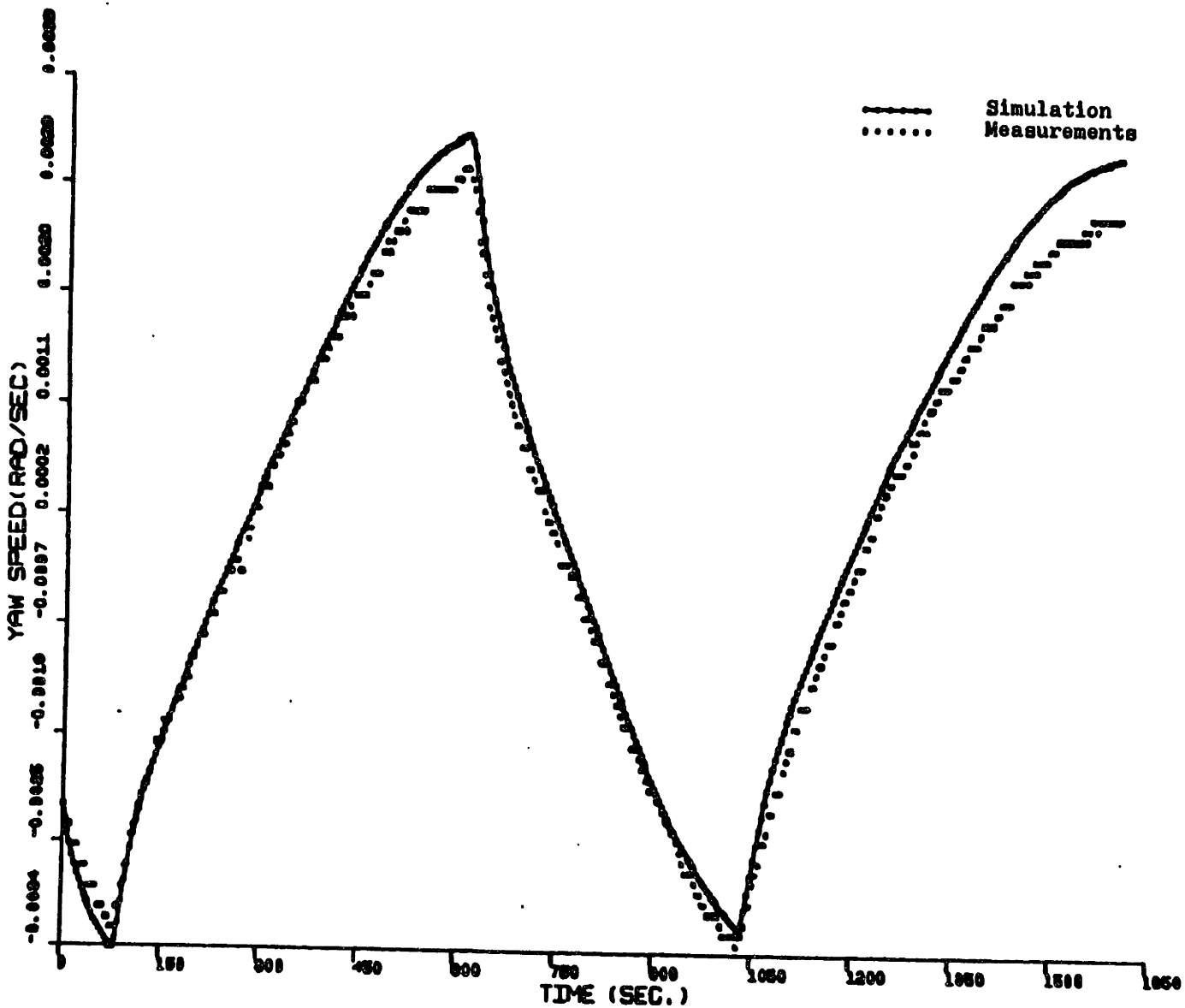

fig.4.3.3(c) Comparison between the Measurements and the Simulation of 10^{o}-10^{o} Maneuver by Using the Coefficients Identified with Measured u, ψ and Derived $\dot{\psi}$----Yaw Speed r.

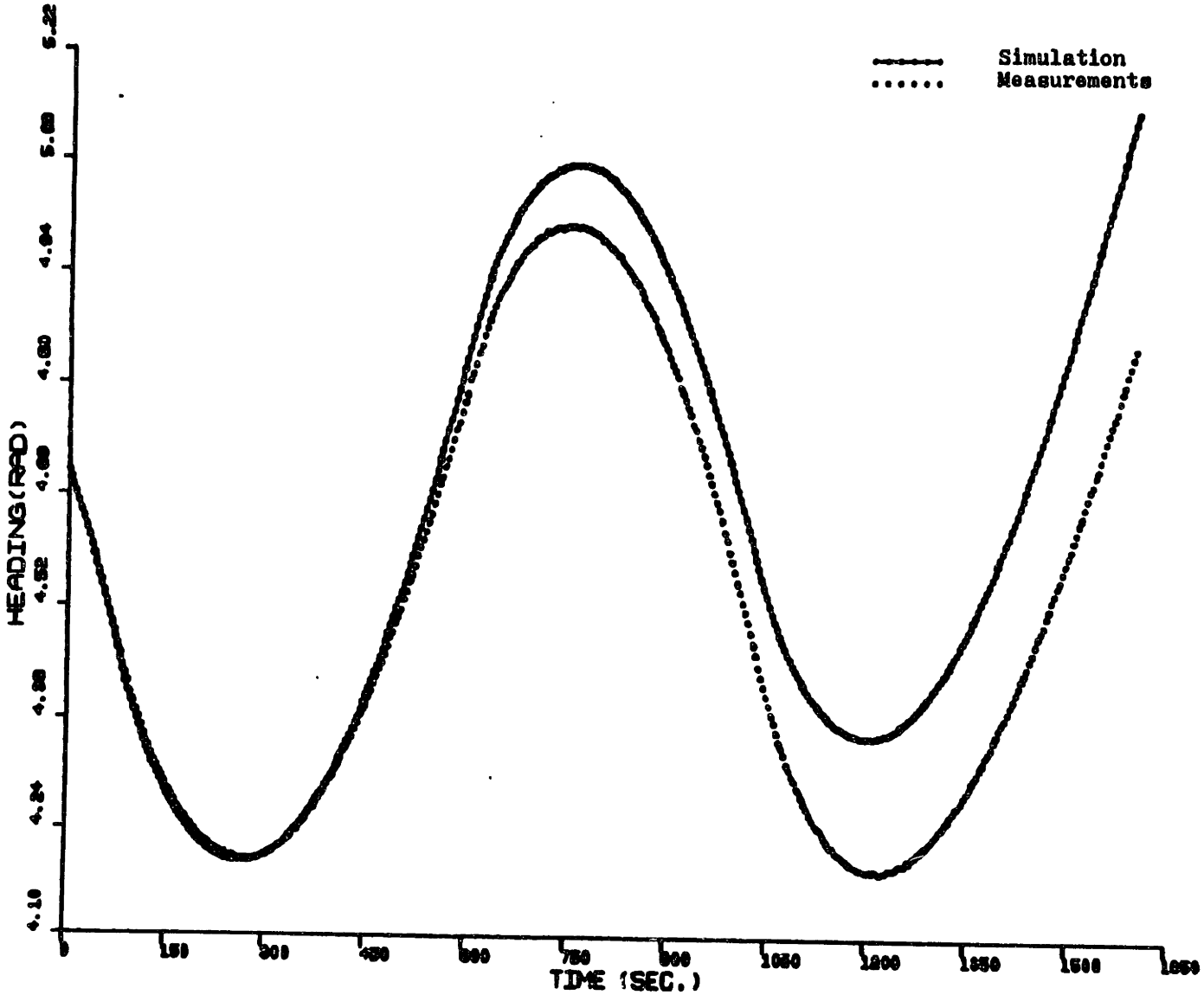

fig.4.3.3(d) Comparison between the Measurements and the Simulation of 10^{o}-10^{o} Maneuver by Using the Coefficients Identified with Measured u, ψ and Derived $\dot{\psi}$----Yaw Angle ψ.

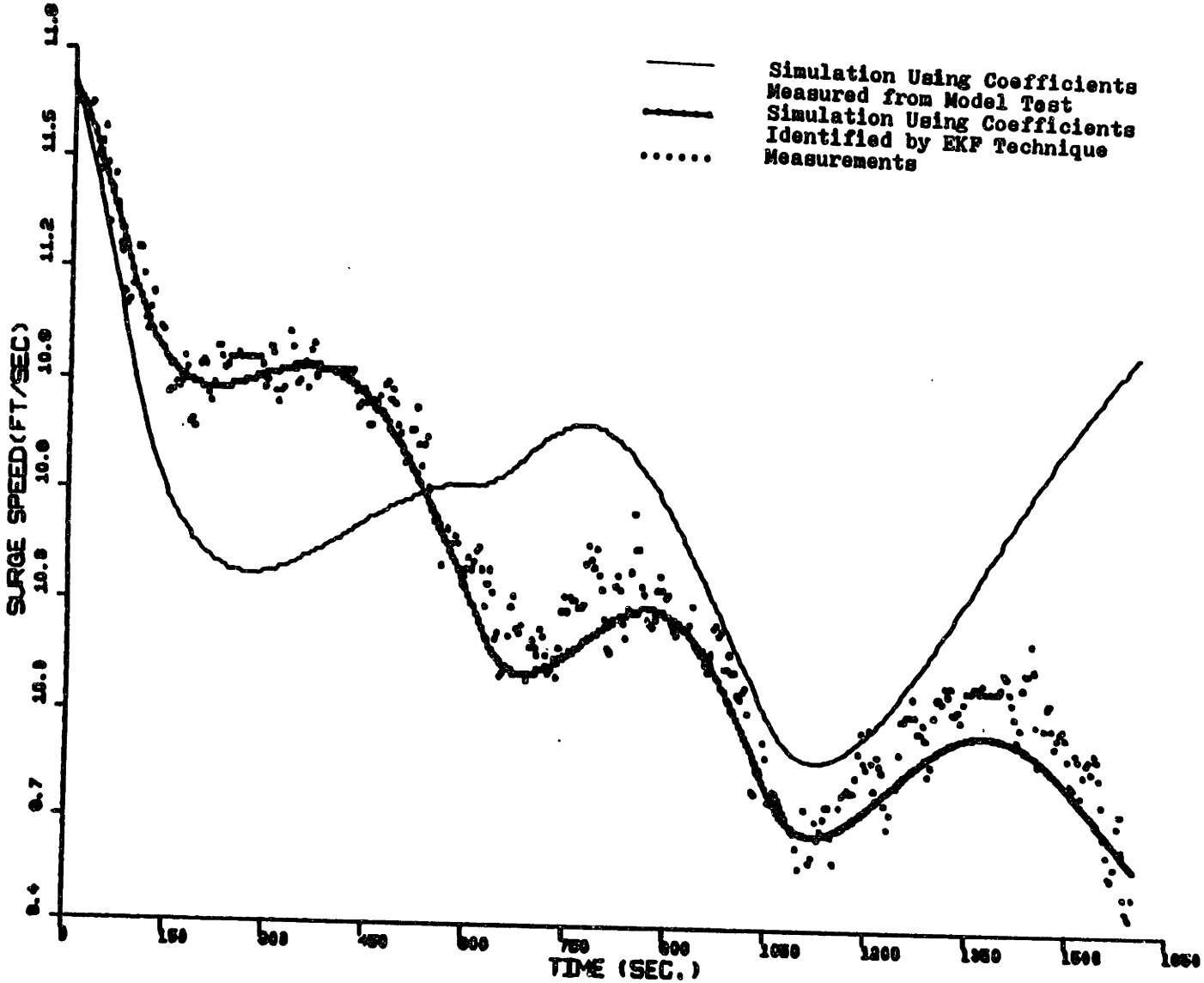

fig.4.3.4(a) Comparison between the Simulations of the Maneuver of 10^{o}-10^{o} Zigzag by Using the Coefficients "Measured" from Model Test and Identified with Measured u, ψ and Derived $\dot{\psi}$----Surge Speed u.

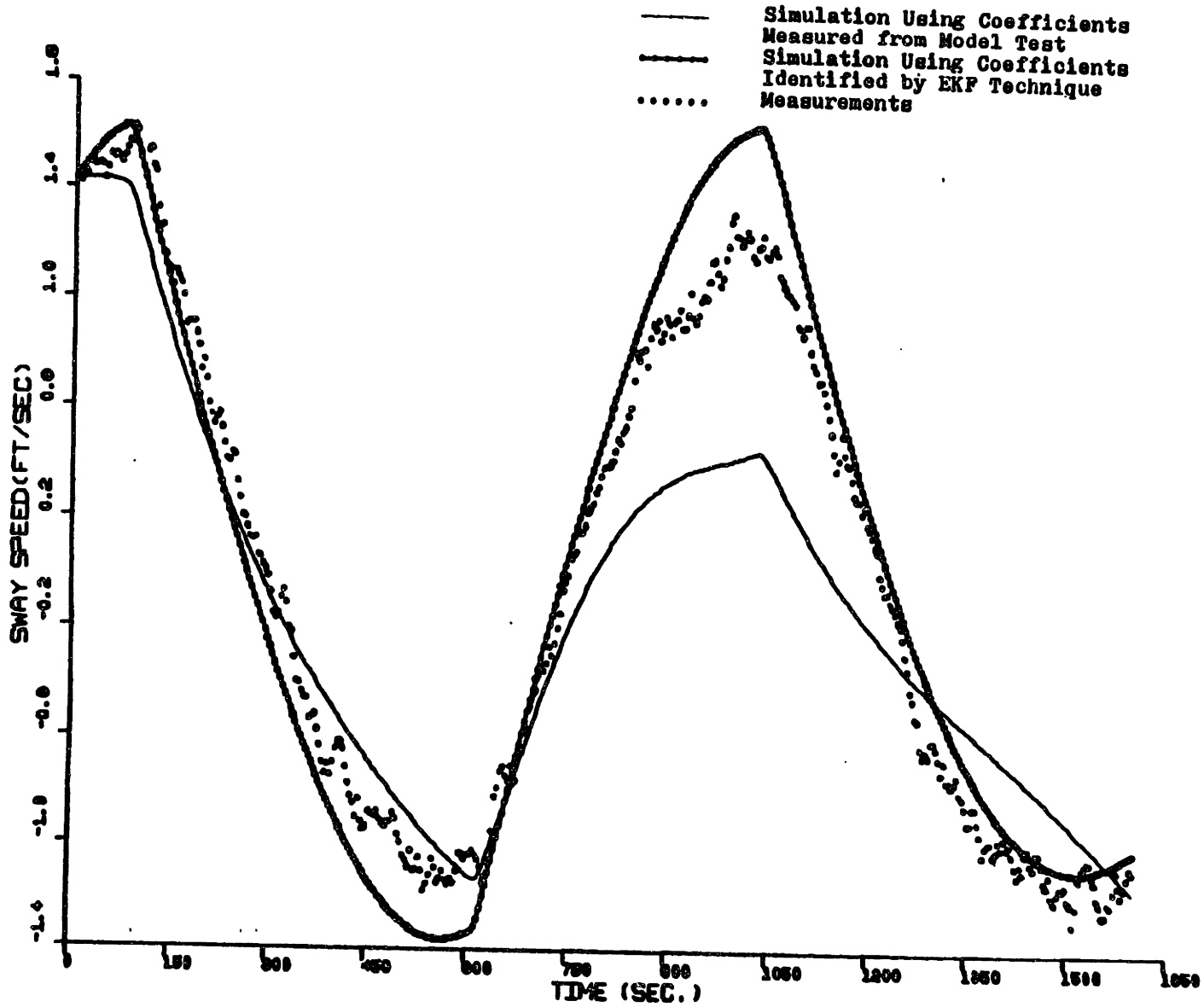

fig.4.3.4(b) Comparison between the Simulations of the Maneuver of 10^{o}-10^{o} Zigzag by Using the Coefficients "Measured" from Model Test and Identified with Measured u, ψ and Derived $\dot{\psi}$----Sway Speed v.

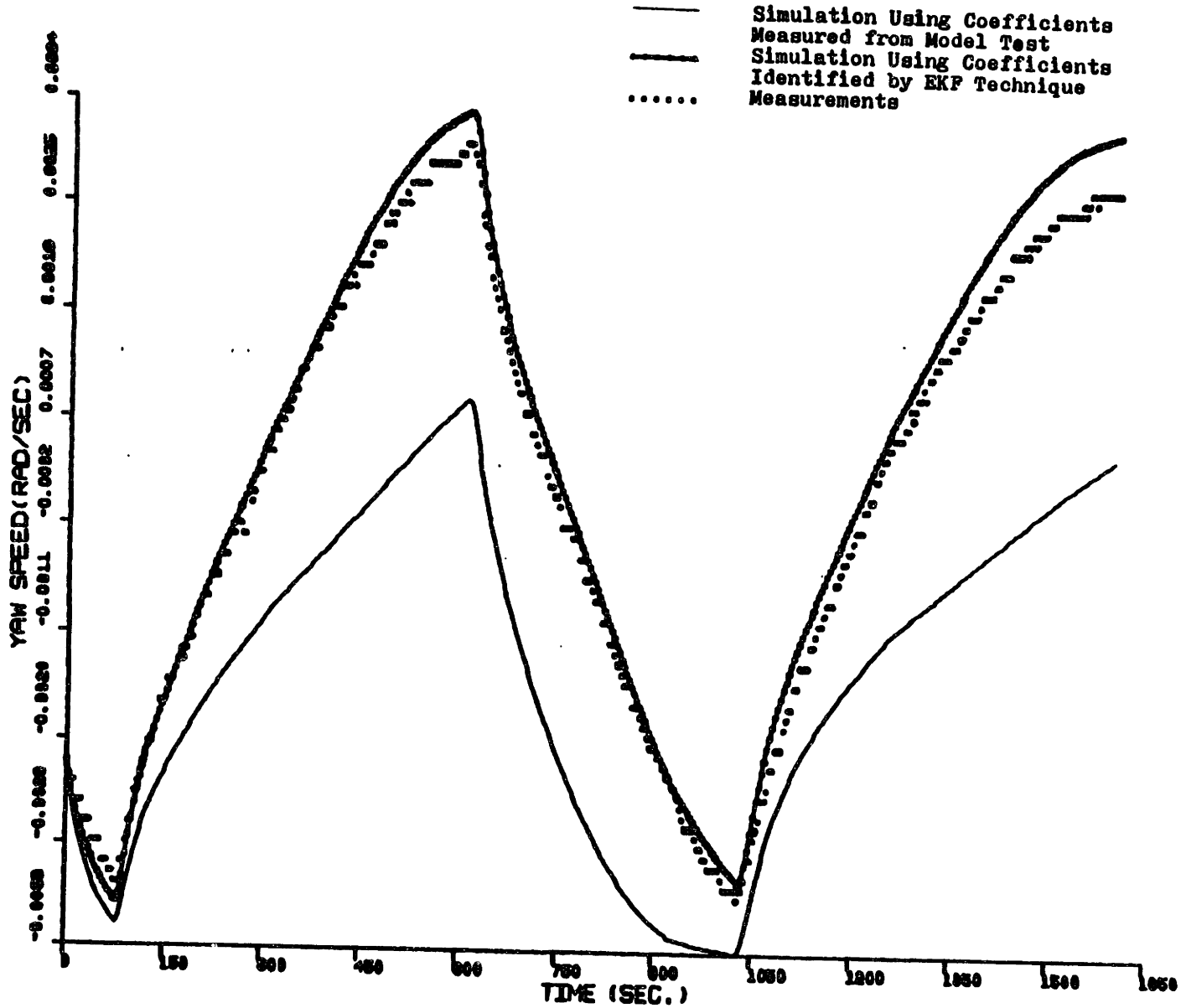

fig.4.3.4(c) Comparison between the Simulations of the Maneuver of 10^{o}-10^{o}Zigzag by Using the Coefficients "Measured" from Model Test and Identified with Measured u, φ and Derived $\dot{\psi}$----Yaw Speed r.

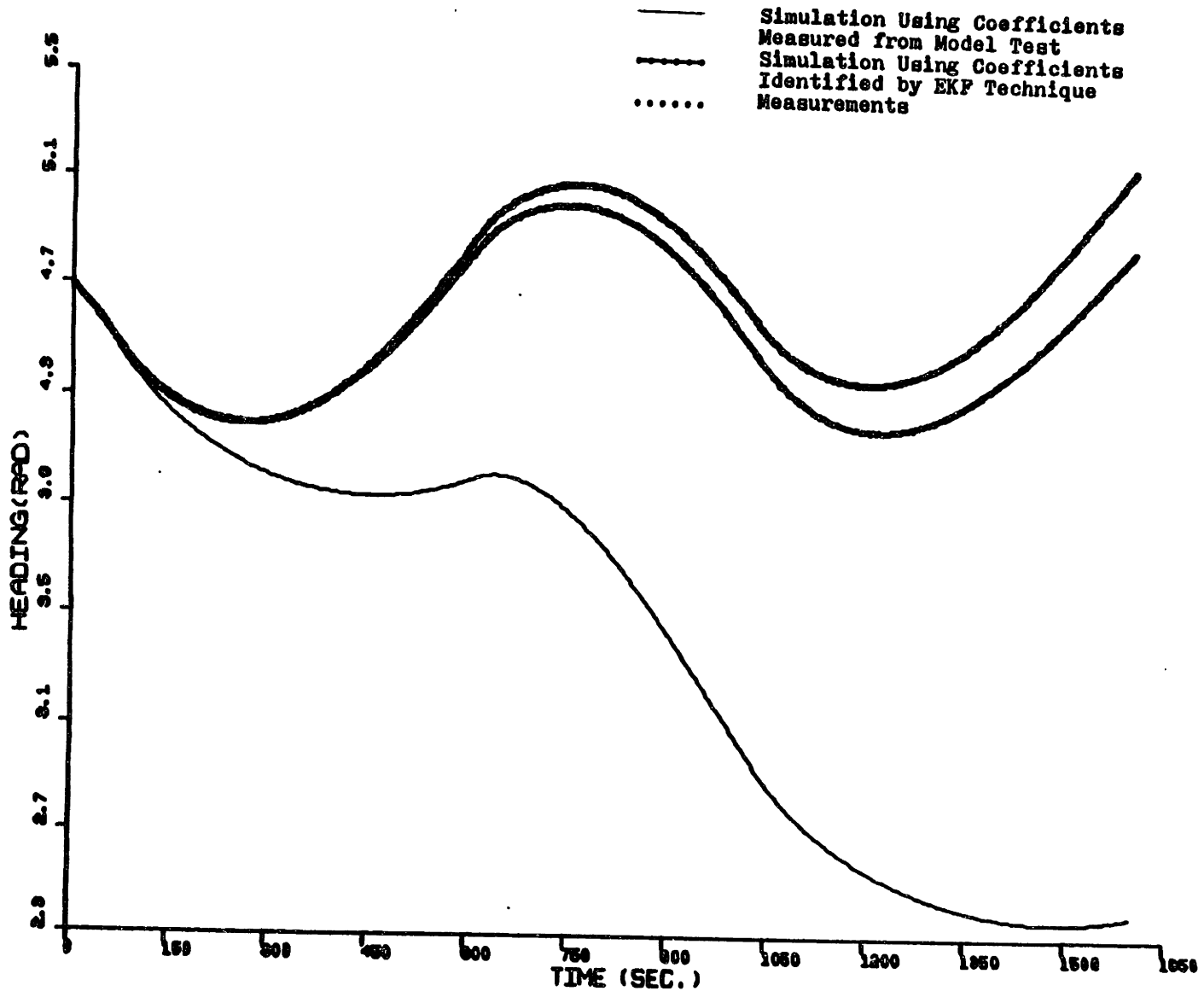

fig.4.3.4(d) Comparison between the Simulations of the Maneuver of 10^{o}-10^{o} Zigzag by Using the Coefficients "Measured" from Model Test and Identified with Measured u, ψ and Derived $\dot{\psi}$----Yaw Angle ψ.

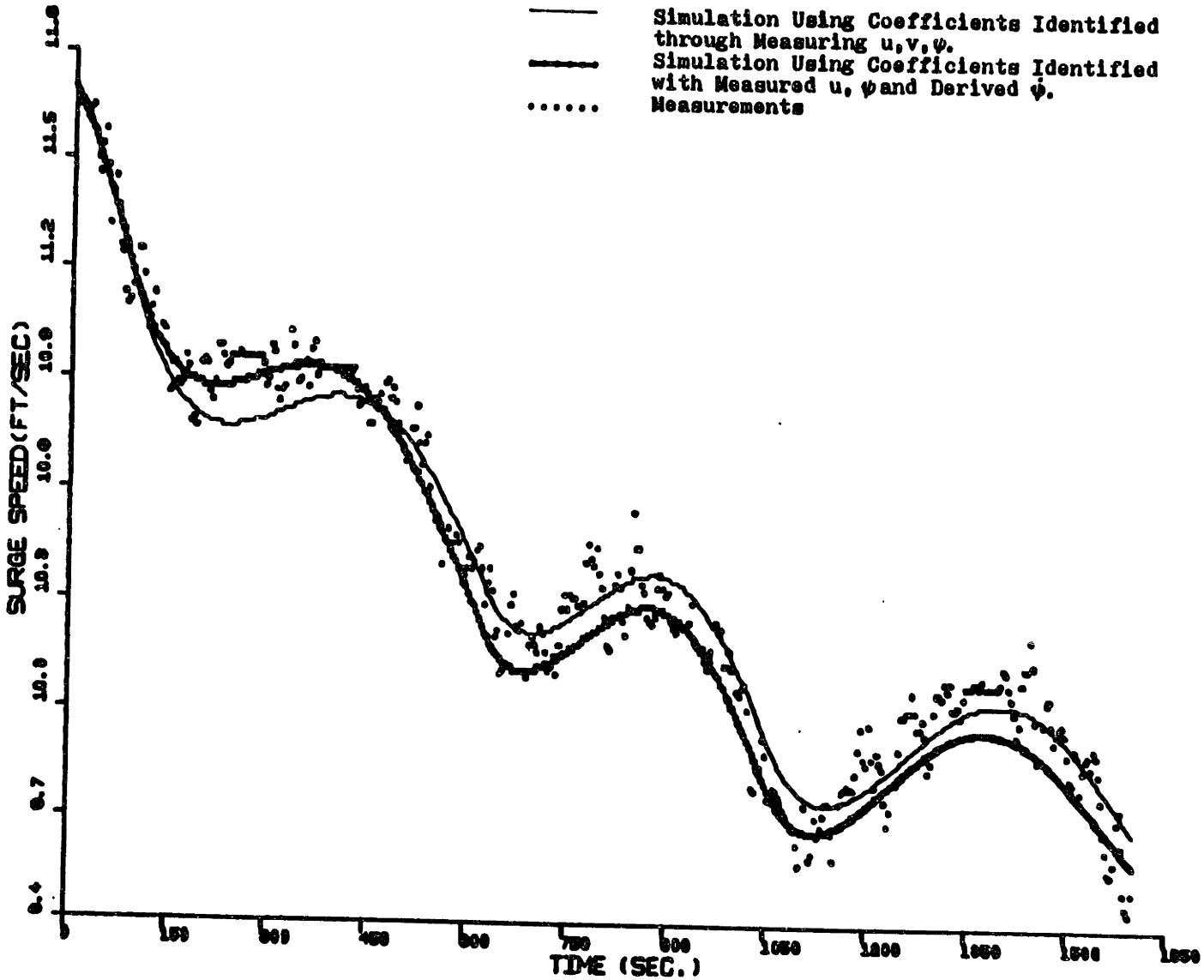

fig.4.3.5(a) Comparison between the 10^{o}-10^{o} Maneuver Simulations by Using the Coefficients Identified with Measured u, v, ψ and with Measured u, ψ and Derived $\dot{\psi}$ Respectively----Surge Speed u.

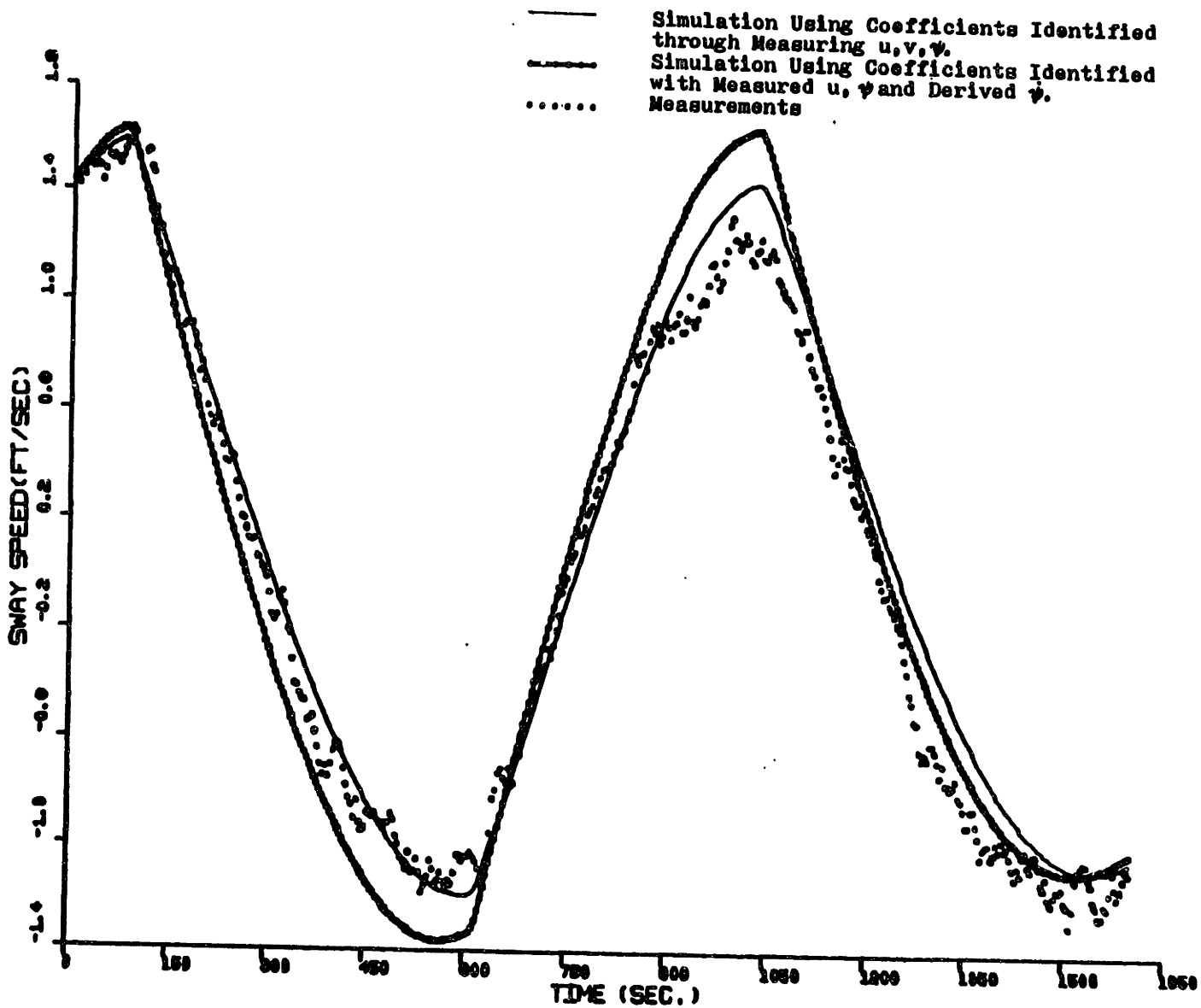

fig.4.3.5(b) Comparison between the 10^{o}-10^{o} Maneuver Simulations by Using the Coefficients Identified with Measured u,v, ψ and with Measured u, ψ and Derived $\dot{\psi}$ Respectively----Sway Speed v.

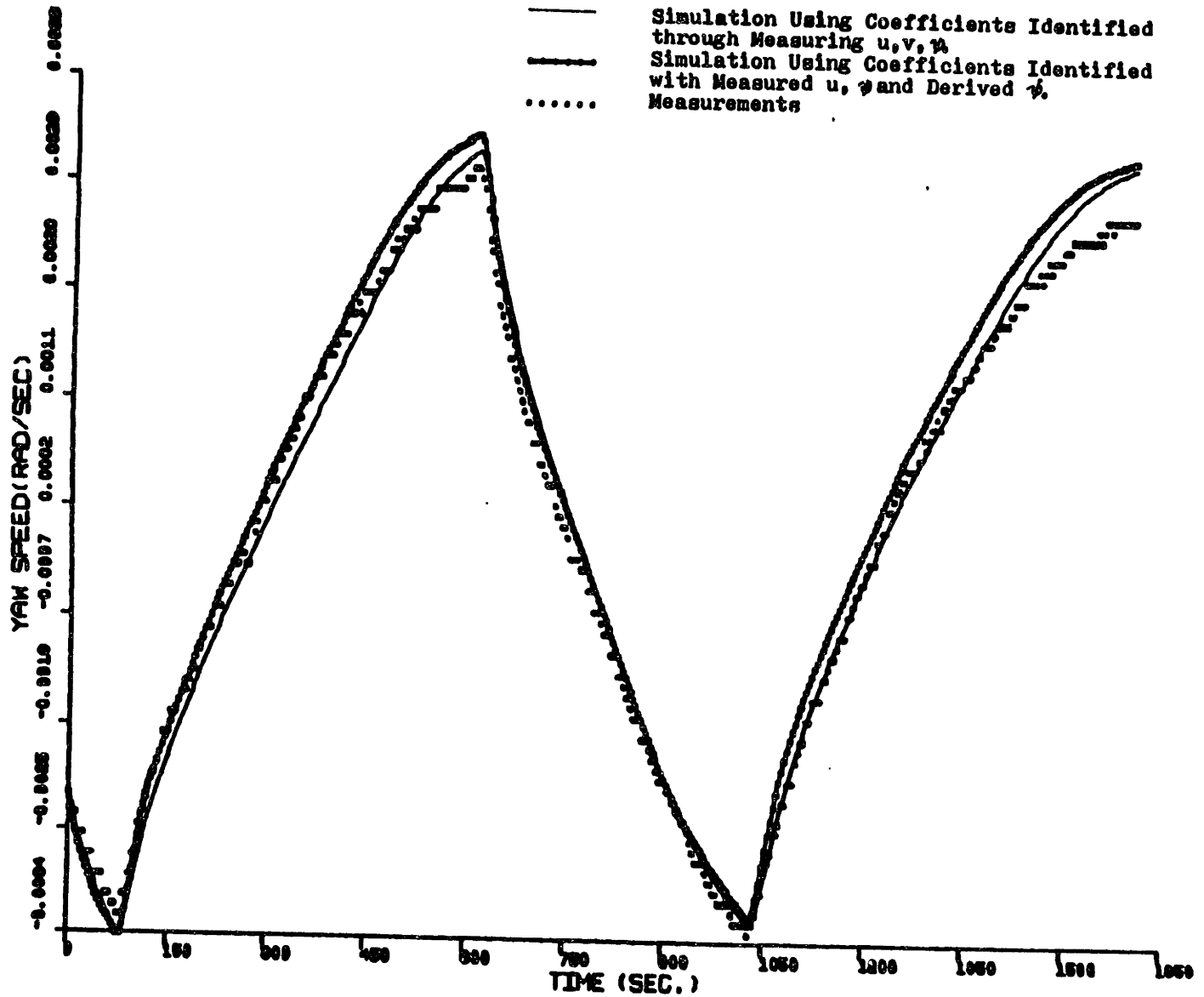

fig.4.3.5(c) Comparison between the 10°-10° Maneuver Simulations by Using the Coefficients Identified with Measured u,v, ψ and with Measured u, ψ and Derived $\dot{\psi}$ Respectively----Yaw Speed r.

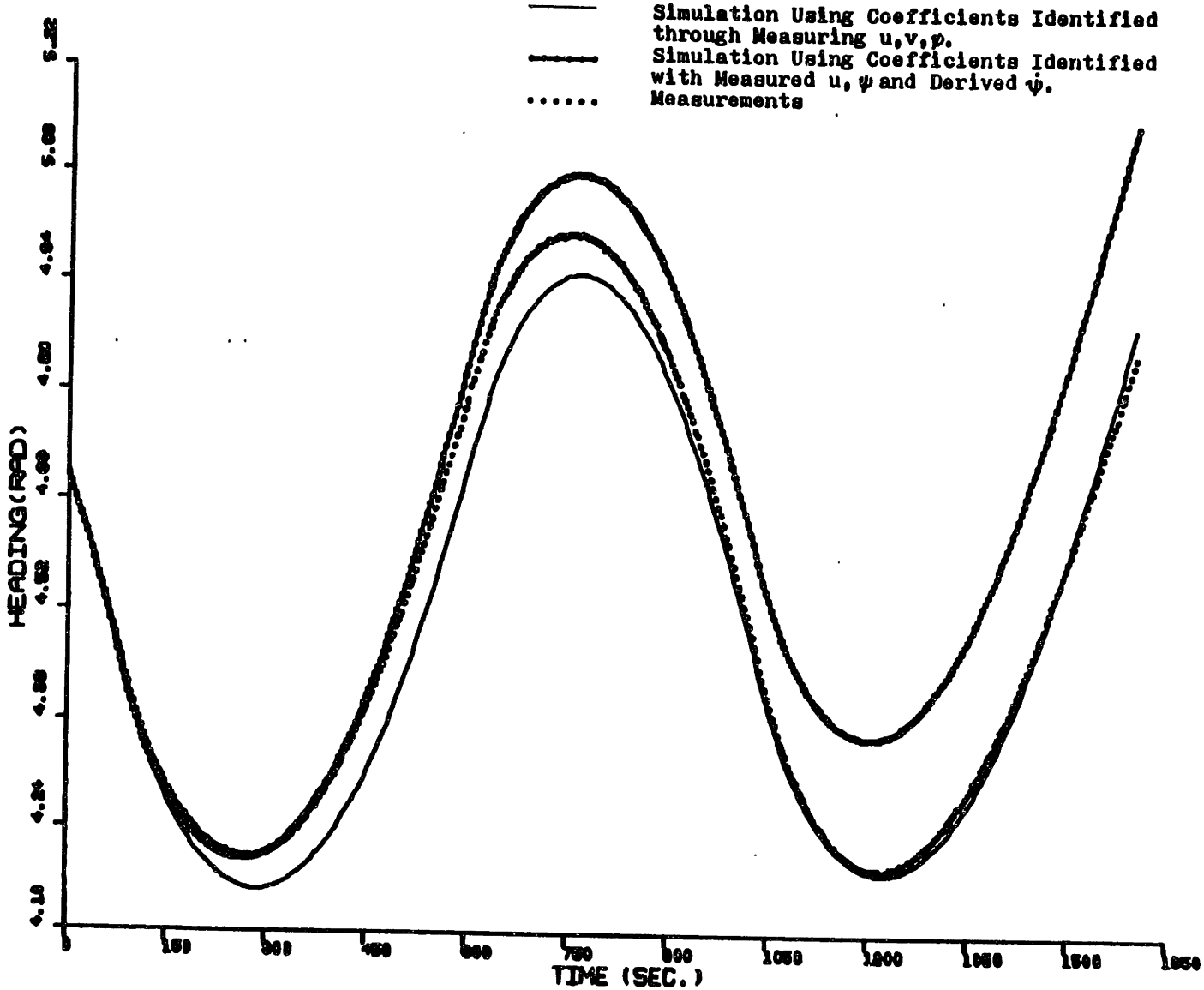

fig.4.3.5(d) Comparison between the 10°-10° Maneuver Simulations by Using the Coefficients Identified with Measured u,v, ψ and with Measured u, ψ and Derived $\dot{\psi}$ Respectively----Yaw Angle ψ.

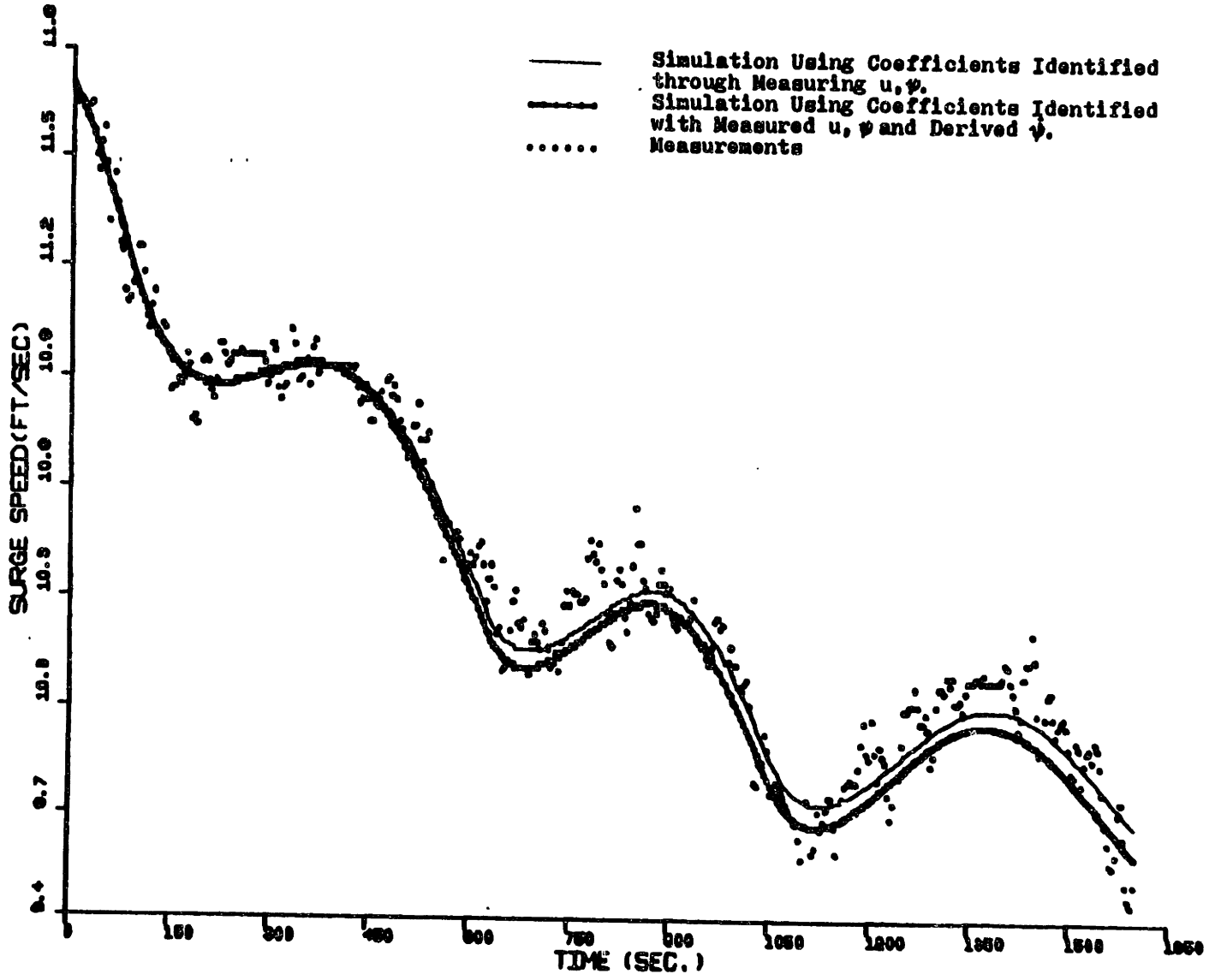

fig.4.3.6(a) Comparison between the 10^{o}-10^{o} Maneuver Simulations by Using the Coefficients Identified with Measured u, ψ and with Measured u, ψ and Derived $\dot{\psi}$ Respectively----Surge Speed u.

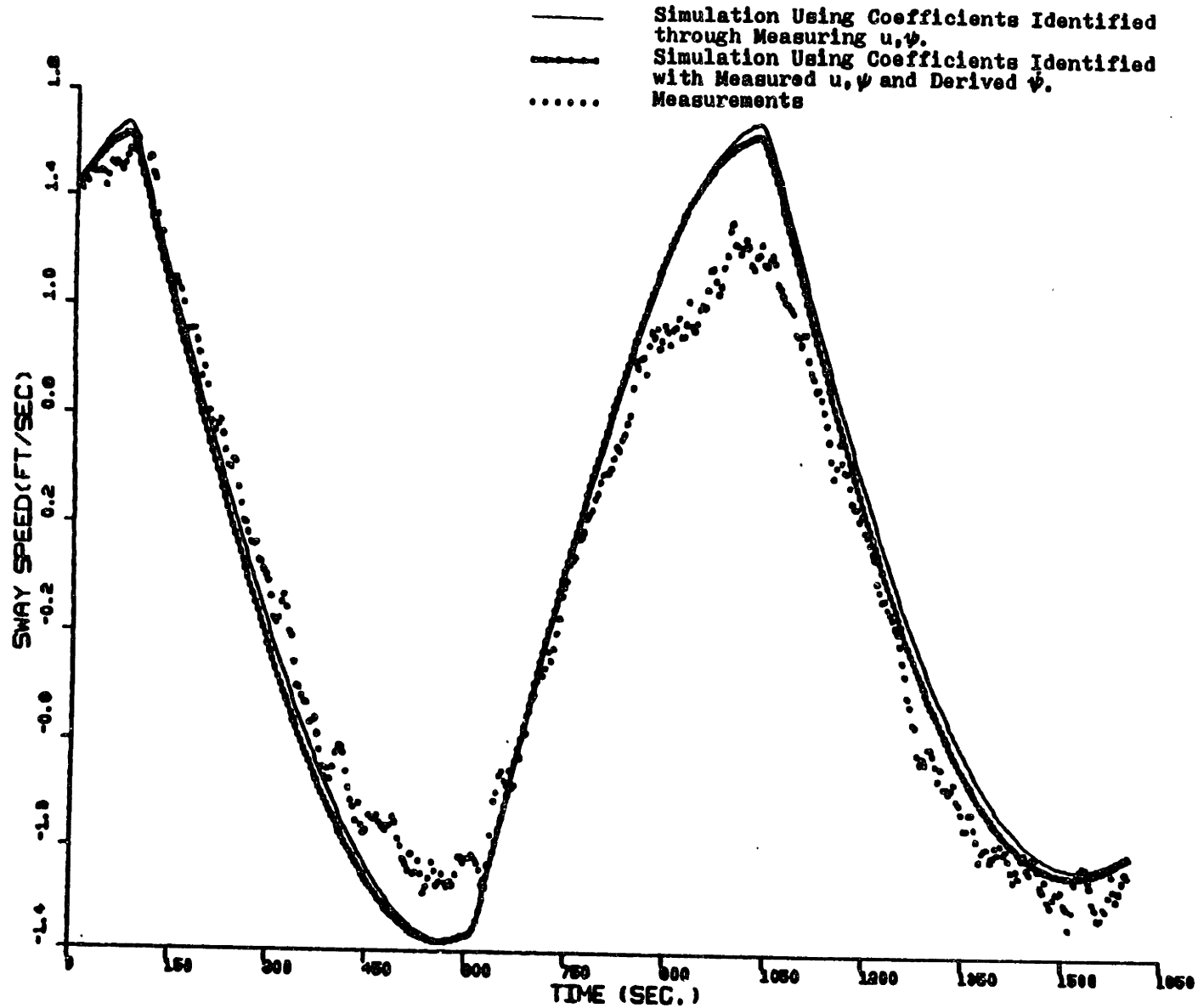

fig.4.3.6(b) Comparison between the 10^{o}-10^{o} Maneuver Simulations by Using the Coefficients Identified with Measured u, ψ and with Measured u, ψ and Derived $\dot{\psi}$ Respectively----Sway Speed v.

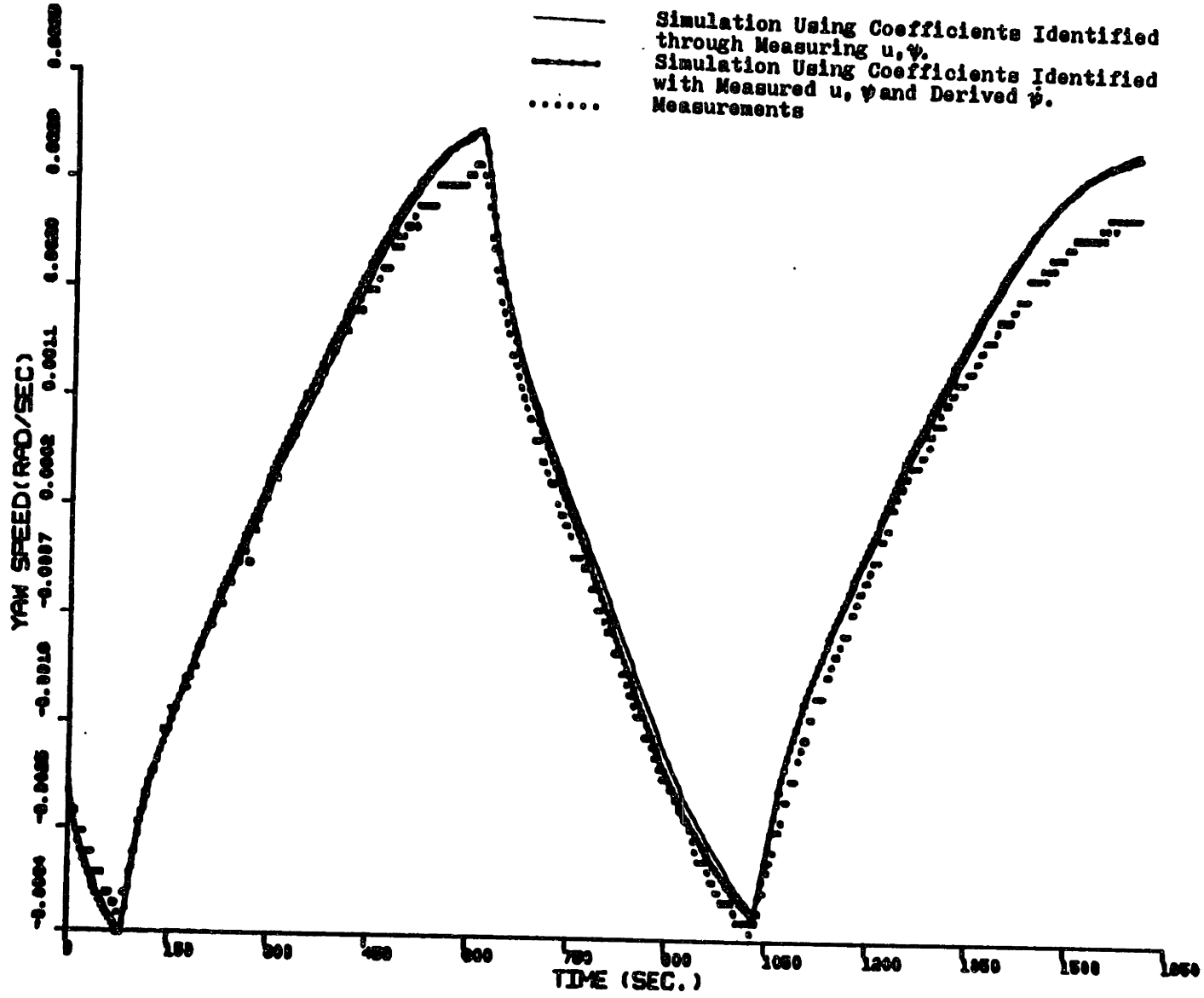

fig.4.3.6(c) Comparison between the 10^{o}-10^{o} Maneuver Simulations by Using the Coefficients Identified with Measured u, ψ and with Measured u, ψ and Derived $\dot{\psi}$ Respectively----Yaw Speed r.

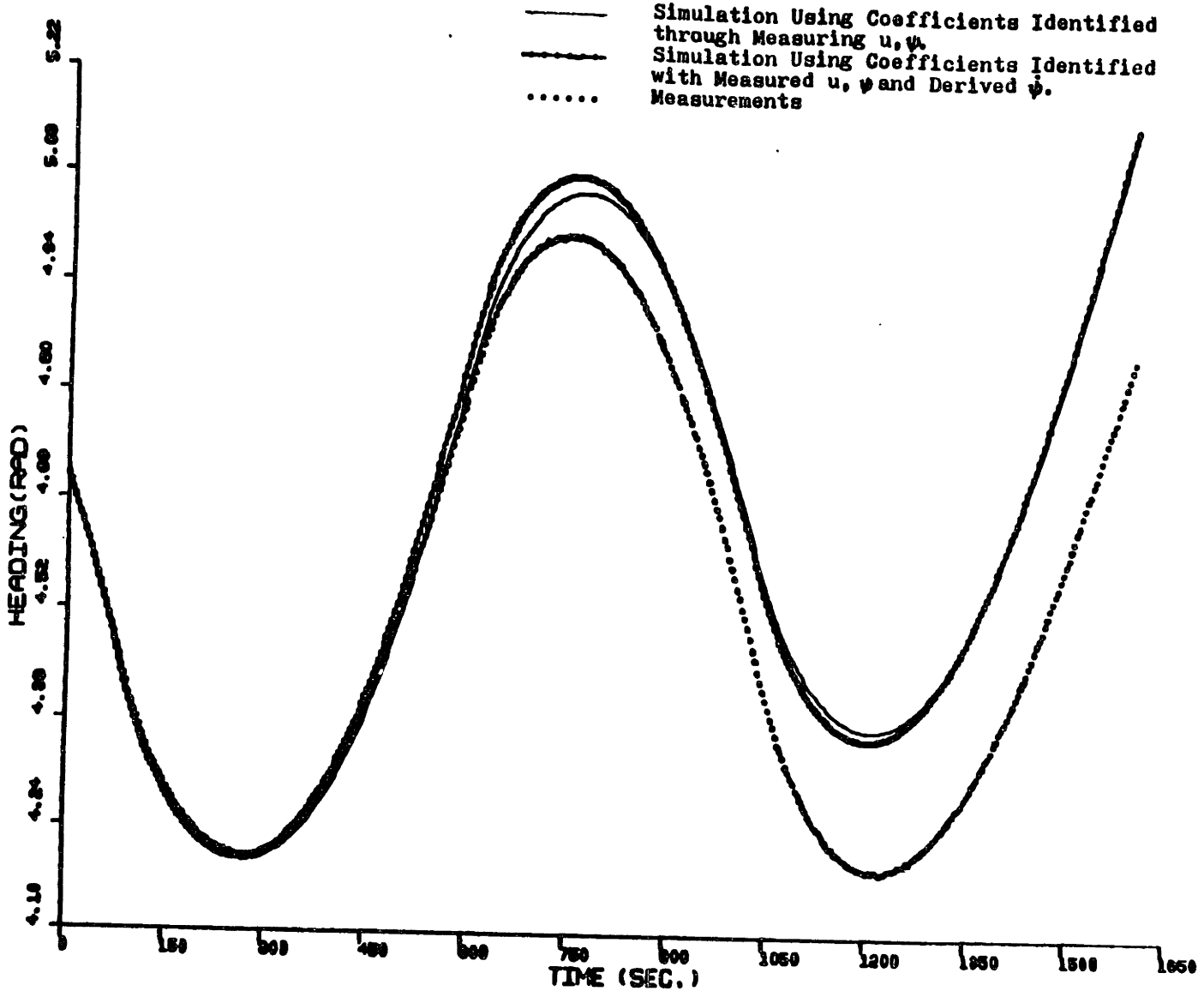

fig.4.3.6(d) Comparison between the 10^{o}-10^{o} Maneuver Simulations by Using the Coefficients Identified with Measured u, ψ and with Measured u, ψ and Derived $\dot{\psi}$ Respectively----Yaw Angle ψ.

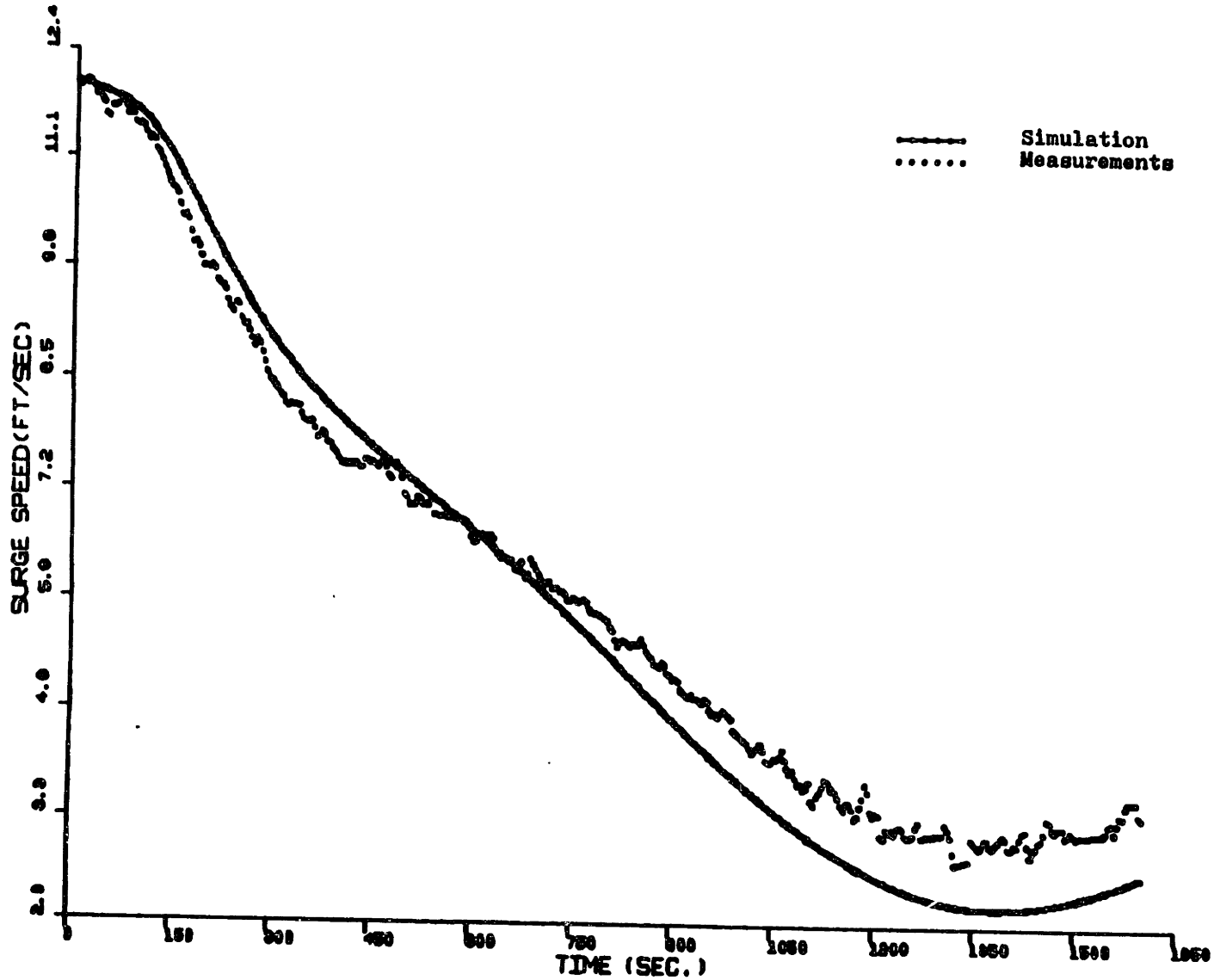

fig.4.3.7(a) Comparison between the Measurements and the Simulation of 35° Maneuver by Using the Coefficients Identified With Measured u, ψ and Derived $\dot{\psi}$----Surge Speed u.

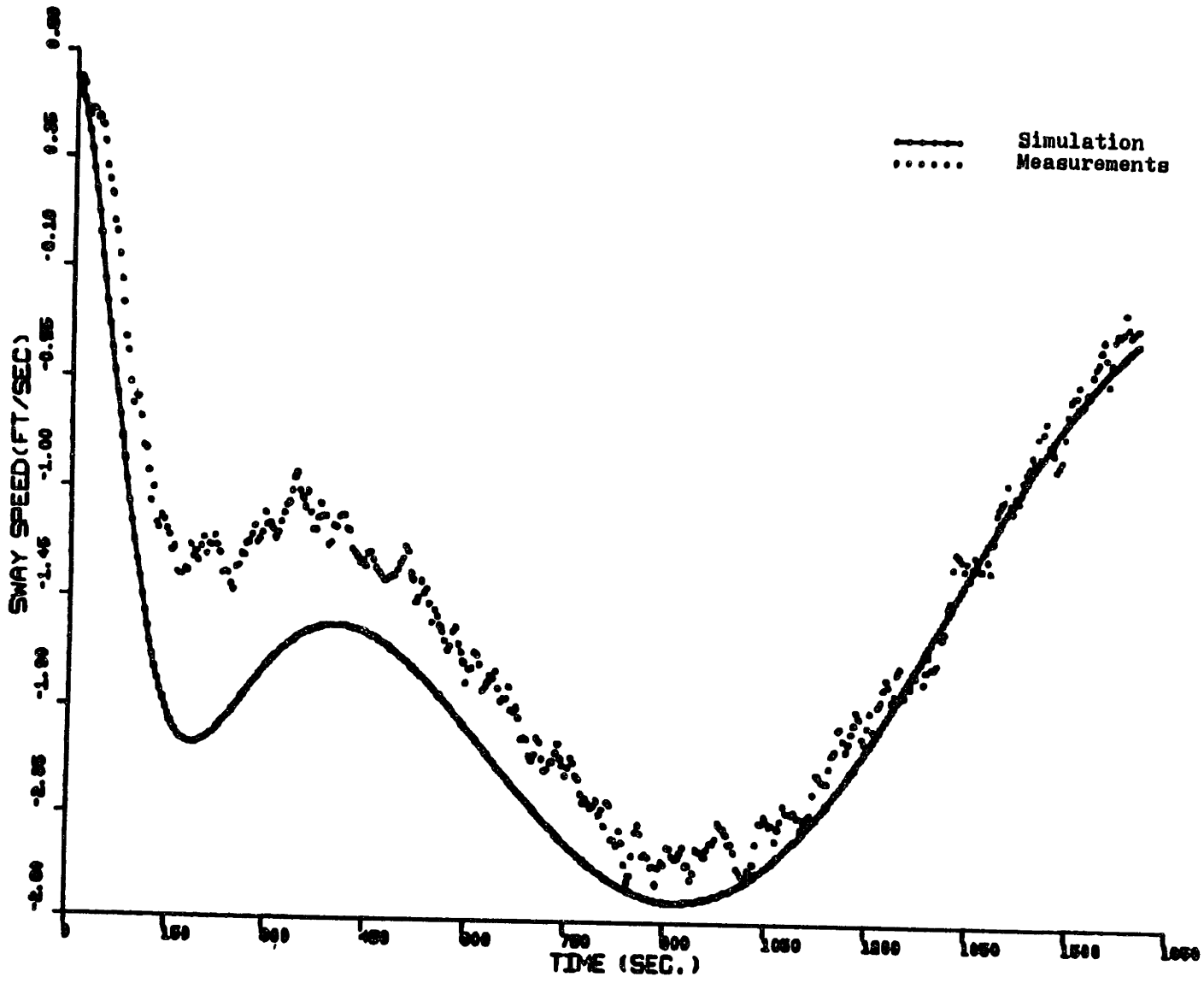

fig.4.3.7(b) Comparison between the Measurements and the Simulation of 35° Maneuver by Using the Coefficients Identified with Measured u, ψ and Derived $\dot{\psi}$----Sway Speed v.

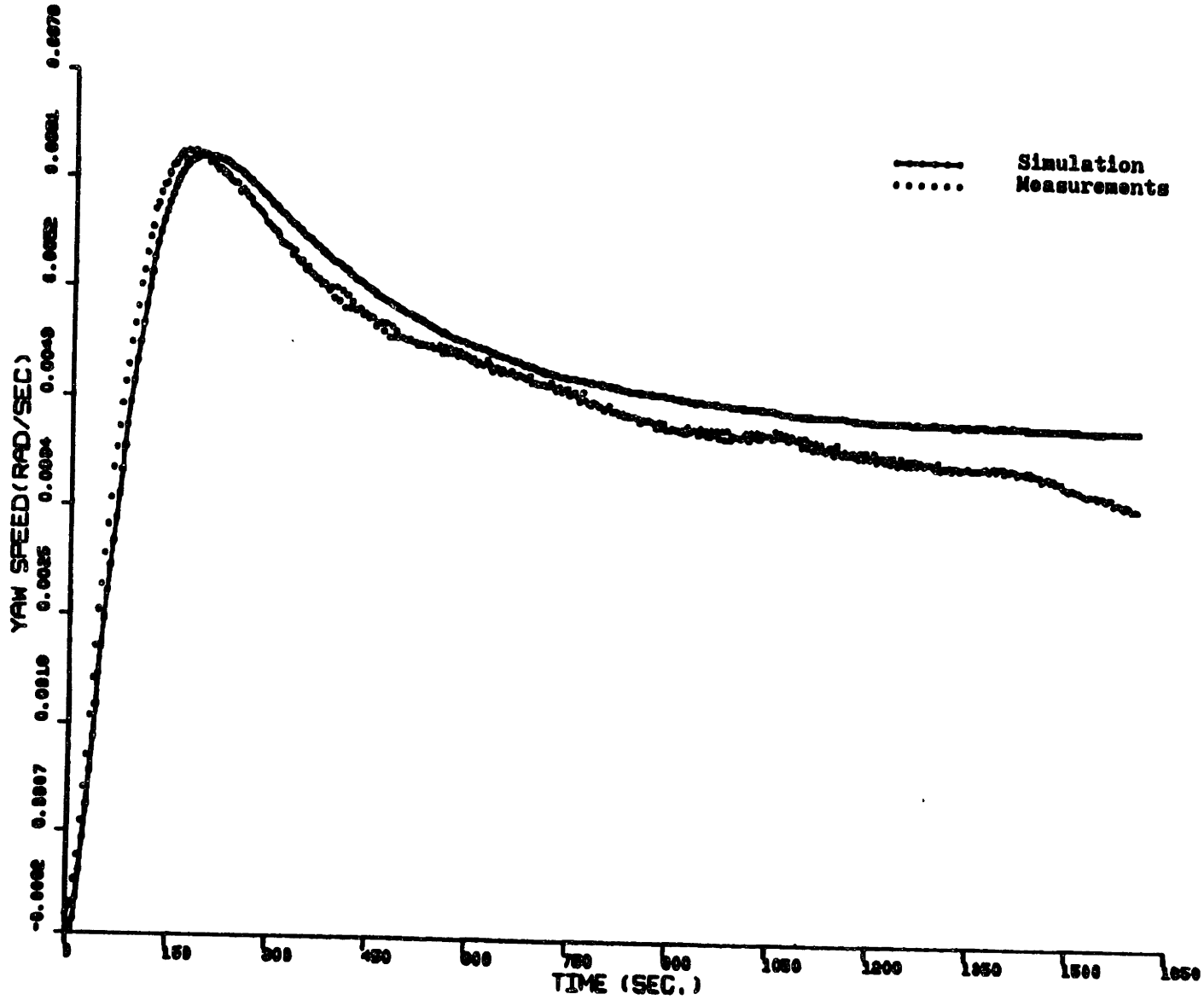

fig.4.3.7(c) Comparison between the Measurements and the Simulation of 35^{o} Maneuver by Using the Coefficients Identified with Measured u, ψ and Derived $\dot{\psi}$----Yaw Speed r.

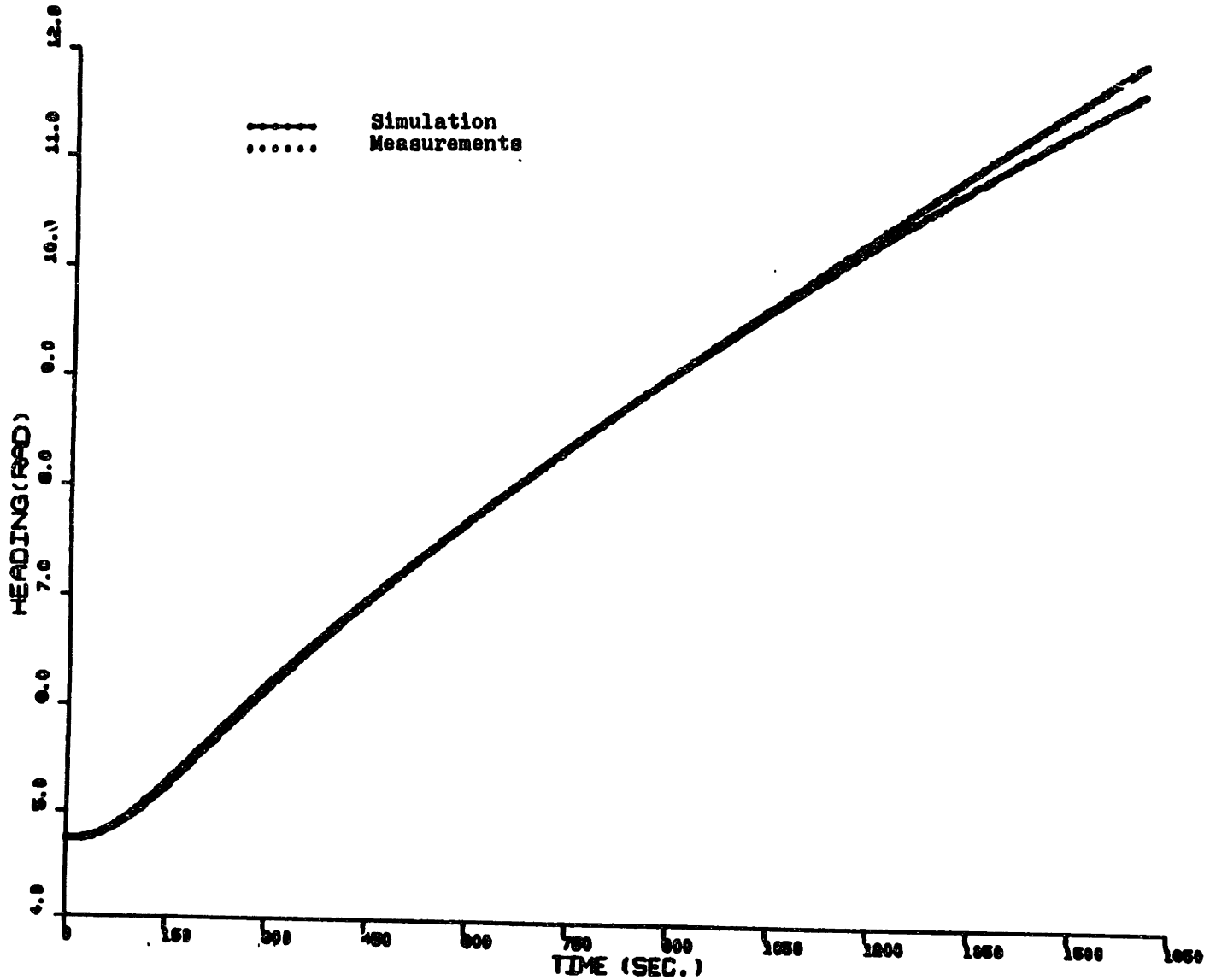

fig.4.3.7(d) Comparison between the Measurements and the Simulation of 35° Maneuver by Using the Coefficients Identified with Measured u, ψ and Derived $\dot{\psi}$----Yaw Angle ψ.

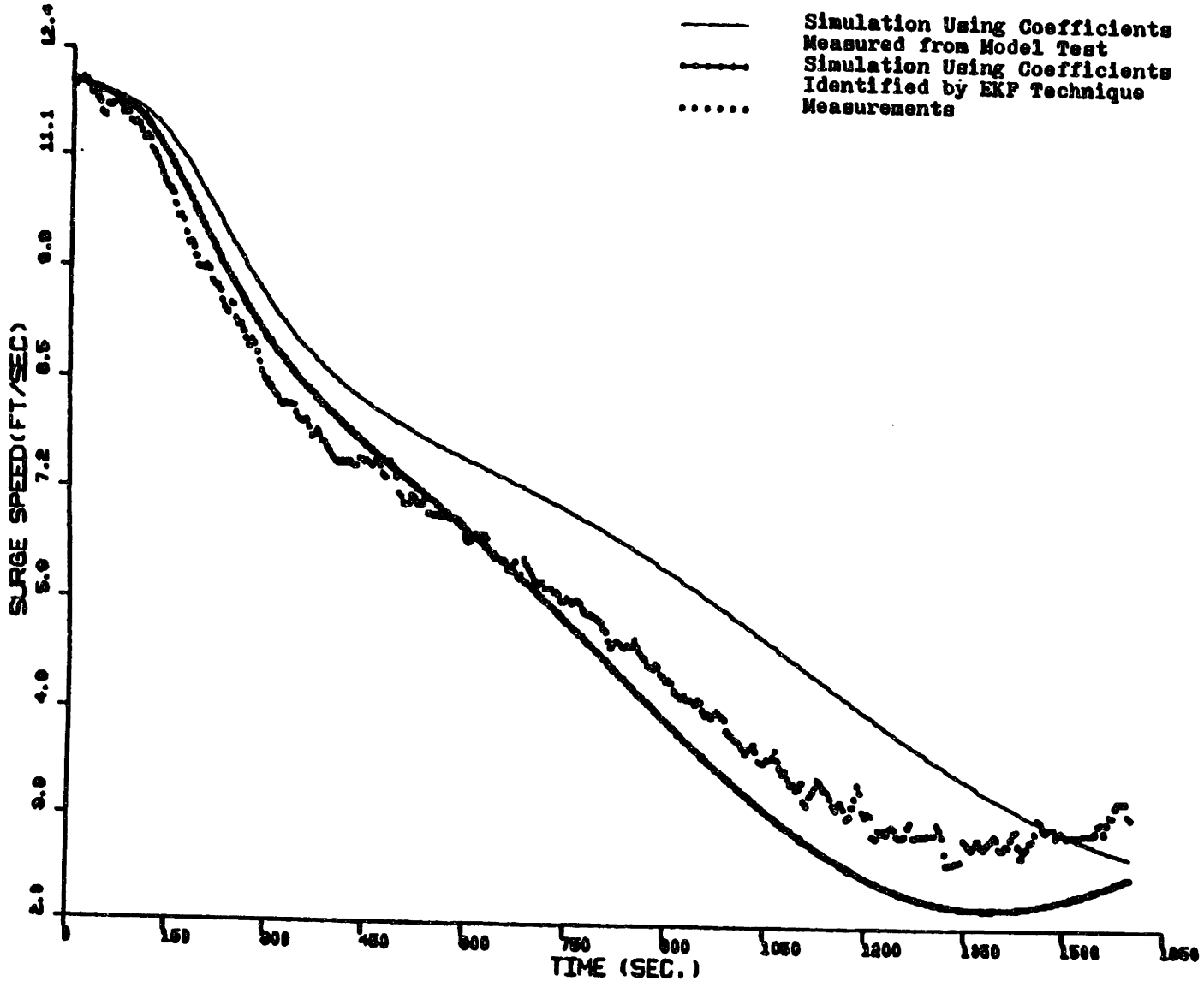

fig.4.3.8(a) Comparison between the Simulations of the Maneuver of 35^{o} Turning by Using the Coefficients "Measured" from Model Test and Identified with Measured u, ψ and Derived $\dot{\psi}$ ----Surge Speed u.

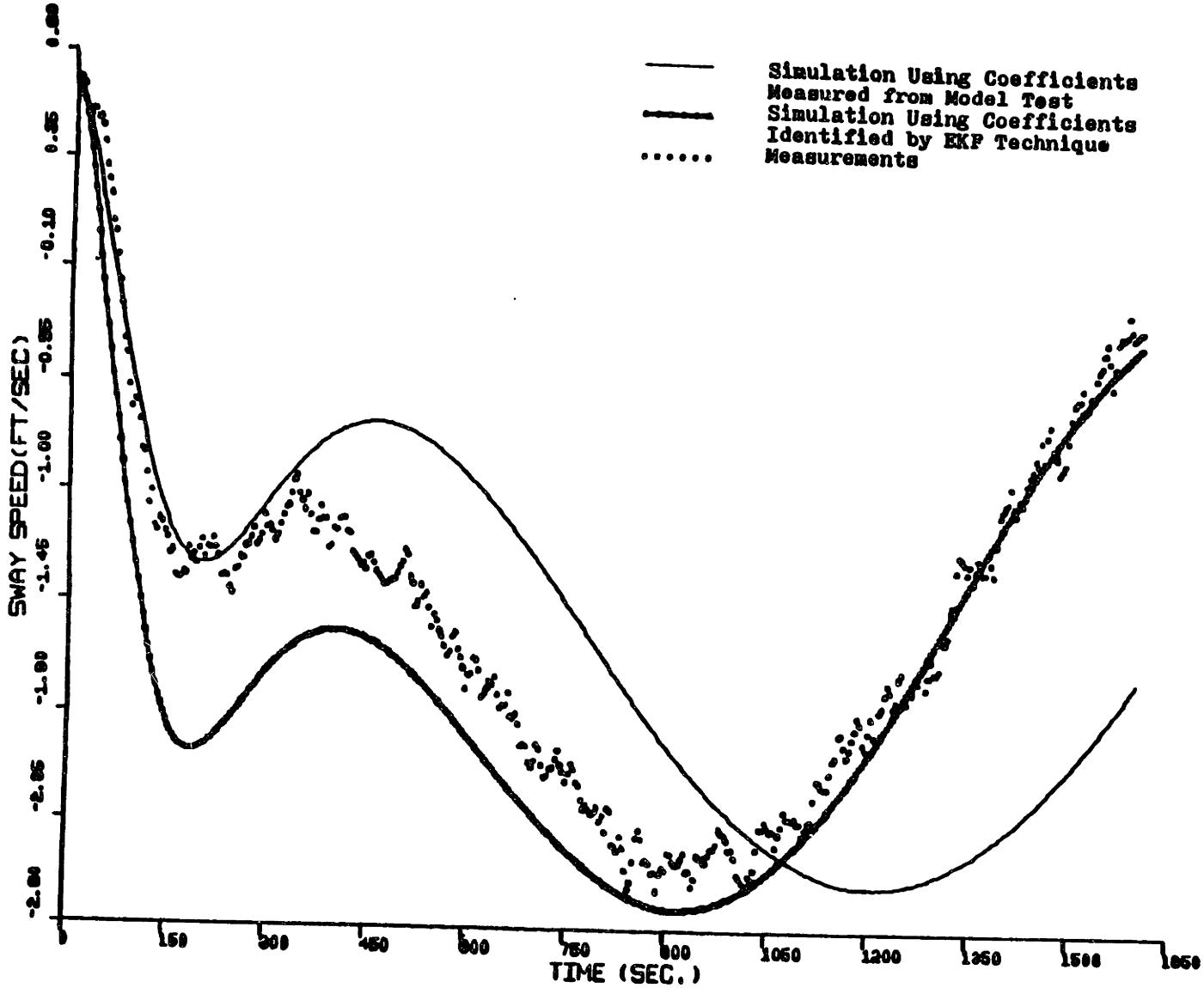

fig.4.3.8(b) Comparison between the Simulations of the Maneuver of 35^{o} Turning by Using the Coefficients "Measured" from Model Test and Identified with Measured u, ψ and Derived $\dot{\psi}$----Sway Speed v.

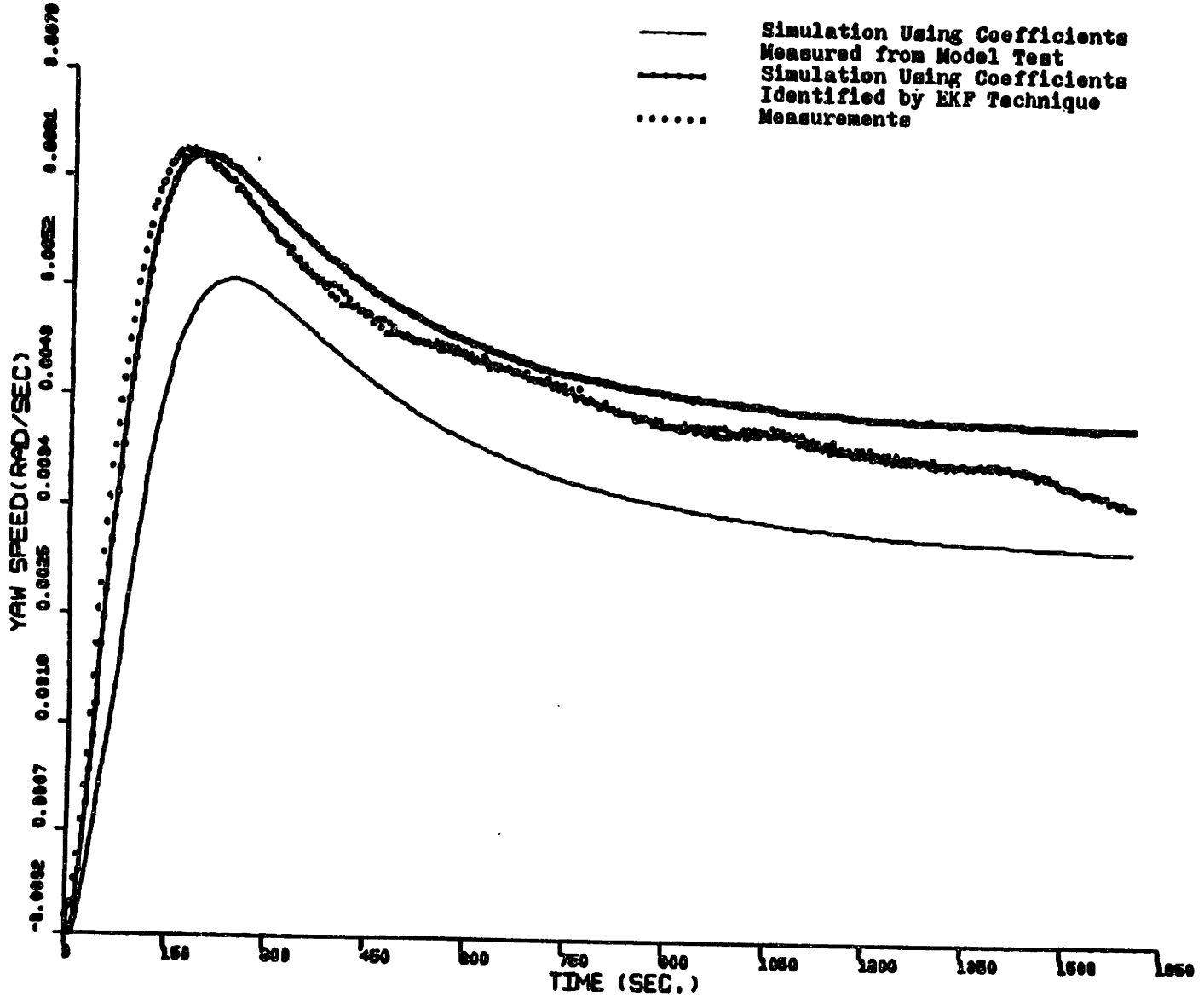

fig.4.3.8(c) Comparison between the Simulations of the Maneuver of 35° Turning by Using the Coefficients "Measured" from Model Test and Identified with Measured u, ψ and Derived $\dot{\psi}$----Yaw Speed r.

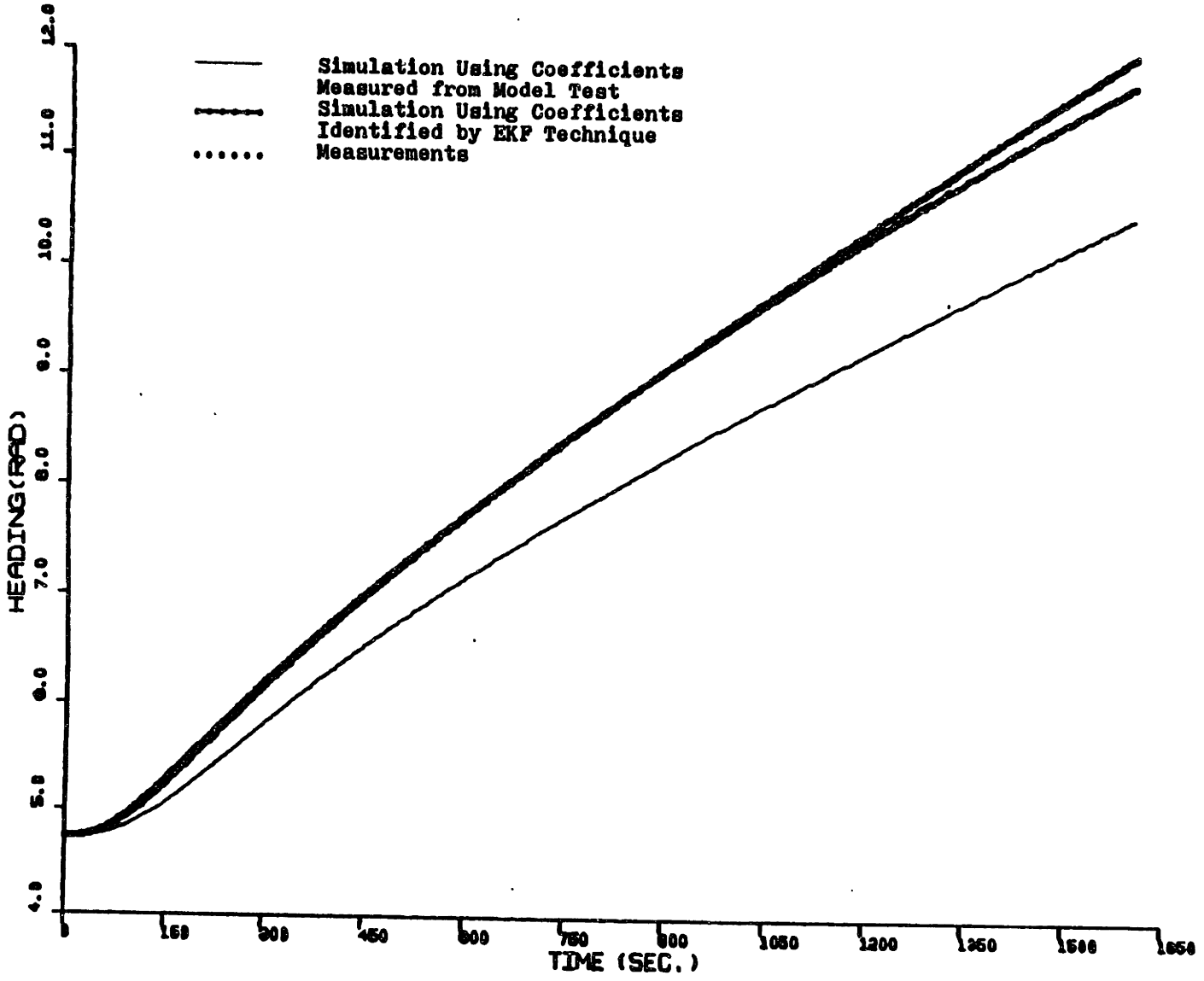

fig.4.3.8(d) Comparison between the Simulations of the Maneuver of 35° Turning by Using the Coefficients "Measured" from Model Test and Identified with Measured u, ψ and Derived $\dot{\psi}$----Yaw Angle ψ.

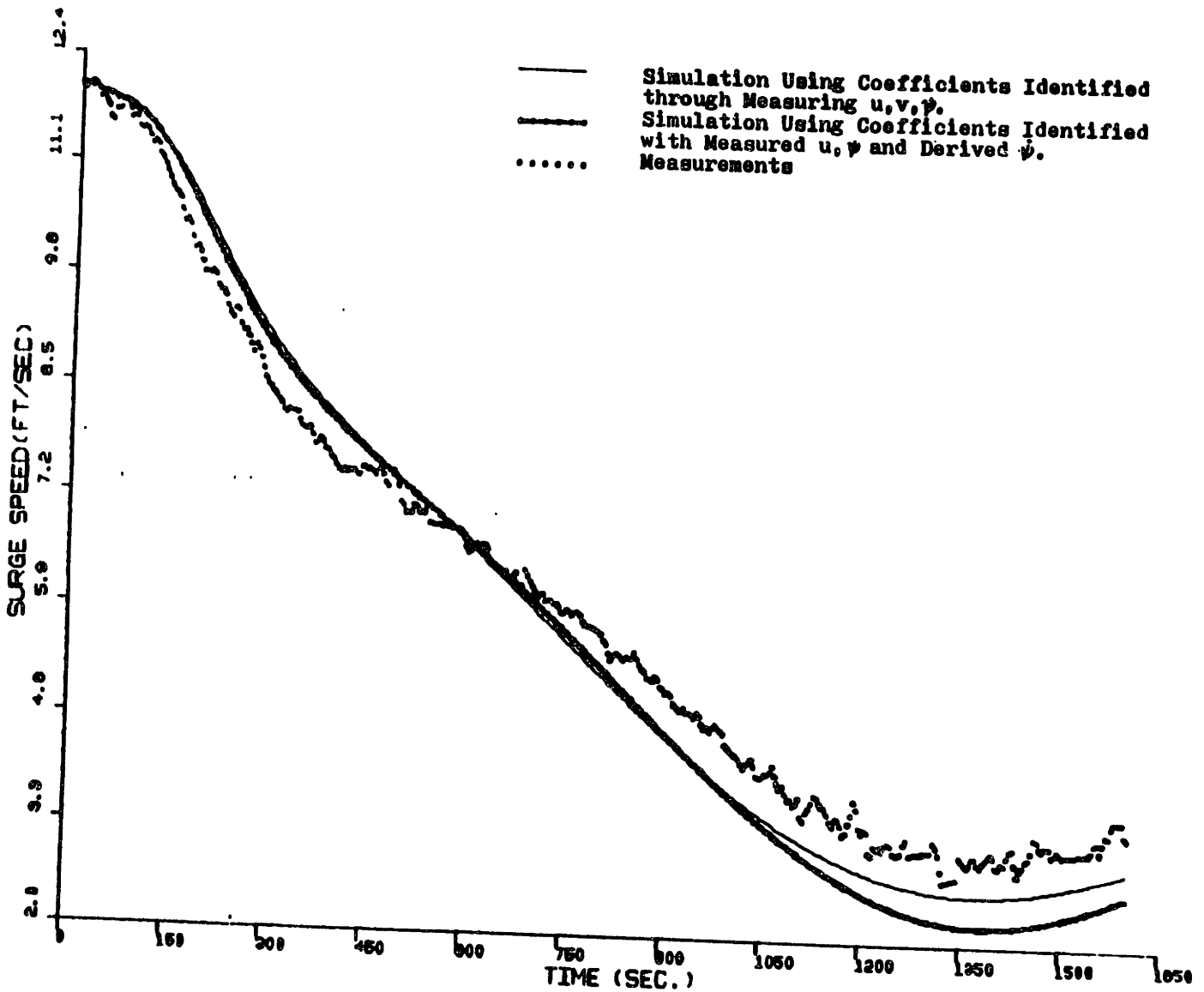

fig.4.3.9(a) Comparison between the 35° Maneuver Simulations by Using the Coefficients Identified with Measured u, v, ψ and with Measured u, ψ and Derived $\dot{\psi}$ Respectively----Surge Speed u.

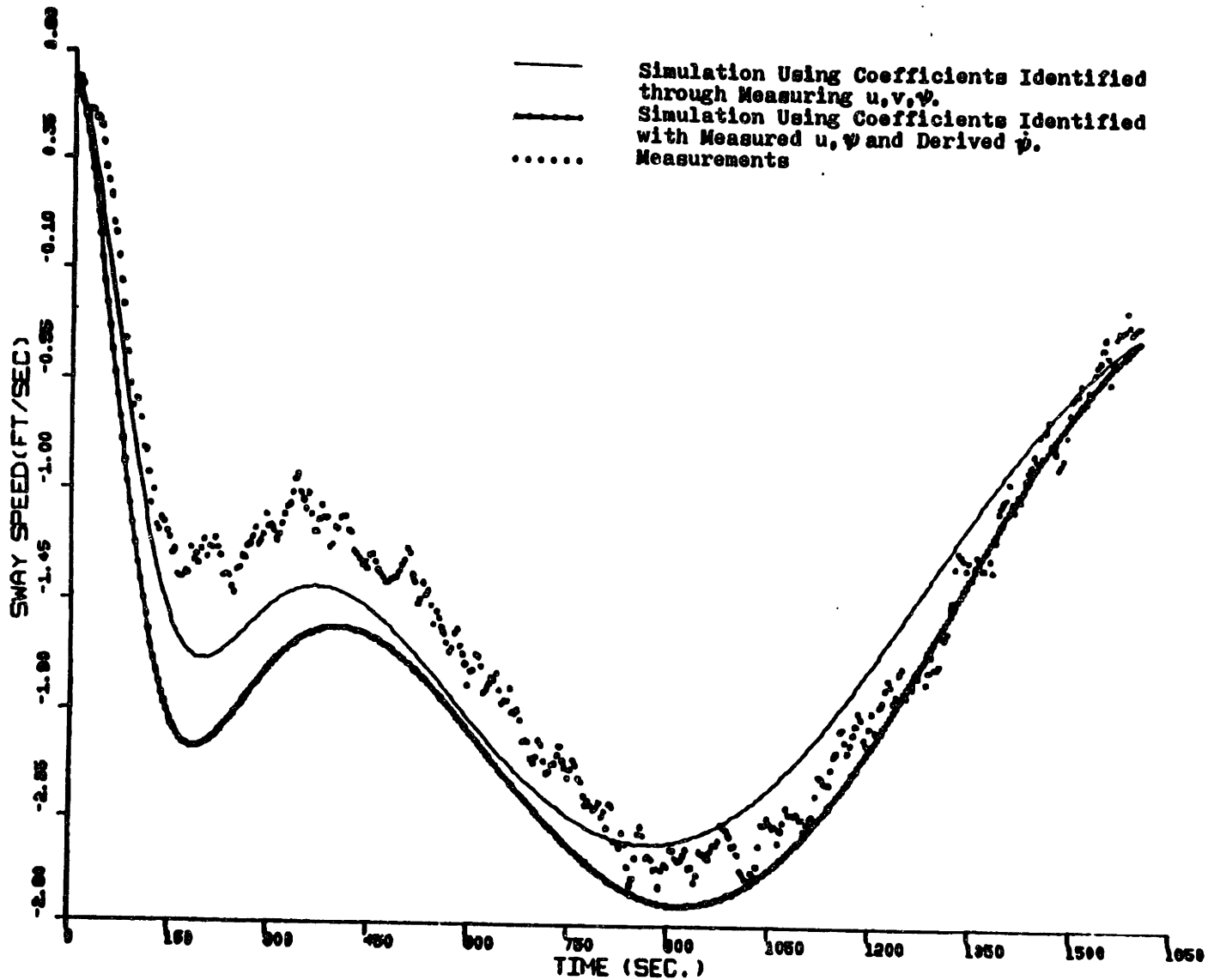

fig.4.3.9(b) Comparison between the 35^{0} Maneuver Simulations by Using the Coefficients Identified with Measured u,v,ψ and with Measured u,ψ and Derived $\dot{\psi}$ Respectively----Sway Speed v.

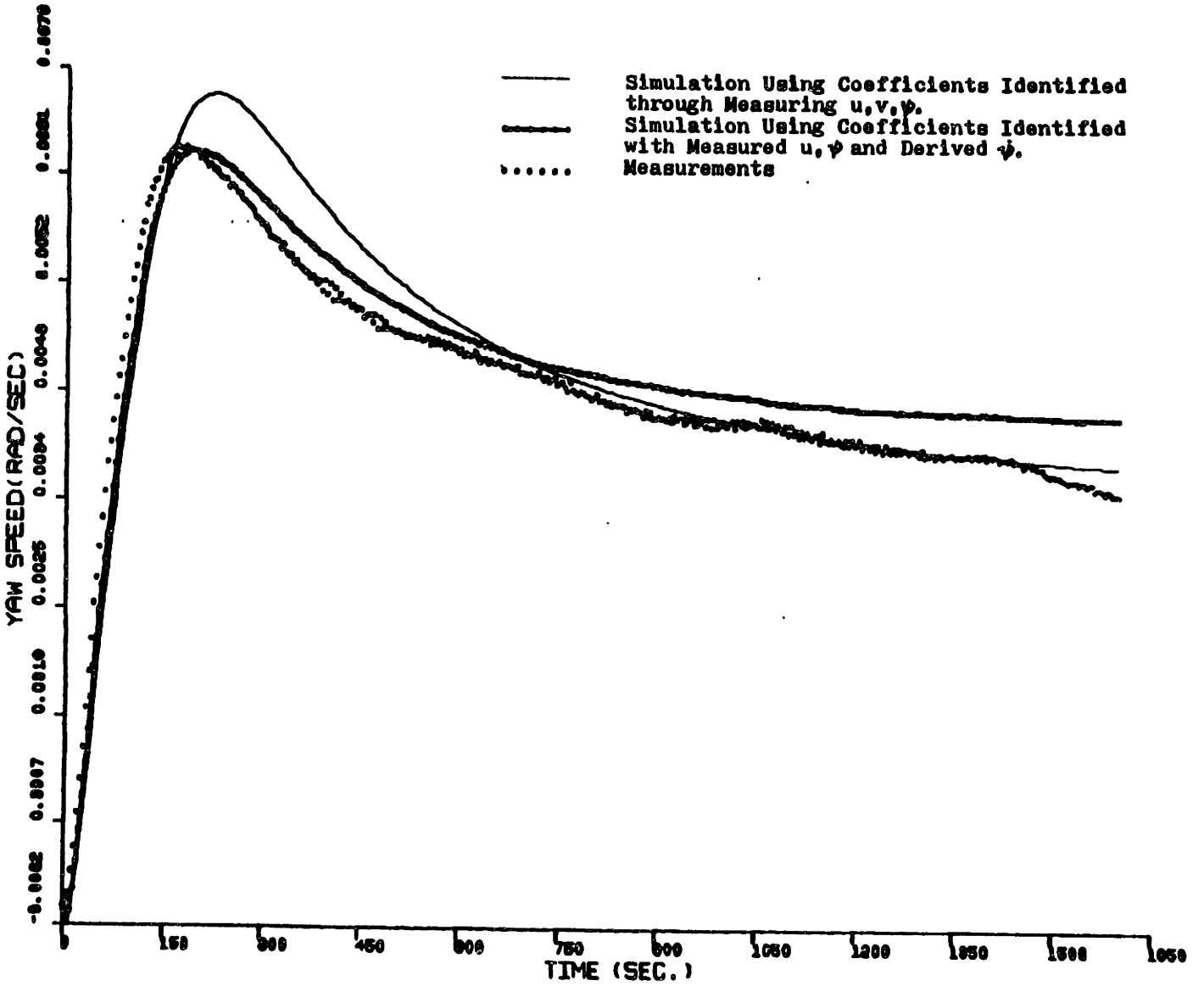

fig.4.3.9(c) Comparison between the 35° Maneuver Simulations by Using the Coefficients Identified with Measured u,v,ψ and with Measured u,ψ and Derived ψ̇ Respectively----Yaw Speed r.

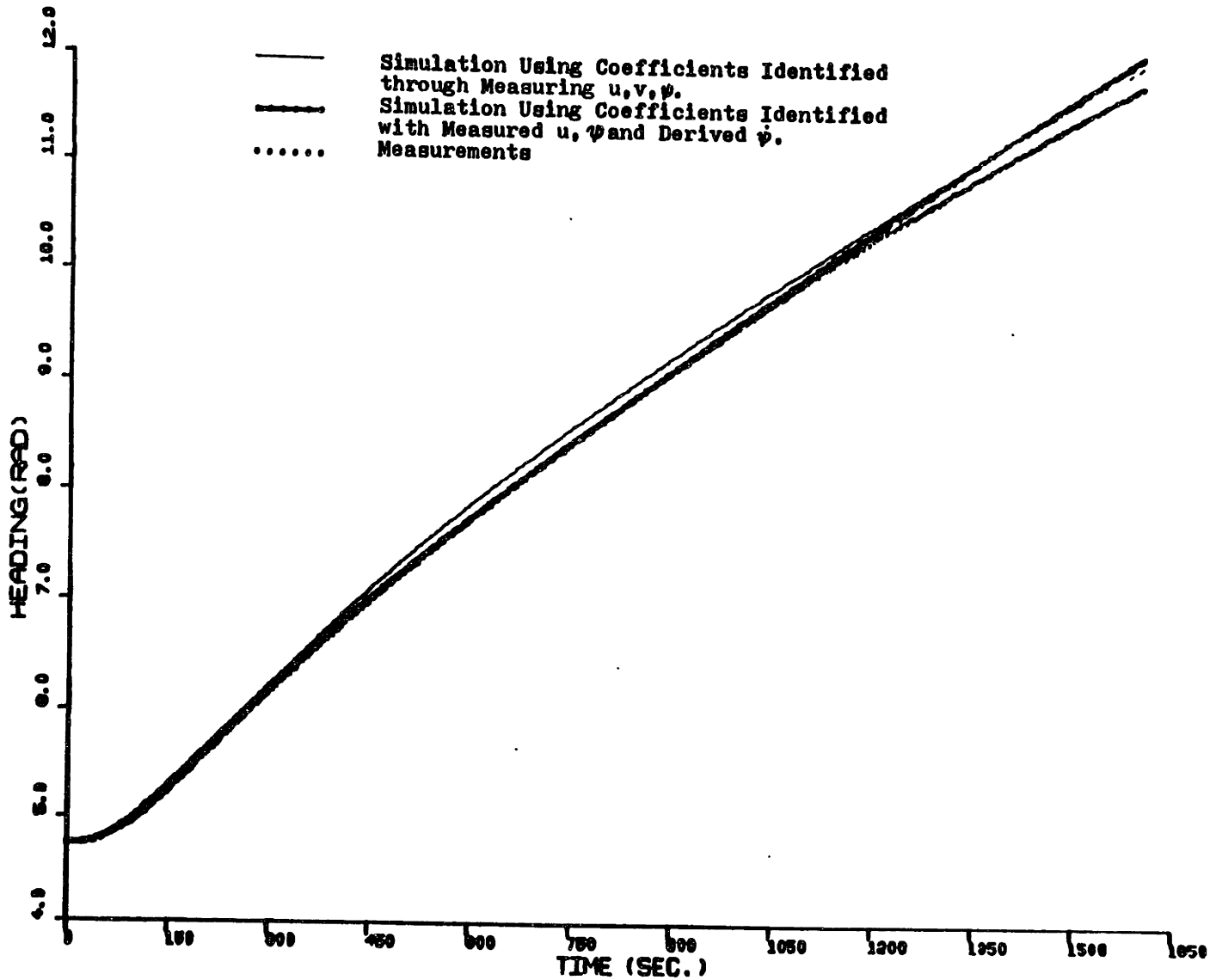

fig.4.3.9(d) Comparison between the 35°Maneuver Simulations by Using the Coefficients Identified with Measured u,v,ψ and with Measured u,ψ and Derived $\dot{\psi}$ Respectively----Yaw Angle ψ.

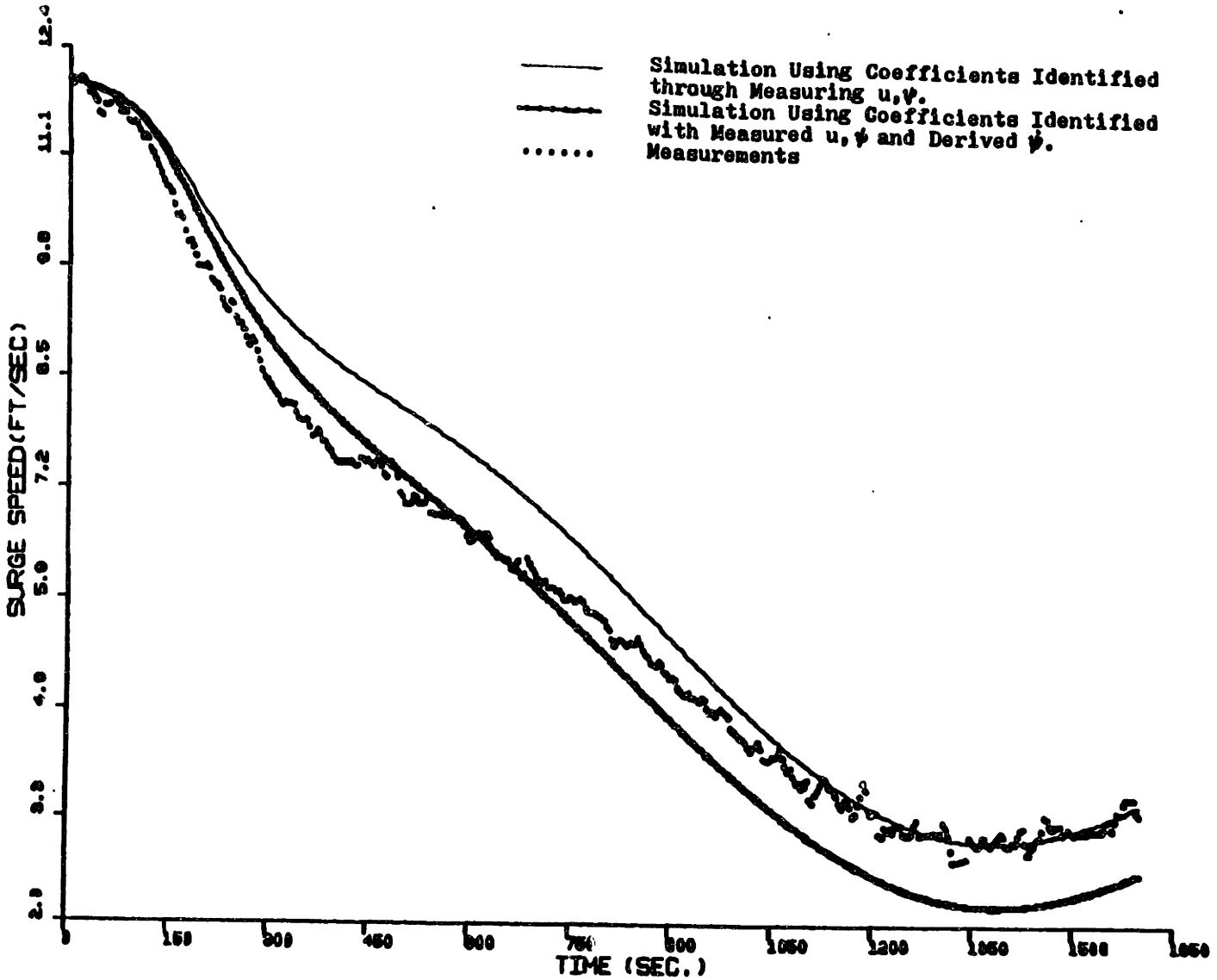

fig.4.3.10(a) Comparison between the 35° Maneuver Simulations by Using the Coefficients Identified with Measured u, ψ and with Measured u, ψ and Derived $\dot{\psi}$ Respectively----Surge Speed u.

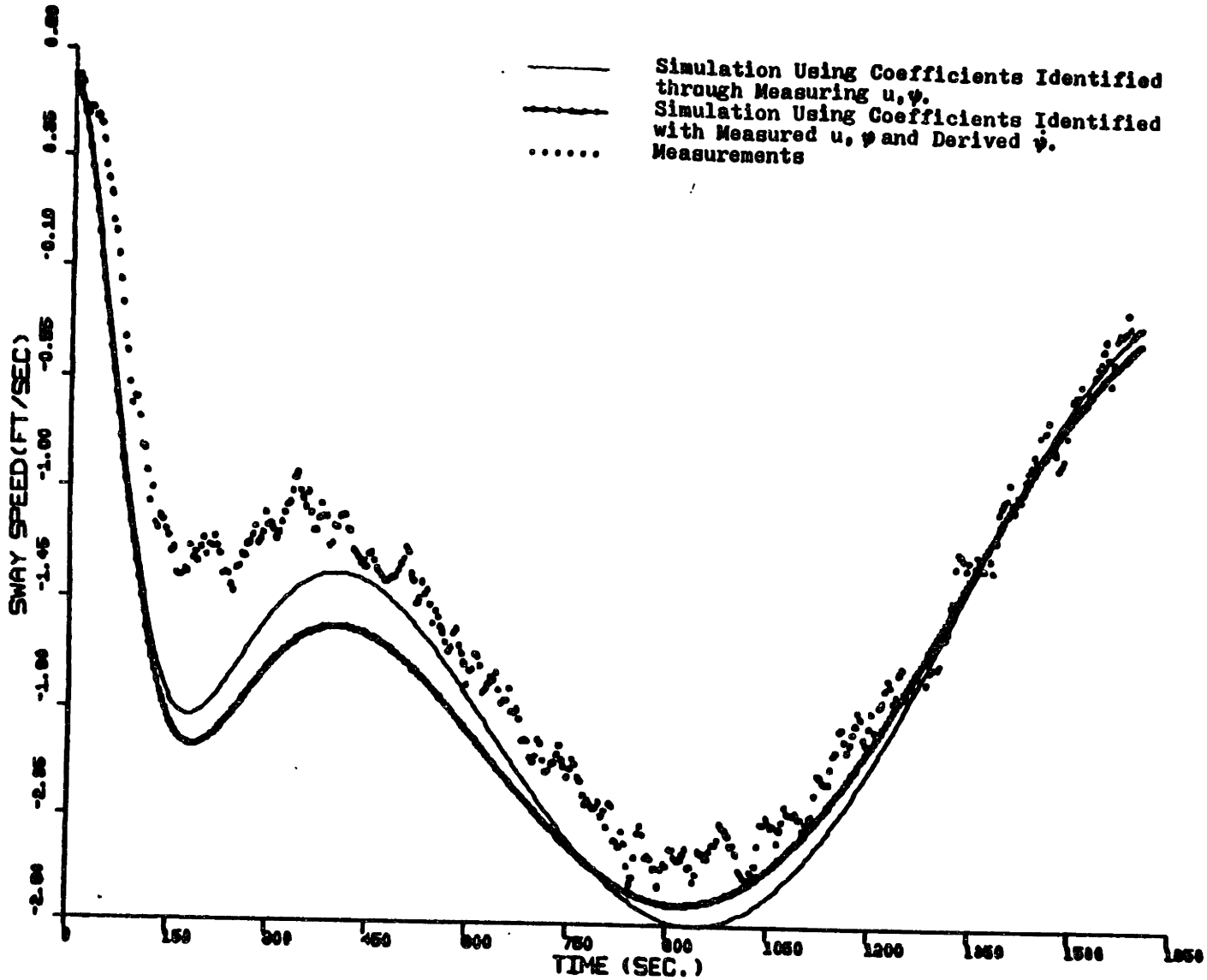

fig.4.3.10(b) Comparison between the 35° Maneuver Simulations by Using the Coefficients Identified with Measured u, ψ and with Measured u, ψ and Derived $\dot{\psi}$ Respectively----Sway Speed v.

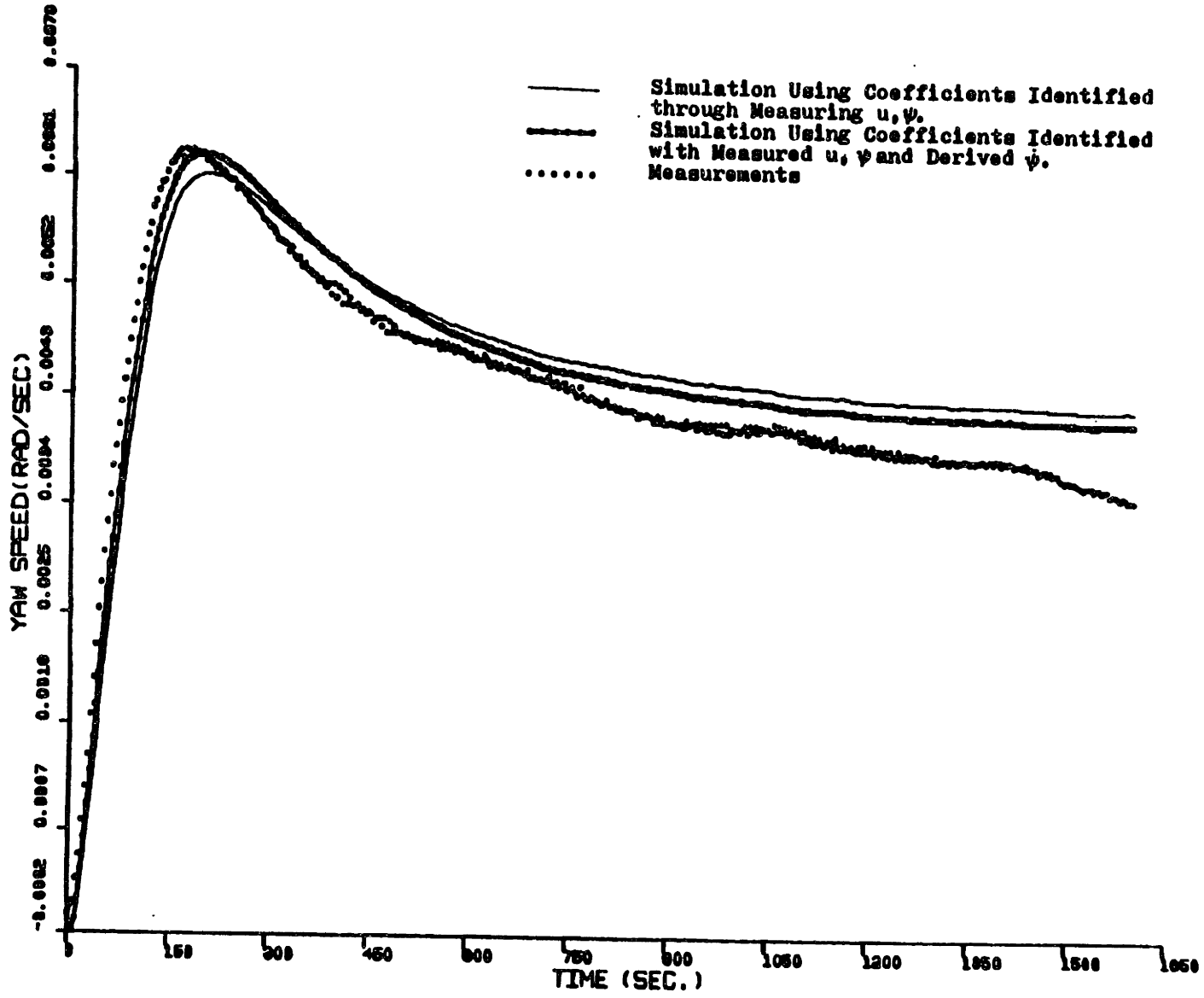

fig.4.3.10(c) Comparison between the 35^{o} Maneuver Simulations by Using the Coefficients Identified with Measured u, ψ and with Measured u, ψ and Derived $\dot{\psi}$ Respectively----Yaw Speed r.

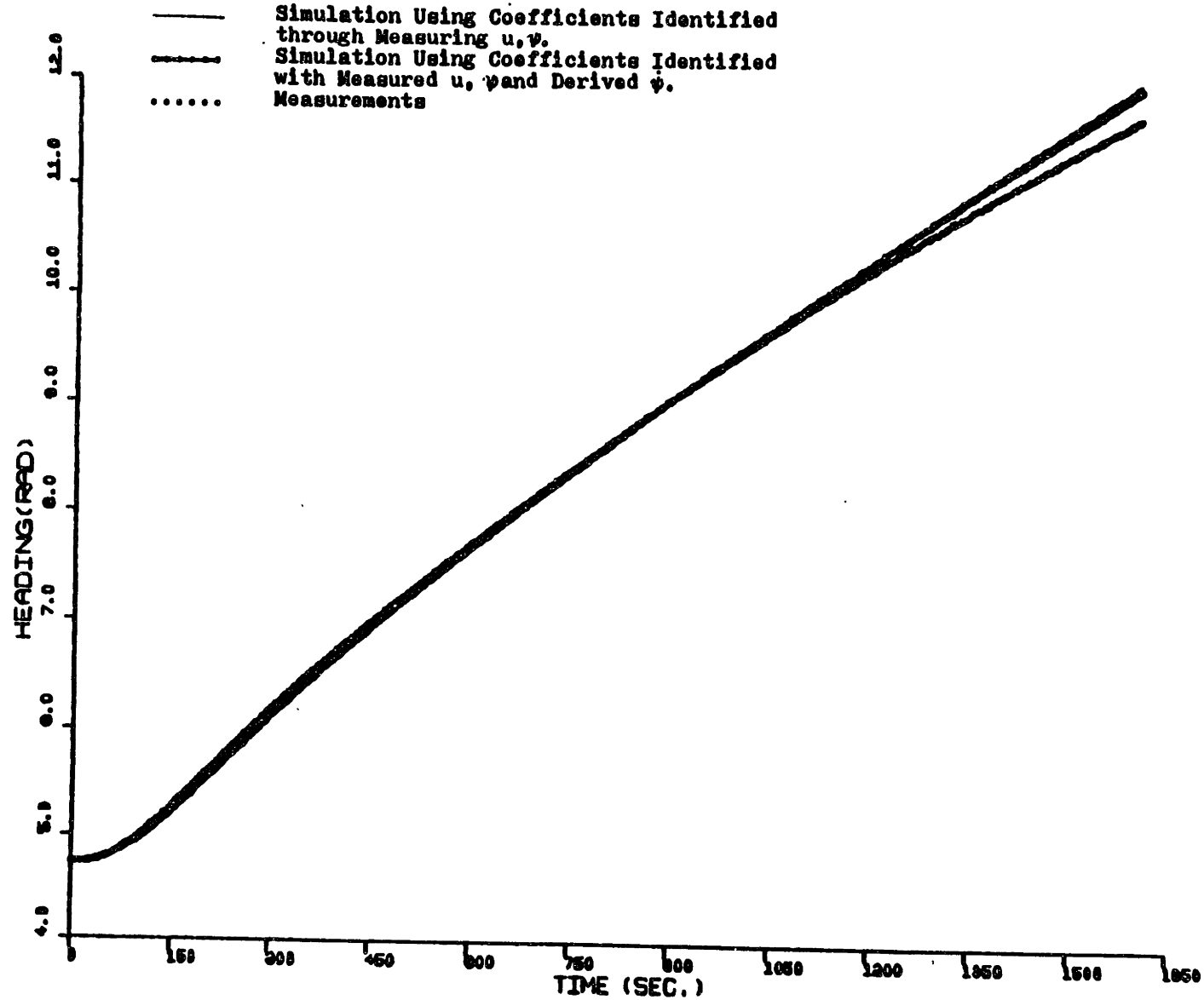

fig.4.3.10(d) Comparison between the 35° Maneuver Simulations by Using the Coefficients Identified with Measured u, ψ and with Measured u, ψ and Derived $\dot{\psi}$ Respectively----Yaw Angle ψ.

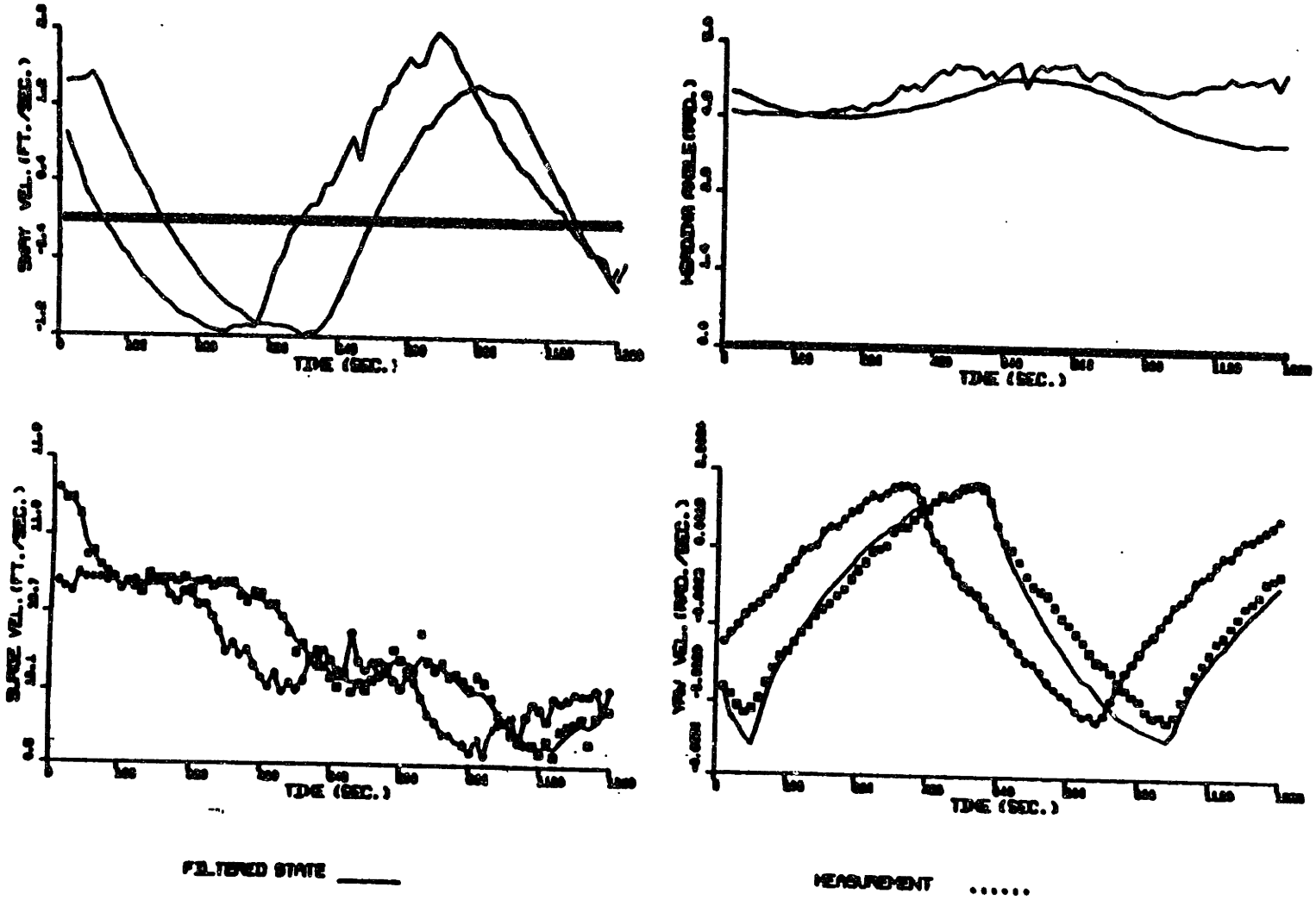

fig.4.4(a) Results of Identification of Coefficients with Measured u and Derived $\dot{\psi}$ Instead of ψ. No Improvement to the Results with Measured u and ψ.

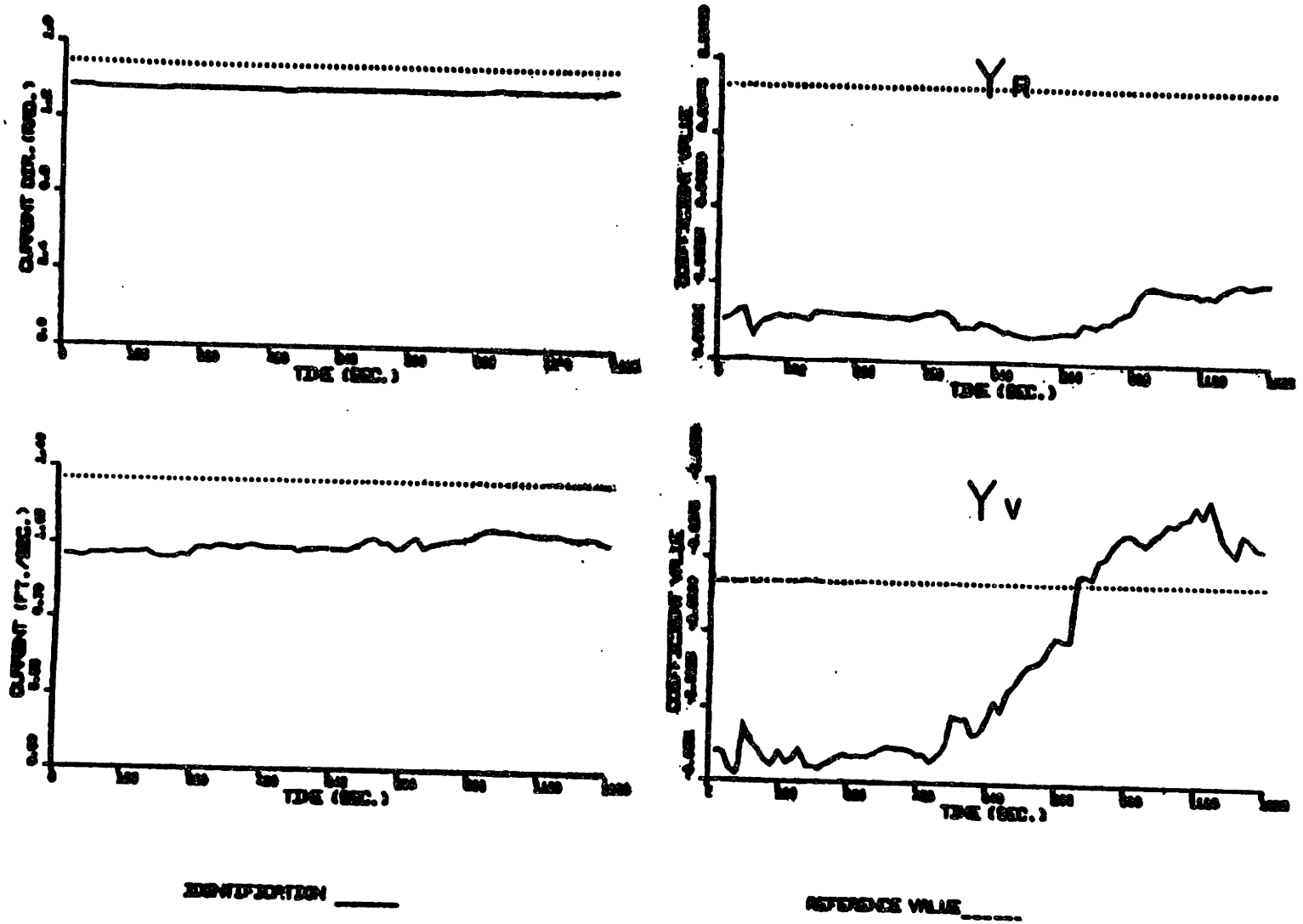

fig.4.4(b) Results of Identification of Coefficients with Measured u and Derived $\dot{\psi}$ Instead of ψ. No Improvement to the Results with Measured u and ψ.

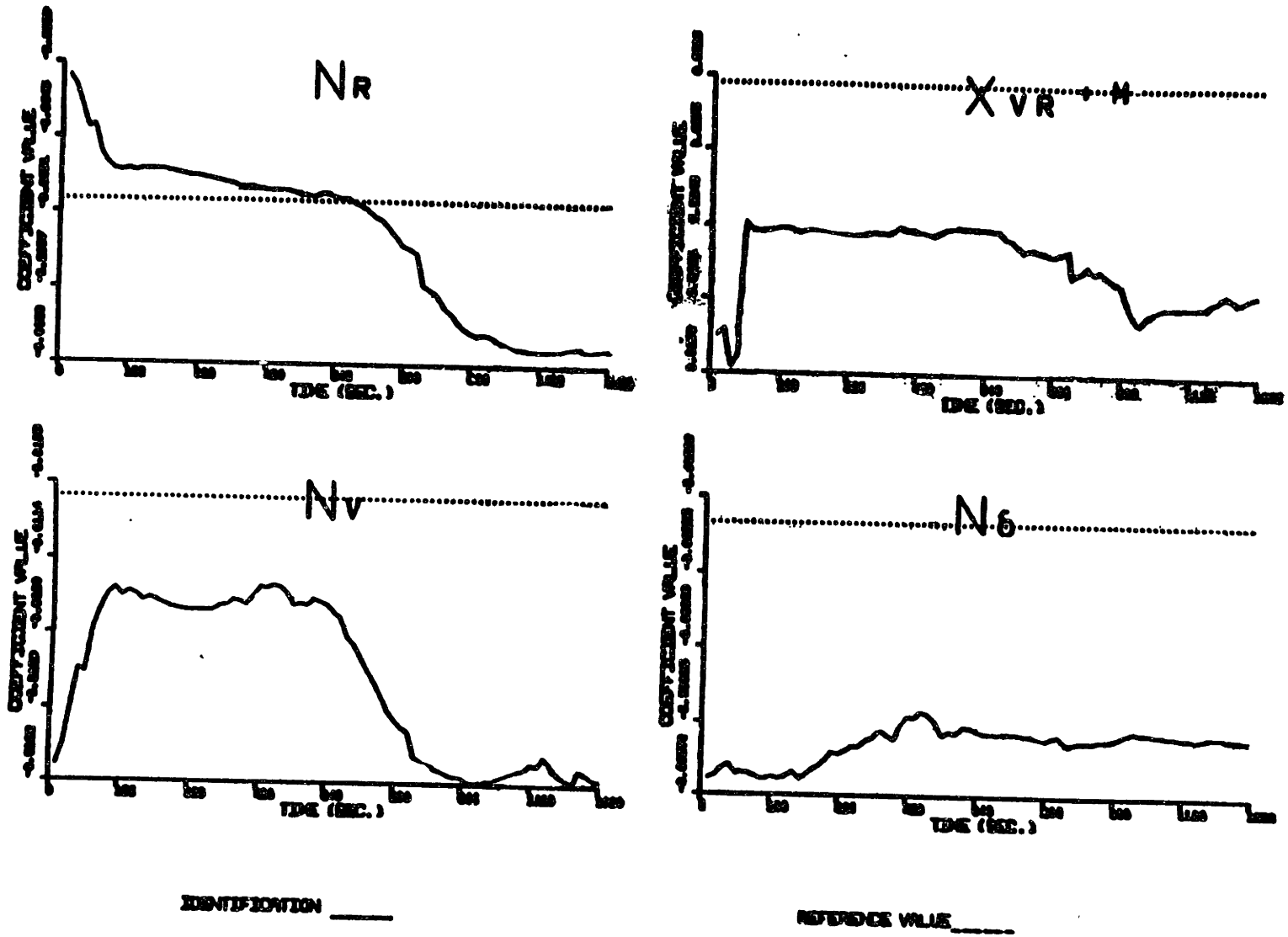

fig.4.4(c) Results of Identification of Coefficients with Measured u and Derived $\dot{\psi}$ Instead of ψ. No Improvement to the Results with Measured u and ψ.

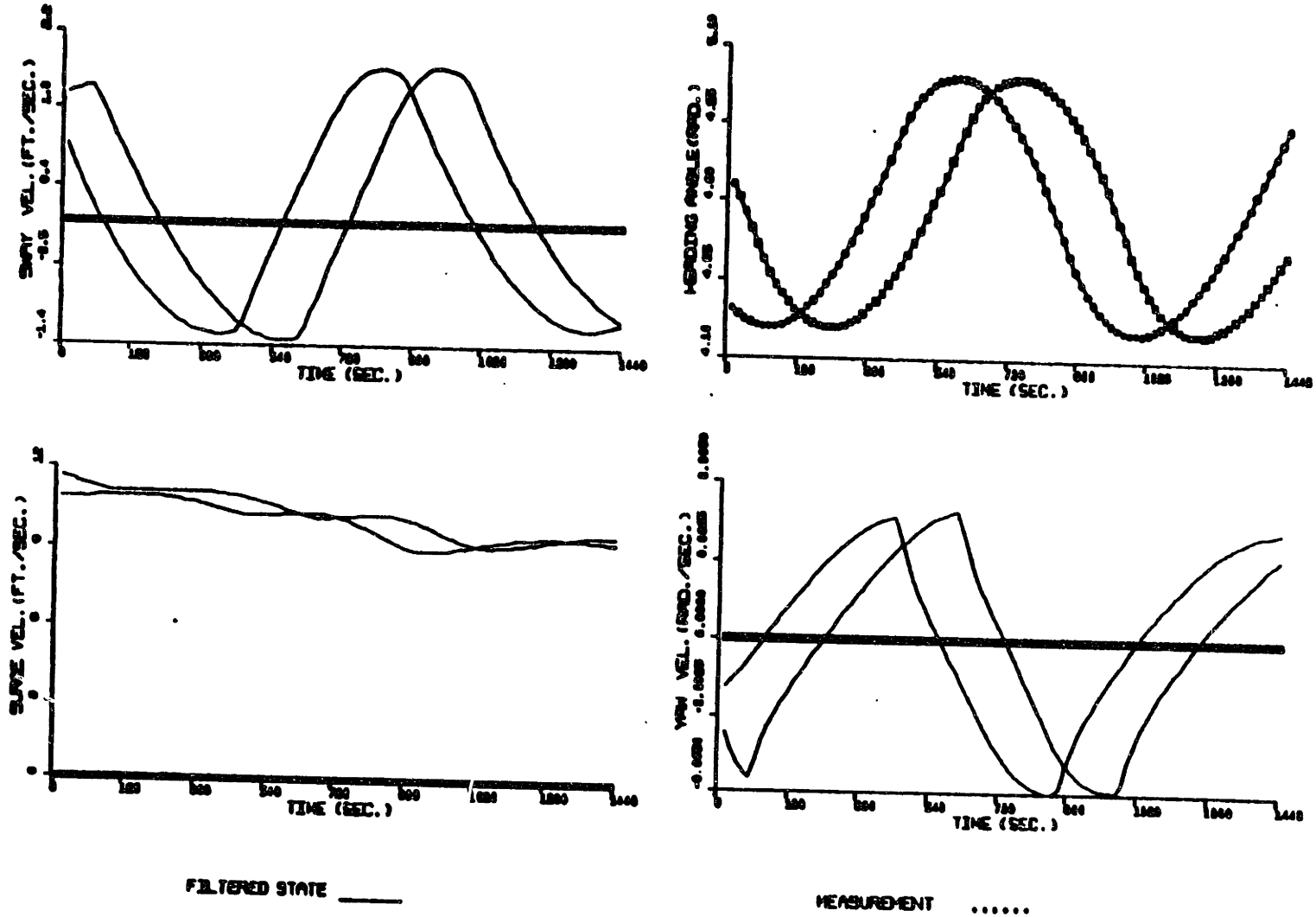

fig.4.5(a) Results of Identification of Coefficients with Measured ψ Only. The Results Are Not Qualified.

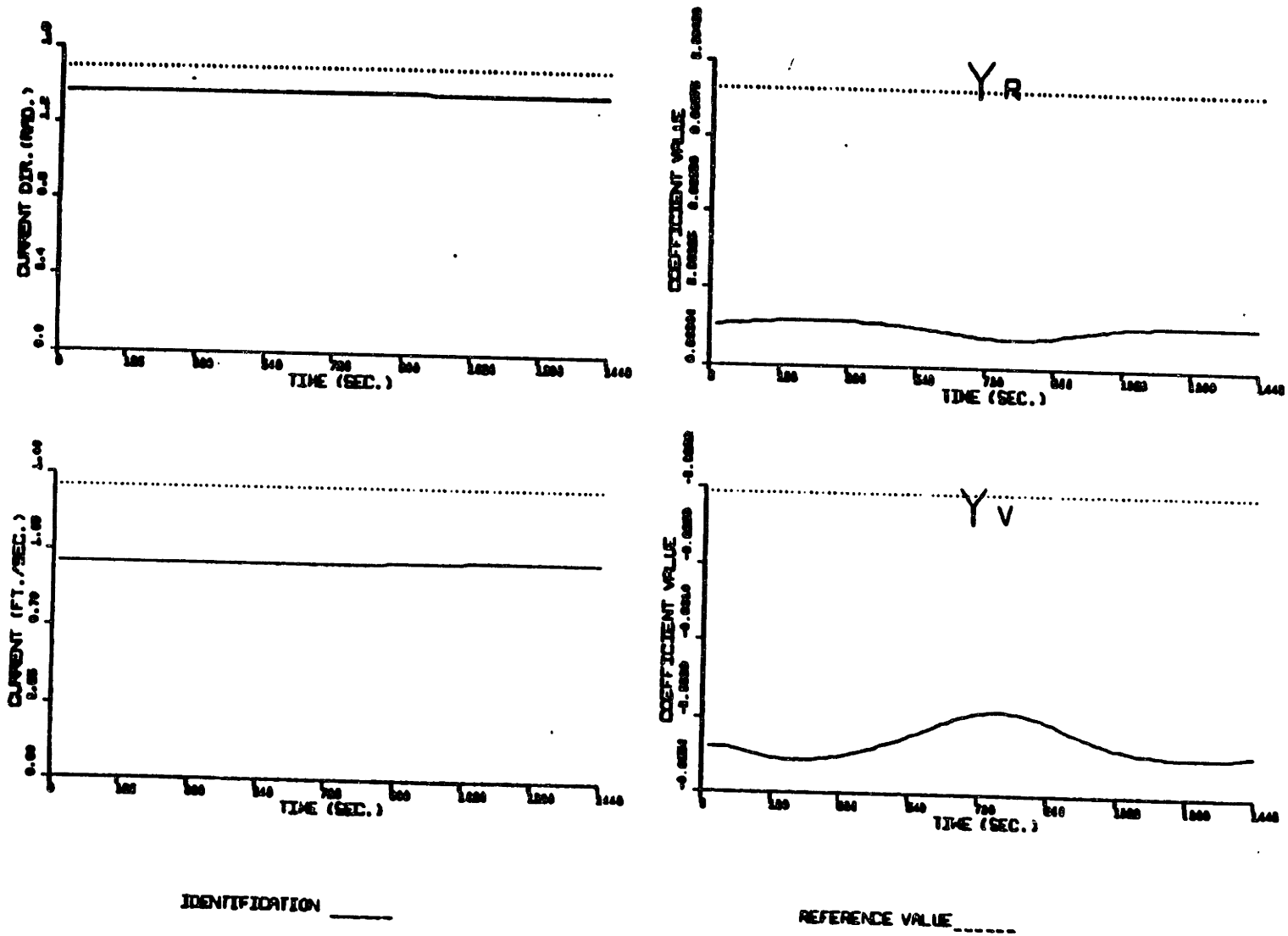

fig.4.5(b) Results of Identification of Coefficients with Measured ψ Only. The Results Are Not Qualified.

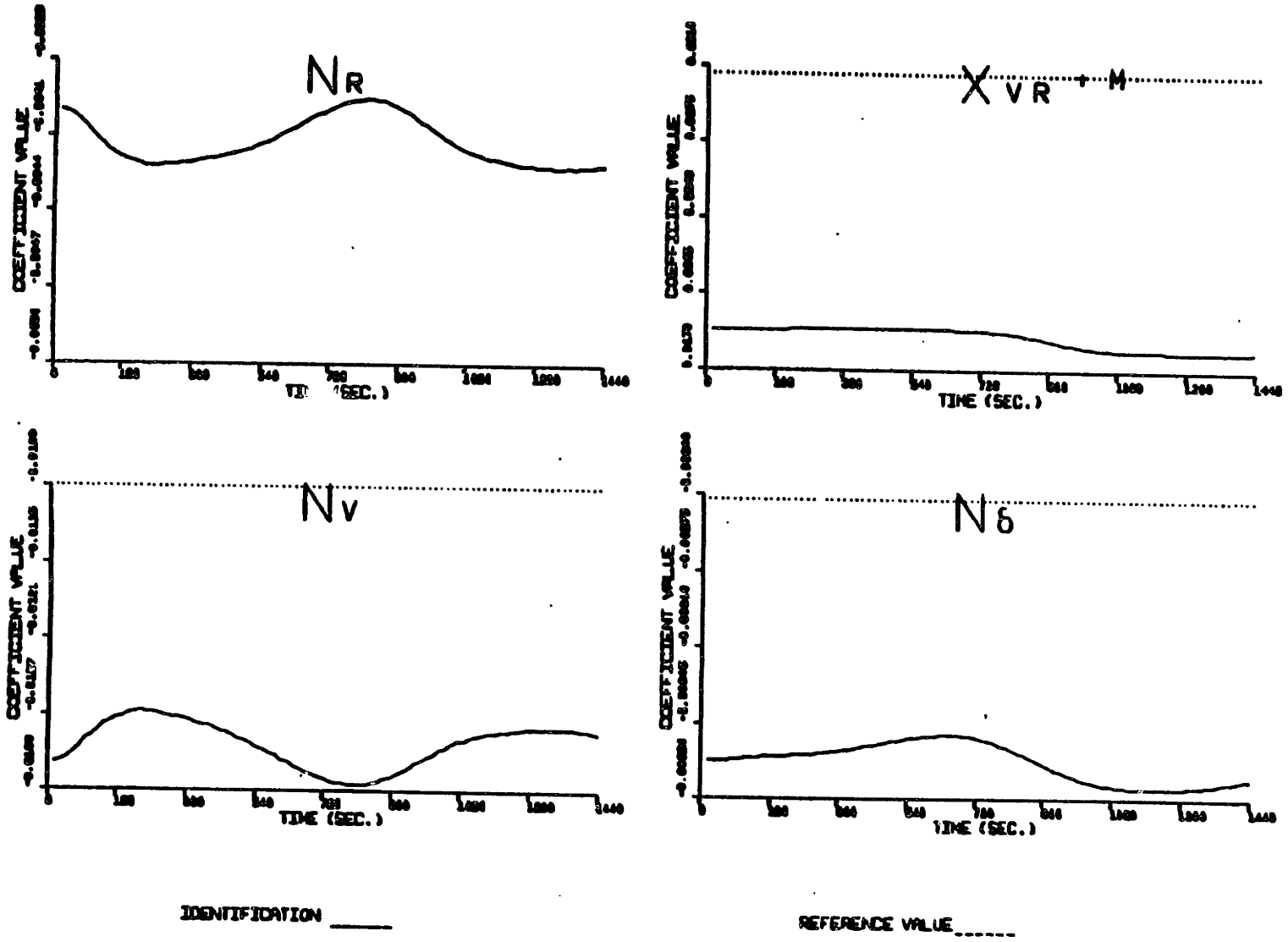

fig.4.5(c) Results of Identification of Coefficients with Measured ψ Only. The Results Are Not Qualified.

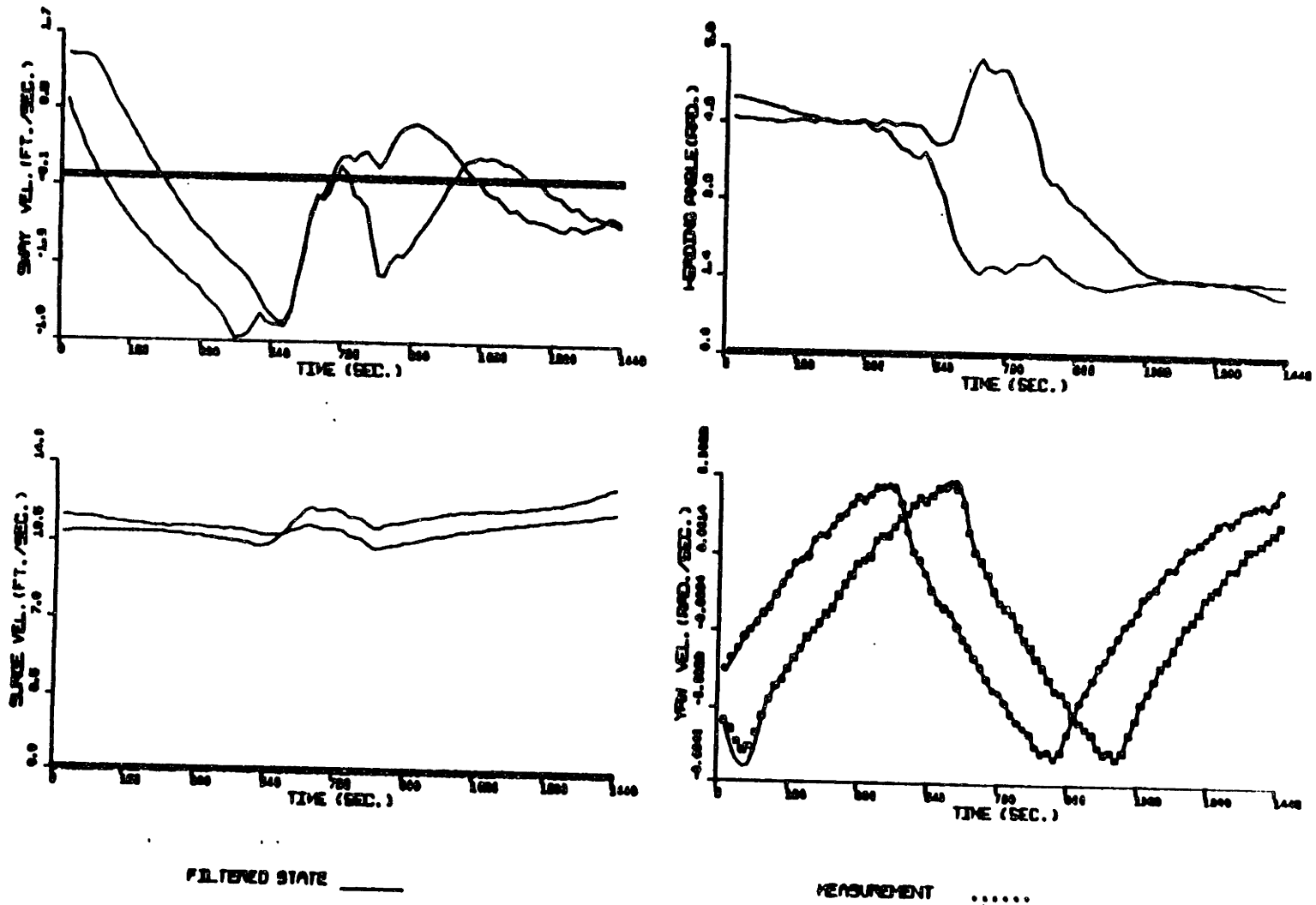

fig.4.6(a) Results of Identification of Coefficients with Derived $\dot{\psi}$ Only. The Results Are Not Qualified Either.

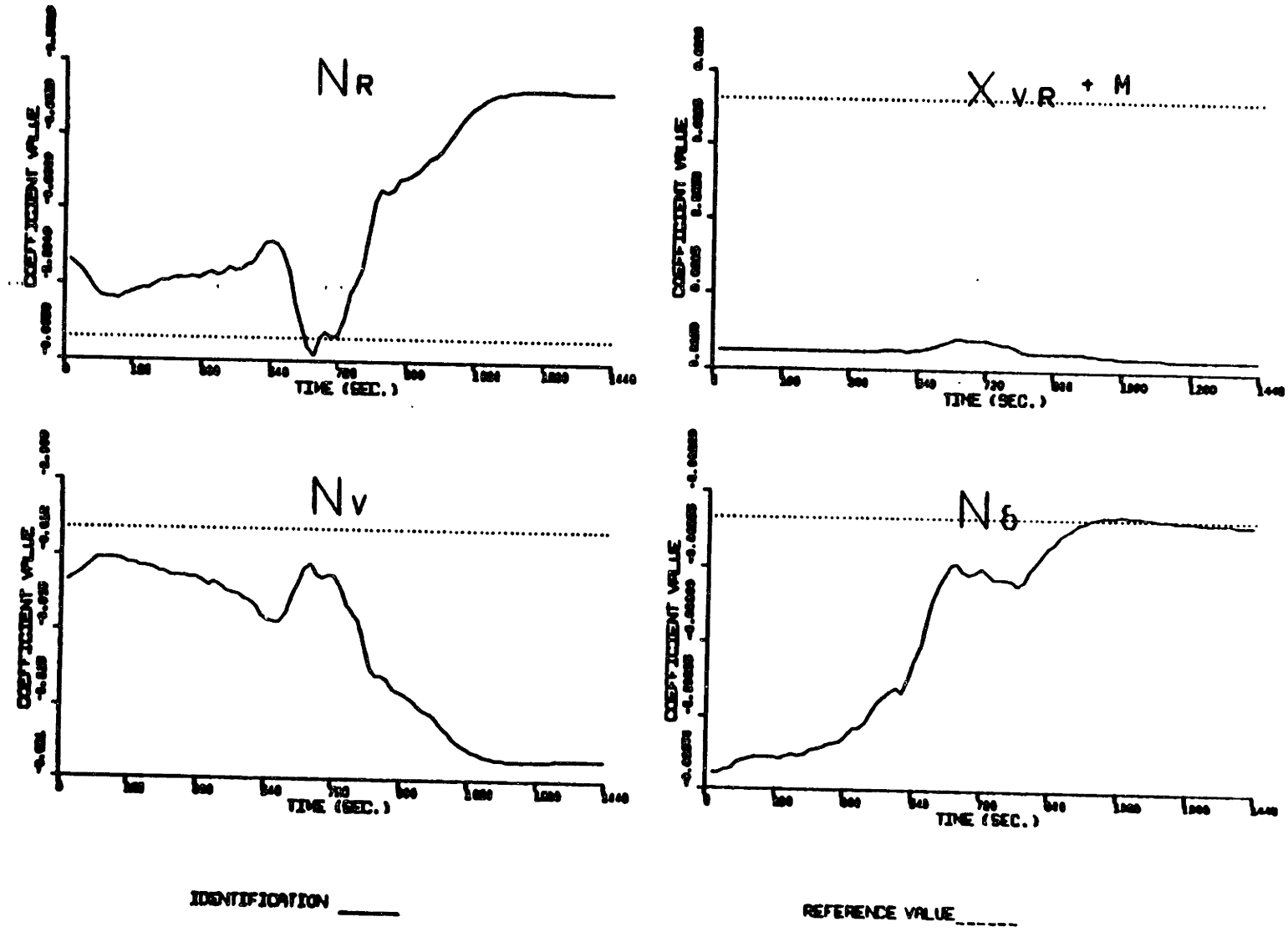

fig.4.6(b) Results of Identification of Coefficients with Derived $\dot{\psi}$ Only. The Results Are Not Qualified Either.

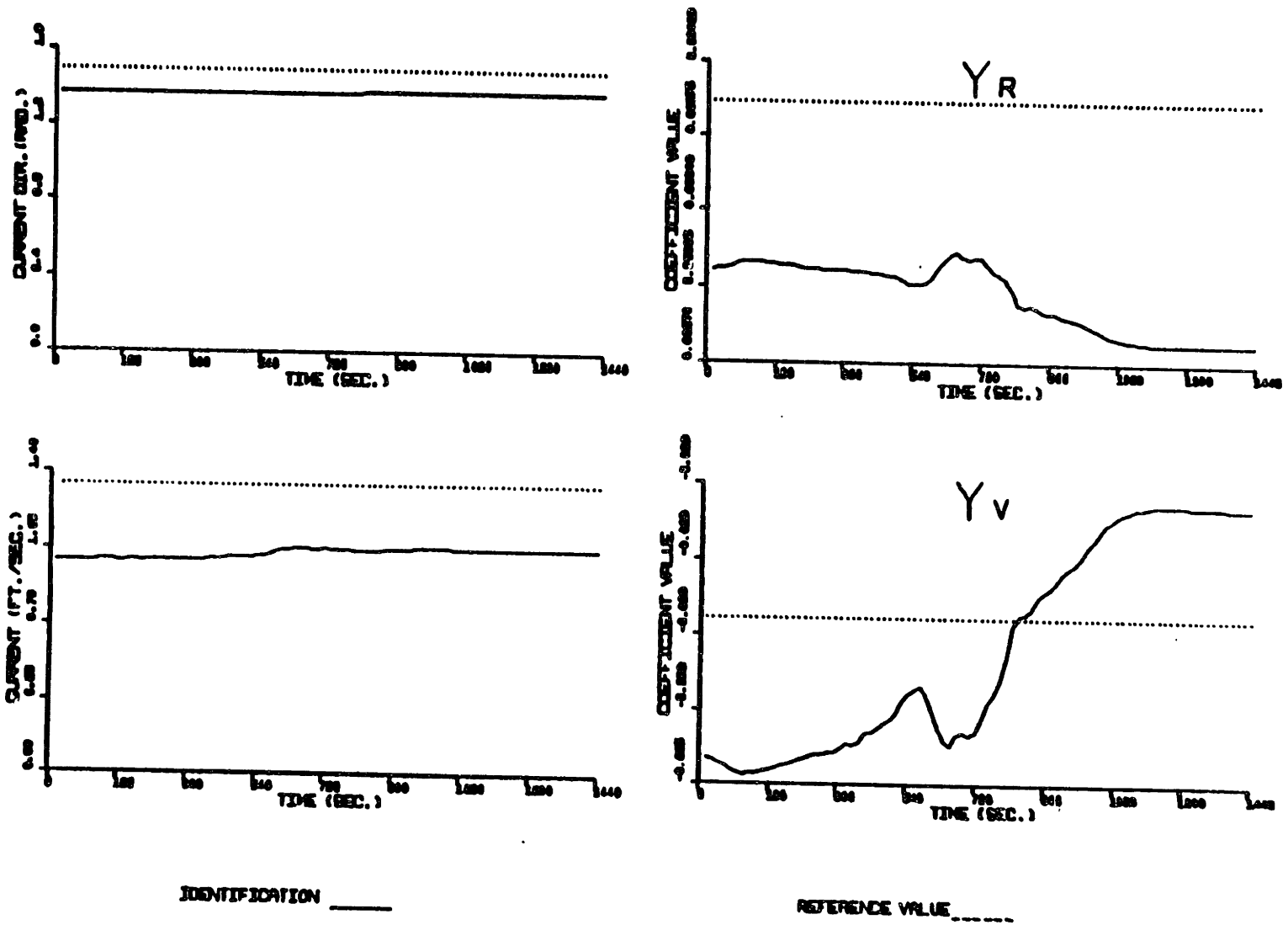

fig.4.6(c) Results of Identification of Coefficients with Derived $\dot{\psi}$ Only. The Results Are Not Qualified Either.

Coefficients & Current		Measurements			
		(4)	(3)	(2)	
		u,v,r,ψ	u,v,ψ	u,ψ	u,ψ,$\dot{\psi}$
6	Y_v	-0.02608	-0.02551	-0.02401	-0.02569
7	Y_r	0.00365	0.00339	0.00340	0.00321
12	N_v	-0.01406	-0.00613	-0.01393	-0.01286
13	N_r	-0.00480	-0.00247	-0.00699	-0.00630
14	N	-0.00283	-0.00233	-0.00337	-0.00322
21	X_{vr}+M	0.02660	0.02328	0.02013	0.02121
38		86.5^o	74.9^o	76.9^o	78.7^o
39	C(ft/s)	0.958	1.119	1.212	1.138
15	N_{vrr}	0.00337	0.00240	0.00260	0.00237
20	X_{ee}	-0.000996	-0.00211	-0.00124	-0.00142
22	X_{vvrr}	-0.00278	-0.00467	-0.00446	-0.00454
31	N_{eee}	0.00116	-0.00051	0.00084	-0.00043
35	Y_{vrr}	-0.03985	-0.03335	-0.04817	-0.03259
38		74.6^o	80.4^o	88.4^o	86.9^o
39	C(ft/s)	1.042	0.985	1.179	1.077

Table4.1 Results of Identification with Different Measurements

Chapter 5 CONCLUSIONS AND SUGGESTIONS

5.1 Conclusions

From our work, the following conclusions can be drawn:

1) For displacement surface ships like Esso Osaka, their dynamics in horizontal plane can be very well described by a linearized model of third order. With measurements of only the surge velocity u and yaw angle ψ, the main linear and nonlinear hydrodynamic coefficients can be identified satisfactorily by using EKF. Hence, with further work on different type of ships, we can expect that in the future, the simulation technique may be extensively applied to most of the ships equipped only with gyrocampass and a surge speed measuring device like speed log or Doppler sonar. Because, with them, through very simple sea trials during normal operation, the hydrodynamic coefficients can be "measured" with satisfactory accuracy.

2) The result of using three measurements u, v and ψ is even better, and does not differ from that of using four measurements of u, v, r and ψ. For the modern ships installed with dual axis Doppler sonar and heading rate gyro, three measurement is recommended. The results are better than that of the two measurement model, while no more work is involved during the sea trials.

3) With our state model and the already designed sea trials, the hydrodynamic coefficients of the ship can not be well identified by merely using the measurement of ψ with EKF.

4) Through our work, EKF is again confirmed to be a powerful tool in the identification of the hydrodynamic coefficients in the maneuvering simulation model. Also the skills of parallel processing and over- and under- estimated initial guesses are proved very useful during the identification.

5.2 Suggestions

The following suggestions are raised for achieving further improvements on the application of system identification theory to ship maneuvering study:

1) It is worthwhile to see if the following trade-off is valuable. We change the model structure by eliminating ψ from the state model:

$$\begin{aligned}
\dot{u} &= \dot{u}_r - (v - v_r)r \\
\dot{v} &= \dot{v}_r + (u - u_r)r \\
\dot{u}_r &= \frac{f_1}{m - X_{\dot{u}_r}} \\
\dot{v}_r &= \frac{1}{f_4}[(I_z - N_{\dot{r}})f_2 - (mx_G - Y_{\dot{r}})f_3] \\
\dot{r} &= \frac{1}{f_4}[(m - Y_{\dot{v}_r})f_3 - (mx_G - N_{\dot{v}_r})f_2]
\end{aligned} \qquad \text{.....(5.1)}$$

and then in the measurement model use $r = \dot{\psi}$ instead of ψ.

In this way the model of the system will be more standardized and the process noise of the state model can be decreased while the measurement noise does not increase at the same time. This will do good to the whole system. But

at the same time, since the current speed u_c and current direction angle α are also eliminated from the model, we can not identify the current directly.

2) As we mentioned in Chapter3, because of the mutual influence between state model and measurement models, when we try to use measurements of less numbers of variables, work on the state model is also needed to improve the efficiency of the process, including engineering and mathematical analyses to see what modification is needed. Also from our work and the work done by Hwang and Kwok[8,9], we know that state model of Esso Osaka does have some inadequacy which is apparent when the nonlinear hydrodynamic coefficients were identified. Modifications and revisions are needed for future development.

3) The sea trials may need new designs when the system model is modified. And because this is a new area, more practices on the ships with different sea trials designs are needed. Through comparison of the results, more effective designs may be developed.

4) A similiar study can be carried out on the different types of ship in order to make the application of system identification technique more practical.

REFERENCES

1. Abkowitz, M. A., 1969, STABILITY AND MOTION CONTROL OF OCEAN VEHICLES, The M.I.T. Press, Cambridge, Mass.

2. Abkowitz, M. A., 1980, MEASUREMENT OF HYDRODYNAMIC CHARACTERISTICS FROM SHIP MANEUVERING TRIALS BY SYSTEM IDENTIFICATION, SNAME, Annual Meeting.

3. Gelb, G., 1977, APPLIED OPTIMAL ESTIMATION, The M.I.T. Press, Cambridge, Mass.

4. Athans, M., 1971, THE ROLE AND USE OF THE STOCHASTIC LINEAR-QUADRATIC- GAUSSIAN PROBLEM IN CONTROL SYSTEM DESIGN, IEEE, Transaction on automatic control, Vol. AC-16, No.6

5. Fitzgerald, R. J., 1971, DIVERGENCE OF THE KALMAN FILTER, IEEE, Transaction on automatic control, Vol. AC-16, No. 6, pp.736--747

6. Rhodes, I. B., 1971, TUTORIAL INTRODUCTION TO ESTIMATION AND FILTERING, IEEE, Transaction on automatic control, Vol. AC-16, No. 6, pp.

7. Sage, A. P. and Melsa, J. L., 1971, SYSTEM IDENTIFICATION, Academic Press, New York and Landon.

8. Hwang, W. Y., 1980, APPLICATION OF SYSTEM IDENTIFICATION TO SHIP MANEUVERING, Ph.D. Thesis, Department of Ocean Engineering, M.I.T., Cambridge, Mass.

9. Kwok, C. L., 1981, SELECTION OF HYDRODYNAMIC COEFFICIENTS FOR SUPERTANKER SIMULATION, M.Sc. Thesis,

Department of Ocean Engineering, M.I.T., Cambridge, Mass.

10. Hayes, M. N., 1971, PARAMETRIC IDENTIFICATION OF NONMINEAR STOCHASTIC SYSTEM

APPLIED TO OCEAN VEHICLE DYNAMICS, Ph.D. Thesis, Department of Ocean Engineering, M.I.T., Cambridge, Mass.

11. Szeto, F. F., 1977, SYSTEM IDENTIFICATION FROM SHIP MANEWUVERS IN CURRENTS , Engineers Thesis, Department of Ocean Engineering, M.I.T., Cambridge, Mass.

12. Lundblad, J. G., 1974, APPLICATION OF THE EXTENDED KALMAN FILTERING TECHNIQUE TO SHIP MANEUVERING ANALYSIS, M.Sc. Thesis, Department of Ocean Engineering, M.I.T., Cambridge, Mass.

13. Brinati, H. L., 1973, SYSTEM IDENTIFICATION APPLIED TO MANEUVERING TRIALS, Engineers Thesis, Department of Ocean Engineering, M.I.T., Cambridge, Mass.

14. Ogata, K., 1970, MODERN CONTROL ENGINEERING, Prentice-Hall, Inc., Englewood

Cliffs, N.J.

15. Kim, J.S., 1983, APPLICATION OF MANEUVERING SIMULATION MODELS TO SHIP DESIGN DEVELOPMENT, M.Sc. Thesis, Department of Ocean Engineering, M.I.T., Cambridge, Mass.